School of Civil Engineering

Small and Large Strain Rheological and Fatigue Characterisation of Bitumen-Filler Mastics

By

Min-Chih Liao

Thesis submitted to The University of Nottingham
for the degree of Doctor of Philosophy

October 2007

Abstract

Bituminous binder in asphalt mixtures does not occur as bitumen alone, but is mixed with mineral fillers forming bitumen-filler mastic. There could be possible interactions between filler and bitumen, which does not get reflected in the rheological and mechanical properties of plain bitumen. The rheological and mechanical properties of the mastics rather than those of the bitumen are more appropriate in terms of establishing a correlation with asphalt paving mixture performance. Additionally, since bituminous binders exist as thin films in asphalt mixtures, they may perform in the non-linear range due to the considerable difference between the modulus of aggregates and the modulus of binders.

This thesis investigates the use of a Dynamic Shear Rheometer (DSR) to quantify the rheological properties and fatigue characterisation of various bitumen-filler mastics under small and large strain conditions. A set of fundamental rheological tests was performed on a range of the bitumen-filler mastics with three filler types (limestone, cement and gritstone) and three filler concentrations (15, 35 and 65% by mass). The bitumen-filler mastics having 15 and 35% filler concentrations by mass were considered as enhanced binders since filler suspension was present in the base bitumen, while the mineral filler particles established physical contacts with other particles through the bitumen medium (filler skeleton) for the 65% bitumen-filler mastic.

This research is concerned with small strain rheological analysis, steady state rheological analysis and fatigue characterisation (large strain) of the bitumen-filler mastics. The strain and stress linear viscoelastic (LVE) limits, stiffening effect of mineral filler on complex modulus and zero shear viscosity (ZSV), ZSV extrapolation using various techniques and fatigue characteristics have been presented in this thesis. Dynamic shear testing (stress sweeps, frequency sweeps and time sweeps) and rotational shear testing (viscometry testing and creep testing) of the bitumen-filler mastics have indicated that the rheological characteristics and fatigue characterisation differ considerably between the filler enhanced binder (15 and 35% mastics) and the filler highly modified binder (65% mastics). The 15 and 35% bitumen-filler mastics showed

similar patterns of rheological and fatigue behaviour to the pure bitumen, while the 65% bitumen-filler mastics showed a significant stiffening effect on ZSV and a similar pattern of fatigue characteristics to a 10 mm DBM.

Acknowledgements

I would like to thank a large number of people who have provided encouragement, assistance and funding without which this Ph.D. research would not have been possible.

I am greatly indebted to my supervisor Dr. Gordon D. Airey for his invaluable guidance, support and enthusiasm throughout the research period. My thanks also go to Professor Andrew C. Collop and Dr. Nick H. Thom for their advice and support. I would also express my appreciation to Dr. Salah E. Zoorob and Mr. Murray Parry who acted as mentors and offered valuable suggestions while studying and working in the Nottingham Transportation Engineering Centre (NTEC).

I would like to express my appreciation and thanks to Mr. Barry Brodrick, Mr. Chris Fox and Mr. Kevin Gilbert who assisted me during the experimental work. I would like to express my deep gratitude to all of those individuals who assisted me while working in the NTEC laboratory, particularly Jonathan Watson, Mick Winfield, Richard Blakemore, Martyn Barrett, Nancy Hodge, Richard Meehan, Neil Parkes, Michael Pepper and Lawrence Pont. I also thank all administration staff for their help during the course of the study. I am grateful to all the researchers and colleagues of the NTEC at the University of Nottingham. Thanks to all those who have helped me in some way but are not mentioned above by name.

I would also like to express my sincere appreciation to all my colleagues at the National Cheng Kung University who provided me with the inspiration to undertake the work herein. I have to be greatly indebted to Professor Jian-Shiuh Chen for his constant encouragement and invaluable advice.

I wish to thank my parents, Mr. and Mrs. Wu, brother and sister-in-law who made my stay in the U.K. possible and beautiful. Finally, I wish to thank Ellen for her patience, love and care as I worked on my Ph.D. research.

Declaration

The research described in this thesis was conducted at the University of Nottingham, School of Civil Engineering between October 2003 and October 2007. I declare that the work is my own and has not been submitted for a degree of another university.

Min-Chih Liao
Nottingham
October 2007

Table of Contents

Page

List of Figures

List of Tables

Introduction

1.1 Background

Bitumen has been used for a wide variety of applications, particularly in road construction. The most common bitumens are manufactured from crude oil by distillation. Bitumen is a complex mixture of components which are composed of hydrocarbon molecules and other molecules containing heteroatoms such as oxygen, sulphur and nitrogen. The precise composition of bitumen varies according to the source of crude oil.

Bitumen is a thermoplastic material and is used to adhere and lubricate mineral aggregates to form an asphalt mixture for paving construction. When bitumen is subjected to a load, it performs in an elastic and brittle manner at low temperatures and in a viscous and fluid manner at high temperatures. At intermediate temperatures, bitumen performs as a time and temperature dependent material and possesses a combination of both elastic and viscous behaviour described as viscoelasticity. The viscoelastic property of bitumen plays an important role for paving construction and it influences the mechanical properties of asphalt mixtures.

The use of bitumen in combination with aggregates, fillers and air to form an asphalt mixture layer contributes to a smooth and stiff structural layer in flexible pavements to spread loads and protect the underlying unbound layers by distributing wheel loads. The mechanical properties (stiffness, permanent deformation and fatigue cracking) of asphalt mixtures are strongly dominated by binder properties, aggregate skeleton, and the volumetric proportions of bitumen, aggregate and air.

Asphalt pavements do not fail suddenly other than due to large thermal or ground movements, but gradually deteriorate over a long period to a terminal condition which

can be defined as failure. Permanent deformation and fatigue cracking are the two primary modes of failure caused by repeated traffic loading, temperature variations and construction practices generating stresses and strains in the asphalt layers. Primary concerns of pavement engineers are the improvements in material properties and developments of proper pavement design methods. The material properties can be improved by the use of high quality of aggregates and binders, and also can be improved by proper asphalt mixture design. The proper pavement design methods are obtained from a better understanding of behaviour of pavement structure and mechanical properties of the materials.

1.2 Review of Bituminous Binders

1.2.1 Bituminous Binders

The most common bitumens are manufactured from crude oil and they can be supplied in a number of different forms such as: penetration grade bitumens, cutback bitumens, bitumen emulsions and modified bitumens for road applications. Bitumen plays a major role in pavement performance and it is responsible for the viscoelastic characteristics of asphalt mixtures. A change in bitumen strain is generally attributed to viscous flow as a function of the increase in temperature and loading time. Due to a considerable increase in traffic level, tyre pressure and heavier trucks, bitumen modification is a solution to overcome the distresses in flexible pavements. The aim of bitumen modifier is either to stiffen bitumens to reduce the total viscoelastic response of asphalt mixtures or to increase the elastic component of bitumens to reduce the viscous component.

A variety of modified bitumens and specialist bitumens are currently being used in paving applications in order to improve the performance of asphalt paving mixtures. Various additives are used as bitumen modifiers such as reclaimed rubber products, fibres, catalysts, extenders, polymers and fillers.

1.2.2 Empirical Testing

Many empirical tests have been used to characterise the physical properties of bitumen under particular temperature and loading time conditions, such as the penetration test in

the United Kingdom. In addition, the softening point test and viscosity test are routinely used for the determination of the physical properties of bitumens.

Penetration Test (BS EN 1426:2000)

The penetration test can be considered as an indirect measurement of the viscosity of the bitumen at 25^{o}C, and is a common test used in the United Kingdom to specify different grades of bitumens. In the penetration test, a needle penetrates a sample of bitumen under a load of 100 grams at a temperature of 25^{o}C for a loading time of 5 seconds. The definition of penetration, which is measured in decimillimetres (dmm) is the distance traveled by the needle into the bitumen sample under the loading conditions. Harder bitumen results in lower values of penetration, whereas softer bitumen has higher values of penetration. A variety of bitumens can be easily graded and specified based on the penetration results.

Ring and Ball Softening Point (BS EN 1427: 2000)

The ring and ball softening point test is commonly conducted to determine the consistency of bitumens by measuring the equiviscous temperature at the beginning of the fluidity range of bitumens. In the softening point test, a steel ball (3.5 g) is placed on a bitumen sample contained in a brass ring that is suspended in a water or glycerol bath, in which the bath temperature is raised at 5^{o}C per minute. The softening point is the temperature measurement when the bitumen softens and eventually deforms slowly with the ball through the ring to touches a base plate 25 mm below the ring.

Viscosity Test

Viscosity is a fundamental characteristic of a bitumen's fluidity at a given temperature and loading time. The viscosity values for a bitumen can be measured by means of various techniques. The sliding plate viscometer is used to measure the absolute or dynamic viscosity in pascal seconds (Pa.s) for a bitumen, while the capillary viscometer is used to measure the kinematic viscosity in mm^2/s for a fluid bitumen. The rotational viscometer is routinely used to determine the absolute viscosity (Pa.s) for a bitumen at pavement service temperatures. A torque is applied to a cylindrical-shaped spindle submerged and rotated in a tube which contains a bitumen sample. The absolute

viscosity values are converted from the measurements of the torque applied to a bitumen sample in response to the applied shear rate over a wide range of temperature and shear rate conditions.

1.2.3 Fundamental Rheological Testing

The performance of asphalt pavements are not easily characterised by physical properties as asphalt pavements are subjected to complex environmental and loading conditions. Additionally, various polymer modified bitumens (PMBs) and multi-grade bitumens can not necessarily be charaterised by empirical properties. It is essential to understand the stress-strain behaviour of bituminous binders over a wide range of temperature and loading time conditions. Thus, fundamental tests were introduced and developed to investigate mechanical properties and viscoelasticity of binders under different environmental conditions. In the United States, the Strategic Highways Research Program (SHRP) was a coordinated effort to produce binder specifications which were classified based on a performance-grade system in accordance with fundamental testing results (Petersen et al., 1994; Anderson et al., 1994).

Dynamic Shear Rheometer Test (AASHTO T315-02)

The Dynamic Shear Rheometer test is used to measure the elastic and viscous nature of bituminous binders within a linear viscoelastic region across a range of temperatures and frequencies. The oscillatory-type test is conducted on binders at different temperature, frequency, stress and strain levels. In the test, a bitumen sample sandwiched between two parallel plates is subjected to a sinusoidal torque or a sinusoidal angular displacement of constant angular frequency. The various rheological parameters are converted from the measurements of the torque applied to a specimen in response to the applied shear stresses or strains.

Bending Beam Rheometer Test (AASHTO: T313-02)

The Bending Beam Rheometer test is used to measure the creep response of binders at low temperatures. In the test, a constant load is applied to a prismatic bitumen beam measuring 125 mm by 12.5 mm by 6.25 mm in simple bending at its midpoint. Creep stiffness values are obtained at several loading times ranging from 8 to 240 seconds (six

loading times: 8, 15, 30, 60, 120 and 240). The m value is the slope of the log creep stiffness versus log time curve. SHRP binder specification states if the creep stiffness is less than or equal to 300 MPa together with the m value being greater than 0.30, the binder meets the specification (Petersen et al., 1994).

Direct Tension Test (AASHTO: T314-02)

The Direct Tension test is used to provide tensile failure properties of bitumens at low in-service temperatures. A dog-bone-shaped specimen is contained in a silicone rubber mold and pulled in tension at a single temperature and rate of elongation until rupture occurs. The DTT test is valid when a specimen fractures in a brittle-ductile region where the strain to failure ranges from 0.1 to 10 percent. A binder acts as a brittle material where the strain to failure is less than approximately 1 percent. In SHRP binder specification, it should be ensured that the strain at failure at the minimum pavement design temperature is greater than 1.0 percent (Petersen et al., 1994).

1.3 Review of Asphalt Mixtures

1.3.1 Types of Asphalt Mixture

Various types of asphalt mixtures exist if considering the possible combinations of the aggregate particle size distributions and binder contents. Traditionally, the asphalt mixtures are designed as either continuously graded or gap graded. A continuously graded asphalt mixture is one that contains continuous aggregate particle size distribution from the maximum size down to filler, while a gap graded asphalt mixture is one that the aggregate particle size distribution is discontinuous. The types of asphalt mixture in terms of aggregate particle size distribution are described as follows:

Continuously Graded Mixtures

1. Dense Bitumen Macadam (DBM)

Dense Bitumen Macadam (DBM) is a traditional mixture incorporating 100 or 200 pen grade bitumen. It is a continuously graded asphalt mixture, and its strength is derived

from the interlock of coated aggregates. DBM can also be incorporated with 50 penetration grade bitumen, identified as DBM 50.

2. Heavy Duty Macadam (HDM)

Heavy Duty Macadam, which is one of the improved dense coated macadams, is a continuously grade asphalt mixture with an increased filler content ranging from 7% to 11% by mass in mixtures. 100/150 penetration grade bitumen is replaced by 40/60 penetration bitumen together with a higher filler content, which results in a significant increase in stiffness for asphalt mixtures. This improves the resistance of permanent deformation as well as reducing the tensile strains induced at the bottom of a base layer.

3. High Modulus Base (HMB)

High Modulus Base material is another one of the improved dense coated macadams and is manufactured with 30/45 penetration bitumen. The HMB provides a significant increase in stiffness compared to the conventional asphalts and as a result can be laid thinner.

Gap Graded Mixtures

1. Hot Rolled Asphalt (HRA)

Hot Rolled Asphalt (HRA) is a gap graded asphalt mixture with a relatively high binder content and consists of a single size coarse aggregate mixed with a bitumen/sand/filler mortar. The strength of HRA is derived from the characteristics of mortar. The use of HRA in paving construction can provide a good resistance to fatigue cracking and increase durability caused by the relatively high binder content making the mixtures impermeable to air and water. However, HRA is now not commonly used in the UK due to rutting problems.

2. Stone Mastic Asphalt (SMA)

Stone Mastic Asphalt originally developed in Germany and Scandinavia is a gap graded asphalt. SMA has a coarse aggregate skeleton with the voids being filled with a fine

aggregate/filler/bitumen mortar. It is a durable material with high stability due to the stone-stone interlock of its coarse aggregate skeleton.

3. Porous Asphalt

Porous Asphalt (PA) is a gap graded material and used as wearing courses. PA has interconnecting voids so that it allows water to flow freely through the PA to the binder course. The use of modified binders or fibres is necessary due to the bitumen being exposed to oxygen in the atmosphere and therefore oxidising relatively quickly.

1.3.2 Mechanical Properties of Asphalt Mixture

It is essential to consider the two aspects of material properties in the analytical design of asphalt pavements: (1) the stress-strain behaviour of asphalt mixtures used to analyse critical stresses and strains in the pavement structure and (2) the performance of asphalt pavements included the resistance of permanent deformation and fatigue cracking (Airey, 1997; Read and Whiteoak, 2003; Osman, 2004). The mechanical properties of stiffness, permanent deformation and fatigue cracking are presented as follows:

Stiffness Modulus

The stiffness modulus of asphalt mixtures is not a constant, but a function of temperature and loading time. The strain-stress behaviour of asphalt mixtures occurring at low temperatures or short loading times (high stiffness modulus) is elastic and used to calculate the stresses and strains in analytical pavement design, whereas that of asphalt mixtures at high temperatures or long loading time (low stiffness modulus) is used to evaluate the permanent deformation.

Fatigue Cracking

Fatigue cracking is defined as a phenomenon of fracture under repeated or fluctuating stress having a maximum value generally less than the tensile strength of the material. In asphalt pavements, fatigue cracking is one of the primary distresses and consists of two main phases, crack initiation and crack propagation, resulting from accumulative damage under load repetition, temperature variation and construction practices which induce stress below the tensile strength of asphalt materials (Read, 1996; Rowe, 1996).

The progressive damage results in cracks which initiate at the bottom of the bituminous layers and then propagate to the pavement surface in thinner asphalt pavements, whereas cracks start at the pavement surface and then propagate towards the bottom of bituminous layers in thicker asphalt pavements. Due to the fatigue behaviour of asphalt mixtures it is necessary to incorporate a fatigue factor into the pavement design.

Permanent Deformation

Permanent deformation is one of the primary distresses found in bound and unbound layers in asphalt pavements caused by repeated vehicle loading at high pavement temperatures and inadequate compaction during construction. The deformation in asphalt pavements develops primarily through two mechanisms consisting of densification (compaction) and shear flow. The accumulation of permanent deformation or irrecoverable deformation usually results in rutting in the road surfacing layers. Non-structural rutting problems exhibit distinctive shoulders on the road surfacing caused by accumulated permanent vertical strain confined to the bituminous layers, which can be solved by the overlap of wearing courses. Structural rutting problems caused by accumulated vertical strain can be due to incorrect pavement design. The permanent deformation occurs in the whole pavement structure (bound and unbound layers).

1.4 Problem Statements

1.4.1 Material Considerations

The mechanical properties of asphalt mixtures are significantly influenced by the rheological and mechanical properties of bituminous binders. However, the bituminous binder in asphalt mixtures does not occur as bitumen alone, but is mixed with mineral fillers forming mastic. The physical properties and chemical constituents of the mineral fillers could affect the rheological and mechanical properties of bitumen-filler mastics. There could also be the possible interactions between filler and bitumen, which does not get reflected in the rheological and mechanical properties of plain bitumen. Bitumen-filler mastics may provide a better correlation to asphalt mixtures since they take account of physicochemical aspects of the interactions between bitumen and mineral filler. The rheological and mechanical properties of mastics rather than those of bitumen

may be more appropriate in terms of establishing a correlation with asphalt paving mixture performance.

1.4.2 Testing Considerations

Empirical tests such as penetration, softening point and viscosity have been routinely used to represent the physical properties of bituminous binders and link these to the performance of asphalt mixtures. However, these conventional specifications and tests only determine the characteristics of the binders at particular temperature and loading rate conditions. Additionally, the possible physicochemical interaction between mineral filler and bitumen may be not necessarily characterised by the traditional parameters from these empirical tests.

Fundamental rheological testing (oscillatory-type) using a DSR has also been routinely performed to characterise the rheological behaviour of bituminous binders within a linear viscoelastic domain and it enables the binder's complete rheological properties to be determined. However, practically, since bituminous binders exist as thin films in asphalt mixtures, they might perform in the non-linear range due to the considerable difference between the modulus of aggregates and the modulus of binders. The strain domains within the binders are much higher than the bulk strain within the asphalt mixtures. Therefore, the bitumen-filler mastic investigation should be concerned with a set of rheological tests which are related to stiffness modulus, permanent deformation and fatigue characteristics of asphalt mixtures.

1.5 Research Methodology

1.5.1 Material

In this investigation, a straight-run bitumen (base bitumen) with three types of mineral filler were tested using a dynamic shear rheometer (DSR). The filler concentration levels in bitumen-filler mastics were selected as (1) filler particles are suspended in the bitumen (low filler concentration) and (2) filler particles form a skeleton in the bitumen (high filler concentration). At the low filler concentration, the bitumen/filler ratio used in bitumen-filler mastic was similar to that used in Dense Bitumen Macadam (DBM).

At the high filler concentration, physical contacts between mineral filler particles were present in the bitumen-filler mastic. The mechanical behaviour of the highly modified mastic having a filler skeleton might reflect that of DBM having an aggregate skeleton.

1.5.2 Research Objectives

Taking into consideration the problem statements, the research objectives in this thesis are concerned with three areas:

1. Small Strain Rheological Analysis

The small strain rheological testing (oscillatory-type) using a dynamic shear rheometer (DSR) enables the complete rheological mastic properties to be determined. Using the DSR, the linear viscoelastic properties of the mastics can be characterised over a wide range of temperature and loading time conditions. Oscillation testing using stress sweeps and frequency sweeps was performed on the base bitumen and bitumen-filler mastics.

2. Steady State Rheological Analysis

As bitumen and bitumen-filler mastics tend to show non-Newtonian behaviour at pavement service temperatures, the viscosity needs to be determined in the form of zero shear viscosity (ZSV), which is independent of shear rate and testing condition (steady state). Within this linear region, the ZSV reflects dissipated motions in a negligibly perturbed, equilibrium "no-flow" structure (Phillips and Robertus, 1995). The use of the concept of ZSV has therefore been suggested as a more appropriate rutting parameter (Phillips and Robertus, 1996; Sybilsky, 1996a).

This research objective looks at the suitability of different laboratory testing techniques at measuring zero shear viscosity (ZSV) of bitumen-filler mastics and the relative effect of filler type and concentration on the measured ZSV. Various techniques were used to measure ZSV, including small amplitude, low frequency oscillations, low stress creep tests and low shear strain rate viscometry measurements.

3. Fatigue Characterisation (large strain)

Attempts have been made to include a binder parameter in asphalt mixture fatigue prediction with the Superpave fatigue criterion, G*sinδ, being the most recent. However, these parameters determined in the linear viscoelastic region at low strain levels have generally failed to establish a comprehensive correlation with asphalt mixture fatigue performance (Bahia et al., 2002). Bahia et al. (1999) claimed that strains within binder films could be as high as 10 to 100 times of the bulk strains of asphalt mixture. Since binders exist as thin films, they can be performing in the non-linear region due to the considerable difference between the modulus of mineral aggregates and the modulus of binders.

Since the introduction of the DSR, direct testing of bituminous binders in fatigue has become relatively common with a number of research groups having successfully generated fatigue characteristics for both pure and modified bitumens by means of time sweep tests using the DSR. In this study, oscillation tests using time sweeps were performed using large strains and stresses to investigate fatigue characteristics of bitumen and mastics. To establish a picture of the factors affecting pavement fatigue at every stage from bitumen to mixture, comparisons of fatigue characteristics of bitumen, mastics and mixtures were discussed.

1.6 Thesis Structure

Chapter 1 provides a background of bitumens and asphalt mixtures that are used for asphalt paving construction. The mechanical properties of stiffness, permanent deformation and fatigue cracking are described. This is then followed by the introduction of empirical and fundamental testing for bituminous binders. This chapter also includes the research methodology and thesis structure.

Chapter 2 provides an introduction of bitumen constitution and structure, mineral filler properties in terms of physical and chemical aspects, bitumen-filler systems and the role of mineral filler in asphalt mixtures. This is then followed by the review of recent research into dynamic mechanical analysis of bitumens by means of dynamic shear

rheometry, permanent deformation testing of bitumens and fatigue testing of bitumens. This chapter also concludes with the review of bitumen viscosity under steady state conditions and fatigue analysis using phenomenal and dissipated energy approaches.

Chapter 3 describes the physical properties of the base bitumen and mineral fillers as well as the filler concentrations by mass and volume in bitumen-filler systems. The strain and stress linear viscoelastic (LVE) limits of the bitumen and mastics are established by performing stress sweeps using a DSR. The rheological testing is carried out over a wide range of temperature and frequency conditions using small strains. The dynamic mechanical analysis of bitumen-filler mastics are also presented in this chapter.

Chapter 4 presents the viscosity measurements of the bitumen and bitumen-filler mastics obtained using the oscillation, viscometry and creep techniques. The extrapolation of ZSV using mathematical models and the filler stiffening effect on ZSV are presented in this chapter.

Chapter 5 presents the fatigue characteristics of bitumen and bitumen-filler mastics by performing time sweeps in the linear and non-linear regions (large strains and stresses) using a DSR. The comparison of fatigue behaviour of pure bitumen, mastics and asphalt mixtures are included in this chapter.

Chapter 6 summarises conclusions from this research and presents recommendations for future work.

2

Literature Review

2.1 General

Asphalt mixtures consist of three components of aggregate, bituminous binder and air. The bituminous binder occurs not as bitumen alone, but is mixed with mineral filler forming the mastic. The combination of the bitumen and mineral filler, called bitumen-filler mastic in an asphalt mixture, has a significant influence on the performance of asphalt paving mixtures. The mastic influences the lubrication between large aggregate particles and thus affects workability (Anderson, 1987). The bitumen-filler mastic must have enough stiffness to prevent the drain-down of the mastic due to gravitational forces during storage and handling, particularly in gap- or open-graded mixtures. Additionally, the mechanical properties of bitumen-filler mastic need to be assessed by the use of various binder modification techniques such as dynamic shear rheometer (DSR).

This chapter is a review of considerable work which has been conducted to measure empirical and fundamental properties of bitumen, mineral filler and bitumen-filler mastics. The dynamic mechanical analysis and mechanical properties of bituminous binders are also included in this chapter.

2.2 Bitumen-Filler System

2.2.1 Bitumen

2.2.1.1 Bitumen Constitution

Bitumen is a fractional residue distillated from crude oil and is composed of a mixture of organic molecules that vary widely in composition from non-polar saturated hydrocarbons to highly polar and highly condensed aromatic ring systems (Petersen, 1984). Predominant hydrocarbons with appreciable amounts of compounds containing

oxygen, sulfur, and nitrogen as well as minor amounts of metals such as vanadium, nickel, iron, magnesium, calcium and other elements exist in a bitumen constitution (Romberg et al., 1959). Because the types of compounds and their molecular weights cover wide ranges, it is difficult to specify the precise composition from tests on the entire bitumen. Read and Whiteoak (2003) summarised that most bitumens distillated from a variety of crude oil contain:

- carbon 82-88%
- hydrogen 8-11%
- sulphur 0-6%
- oxygen 0-1.5%
- nitrogen 0-1%

The exact chemical composition of a bitumen varies in accordance with the original crude oil, bitumen manufacturing processes (semi or full blowing procedure) and bitumen modification.

In addition to the elemental analysis of bitumen, the SARA analysis (Saturates, Aromatics, Resins, and Asphaltenes, SARA) is used to define the bitumen constitution. Generally, bitumen constitution can be separated into four component groups and the metallic constituents. Saturates are non-polar viscous oils which are straw or white in colour; aromatics are dark brown and non-polar viscous liquids with high dissolving ability; Resins (polar) are dispersing agents for asphaltenens; asphaltenes (polar) are generally considered to be highly polar and complex aromatic materials of fairly high molecular weight. Asphaltenes dispersed in maltenes (saturates, aromatics and resins) are the principle viscosity enhancing components in bitumens.

The rheological properties of pure bitumens strongly depend on the chemical compositions of bitumens, particularly on the asphaltene content (Read and Whiteoak, 2003). Mack (1932) conducted viscosity tests using Pocchetino's falling cylinder apparatus on a blown Mexican bitumen with different asphaltene contents (0% to 20%) at five test temperatures ranging between 0^{o}C and 120^{o}C. The apparatus consisted of two

vertical coaxial cylinders and the bitumen was poured between the cylinders to a certain height. They found a considerable influence of asphaltene content on bitumen viscosity. The bitumen viscosity increased as the asphaltene content increased. Much work has shown in the literatures reporting that the bitumen rheological properties such as penetration, softening point and viscosity were influenced by bitumen constitution (Saal and Labout, 1940; Traxler, 1936a, 1936b and 1938; Traxler and Coombs, 1936; Traxler and Romberg, 1952).

2.2.1.2 Bitumen Structure

Bitumen is traditionally regarded as a colloidal dispersion of compounds of high molecular weight of varying composition in oils also of diversified constitution. Although the chemical composition is extremely complex, bitumen structure can be broadly separated into the several groups as considering bitumen as belonging to the realm of colloid-chemistry. Much work has been published in the literature suggesting that bitumen is a colloidal system, consisting of asphaltene micelles dispersed in a lower molecular weight medium (maltene) (Gidler, 1965; Little and Petersen, 2005; Traxler, 1936a and 1936b; Traxler and Coombs, 1936 and 1938; Traxler and Romberg, 1952). Mack (1932) proposed that the three main constituents of bitumens are oily constituents, asphaltic resins and asphaltenes. He considered the asphaltene as the dispersed phase and the mixture of asphaltic resins and oily constituents as the dispersion medium. The three main constituents are described as follows:

- Oily Constituents: These compounds appear as a viscous oil similar to cylinder oil and are usually fluorescent. They are hydrocarbons, and generally contain small percentages of sulfur and oxygen.
- Asphaltic Resins: The asphaltic resins represent the intermediate products formed in the transformation of oily constituents into asphaltenes by oxidation with air. The resins contain oxygen and are oxidation products of the oily constituents.
- Asphaltenes: Asphaltenes are formed from asphaltic resins by further action of sulfur or oxygen. They appear as a dark brown to black powder. On heating they do not melt and soften but decompose, swell and finally sinter together.

Pfeiffer and Saal (1940) proposed that the asphaltene fraction distinguishes from the soluble or maltene fraction consisting of heavy, purely viscous oil. The asphaltene consists of high molecular hydrocarbons of a predominantly aromatic character, with a comparatively low hydrogen content. Most asphaltenes have a marked tendency to adsorb aromatic hydrocarbons of lower molecular weight. In the bitumens the asphaltenes are the centres of micelles which are formed by adsorption, and partly by absorption, of part of the maltenes on the surfaces or in the interiors of the asphaltene particles. This part of the maltenes consisting chiefly of hydrocarbons of an aromatic is called resins, and the other part of maltenes is often referred to as oily constituents.

According to Pfeiffer and Saal's conception, the structure of such a micelle is such that the bulk of the substances with high molecular weight and with aromatic nature are arranged most closely to the nucleus. These are surrounded by oily constituents until a gradual and nearly continuous transition to the intermicellar phase is formed, as shown in Figure 2.1. It is noted that there is no sharp and rigid distinction between the resins and the oily constituents. When the entire system contains sufficient constituents for the formation of the outer regions of the micelles, the asphaltene are fully peptised and able to move through the bitumen. Such a system will show almost purely viscous flow. It is known as a sol type structure.

If there is a shortage of asphaltic resins, part of the forces causing the formation of the micelle are not compensated by adsorption of asphaltic resins, and the micelles will be subjected to mutual attraction. The micelles will form a kind of bond in places where they accidentally approach so closely, as shown in Figure 2.2. It also can be interpreted that when the concentration and the size of the molecular agglomerates (asphaltene) increases to where they begin to interact with one another, larger agglomerated networks are formed. It is known as a gel type structure, as shown in Figure 2.3. In practice, most bitumens are of intermediate character between sol and gel types.

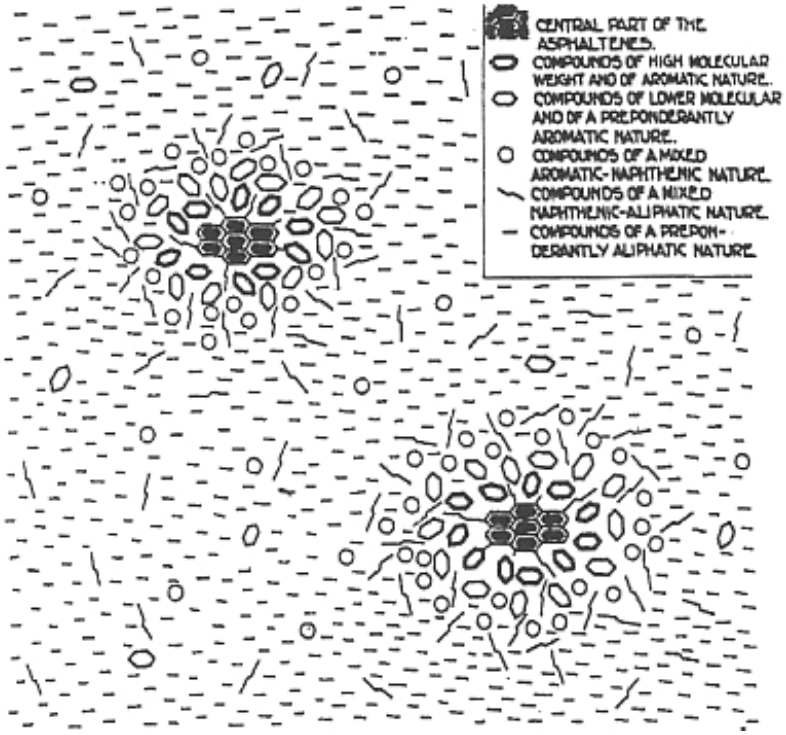

Figure 2.1: Schematic representation of peptised asphaltene micelles (Pfeiffer and Saal, 1940)

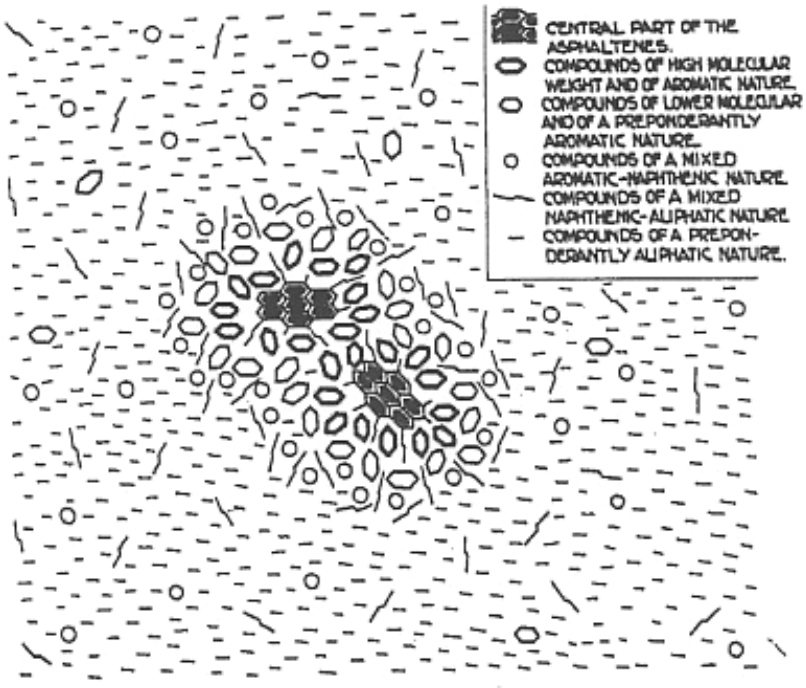

Figure 2.2: Schematic representation of flocculated asphaltene micelles (Pfeiffer and Saal, 1940)

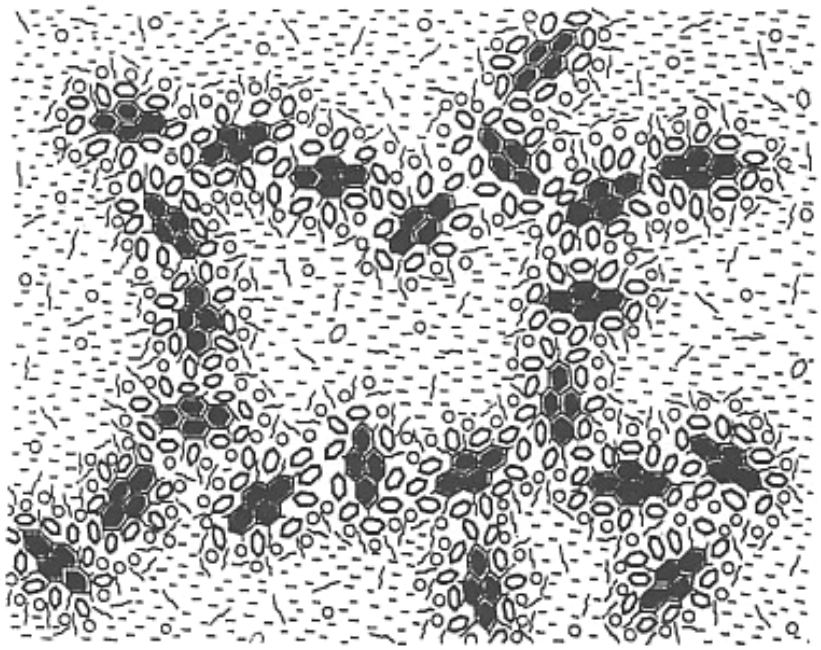

Figure 2.3: Schematic representation of a GEL type bitumen (Pfeiffer and Saal, 1940)

2.2.2 Mineral Filler

The term mineral filler refers to the fraction of the mineral aggregate, which mostly passes the 75μm sieve. Many different materials such as limestone dust, volcanic ash, silt, powdered shale, portland cement, mineral sludge, hydrated lime, rock flour, diatomaceous earth and fly ash, referred to as filler types, can be described in this way (Tunnicliff, 1962). Usually asphalt mixtures have been designed to include mineral filler. Different filler types may be used interchangeably, and different quantities of one type may satisfy a single mixture design situation. The filler is important because of the surface area involved, and that properties of an asphalt pavement may be improved by the use of filler include strength, plasticity, amount of voids, resistance to water action and resistance to weathering (Tunnicliff, 1962). Traxler and Miller (1936) classified filler characteristics as follows:

- Primary characteristics of fundamental importance: particle size, size distribution, and shape.
- Primary mineralogical characteristics of less importance: texture, hardness, strength, specific gravity and wettability.

- Secondary characteristics dependent on one or more primary characteristics: void content, average void diameter and surface area.

Kavussi and Hicks (1997) mentioned that in the early times, the evaluation of mineral filler in asphalt mixtures, relied on routine laboratory tests, most from soil mechanics. These tests involved liquid limit, plasticity index, cementation (to test coagulation or cohesion properties), shrinkage test, and water-bitumen preferential test (to reject hydrophilic fillers). As researchers became more experienced with mineral fillers, tests such as particle density, shape, surface texture, size distribution, surface area, air permeability, bulk density, fractional voids in dry compacted filler, pore diameter and permeability of packed filler to water were recogonised to be the importance to evaluate filler. In order to provide satisfactory engineering properties to an asphalt mixture, a filler should not possess high porous particles and at the same time, having a hydrophobic surface, with high affinity to bitumen. Under these conditions, it might absorb the lighter oily fractions of the bitumen present in the mixture, tending to stiffen it. Additionally, it should not have an adverse chemical reaction with bitumen, and not possess hydrophilic surface in order to ensure good adhesion between binder and aggregates. The generally physical properties and testing of the mineral filler are summarised as follows:

Particle Size Distribution (BS 812-103.1:1985)

The particle size distribution of fillers can be determined by sieving. The grading curve is a graphical representation of the particle size, and is therefore useful in itself as a means of describing the material.

Voids of Dry Compacted Filler (BS EN 1097-4:1999)

The voids of dry compacted filler can be determined by means of Rigden apparatus, as shown in Figure 2.4. It is used for example to determine their bitumen carrying capacity. The percentage air voids are the volume of air filled space in the filler, expressed as a percentage of the total volume of the filler after compaction by a standard method. The volume of the compacted filler is determined using the height of the compacted filler

bed. Using the known particle density of the compacted filler, the air void content of the compacted filler is calculated.

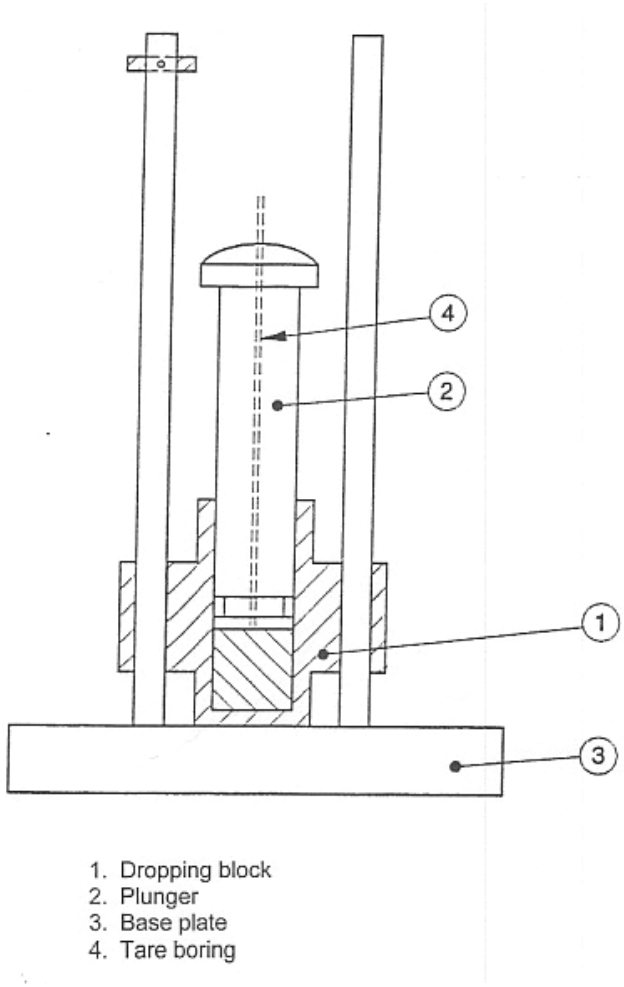

Figure 2.4: Compaction apparatus for dry filler (BS 1097-4, 1999)

Particle Density of Filler (BS EN 1097-7:1999)

The particle density of filler can be determined by means of a pyknometer. The pyknometer method is a well known method for determining the volume of irregularly formed samples. When the mass of the sample is known, the density can be calculated. The principle is based on the replacement of a certain amount of liquid of known density with the test portion. A pyknometer with know volume, containing the test portion, is topped up with the liquid. The volume of the liquid is calculated by dividing the mass of

the liquid added by the liquid density. The volume of the test portion is calculated by subtraction of this volume from the pkynometer volume.

Specific Surface Area (BS 4359-1:1996)

The surface area is the external surface of a solid plus the internal surface of its accessible macro-and mesopores. The specific surface area of filler can be determined by the measurements of the amount of physically adsorbed gas according to the method of Brunauer, Emmett and Teller (BET method). The method specified involves the determination of the amount of adsorptive (measuring gas to be adsorbed) gas required to cover the external and the accessible internal pore surfaces of a solid with a complete monolayer capacity can be calculated from the adsorption isotherm using the BET equation. Any gas may be used, provided it is physically adsorbed by weak bonds at the surface of the solid (van der Waals forces), and can be desorbed by a decrease in pressure at the same temperature.

Traxler et al. (1933) proposed that a mineral filler depended chiefly on its physical properties, of which the void content was one of the most important to influence the properties of fabricated products such as bituminous binders. The filler particle size, shape and texture considerably influence voids of dry compaction. They conducted dry compaction tests for eight types of fillers including limestone, silica, marble, trap rock, argillaceous silica, black slate, soapstone and Tripoli. Dry filler was compacted by hand tapping in a weighed, graduated glass cylinder. The weight and volume of the compacted filler were determined and the bulk density in grams per cubic centimeter was calculated. At least 90 percent of each of the fillers passed a U.S. Standard No. 200 screen (74μm). Each type of filler was separated into five or six fractions. The particle diameters of the various fractions were as follows: <2, 2 to 5, 5 to 10, 10 to 20, 20 to 40 and 40 to 75 micron. They found that the results for limestone, silica, marble, and black slate indicated that particle size had no significant effect on the void content, but those for trap rock and soapstone did not agree with this generalisation. They also concluded that since the fractions of about the same size distribution were compared, the differences in void content of trap rock and soapstone fillers might be attributed to differences in particle shape and texture.

Rigden (1947) indicated that the voids of dry compaction were of major importance for the behaviour of fillers. The volumetric proportion of filler including these voids was a main parameter for the rheological properties of bitumen-filler system. He developed a method for determination of the voids in dry compacted fillers. The apparatus consists of a cylindrical container and a ram of specified dimensions and weight. The compaction of the filler is obtained by repeated dropping of the whole apparatus over a specified height. The bulk density or voids of filler can be calculated since the bulk volume of a known weight of filler is measured. However, some fillers require extra care because the fragile granules might be crashed.

Warden et al. (1959) also developed a kerosene adsorption test for determining the void-forming properties of dry filler powders. Kerosene was gradually added to dry filler, shaken in a dish, till a ball was formed which just had taken up all the filler granules. The compaction effort was delivered by the surface tension of kerosene. Heukelom (1965) found the relationship of the voids volume measurements between Rigden voids, V_{fR}, and voids volume of the kerosene, V_{fK}, was given by:

$$V_{fK} = 0.97V_{fR} \tag{2.1}$$

Table 2.1 shows Rigden voids of some types of mineral filler from Harris and Stuart's (1995) work. They found the Rigden voids can be used to distinguish between bad and good performing fillers for stone matrix asphalt (SMA). The bad and good performance was based on field experience during the SMA pavement construction in three European countries. They also concluded that a filler with high Rigden voids (greater than 39%) would result in a very stiff SMA mix that was difficult to lay-down and cause cracking. A filler with low Rigden voids (less than 34%) would not stiffen the SMA mix enough and thereby cause bitumen drain-down after lay-down. Table 2.1 shows the ranges of the Rigden voids for the mineral fillers are basically between 30% and 40%.

Table 2.1: Rigden voids of mineral fillers used in SMA (Shashidhar et al., 1998)

Designation	Performance	Type	Rigden Voids (%voids)	Specific Gravity
SWE1	bad	Crushed Ignitious	40.4	2.82
SWE2	good	Granite	36.5	2.84
SWE3	good	Granite	38.2	2.74
SWE4	good	Granite	38.0	2.72
SWE5	good	Granite	37.3	2.91
SWE6	bad	Granite	40.0	2.84
SWE7	bad	Limestone	33.1	2.74
GER1	good	Pure limestone	35.2	2.74
GBER2	good	Dolomitic limestone	34.8	2.87
GER3	good	Very pure limestone	34.5	2.74
GER4	bad	Granite	45.7	2.76
GER5	good	Very pure limestone	37.3	2.75
GER6	bad	Impure limestone	42.5	2.81
GER7	bad	Fly-ash	69.2	3.18
GER8	good	Limestone	32.1	2.75
GER9	good	Limestone	38.2	2.74
CHE1	good	Sandstone	38.5	2.76
CHE2	bad	Limestone	32.8	2.76

2.2.3 The Role of Mineral Filler in Bitumen-Filler Mastic

The following two sections look at the influences of physical and chemical mechanisms on bitumen-filler mastic.

2.2.3.1 Physical Mechanism

Chen and Peng (1998) investigated the effect of mineral fillers on tensile strength of bitumen-filler mastics. The direct tensile failure strength tests using a direct tension device was carried out on bitumen-filler mastics at three temperature levels of 10^{o}C, -15^{o}C and -20^{o}C. A AC-20 bitumen was used to mix with two graded silica fillers. The silica filler was considered to be a chemically stable material, and bituminous binders were shown to have little reaction with silica. Two types of particles containing different size distributions were graded and used in this study. One type of size distribution was 100% passing 5μm (surface area = 6.57 m^2/g, bulk density = 0.834 g/cm^3 and specific gravity = 2.464), and the other was 100% passing 75μm (surface area = 0.71 m^2/g, bulk density = 1.163 g/cm^3 and specific gravity = 2.464). Five free bitumen (described in section 2.2.5) contents of 30%, 40%, 50%, 60% and 80% by volume were tested in this study. At a 30% ratio the mineral filler was floating in the binder and particle-particle

contact between mineral fillers no longer existed. The free bitumen content at 30% was a typical minimum design value for mineral fillers used in an asphalt mixture. In the direct tensile test, the sample was shaped like a dog bone with 100 mm in overall length, including the end insert. The bitumen portion of the specimen was 40 mm long with a gauge length of 18 mm and cross-sectional dimensions of 6 mm wide by 6 mm thick. The sample was tested at an elongation rate controlled at 1 mm/min. The failure typically occurred in the midpoint of samples.

They found a considerable effect of particle size on tensile strength of bitumen-filler mastics containing silica fillers. The 5μm bitumen-filler mastic (size distribution was 100% passing 5μm) exhibited higher tensile strength than the 75μm bitumen-filler mastic (size distribution was 100% passing 75μm). At a given filler concentration, smaller particles with higher surface areas carried more tensile loads than bigger ones. Additionally, the larger the particles were, however, the larger the stress concentration area. If the distance between particles was smaller than the stress concentration area, there would be an overlap area between particles, whereas the strength of the particulate-filled composite was deteriorated. Figure 2.5 shows the phenomenon. They also concluded that the particle distance with a higher packing density (high bulk density) was smaller. The stress concentration was maximum where the particle spacing distance was thin. It was around these regions that the bitumen-filler system might start to fail. In addition, the smaller particles had larger surface areas than larger particles at the same filler concentration, and thus exhibited the higher tensile strength.

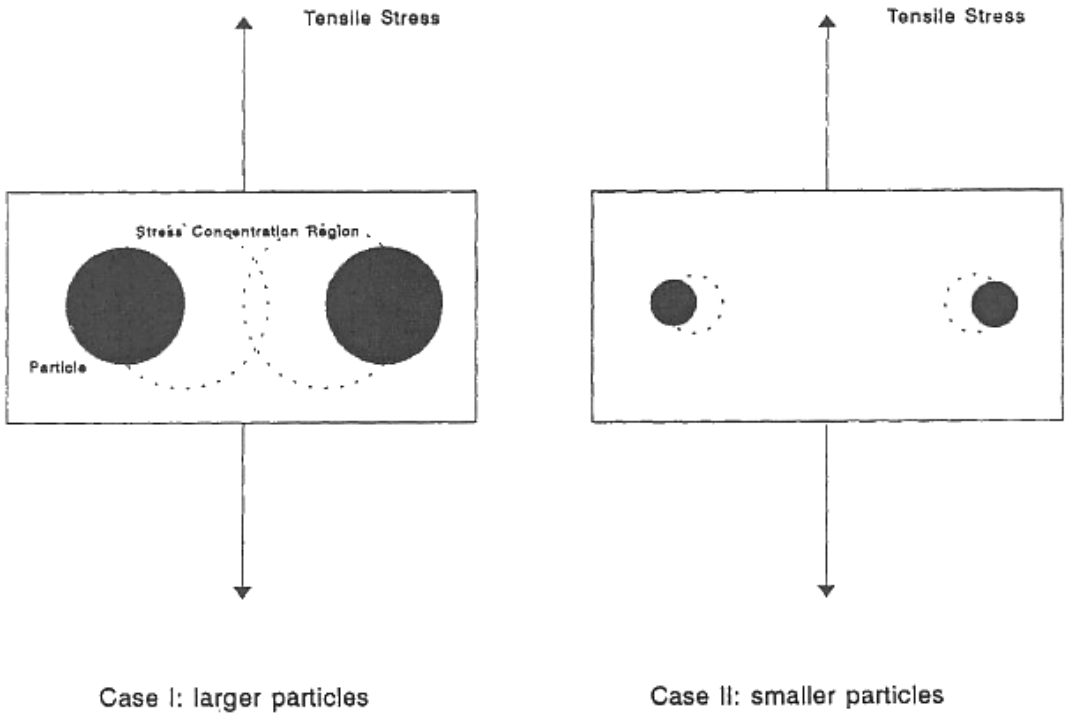

Figure 2.5: Stress concentration due to particle size (Chen and Peng, 1998)

Kavussi and Hicks (1997) evaluated that the effects of filler grading and shape on the physical and rheological properties of bitumen-filler mastics. A Persian Gulf 100 penetration grade bitumen and four types of mineral fillers (limestone, quartz, fly ash and kaolin) were tested. In this investigation, quartz had large and angular particles, limestone had angular particles but they were rather smaller than quartz, fly ash had spherical particles but they were smaller than limestone, and kaolin had the finest particles. Bitumen-filler mastics containing different filler contents, from suspended filler in bitumen (filler/bitumen ratio by weight = 0.26) to very high filler contents (filler/bitumen ratio by weight = 7.2). Empirical tests such as penetration, softening point, Fraass breaking point and viscosity (using rotational viscometer) tests were performed on these bitumen-filler mastics. They found a filler with fine and spherical characteristics had less effect on penetration and softening point than a filler with large and angular particle. The kaolin particles were rather fine and became more incorporated with the bitumen, resulting in stiffer mastics. For Fraass breaking point test, the kaolin particles had a slight improvement in brittle behaviour of the binder by reduction of the Fraass point at low filler concentrations compared to other filler particles. This might be

because of high incorporation of a fine filler into the binder imparting a certain degree of flexibility. Fly ash which was a porous filler was more susceptible to brittleness, and thus had the highest Fraass breaking point. Additionally, the viscosity test was performed at a shear rate of 0.04 1/s and a temperature of 60^{o}C. Again, the kaolin and fly ash had higher viscosities due to their fineness characteristic and spherical particle shapes. The pattern for viscosities exhibited a trend from less to most stiff for quartz, limestone, fly ash and kaolin. They concluded that the particle size and shape had pronounced effects on physical properties of bitumen-filler mastics.

Soenen and Teugels (1999) examined possible bitumen filler interaction by means of dynamic shear rheology. Mastics were prepared using four penetration grade bitumens (penetration: 192, 214, 180 and 205) from different sources and three mineral fillers (quartz, rhyolite and tuff rhyolite) having similar physical properties of bulk density and specific surface. The filler concentrations of bitumen-filler mastics were 30%, 45% and 55% by volume. The frequency sweep tests using stress controlled loading were carried out at every 5^{o}C, covering a mastic modulus range from 100 Pa to 10^{8} Pa within the linear viscoelastic region. The stiffening ratios of complex modulus (G*mastic/G*bitumen) were presented. The results showed that the effect of a possible chemical interaction between bitumen and filler on the linear viscoelastic behaviour of the mastics was very low. The stiffening ratios for the bitumen-filler mastics were not exactly the same as testing at the same filler concentration (30%) due to filler packing effect. At high filler concentration (55%), the filler skeleton gradually started to influence the shear modulus. The effect of the filler skeleton gradually became visible in the rheological measurements as temperature increases, or frequency decreased, as shown in Figure 2.6. The modulus of the bitumen dropped below the stiffness developed due to the filler skeleton. They concluded that the relative stiffening effect was only dependent on the filler volume concentration, but independent on the type of filler as well as on the origin of the bitumen.

As a consequence, the particle size distribution, particle shape, void of dry compaction (Rigden void), specific surface area and specific gravity as well as filler concentration strongly influence the physical and mechanical properties of bitumen-filler mastic

(under the same base bitumen condition). In addition to physical mechanisms of mineral filler, the study of bitumen filler interaction (chemical mechanism) should also be considered.

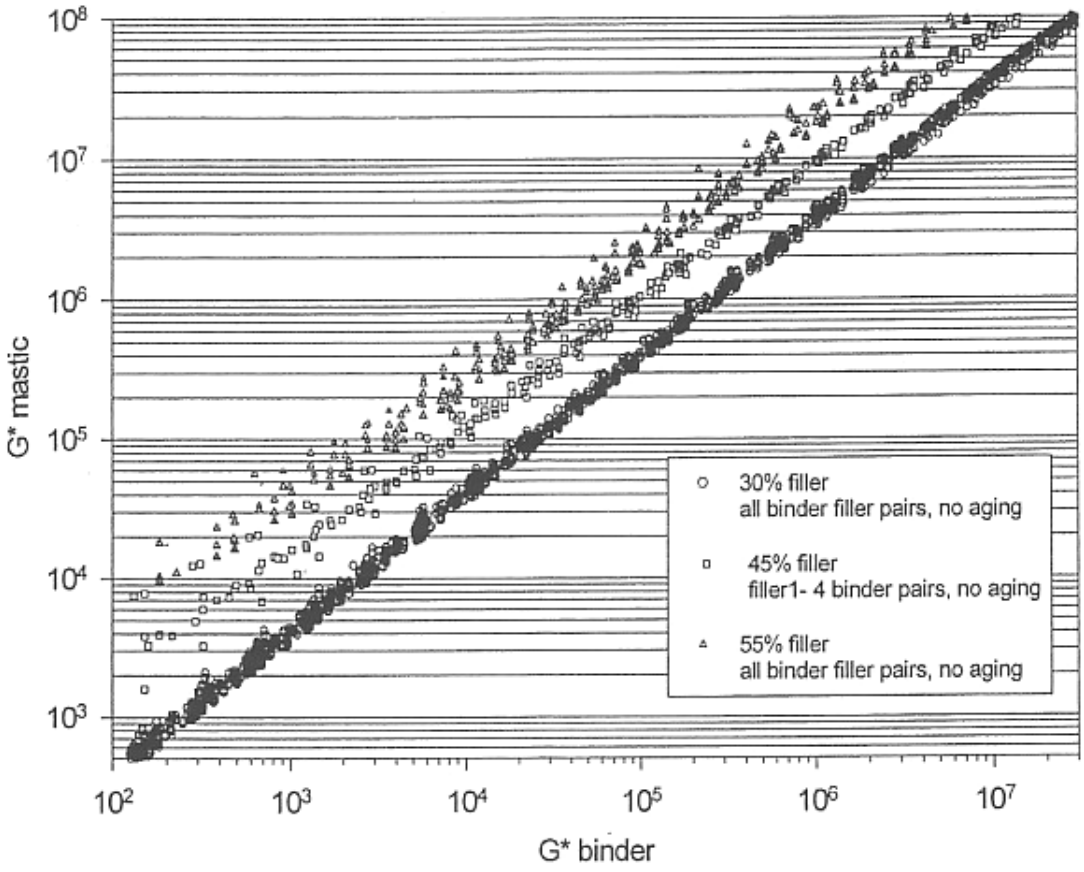

Figure 2.6: The influence of filler concentration on complex modulus values of bitumens and mastics (Soene and Teugels, 1999)

2.2.3.2 Chemical Mechanism

In addition to physical mechanism, the chemical mechanism of "active" mineral filler should be considered due to the bitumen and filler compositions. Because of chemical compositions, filler might sever as an active material such as hydrated lime filler containing calcium hydroxide, the activity being manifested in the properties at the interface between the filler and the bitumen. Little and Petersen (2005) investigated the effect of hydrated lime filler on the rhological properties of bitumen-filler mastics in terms of physical and chemical interactions. They evaluated the rheological data based on the previous work (Petersen et al., 1987). Rheological tests were performed at 60^{o}C

using a mechanical spectrometer. Four types of unaged and aged bitumens with two types of fillers (limestone filler and hydrated lime filler) at one filler content of 20% were tested in the programme. The two types of mineral fillers had similar particle size distributions. The rheological results showed the hydrated lime filler had more considerable impact on the loss tangent (tan δ) (the difference in complex modulus is not significant) of bitumen-filler mastic than the limestone filler, but the impact was bitumen dependent.

Unlike typically inert fillers, hydrated lime filler contains calcium hydroxide, $Ca(OH_2)$, and has a high relative concentration of reactive chemical functionality. It reacts readily with acidic materials such as carboxylic acids to form calcium salts that are virtually insoluble. Carboxylic acids and related chemical functionality such as 2-quinolone types in bitumen react irreversibly with the hydrated lime filler. Because the hydrated lime filler is insoluble in the bitumen, this reaction removes these acidic components from the bitumen phase of the matrix by their adsorption on the surface of the hydrated lime particles (Little and Petersen, 2005).

Little and Petersen (2005) also evaluated the data of two SHRP core bitumens of AAD-1 and AAM-1 which were substantially difference in chemical composition based on the previous works (Lesueur and Little, 1999; Petersen et al., 1987). AAD-1 had high asphaltene and polar chemical functional group content, while AAM-1 had very low asphaltene content and less polar components. The AAD-1 had 60% of the carboxylic acids and more than 90% of the 2-quinolone. They found the AAD-1 adsorbed on the surface of the hydrated lime filler particle and thus increasing loss tangent, while the AAM-1 was relatively deficient in both asphaltene and polar chemical functionality and thus having less impact on the loss tangent.

Lesueur and Little (1999) also explained that the level of interaction between hydrated lime and bitumen was bitumen dependent. This interaction caused hydrated lime to strongly affect high temperature rheology in certain “compatible” bitumens, but it had less of an effect in other bitumens. Hydrated lime adsorbed an interactive molecular

layer from the compatible bitumen that may significantly affect the high temperature rheology to a much higher degree than other inert fillers.

2.2.4 The Role of Mineral Filler in Asphalt Mixtures

Asphalt paving mixtures have been designed to include mineral filler since about 1890 (Tunnicliff, 1967). The filler plays an important role in determining the properties and behaviour of the mixture. The role of mineral filler in the paving mixture can be divided into two parts. The filler serves as an inert material for filling the voids between coarser aggregate in the mixture. On the other hand, the filler serves as an active material, the activity taken place in the properties at the interface between the filler and the bitumen, because of its fineness and surface characteristics.

The workability and practical performance of asphalt mixtures depend largely on the proportion and type of filler used. Generally, the addition of filler results in a decrease in percentage of air voids in asphalt mixtures. The difference in densification is one of the reasons why mixtures containing different quantities of filler possess different mechanical properties. Anderson (1987) indicated the mineral filler may affect asphalt paving materials in a number of ways such as: stiffen and extend the bitumen, alter the moisture resistance, affect the ageing characteristics, and affect the workability and compaction characteristics of the asphalt mixtures. Generally, the effect and role of filler in asphalt mixtures can be discussed in terms of physical and chemical aspects.

2.2.4.1 Physical Aspect

Tunnicliff (1967) proposed that the functions of two asphalt mixture components were distinctly different for load bearing purposes: (1) aggregate resisted deformation because of its internal stability (mechanical effect), (2) bituminous binder, within a mass of filler, resisted shear deformation due to its cohesion (cohesive effect). Failure occurred when the arrangement of particles was disturbed, and the cohesive component shears simultaneously. He also performed triaxial compression tests on a sheet asphalt mixture containing binder (93 penetration grade bitumen and limestone dust mineral filler) with a sand passing the number 10 sieve (2mm) at room temperature of 76^{o}F. The Rigden

voids of limestone filler was 32.2%. A set of asphalt mixture specimens contained binder contents ranging from 25 to 35 percent with filler-bitumen ratios (by mass) ranging from 0.2 to 1.2. Load was applied to the upper bearing block such that vertical deformation of the specimen was 0.1 inches per minute until failure occurred. Failure was the maximum load sustained. The confining pressure of 10 psi was used in order to develop definitive comparisons between internal stability and cohesion.

He found that at high filler concentrations, the influence of filler on mechanical and cohesive effects for the sheet asphalt mixture were significant, indicating stronger pavements at high filler concentrations, resulting from better cohesion as well as better internal stability. At low filler content (filler-bitumen ratio was 0.2), the cohesive effect was greater than the mechanical effect, but the difference was not large. He explained that filler was suspended and contributed to shear resistance due to cohesion. The explanation of the mechanical effect might be that some filler particles acted like aggregate, but this explanation was not consistence with all of the data. Sand voids (volume of air and binder in a compacted specimen) increased as filler-bitumen ratio increased. The decrease in shear resistance might be caused by the increase in sand voids. He concluded that the shear resistance and internal ability of paving mixtures were a function of filler concentration as long as filler particles were suspended in bitumen.

Huschek and Angst (1980) also investigated the effect of filler on mechanical properties of bitumen-filler mastics at high and low service temperatures. Four types of penetration grade bitumens (Penetration were 170, 73, 29 and 70) and four types of mineral filler including limestone, silicious limestone, schist flour and bauxite residue (Rigden voids were 34%, 32%, 38% and 59%) were tested at different bitumen/filler ratios (by weight) from 30/70 to 80/20. In this investigation, the “effective volume concentration” of filler in a bitumen-filler mastic was calculated based on Rigden voids. They performed viscosity tests at 40^{o}C using a squeeze film viscometer on specimens to characterise the behaviour of bitumen-filler mastics at high service temperatures. A mastic specimen was sandwiched between two polished steel plates. Through an axial stress, the plates approached each other. The viscous mastic was squeezed out and thus the viscosity was determined in terms of normal stress, test time and the change in thickness of bitumen

film. They also performed indirect tensile splitting tests at -15^{o}C on specimens to characterise the behaviour of bitumen-filler mastic at low service temperature. Cylindrical samples were loaded between two load-bearing fillets at constant deformation rate. Two deformation rates of 52 and 200 mm/min were chosen. The tensile stresses and strains at failure were recorded. Additionally, the asphalt mixtures (Marshall specimens) containing the identical quantity of bitumen-filler mastic (14% by mass) were tested -15^{o}C by the use of indirect tensile splitting tests in order to compared with bitumen-filler mastics.

They found that opposing tendencies of the strengths using indirect tensile splitting tests as a function of the effective filler volume content for the bitumen-filler mastics and sand-chippings mixtures. The tensile strength of the bitumen-filler mastics increased, but for the mixtures it reached a maximum at the effective filler volume concentration of 60% in mastic. At the high effective filler volume concentration, the decrease in tensile strengths for mixtures was attributed to be insufficiently compacted (workability) and the deficient adhesive force of the bitumen-filler mastics. In addition, they found that the magnitude of the maximum elongation at failure was dependent upon the hardness of bitumen (penetration) as well as the type of filler. High penetration bitumen (170 pen) with finer and flat filler (schist flour) had the maximum value of elongation at failure compared to other mastics. They also found the elongation at failure might not be related to Rigden void. The mastic with bauxite residues (Rigden void = 59%), despite greatly differing void contents yield approximately the same elongation at failure as mastics with limestone filler (Rigdon Void = 34%). They compared the viscosity of bitumen-filler mastic at 40^{o}C with the elongation at failure at -15^{o}C and summarised that harder bitumens generally behaved unfavourably at low temperatures compared to softer bitumens. An increasing filler concentration had a favourable effect on the low temperature behaviour up to a certain effective volume concentration. The optimum effective volume concentration lied in the range 0.4 to 0.6. They also concluded that the Rigden void was important only for the viscosity at high temperatures, but not for the behaviour at cold temperatures.

Anderson (1987) investigated the use of baghouse fines including limestone, granite, traprock and quartz as mineral fillers in asphalt mixtures. Each filler was added to a 73 penetration grade bitumen at three filler/bitumen ratios of 0.2, 0.4 and 0.6 by volume. In this investigation, he used the filler/bitumen ratio as well as the "free bitumen" volume content within the bitumen-filler mastic (described in section 2.2.5) to evaluate the mechanical properties of asphalt mixtures. In addition to bitumen-filler mastics, Marshall compaction was used to compact asphalt mixture specimens that were tested for indirect (diametral tension) resilient modulus and creep tests at 39.2, 77 and 104^{o}F, and diametral tensile strength test at 77^{o}F. The mechanical properties of the mixtures were then compared with the free bitumen volume ratios of the bitumen-filler mastics and with the particle size distribution of the fillers.

The results showed that the resilient modulus and tensile strength increased as an increase in filler/bitumen ratio. A repeatable relationship between percent free bitumen and the mechanical properties of resilient modulus, tensile strength and strain had been demonstrated except for the very fine fillers (quartz) at the larger filler/bitumen ratios. The quartz filler was very fine, predominantly minus 5 micrometers and had high stiffening effect on bitumen-filler mastic. The low resilient modulus, tensile strength of asphalt mixtures containing high quartz filler content might be caused by the worse workability during the mixing procedure. Thus, he suggested that the percent free bitumen in the filler fraction should be maintained at 40 percent or less. Additionally, in terms of the gradation of the filler fraction, anomalous behaviour in asphalt mixtures would be expected as the filler (quartz) was one-size and finer than 10-15 μm, or when the filler (such as coarse cyclone filler in this study) was coarse and lacking material less than 10-20 μm. He recommended that the well-graded fillers tended to behave in a more predictable manner.

2.2.4.2 Chemical Aspect

Mineral filler such as hydrated lime filler can serve as an active filler and show physio-chemical activity in the aggregate-mastic interface. Ishai and Craus (1977) investigated the effect of the filler on aggregate-bitumen adhesion properties in sand asphalt mixtures. Two typical cases involving two useful fillers, limestone (specific surface = 258 m^2/kg

and voids of dry compacted filler = 42.4%) and hydrated lime (specific surface = 750 m^2/kg and voids of dry compacted filler = 54.8%) with a 60/70 penetration grade bitumen and a well-graded quartzite sand (80% SiO_2) were involved in this study. The filler proportions for the hydrated lime were between 0 to 20 percent and for the limestone filler were between 5 to 25 percent by weight of the entire aggregate in the mixture. The sand asphalt mixtures were produced according to the Marshall procedure. The resilient modulus tests were performed using Resilient Modulus device on the sand asphalt mixtures at 25^{o}C using Resilient Modulus device. Before or after testing, the Marshall specimens were conditioned under different environmental conditions of water immersion at 25^{o}C and/or 60^{o}C with or without vacuum saturation. Therefore, the percent retained resilient modulus of the sand asphalt mixtures was compared with the filler content as well as filler type in mixtures. The results showed that the behaviour of silicious sand asphalt mixtures with hydrated lime filler showed, under variable environmental conditions and especially with optimum filler content (10-15%), high adhesion potential compared to that with limestone filler.

Ishai and Craus (1977) explained the physio-chemical activity in the aggregate-mastic interface as shown in Figure 2.7. A substantial modification of the interface phenomenon could be observed as a hydrophilic aggregate (silicious aggregate) which was coated with a hydrated lime-bitumen mastic. If initially the water was present in the interface, a chemical adsorption was developed and the calcium ions replaced the hydrogen ions of the silicic acid. In this process calcium silicate was formed at the active points of the interface. The aggregate surface which was initial acidic became basic from the coating of the calcium ions. These ions had an affinity to the acidic components of the bitumen and the calcium ions which coated the aggregate surface. The excess hydrated lime solution in the interface was incorporated into the mastic, forming an inverse asphaltic emulsion. However, it should be noted that the contribution of the hydrated lime to adhesion was valid in the presence of water. In dry conditions, the hydrated lime might serve as an inert filler in the mastic without any physio-chemical activity.

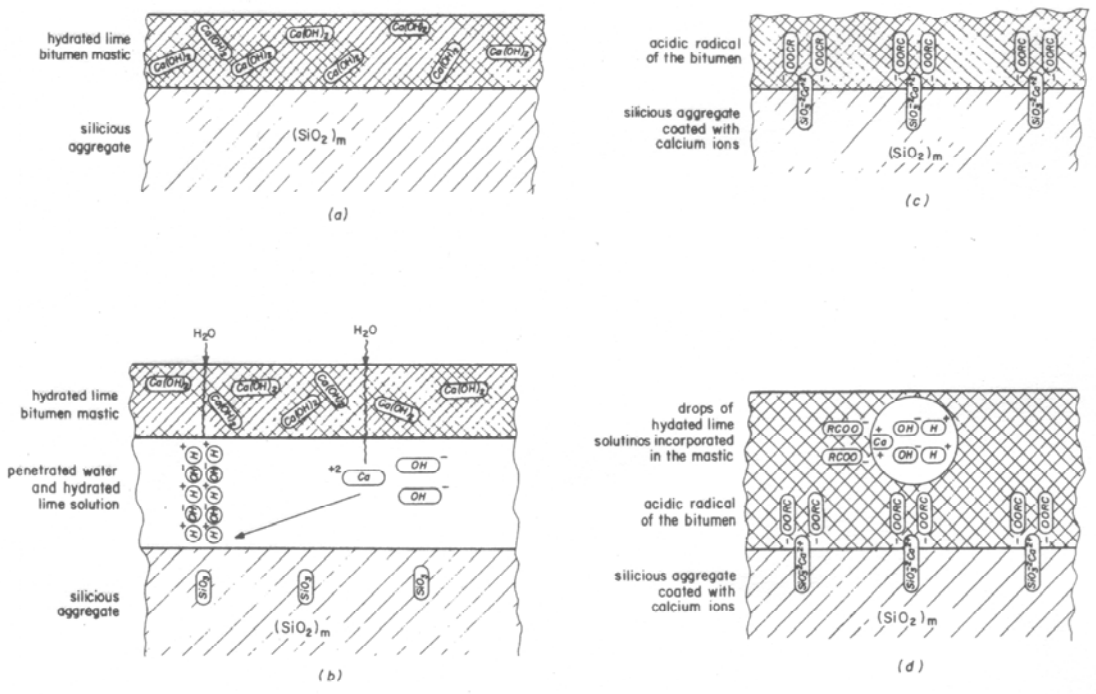

Figure 2.7: Schematic description of the adhesion mechanism in the interface between hydrated lime mastic and silicious aggregate (Ishai and Craus, 1977)

2.2.5 Packing Fraction of Filler in Bitumen-Filler System

Tunnicliff (1967) described that packing referred to the degree of dispersion of filler particles in bitumen-filler system. It was related to concentration, since filler particles were widely dispersed at low concentrations, and they were tightly packed at high concentrations. Packing and concentration were not the same because concentration was concerned only with the volume occupied by particles, whereas packing involved space between particles.

Anderson (1987) explained the voids in a compacted bed of dust (filler), as illustrated in Figure 2.8. As bitumen was added to the dust (filler), the bitumen first filled the voids. Any bitumen within these voids was called fixed asphalt (bitumen) since it was fixed within the minimum void structure. Bitumen in excess of the fixed bitumen was called free bitumen because it was free of the voids and was free to lubricate the filler particles.

This free bitumen pushed the particles apart, lubricating the bitumen-filler mastic and thereby enhancing its fluidity.

Heukelom (1965) demonstrated that the functional volume percentages of solid and fluid phases differed from the compositional volume percentages of filler granules and asphaltic bitumen, as shown in Figure 2.9.

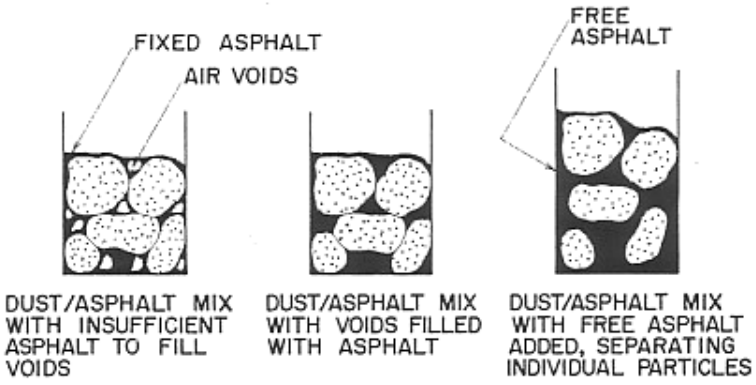

Figure 2.8: Fixed and free bitumen (Anderson, 1987)

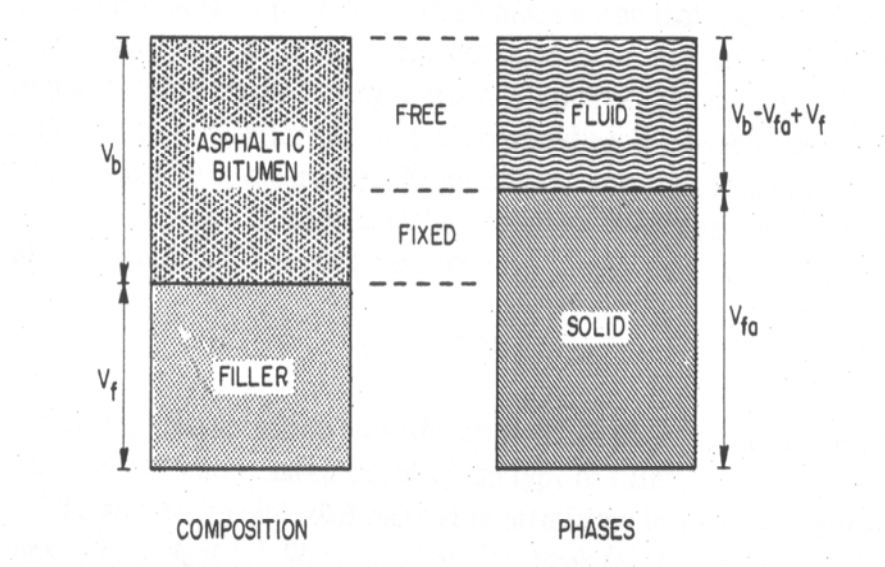

Figure 2.9: Basic concept of fractional voids (Heukelom, 1965)

The Rigden test can determine the air voids in dry compacted filler, V_{fR}. In a bitumen-filler system with a filler content, V_f, of granules, the volume percentage of solid phase equals the effective bulk volume percentage of filler, V_{fa} (solid phase), which is given by:

$$V_{fa} = \frac{100}{V_{fR}} V_f \tag{2.2}$$

At this filler concentration a proportion, V_{fa}-V_f, of bitumen is fixed. As the mastic with a bitumen content, V_b, of bitumen, the remaining volume percentage of free bitumen (fluid phase) equals:

$$V_b - V_{fa} + V_f = V_b - \left(\frac{100}{V_{fR}} - 1 \right) V_f \tag{2.3}$$

Therefore, the functional volume percentages can be calculated from the percentages of bitumen and filler, as the type of filler is represented by the value of V_{fR}.

2.2.6 Stiffening Effect of Fillers Using Rheology-Based Models

The stiffening effect of fillers at different filler concentration levels in mastic has been studied extensively using rheological models which take into account variance of rheological properties due to particle size, particle dispersion and particle aggregation. Shashidhar et al. (1999) selected the Nielsen modified Kerner's equation to understand the nature of bitumen-filler system. The equation relates the increase in any modulus with the addition of fillers, and also takes account into such factors as generalized Einstein coefficient, K_E, maximum packing fraction of the filler, Φ_m, and Poisson's ratio of the matrix as given below:

$$M/M_1 = (1+AB\Phi_2)/(1-B\Psi\Phi_2) \quad (2.4)$$

$$\Psi = 1+[(1-\Phi_m)/\Phi_m]\Phi_2 \quad (2.5)$$

Where

M = modulus of mastic

M_1 = modulus of bitumen

$A = K_E-1$

B = constant

Φ_2 = filler volume fraction

The filler volume fraction, Φ_2, is defined as a volume of filler is added to a volume of bitumen. The maximum amount of filler that can be added to the bitumen without any air voids is defined as the maximum volume fraction of the fillers, Φ_m. When a mastic has $\Phi_m = \Phi_2$, the particles are all touching one another with bitumen occupying all the void spaces.

The rheology-based model was fitted to bitumen-mastic data of different filler volume contents through calibrating the two parameters of K_E and Φ_m. Shashidhar et al. (1999) also reported the two parameters can be estimated from the dynamic complex modulus (G*) data for any given bitumen-filler mastic system. A knowledge of the variation of K_E and Φ_m for different mastic systems as a function of properties of interest may lead to the selection of appropriate fillers to improve such properties. Figure 2.10 shows the effect of changing Φ_m when keeping K_E constant. The Φ_m acts as a vertical asymptote to the stiffness curve. Figure 2.11 shows the variation of stiffness curve with K_E at constant Φ_m. As K_E increases, the slope of the curve at an given filler volume fraction increases. K_E is an indicator of the rate of increase of stiffness with addition of filler particles. Therefore, they concluded that the stiffening of bitumen as fillers are added can be

quantified by K_E and Φ_m. The fillers studied had Φ_m ranging from 0.28 to 0.45 and K_E between 2.5 and 4.5. Kim and Little (2004) investigated the rheology-based models in characterizing the dynamic mechanical behaviour of bitumen-filler mastics. They summarised the rheology-based models could capture the stiffening effect of limestone fillers up to a volume fraction of 25%.

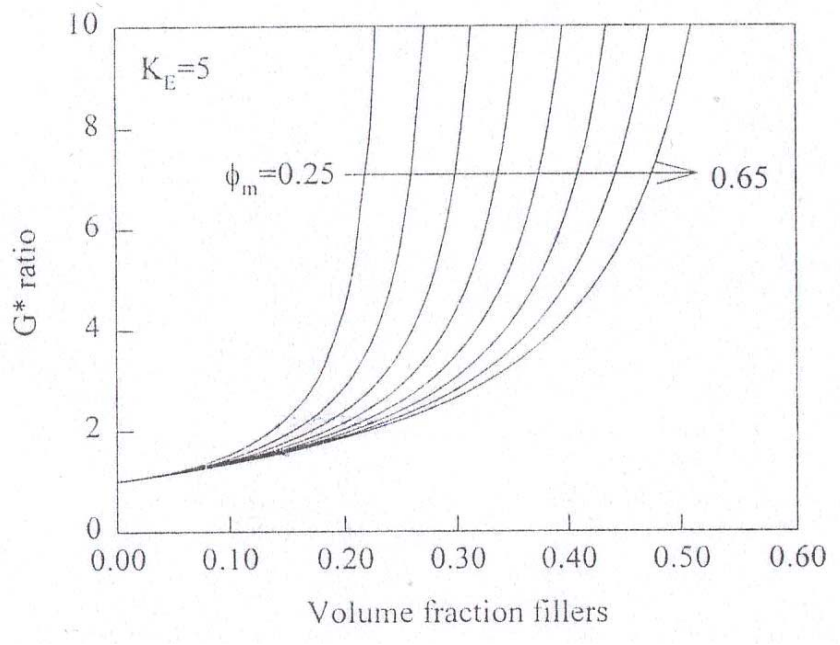

Figure 2.10: The effect of changing Φ_m (Shashidhar et al., 1999)

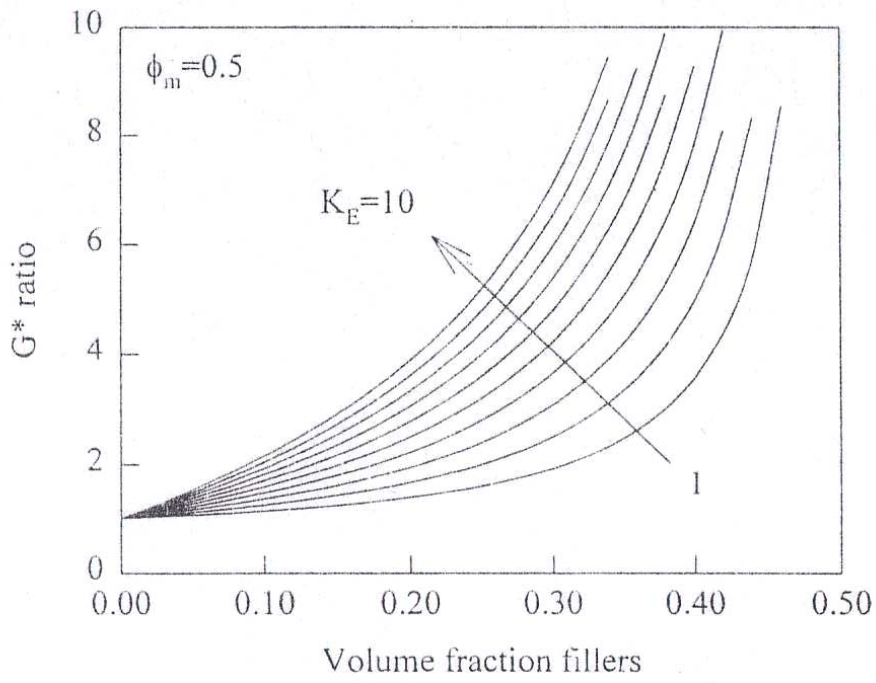

Figure 2.11: The effect of changing K_E (Shashidhar et al., 1999)

2.3 Dynamic Oscillatory Testing Using a DSR

2.3.1 Introduction of Dynamic Shear Rheometer (DSR)

DSR is the acronym for Dynamic Shear Rheometer and is used to measure the dynamic shear modulus and phase angle of bituminous binders at intermediate and high pavement temperatures. In the DSR dynamic oscillatory testing, the shear stresses and shear strains vary with time from positive to negative in a sinusoidal fashion. The DSR provides stress-strain moduli at different rate of loading expressed in terms of frequency at different test temperatures (Anderson et al., 1994). The DSR equipment used in bituminous binders characterisation can be divided into two categories : (1) controlled stress, when the rheometer applies a stress to the specimen and measures the resulting strain, and (2) controlled strain, when the rheometer applies a strain to the specimen and measures the resulting stress.

A 1-mm by 25-mm or 2-mm by 8-mm, hockey puck-shaped, sample of bituminous binder squeezed between two parallel metal plates is placed in a temperature controlled

chamber, as shown in Figure 2.12. The chamber for controlling the test specimen temperature by heating or cooling maintains a constant specimen environment. The medium in the environment chamber can be liquid or gas. Due to the extreme temperature dependency of bituminous binders, it is necessary to control the temperature for the rheological testing of bituminous binders to a much finer degree than for most other viscoelastic materials. A change in temperature of 1°C can result in a modulus change of up to 25 percent for some binders (Anderson et al., 1994).

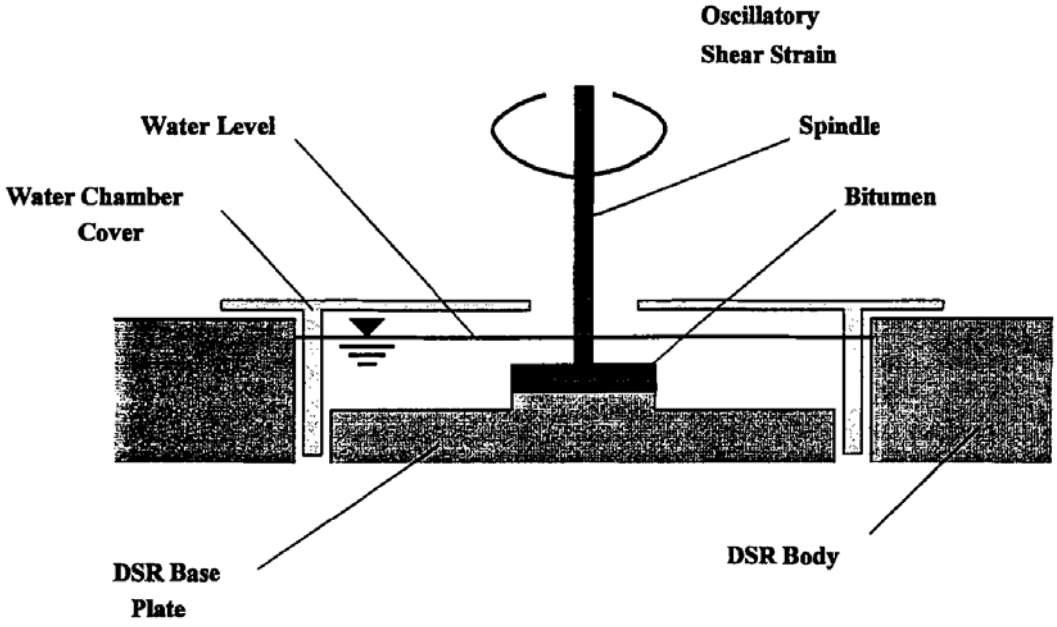

Figure 2.12: Testing arrangement in DSR (Airey, 1997)

Two types of spindles (upper plate) used in the DSR testing are 25-mm diameter parallel plate geometry, and 8-mm diameter parallel geometry. It is essential to select spindle geometry due to the effect of compliance of parallel plate geometry on rheological measurements for the extremely high stiffness binders under dynamic loading at low temperatures. Anderson et al. (1994) suggested that 25-mm parallel plates should be used when the complex modulus ranges from 10^3 to 10^5 Pa; 8-mm parallel plates should be used when the complex modulus ranges from 10^5 to 10^7 Pa; torsion bar or bending beam rheometer should be used when the complex modulus is greater than 10^7 Pa.

During the test, the sample of bituminous binder is sheared between two parallel plates. One of the parallel plates is oscillated with respect to the other at selected frequencies and rotational deformation amplitude (or torque amplitude). As shown in Figure 2.13, the spindle (upper plate) is caused to oscillate sinusoidally while the base plate is fixed during testing. The testing is carried out by oscillating the spindle about its own axis such that a radial line through point A moves to point B, then reverses direction and moves through point A to point C, followed by moving back from point C to point A (Airey,1997).

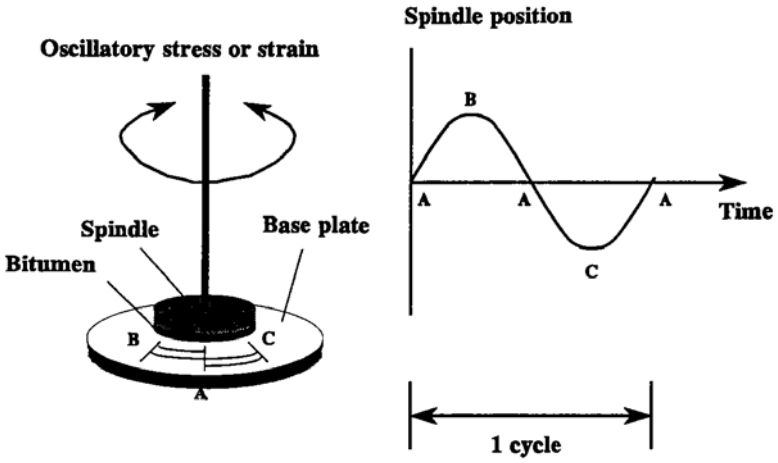

Figure 2.13: Principles involved in DSR test (Airey, 1997)

The procedure during the DSR testing is that the responding strain/stress measurement is determined by applying a torque to a puck-shaped bituminous specimen in response to the applied stress/strain, as shown in Figure 2.14. The calculation of the shear stress and shear strain is given by:

$$\tau = \frac{2T}{\pi r^3} \tag{2.6}$$

where:

τ = shear stress (Pa)

T = torque (N.m)

r = radius of parallel plates (m)

$$\gamma = \frac{\vartheta r}{h} \tag{2.7}$$

where

γ = shear strain

ϑ = deflection angle

h = gap width between two parallel plates (bitumen sample thickness) (m)

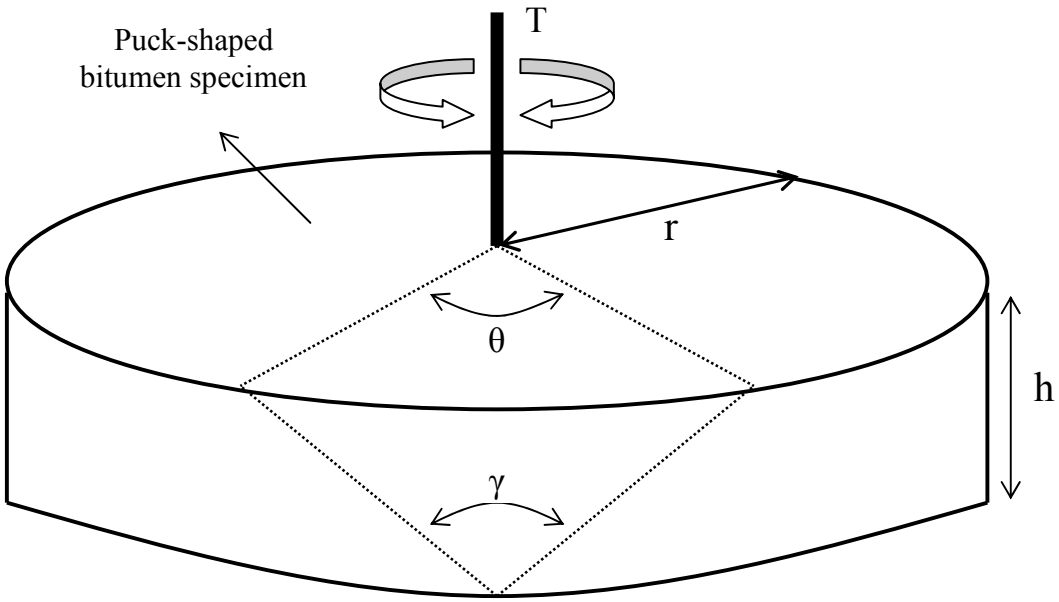

Figure 2.14: DSR testing geometry

It is noted that the non-uniform shear strains and shear stresses are calculated in the parallel plate geometry. The values of shear strain and shear stress are dependent on the radius of the parallel plates and vary in magnitude from the centre to the extremities of disks. The shear stress, shear strain and shear complex modulus, which is a function of the radius to fourth power, are calculated at the outside (maximum value) of the disk.

2.3.2 Dynamic Mechanical Analysis

Dynamic mechanical analysis (DMA) is used to fingerprint the dynamic rheological properties of bitumens by means of oscillatory-type testing using a rheometer to understand the viscous and the elastic nature of bitumens over a wide range of temperatures and loading rates (Goodrich, 1991). The dynamic test may be either stress-controlled or strain-controlled depending upon which of these variables is controlled by the test machine, but strain-controlled testing is more common than stress- controlled testing (Christensen and Anderson, 1992). During the strain-controlled testing, a sinusoidal shear strain is imposed on a bitumen specimen, and the resultant shear stress response is measured as a function of frequency. The primary response of interest in dynamic testing is the complex modulus, G*, which is the ratio between stress and strain:

$$G^*(\omega) = \left(\tau_{max} - \tau_{min}\right) \Big/ \left(\gamma_{max} - \gamma_{min}\right) \tag{2.8}$$

The complex modulus, G*, is a time dependent parameter so that its magnitude depends on the angular frequency, ω. The shear stress, τ, and shear strain, γ, vary sinusoidally with time so that complex modulus, G*, is calculated from the absolute or peak-to-peak stress and strain values (Anderson, et al., 1991), as shown in Figure 2.15.

Figure 2.16 shows that the response to an applied shear strain is instantaneous and the resultant shear stress is in phase with the applied shear strain when the bitumen behaves as an elastic solid, whereas the resultant shear stress is 90^o out of phase with the applied shear strain when the bitumen behaves as a viscous liquid. The phase angle, δ, (see Figure 2.15) varying between 0^o and 90^o, is the lag in the shear stress response compared to the applied shear strain, and therefore it is an important parameter to describe the viscoelastic behaviour of bitumens (Anderson, et al., 1991; Christensen and Anderson, 1992; Goodrich, 1988 and 1991).

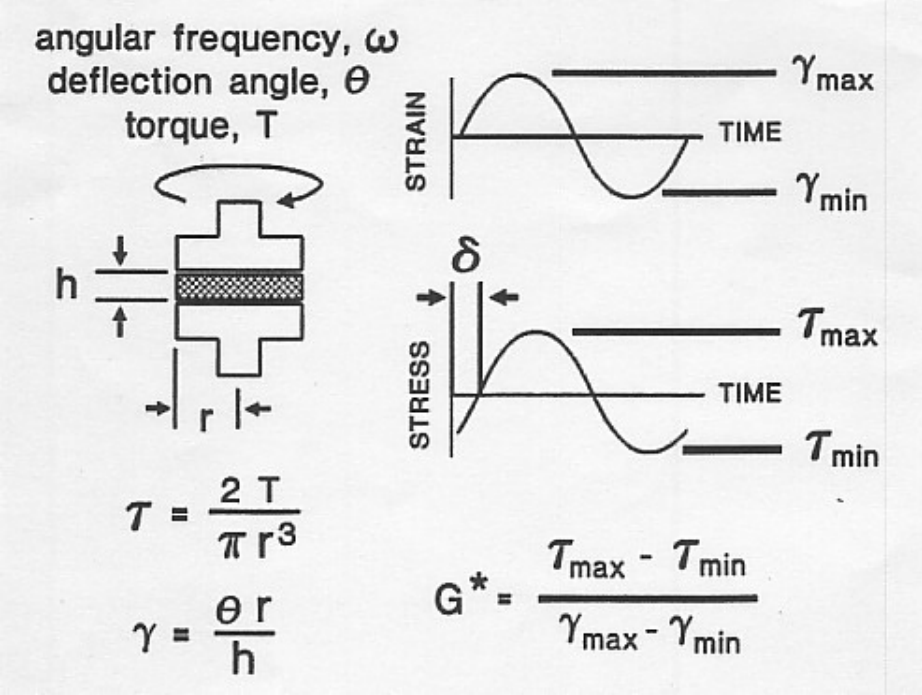

Figure 2.15: Dynamic oscillatory shear measurements using parallel plate geometry (Anderson et al., 1991)

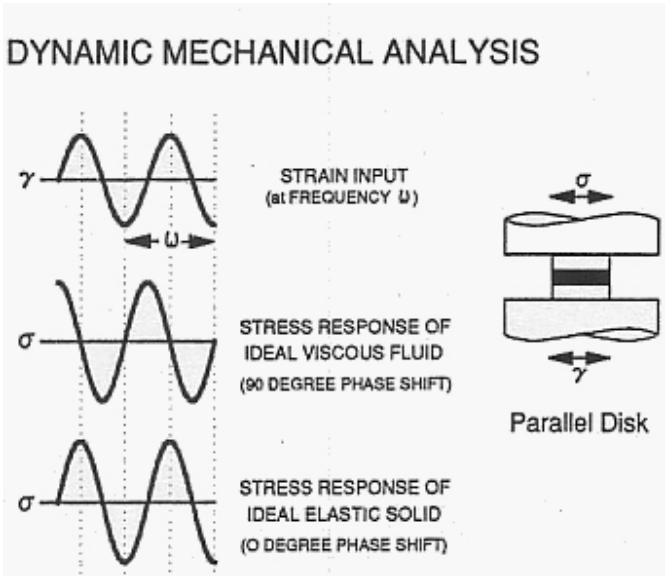

Figure 2.16: Dynamic shear analysis using parallel plate geometry (Goodrich, 1991)

In addition to G*(ω), the other three dynamic parameters: the storage modulus (elastic modulus), G'(ω), the loss modulus (viscous modulus), G"(ω), and the loss tangent, tanδ, are directly related to the complex modulus and the phase angle, and can be computed through a series of relatively simple equations given below:

$$G'(\omega) = G^*(\omega)\cos\delta \tag{2.9}$$

$$G'(\omega) = G^*(\omega)\cos\delta$$

(2.10)

$$\tan\delta = G''(\omega) \Big/ G'(\omega)$$

(2.11)

$$G^*(\omega) = \sqrt{[G'(\omega)]^2 + [G''(\omega)]^2} \tag{2.12}$$

The relationships among complex shear modulus, storage modulus, loss modulus and phase angle can be shown schematically through a trigonometry of a right angle triangle as shown in Figure 2.17.

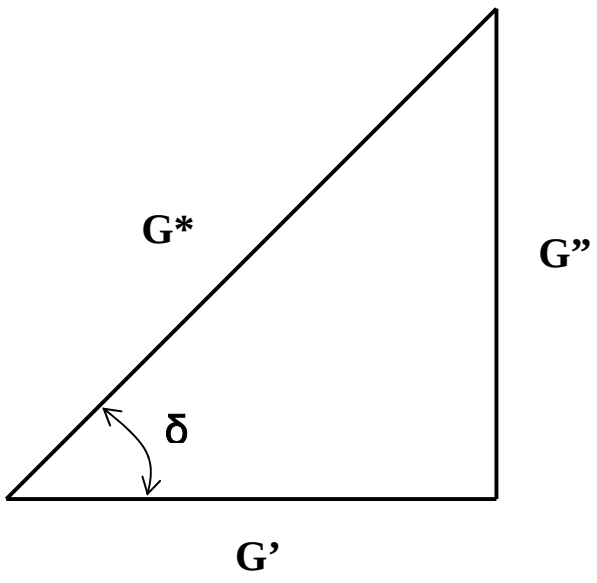

Figure 2.17: Relationship among dynamic complex modulus, storage modulus, loss modulus and phase angle

The storage modulus, G’(ω), represents the in-phase component of complex modulus, whereas the loss modulus, G”(ω), represents the out-of-phase components of the complex modulus. It is noted that the elastic component of the response only represents

part of the storage modulus, and the viscous response only represents part of loss modulus. Most real viscoelastic materials display a delayed elastic response, which is time dependent, but completely recoverable. They can not be strictly interpreted as elastic and viscous moduli (Christensen and Anderson, 1992).

2.3.3 Linearity of Bituminous Binders

In order to predict the engineering performance of any material, it is necessary to understand its stress-strain behaviour. Materials such as bitumen, which exhibit aspects of both elastic and viscous behaviour, are called viscoelastic, and must be characterised with test methods and analytical techniques that account for the time of loading and loading temperature (Anderson et al., 1994). It is usually advisable to confine the characterisation of a bitumen to its linear viscoelastic response to simplify the mathematical modeling of the material, as nonlinear response, particularly for viscoelastic materials, is difficult to characterise in the laboratory and model in practical problems (Airey et al., 2002). Generally, bituminous materials display nonlinear stress-strain behaviour with nonlinearity only becoming negligible at small strains. As the viscoelastic parameters of shear complex modulus, phase angle, storage modulus and loss modulus are all defined under linear viscoelastic conditions, the relationship between stress and strain is influenced only by temperature and loading time (frequency) and not by the magnitude of the stress and strain (Ferry, 1980).

Strain/stress sweeps were usually conducted at selected temperatures and frequencies, and the strain/stress linearity limits were determined as the point beyond which the measured shear modulus reduces to 95% of its zero strain/stress value (Petersen et al., 1994), as shown in Figure 2.18.

In the linearity investigation, strain/stress sweeps were conducted that the response stress/strain values were measured within the linear viscoelastic range to ensure test repeatability, and thus the resultant complex modulus, G*, can be within the LVE limit. Due to considering the operator variability in judging the point at which G* reduces to 95% of zero-strain value and impossibly conducting each asphalt binder at each

temperature, a standard set of strain values was established in SHRP-A-370, as shown in Figure 2.19. Strain sweeps were carried out on more than 40 unaged and aged asphalt binders at selected temperatures at a frequency of 10 rad/sec (1.6Hz) to generate LVE strain and stress limits criteria. The criteria represented the strain/stress levels at which the complex modulus reduced to 95% of zero-strain/stress values. The strain and stress used in the specification testing should be controlled to ± 20% of the following strain and stress equations:

$$\gamma = 12.0/(G^*)^{0.29} \tag{2.13}$$

$$\tau = 0.12(G^*)^{0.71} \tag{2.14}$$

where

γ = shear strain (%)

τ = shear stress (MPa)

G^* = complex modulus (MPa)

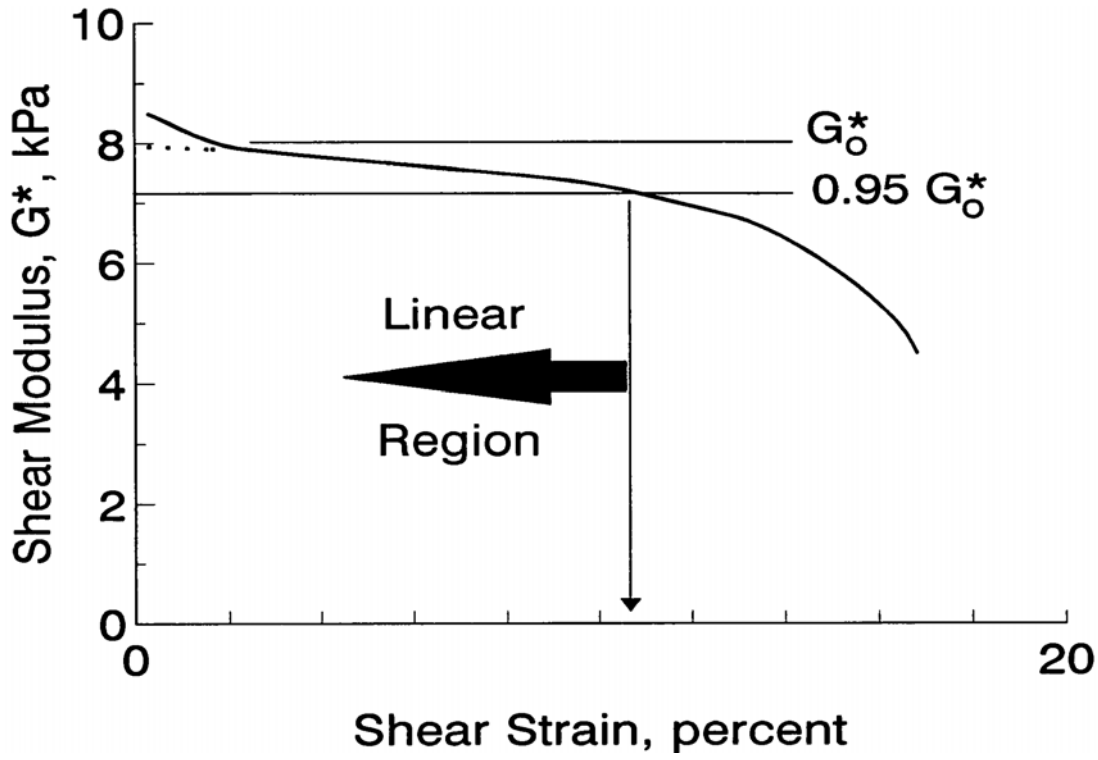

Figure 2.18: Strain sweep used to determine linear region (Petersen et al., 1994)

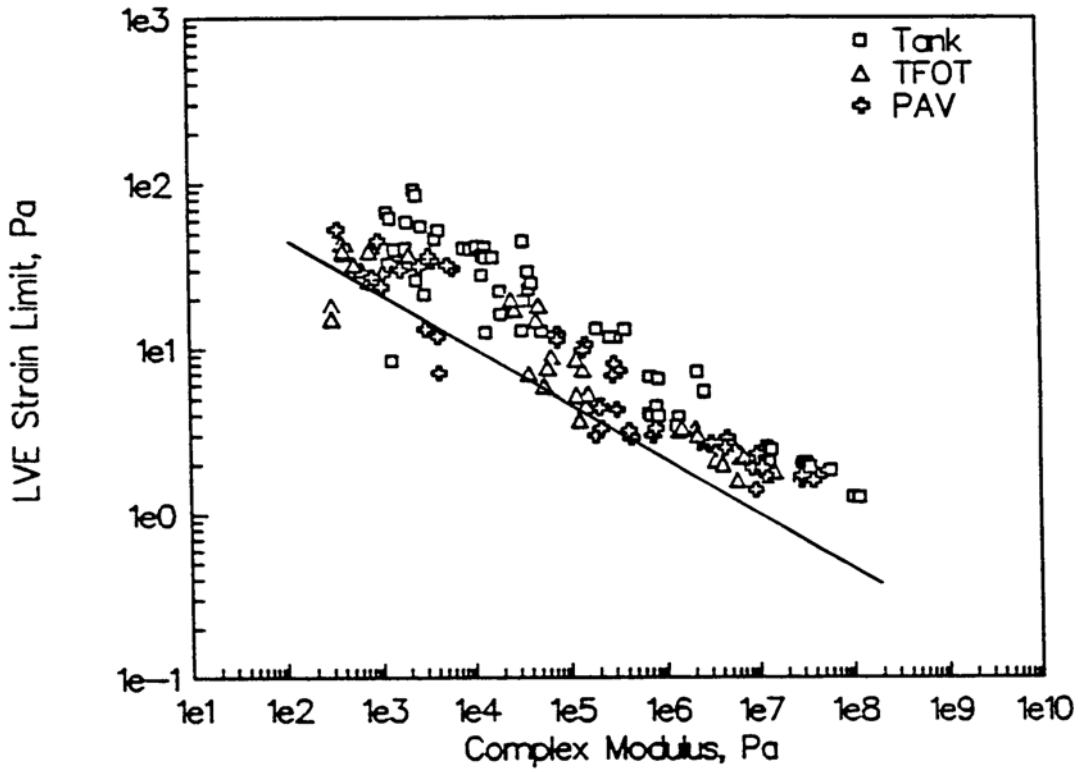

Figure 2.19: Linear viscoelastic strain limit as a function of complex modulus for unaged and aged bitumens (Petersen et al., 1994)

2.3.4 Construction of Master Curves

One of the primary analytical techniques used in analysing dynamic mechanical data for bituminous binders involves construction of master curves. This form of presenting data, as master curve, allows the prediction of the complex modulus, phase angle, storage and loss stiffness modulus at any loading frequency or temperature and the comparison of dynamic data on an equal basis.

In constructing a master curve using time-temperature superposition, dynamic data which consist of a series of curves for the test conducted at each temperature are first obtained over a range of frequencies and temperatures. The data are combined into a single master curve by shifting horizontally individual curves along the time (frequency) axis to form a curve at a single reference temperature.

A horizontal shift factor, a(T), is produced for each curve determined at a particular test temperature. Figure 2.20 illustrates the resulting master curve and its associated

temperature shift factors. These shift factors can be determined by trial and error or by sophisticated computer software. They are generally described using either a Williams-Landel-Ferry (WLF) equation (Ferry, 1980) or Arhennius function:

WLF equation:

$$\log a(T) = \frac{-C_1(T - T_{ref})}{(C_2 + T - T_{ref})} \tag{2.15}$$

where:

$a(T)$ = shift factor

T = temperature, ^{o}K

T_{ref} = reference temperature, ^{o}K

C_1 and C_2 = constants

Arrhenius function:

$$\log a(T) = \frac{\Delta H_a}{2.303}\left(\frac{1}{T} - \frac{1}{T_{ref}}\right) \tag{2.16}$$

where:

$a(T)$ = shift factor

ΔH_a = activation energy, typically 250 kJ/mol

R = universal gas constant = 8.314 J/^{o}K-mol

T = temperature, ^{o}K

T_{ref} = reference temperature, ^{o}K

Generally, the WLF equation is used for colder temperatures whereas the Arrhenius function is used at higher temperatures (Christensen and Anderson, 1992). It is noted that small strains should be used in the testing (within the linear viscoelastic response), and consequently time and temperature superposition will be a reliable method. Anderson et al. (1991) found the WLF equation can accurately describe the shift factors for bituminous binders above a characteristic temperature, called the defining temperature, T_d, for aged and unaged SHRP asphalt binders. They stated that the

constants in the WLF equation were all essentially the same value, with C_1 equals to -19 and C_2 equals to 92. Below T_d, the shift factors could be described by the Arrhenius function.

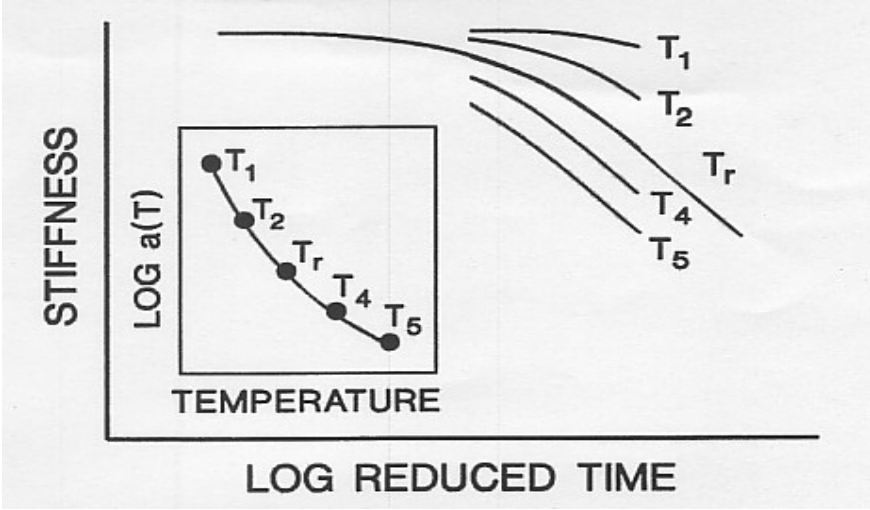

Figure 2.20: Time-temperature superposition in the construction of a master curve (Anderson et al., 1991)

2.4 Permanent Deformation Behaviour and Testing of Bituminous Binders

2.4.1 Creep Characterisation of Bituminous Binders

It is widely recognised that the permanent deformation behaviour of asphalt mixtures is dependent on the flow of bituminous binders. Theoretical considerations show that the binder contribution to rutting is a permanent deformation described by a viscosity (Philips and Robertus, 1995). In a long time creep test for the bituminous binder, the effect of delayed elasticity decreases with time and after a sufficient long time period, the rheological behaviour of the bituminous binder is dominated by viscous flow. Under low stress creep, structures within the bituminous binder deform so slowly that they can continuously adapt thereby maintaining a situation close to equilibrium without building up any significant structural change in the material.

Figure 2.21 shows a viscoelastic response of the behaviour of bituminous binder under creep loading. Three regions of behaviour are included: linear elastic, delay elastic and viscous. The viscous component is operative whenever the bitumen is loaded and is

solely responsible for the non-recoverable deformation. The elastic and delay elastic strain are totally recoverable upon the release of an applied load. The elastic response dominates at short loading times or low temperatures, while the viscous response dominates at long loading times or high temperatures. At intermediate loading times and temperatures the delay elastic response dominates (Anderson et al., 1991).

Collop et al. (2002) performed creep tests using a DSR on 50 and 100 penetration grade bitumens at 20^{o}C over a range of shear stress levels. A typical test result from a creep test is shown in Figure 2.22. The creep curve can be divided into three regions. In the first region, namely primary creep, the shear strain rate (shear strain divided by time) decreases with time and the bitumen behaviour is dominated by elastic and delay elastic effects. In the second region, namely steady-state creep region, the shear strain rate remains approximately constant with time and the bitumen behaviour is dominated by viscous effects. In the third region, namely tertiary creep, the shear strain rate increases with time and the bitumen is progressively damaged.

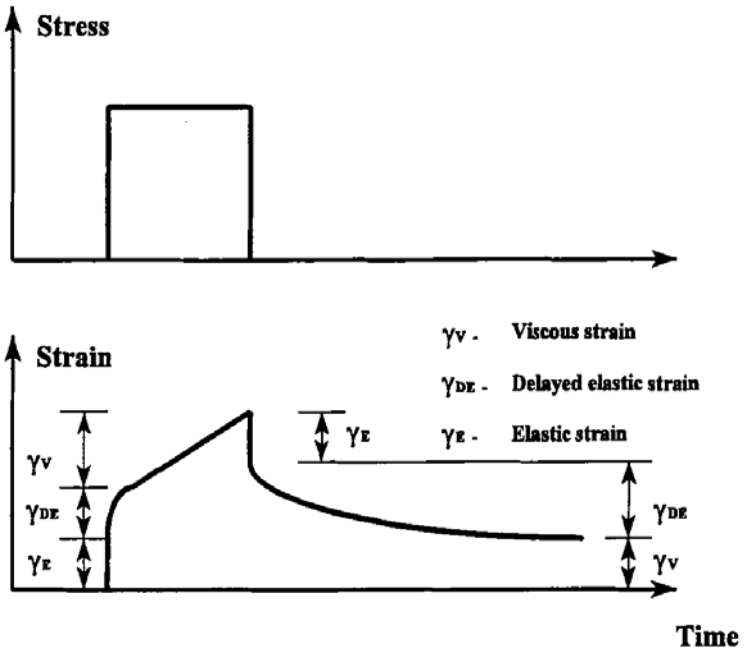

Figure 2.21: Viscoelastic response of bitumen under creep loading (Anderson et al., 1991)

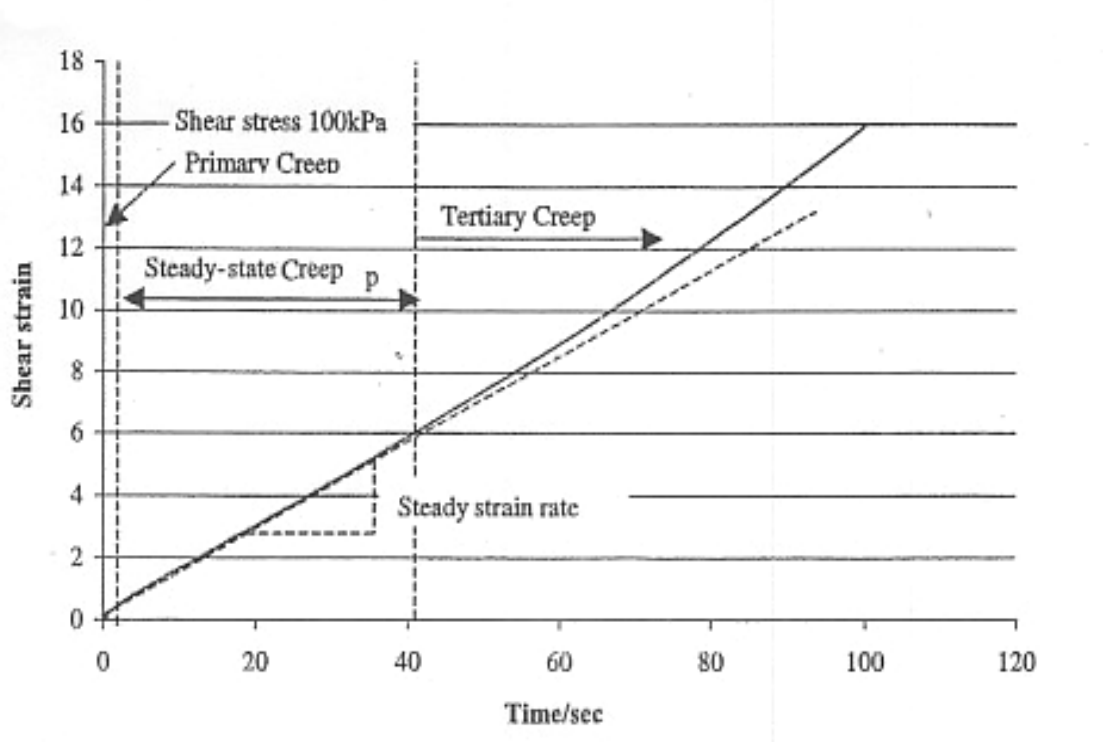

Figure 2.22: Creep test result for bitumen (Collop et al., 2002)

2.4.2 Concept of Zero Shear Viscosity

Zero shear viscosity (ZSV) or the viscosity at zero shear rate is an intrinsic property of a bituminous binder that has been suggested as a more appropriate rutting parameter of most binders, particularly modified binders (Phillips and Robertus, 1996; Sybilsky, 1996ab). Because rational pavement design is customarily based on the premise that wheel loading occurs in the linear region, the corresponding viscosity, so-called zero shear viscosity, is the only viscosity in the linear viscoelastic region and selected to evaluate the permanent deformation resistance of asphalt mixtures. Within the linear region, ZSV is independent of shear rate and it reflects dissipated motions in a negligibly perturbed, equilibrium "no-flow" structure (Phillips and Robertus, 1995).

Desmazes et al. (2000) developed a protocol for reliable measurement of ZSV of bituminous binders. They performed the creep flow followed by creep recovery test on conventional, multigrade and SBS polymer modified bitumens using a DSR for the development of a test method. In creep testing, the applied shear stress has a constant

value, τ_0, and the resulting shear strain, γ, is measured as a function of time. The creep compliance, $J(t)$, is defined as the ratio of shear strain and applied shear stress:

$$J(t) = \gamma(t) / \tau_0 \tag{2.17}$$

Figure 2.23 shows the compliance versus time plot which is similar to strain versus time plot. During the creep and the creep recovery phases, the compliance can be divided into three components, where J_0 is the instantaneous elastic component, J_1 is the delay elastic component and J_2 is the viscous component. During the creep phase, the resulting shear strain is proportional to the applied shear stress in the steady-state part and, therefore, the creep compliance is independent of the stress level. When the applied shear stress is sufficiently low, the viscosity value is independent of the shear stress. The inverse of the slope of the compliance curve in the steady-state part gives the ZSV, η_0:

$$\eta_0 = \lim_{t_{creep} \to \infty} \left(t_{creep} / J_{creep}(t_{creep}) \right) \tag{2.18}$$

During the creep recovery phase, the shear stress is removed and some of the shear strain imposed to the binder is gradually recovered. The ZSV can be derived from the residual compliance:

$$\eta_0 = \lim_{t_{recovery} \to \infty} \left(t_{creep} / J_{recovery}(t_{recovery}) \right) \tag{2.19}$$

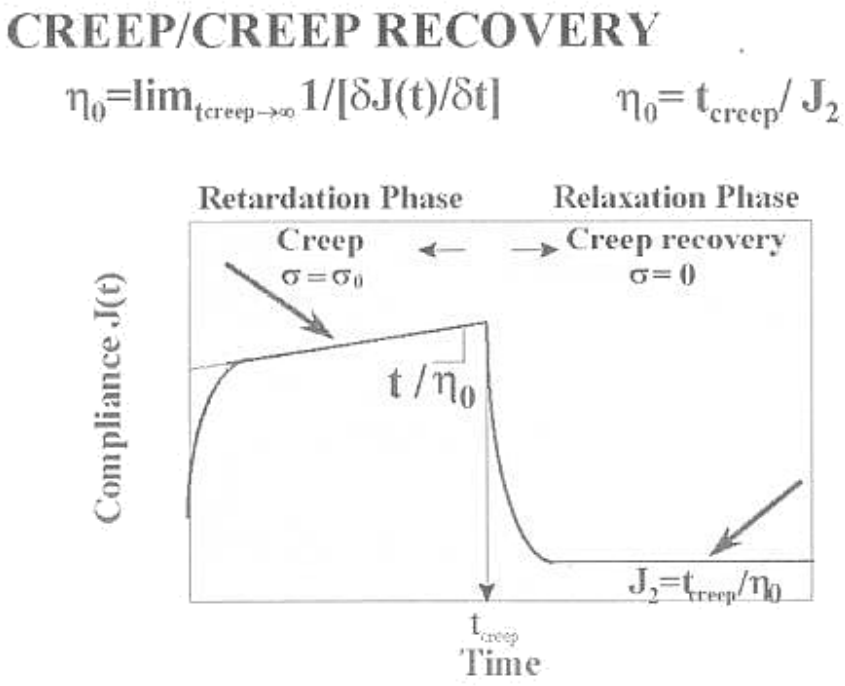

Figure 2.23: Creep/creep recovery compliance curve (Desmazes et al., 2000)

Although ZSV can be determined directly from creep tests, such tests are time-consuming and are difficult to perform on some PMBs (steady-state can not be reached). Anderson et al. (2002) proposed an alternative method of extrapolating the dynamic viscosity to zero frequency. They carried out the sinusoidal oscillation testing with test frequencies ranging from 0.1 to 100 rad/s using a DSR on ten unmodified and modified binders at six temperatures ranging from 52 to 82°C. The complex ZSV, η_0^*, can be measured as a limiting value from the loss modulus, G'', at very low angular frequency of 0.1 rad/s, ω, which is given by:

$$\eta_0^* = \lim_{\omega\to 0}\eta'(\omega) = \lim_{\omega\to 0}\frac{G''(\omega)}{\omega} \tag{2.20}$$

They compared the ZSV values obtained from frequency sweeps with those obtained from single cycle creep recovery tests (performed in linear viscoelastic domain on the same binders) and concluded that a good agreement was shown between the two methods.

Carswell and Green (2000) also carried out an alternative viscosity test at low shear rate levels on sixteen binders consisting of unmodified, multigrade, waxy, elastomeric and plastomeric binders at 45 and 60^{o}C using a DSR. They performed the viscosity test at a range of shear rate from 0.02 to 10 s^{-1}. The unmodified bitumens were relatively independent of shear rate up to 1 s^{-1}, after which their viscosities showed to be increasingly shear dependent, whereas for some PMBs, the viscosities were highly dependent on shear rate. They correlated the viscosities of binders at different shear rate to the wheel tracking rate of HRA mixtures. They found the best correlation for the viscosities of binders at high rate of shear (5 s^{-1}). However, due to either stress limitation of the machine (for stiff binder) or the sample migrating out from the DSR plates (for soft binder), it was not possible to measure the viscosity at higher shear rates.

2.4.3 Creep Testing Using a DSR

A number of researchers have conducted various creep test methods consisting of creep with or without recovery and repeated creep tests using a DSR to investigate the steady-state shear deformation behaviour of bituminous binders. Phillips and Robertus (1995) investigated the correlation of asphalt mixture rutting with binder zero shear viscosity. They performed small amplitude together with low frequency oscillatory test and low stress creep with recovery test (applied stress = 30-100 Pa) at 40^{o}C on conventional unmodified bitumens, multigrade bitumens and SBS polymer modified bitumens containing various polymer contents. The test only slightly perturbed a bituminous material and so enabled ZSV to be measured. In comparative binder testing, dense asphalt mixtures were compared at fixed binder percentage, aggregate type and grading and asphalt compaction. The rutting tests were carried out on these mixtures at a fixed number of wheel passes of 14000 with a test temperature of 40^{o}C in a Laboratory Test Track (LTT) carousel. They concluded that the rutting rate (at 14000 wheel passes) measurements in a LTT carousel correlated well with the ZSV of the binder at the same temperature. The correlation covered unmodified and polymer-modified binders and indicated that ZSV was an appropriate indicator determining the binder contribution to permanent deformation in asphalt pavement rutting. Phillips and Robetus (1996) also

performed the dynamic creep testing on the same asphalt mixtures at the temperature corresponding to an iso-viscosity condition, ZSV=10^6 Pa.s. They found that the creep rate correlated well with ZSV of unmodified as well as polymer modified bitumens.

Desmazes et al. (2000) carried out creep flow followed by creep recovery tests at 40^{o}C using a controlled stress rheometer on conventional, multigrade and SBS polymer modified binders for the development of a test method. For modified bitumens, a stress level of 20-50 Pa was selected, while for unmodified bitumens, a greater value was chosen up to 5000 Pa. The creep and creep recovery time should be long enough to guarantee a steady state. They summarised that the reliable procedure to measure ZSV was suitable for a wide range of binders except highly modified binders where it had been found difficulty to determine the right operating conditions. A steady state creep flow could not be reached and thus an accurate ZSV could not be measured.

Carswell and Green (2000) conducted research to predict the rutting performance of HRA mixtures from ZSVs of bituminous binders. The creep tests using a DSR were performed on sixteen binders consisting of 3 unmodified bitumens, 1 multigrade bitumen, 3 waxy bitumens, 6 elastomeric binders, 3 plastomeric binders and binder/filler blends (binder: filler ratio 8.5: 9.5 by mass) at two stress levels of 100 and 15000 Pa with two test temperatures of 45 and 60^{o}C. The creep compliance was measured after 1000 seconds loading for each binder, and that measured after 100 seconds loading for binder/filler blends. The wheel tracking tests were also undertaken on the HRA wearing course mixtures having a binder content of 7.2% at 45 and 60^{o}C. They found that the relationships between the wheel tracking rate and the creep compliance as well as the wheel tracking rate and steady shear viscosity were poor for binders. For binder/filler blends, the correlations between creep compliance and the steady shear viscosity with wheel tracking rate were encouraging (R^2 = 0.85 and 0.81, respectively). Carswell and Moglia (2003) also proposed an accumulated strain parameter, determined from a repeated creep (pulse creep) test using a DSR on these sixteen binders. The test conditions adopted were the load applied (300 Pa) for 1 second, recovery for 9 seconds, repeated 99 times. They found that the accumulated recovered compliance or the

viscosity did not significantly improve with number of test cycles. The correlations obtained after 1 test cycle were just as good as those obtained after 100 test cycles.

Collop et al. (2002) conducted creep tests on 50 and 100 penetration grade bitumens at 20^{o}C using a DSR over a wide range of stress and strain rate levels to investigate the steady-state shear deformation behaviour in linear and non-linear regions. They found that the steady-state deformation behaviour of both the two penetration grade bitumens is similar. They also concluded that at stress levels less than approximately 50 kPa the deformation behaviour in this region was linear viscous flow. At stress levels greater than approximately 100 kPa, the deformation behaviour was non-linear creep behaviour.

Vlachovicova et al. (2005) performed creep and recovery tests at 60^{o}C on base bitumen (200/300 penetration grade) modified with different amount of radial styrene-butadiene-styrene (SBS) copolymer. Various time durations of creep and recovery were examined. The impact of waiting time between tests on creep compliance and ZSV, and the influence of stress levels ranging from 25 Pa up to 5 kPa were investigated. They found that estimated ZSV as well as steady-state compliance were stress dependent above stress level of 25 Pa. That was because the steady state flow was not reached, especially for the short cycles (1 second loading time and 9 seconds unloading time). They suggested to consider the creep and recovery cycle with higher stress levels.

Bituminous binder permanent deformation tests have been conducted generally using small stresses because binder performs in a linear viscoelastic manner and thus deformation is proportional to stress. However, the stresses and strains under traffic loads can be high enough to make binder reach the non linear region. For evaluating the non linearity of binders, Delgadillo et al. (2006) investigated the stress dependency of binders in repeated creep recovery (RCR) testing using a DSR and the relationship with asphalt mixture performance. The RCR testing of a total of 100 cycles of 1 second loading time and 9 seconds unloading time was carried out on six polymer modified and two oxidised binders at two test temperatures of 46 and 64^{o}C. The binders were RTFO aged before testing. Each binder was tested at six stress levels ranging from 25 to 10000 Pa. The stress sweep testing was also performed at several stress levels between 1 and

50000 Pa on the same binders at 46 and 64°C at 10 Hz. In addition to binder test, a repeated creep recovery testing was also carried out on asphalt mixtures prepared with two types of aggregates (limestone and gravel) and seven different binders. They found that RCR and stress sweeps in cyclic mode showed similar trends when ranking binders with respect to the stress sensitivity. The sensitivity of the RCR test was higher than the stress sweeps because the RCR test was considered at a higher number of cycles (100 cycles). In addition, the correlation between the accumulated strain in the binder and the permanent deformation in the asphalt mixture was found to be good despite of the stress levels used in binder RCR testing. They also concluded that the ability of a binder to resist high stress levels without collapsing seemed to be a good indicator of the asphalt mixture rutting performance.

2.4.4 Extrapolation of Zero Shear Viscosity

Most measurement techniques are performed on a DSR with the ZSV being determining directly from the plotted data or, particularly in the case of the oscillation test, extrapolated to zero frequency using an appropriate mathematical model. The Cross model (Cross, 1965) and Carreau model (Carreau et al., 1968) have been fitted to the bituminous binders measurements allowing extrapolating of the viscosity at zero shear conditions (Anderson et al., 2002; Binard et al., 2004; De Visscher et al., 2004; Dongre and D'Angelo, 2003; Sybilski, 1996ab). The Cross model describes a flow curve of pseudoplastic fluids in the form of a four-parameter equation:

$$\eta = \eta_{\infty} + \frac{\eta_0 - \eta_{\infty}}{\left(1 + k\omega^m\right)} \tag{2.21}$$

where η is the viscosity (Pa.s), η_0 is the zero shear viscosity (Pa.s), η_{∞} is the infinite viscosity (Pa.s) (second Newtonian viscosity), ω is the frequency (rad/s) or shear rate (s^{-1}), and k and m are material constants.

The Carreau model is also fitted to viscosity measurements to obtain the zero shear viscosity, and is given by:

$$\eta = \eta_{\infty} + \frac{\eta_0 - \eta_{\infty}}{\left[1 + (\lambda\omega)^2\right]^n} \quad (2.22)$$

where η is the viscosity (Pa.s), η_0 is the zero shear viscosity (Pa.s), η_{∞} is the infinite viscosity (Pa.s), ω is the frequency (rad/s) or shear rate (s^{-1}), and λ and n are material constants.

Sybilsky (1996a) proposed a simplified version of the Cross model to compute ZSVs of 28 polymer modified bitumens from laboratory measurements with a rotational viscometer. He assumed the η was far greater than η_{∞}, and thus the following simplified three-parameter equation was proposed:

$$\eta = \frac{\eta_0}{\left(1 + k\dot{\gamma}^m\right)} \quad (2.23)$$

where $\dot{\gamma}$ was the shear rate (s^{-1}).

He concluded that the proposed simplified equation enabled the calculation of ZSV of a polymer modified bitumen system from viscosity measurements conducted under varied stress conditions using a rotational viscometer. He suggested that ZSV values as independent from testing conditions could be assumed as an objective material property that could be used for material evaluation. Sybilsky (1996ab) also indicated that the parameter, k, was related to viscosity and was named as consistency. Another parameter, m, was not related to viscosity, but was regarded as a measure of shear compliance.

Anderson et al. (2002) conducted frequency sweeps on ten unmodified and modified bitumens at six temperatures ranging from 52 to 82°C. They applied the Cross model to the dynamic data and they found that an excellent agreement was shown between the graphical (visual) method and the values calculated using the Cross model (shown in

Figure 2.24), which concluded that the Cross model could be used reliably to estimate the ZSV.

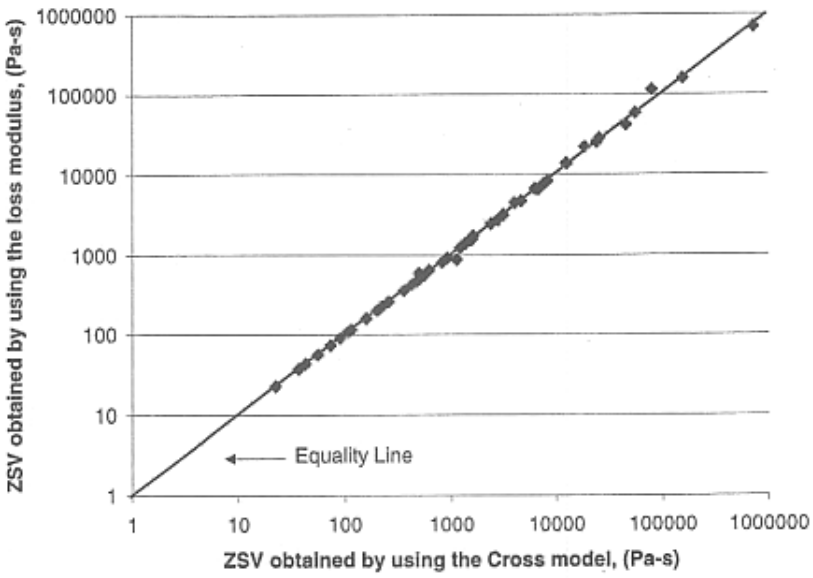

Figure 2.24: Comparison of ZSV from graphical extrapolation of loss modulus to zero frequency and from fitting Cross model (Anderson et al., 2002)

Dongre and D'Angelo (2003) carried out single and multiple creep recovery tests on seven unmodified and modified binders at several temperatures ranging from 46 to 76^{o}C, and five stress levels ranging from1 to 300 Pa. The single creep and recovery tests were performed at a creep load for 5000 seconds duration and unload for 5000 seconds duration. The multiple creep tests were undertaken at a creep load for 1 second duration followed by recovery load of zero for 9 seconds duration. The Carreau Model was then fitted to the log viscosity versus log shear rate data to obtain ZSV. They found that to obtain the accurate ZSVs of bituminous binders, the shear stress should be in the Newtonian region and the steady state should be achieved.

De Visscher et al. (2004) carried out oscillation and repeated creep tests using a DSR on two unmodified binders (straight-run bitumen and waxy bitumen) and two modified binders (SBS and EVA PMBs) at 50^{o}C. For the oscillation test, the frequency sweeps were made from 20 Hz down to at least 0.01 Hz. The Cross model was used to extrapolate measurements of the complex viscosity to very low frequency of 0.001 Hz.

For the repeated creep test, a total of 100 cycles of 1 second loading time and 9 seconds unloading time with a shear stress of 25 Pa was performed. The creep viscosity was determined by fitting the data points of cycles 50 and 51 with the 4-parameter Burgers model. They compared the values obtained for ZSV in the oscillation test to the viscosity from the repeated creep test. The results for the two unmodified binders compared reasonably well. For the modified binders, ZSV was much higher for the creep viscosity than from the repeated creep test. They also suggested that it would be more appropriate to speak in terms of "low shear viscosity" than "zero shear viscosity" since it was not possible to measure down to zero frequency.

Binard et al. (2004) performed frequency sweep, creep and repeated creep tests on thirteen plain and modified binders at 60 and 70^{o}C using a DSR. For the oscillation test, the frequency sweeps were carried out at the test frequency ranging from 0.1 to 100 rad/s. For the creep test, the steady state viscosity was determined at each stress level (10, 25, 50 and 150 Pa). In addition, the repeated and recovery tests were run applying 25 and 50 Pa stresses on a DSR. They consisted of 52 cycles with a 1 second loading followed by a 9 seconds recovery. The Cross model and the Carreau models were both used to extrapolate measurements of the viscosity to very low frequency or shear rate. They found that ZSV value varied a lot for modified binders in the fitting process. For the Carreau model, the curve fitting parameters "forced" the formation of a plateau at low frequencies, artificially bending the curves. Figure 2.25 shows the parameters from the Carreau model lead to a considerable curvature than with the Cross model, resulting in smaller ZSV.

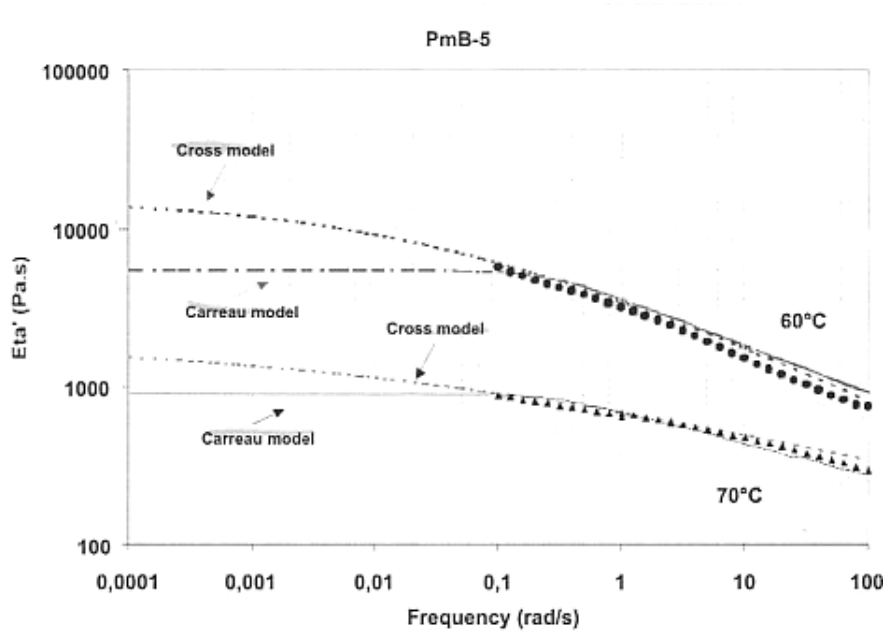

Figure 2.25: Difference in ZSV using the Cross and Carreau models (Binard et al., 2004)

2.5 Fatigue Behaviour and Testing of Bituminous Binders

2.5.1 Fatigue Characterisation of Bituminous Binders

A general definition of fatigue can be described as the phenomenon of fracture under repeated or fluctuating stress having a maximum value generally less than the tensile strength of the material. The repeated stresses which are insufficient in magnitude to produce failure in one cycle nonetheless cause damage in the material with every cyclic loading. This damage accumulates and eventually leads to failure.

The term "fatigue" applied to an asphalt pavement implies a mode of failure of the asphalt pavement resulting from repeated traffic loading, rest periods, construction practices and temperature variations. Research has revealed that fatigue cracks in an asphalt mixture tend to run through the bituminous binder (Hammoum et al., 2002; Hartman and Gilchrist, 2004). Therefore, it is widely accepted that bituminous binder and/or bitumen-filler mastic plays an important role in this failure mechanism, as fatigue cracking tends to take place predominately within the binder itself (Soenen et al., 2004).

Examples of the binder properties influencing asphalt mixture fatigue are stiffness, viscoelasticity and temperature susceptibility.

2.5.2 Fatigue Testing Using a DSR

To investigate the behaviour of bituminous binders under repeated loading can help to understand the binder nature effect on fatigue behaviour of asphalt mixture. The concept of using damage characterisation by performing fatigue testing of bituminous binders has been introduced as an alternative to predict the true fatigue behaviour of binders similar to mixtures (Bahia et al., 1999 and 2002). Since the introduction of the dynamic shear rheometer (DSR), direct testing of bituminous binders in fatigue has become relatively common with a number of research groups having successfully generated load-associated fatigue characteristics for both pure and modified bitumens by means of time sweep tests using the DSR (Anderson et al., 2001; Lu et al., 2003; Planche et al., 2003; Shenoy, 2002; Soenen and Eckmaan, 2000).

Bahia et al. (1999) proposed that dynamic shear rheometer could be used to characterise the fatigue behaviour of asphalt binders. They conducted a non-linear study which was expanded to include fatigue performance of binders at various strain levels in the linear and non-linear range. Two unmodified bitumens, two binders modified with plastomers, two binders modified with elastomers and two modified by oxidation were tested in this programme. The strain sweeps ranging from 1 percent to 50 percent were used to define the strains at which to perform fatigue testing. Specific values of complex modulus were targeted between 2 to 2000 kPa. Three test frequencies of 0.15, 1.5 and 15 Hz were selected in this study. The result indicated the high sensitivity of fatigue to strain level for binders was observed in this study. They summarised that strain level was by far the most important factor controlling fatigue performance although the effects of loading time (frequency) temperature, rest period and binder composition on fatigue disturbance were also significant on fatigue disturbance. The binder fatigue results also confirmed the findings of many research works that have related fatigue damage to strain of asphalt mixtures. They suggested that these effects could be detected in binder testing and

included in a binder specification system which was better related to pavement performance.

Soenen and Eckmann (2000) evaluated DSR as a test method for characterising the fatigue of bituminous binders. They conducted stress-controlled time sweep tests on four straight-run bitumens coming from the same crude origin and differing only in penetration grade. Two oxidised bitumens and some PMBs were also tested in this programme. The tests were performed at binder stiffness levels between 10 MPa and 50 MPa and frequency levels between 10 Hz and 50 Hz. They also observed that hairline cracks started to grow and propagated towards the centre of sample as long as the modulus was sufficiently large. The cracks would slowly heal and a smooth surface would be formed if the sample was left at rest for a longer period of time. For the aged bitumens, their fatigue lines became steeper and more strain dependent. For PMBs, the polymer modification had a considerable effect on the fatigue behaviour, but this was not general. They also reported that the fatigue test results for the binders were compared with fatigue tests performed on asphalt mixtures containing the same binders. Comparisons between the binder and mixture results were encouraging for unmodified bitumens but less correlation for PMBs.

Anderson et al. (2001) carried out strain-controlled time sweep experiments at a test frequency of 10 Hz on one unmodified base bitumen, one base binder modified with SB copolymer, one base binder modified with EVA copolymer and one chemically modified base binder using a DSR. The tests were conducted at equi-stiffness temperatures (initial complex modulus equal to 5 and 45 MPa) and different strain levels. They proposed that two different modes of failure were observed when binders were tested with time sweeps: one was that failure occurred as the result of internal damage (true fatigue) and another in which the loss in modulus was because of flow at the periphery of sample in accordance with a phenomenon known as edge fracture (instability flow). They concluded that true fatigue occurred at temperatures in which the initial complex modulus was greater than 15 MPa, while in the region of 5 MPa edge fracture or instability flow dominated, as shown in Figure 2.26. The dominance of the two failure modes appeared to depend on the modulus of the binder.

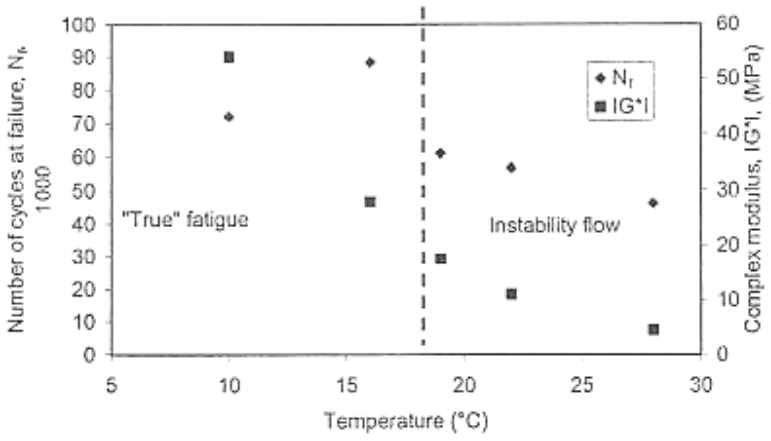

Figure 2.26: True fatigue and instability flow (Anderson et al., 2001)

Since the stiffness of bituminous sample was high, compliance (deformation occurring on DSR spindle) might effect the measurements. Soenen and Eckmann (2000) reported that the stiffness measurements for the same sample were tested at different gap settings. They found that as the gap width decreased, compliance effects influenced the measurements, and the measured stiffness deviated from the true stiffness, as shown in Figure 2.27. Anderson et al. (2001) also mentioned that when testing at binder stiffness of 45MPa at large strains, it was necessary to use torque values that exceed 1000 g-cm. As the complex modulus decreased during time sweep testing, a concomitant increase in the actual strain applied to the sample if the compliance correction remained unchanged, as shown in Figure 2.28. Soenen et al. (2004) reported that the DSR can only be used to evaluate fatigue behaviour in a narrow stiffness or temperature region. They conducted fatigue tests using a DSR time sweep under controlled strain conditions at a frequency of 25 Hz using different gap settings on unmodified and modified bitumens. The fatigue behaviour of binders was investigated at equi-stiffness and equi-temperature levels. They found the different phenomena occurred in the DSR during binder fatigue testing, as shown in Figure 2.29. Three phenomena consisting of pure fatigue, combination of fatigue and flow, and pure flow failure took place at different stiffness or temperature levels. They also suggested that the stiffness level obtained in the binder fatigue test need to be between 60 MPa and 200 MPa due to edge fracture and compliance error.

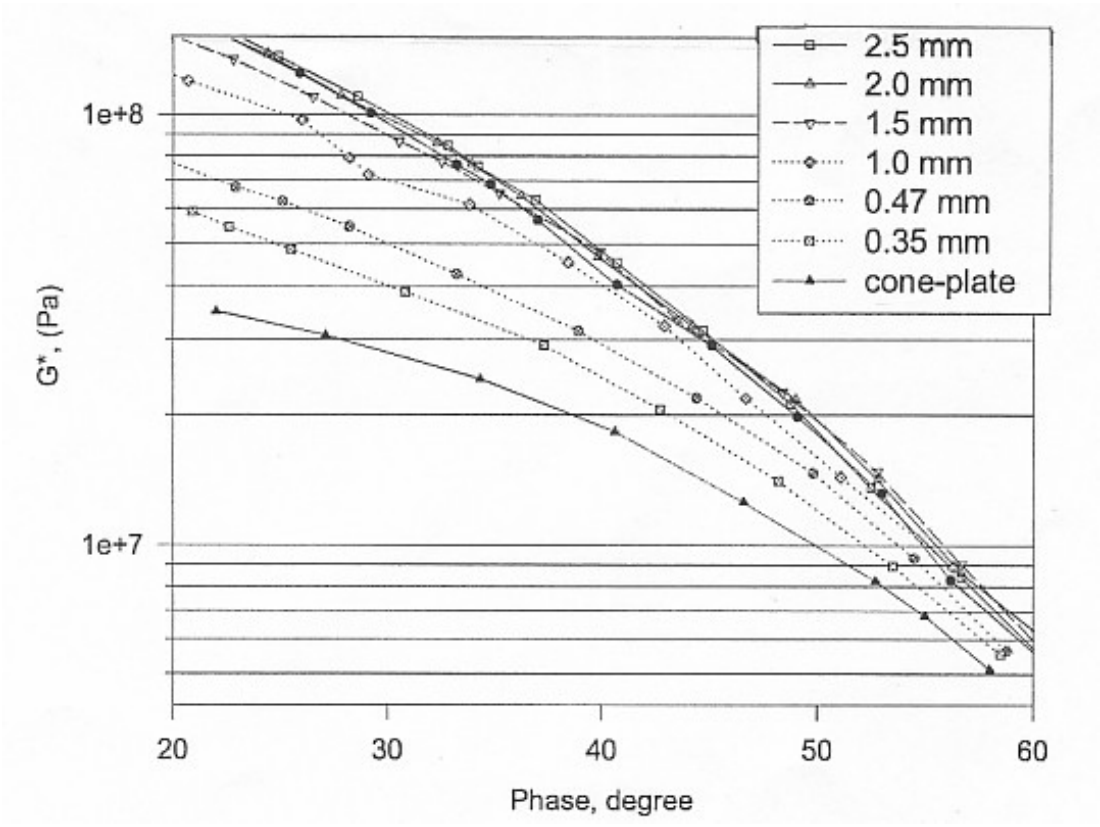

Figure 2.27: Rheological measurements at different gap settings (Soenen and Eckmann, 2000)

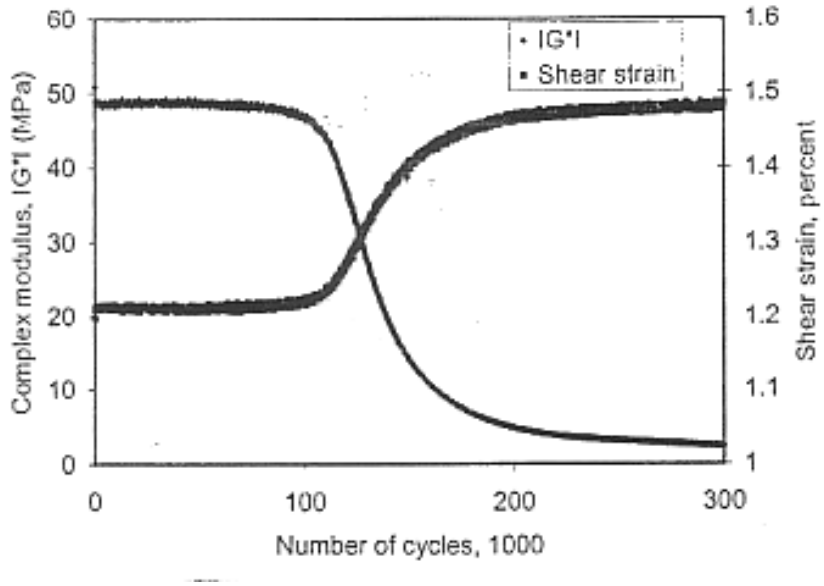

Figure 2.28: Compliance effect (after Anderson et al., 2001)

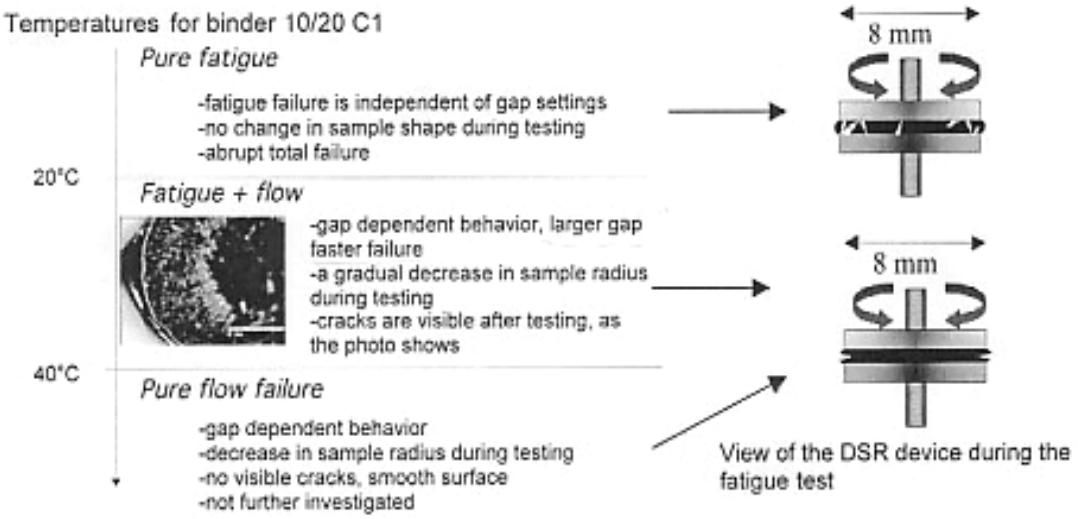

Figure 2.29: Schematic of the phenomena occurring in the DSR binder fatigue testing for 10/20 pen grade bitumen (Soenen et al., 2004)

2.5.3 Approaches of Fatigue Analysis

DSR fatigue tests using time sweeps for bituminous binders have been described earlier in this chapter. During the testing, a number of repetitive loads are applied to a bituminous binder and thus induce the change of material properties until a specimen fails. It is necessary to define fatigue failure in a consistent way for the establishment of the fatigue life in order to assess the fatigue relationship for a bituminous binder. Typically, there are two options of binder failure definition, which are included: (1) phenomenological approach: define fatigue failure using the number of cycles at which the modulus decreased to a predetermined value, and (2) dissipated energy approach: define fatigue failure using a criterion based on changes in dissipated energy.

Phenomenological Approach

The phenomenological approach has been traditionally used for the fatigue failure definition of asphalt mixtures. The definition of fatigue failure for bituminous materials in this approach depends on the modes of loading. In the controlled stress mode of loading, the specimen has a relatively short crack propagation period because the applied stress is held constant and the resulting strain gradually increases as the specimen is damaged until failure, thus, requiring more strain to produce the same stress. In the

controlled strain mode of testing, the specimen has a relatively longer crack propagation period because the strain is held constant and the resulting stress gradually decreases until the specimen is damaged, thus, requiring less stress to produce the same strain (Read, 1996). In the controlled stress mode of loading, the failure point is clearly determined as the specimen is completely fractured, whereas in the controlled strain mode of loading, the failure point is arbitrarily determined as a reduction of the initial stiffness modulus of 50% because the test time could be very long and the failure condition is not obvious, as shown in Figure 2.30.

The fatigue data (number of cycles to failure) are typically plotted against strain or stress. The straight fatigue lines for bituminous materials are generated by means of regression analysis. Figure 2.31 shows the typical fatigue lines for bituminous binders. The steeper line means the binder is more prone to initial shear strain.

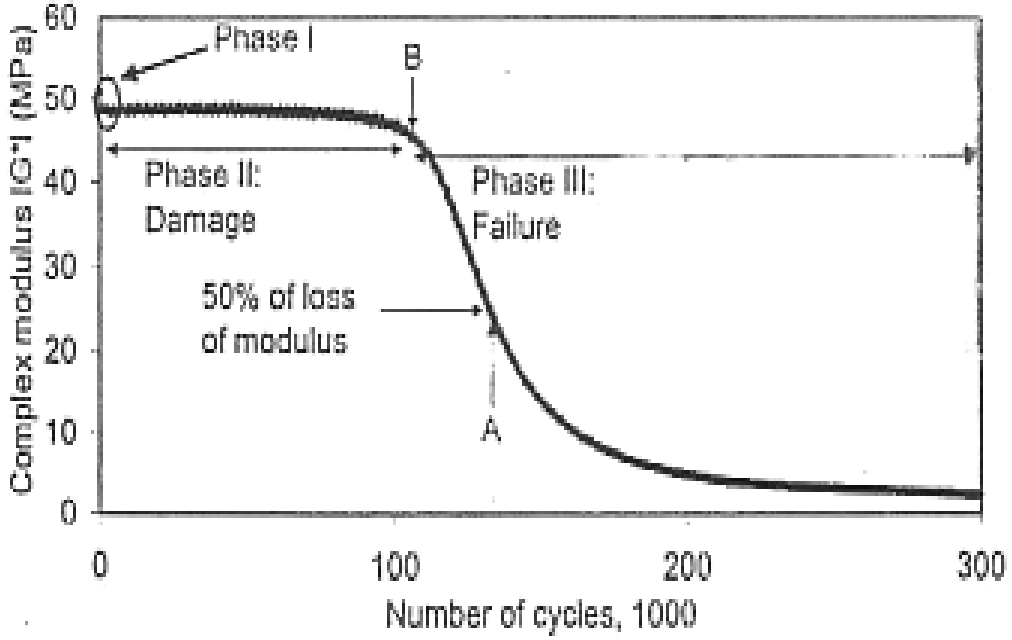

Figure 2.30: Definition of failure point under strain controlled loading mode (after Anderson et al., 2001)

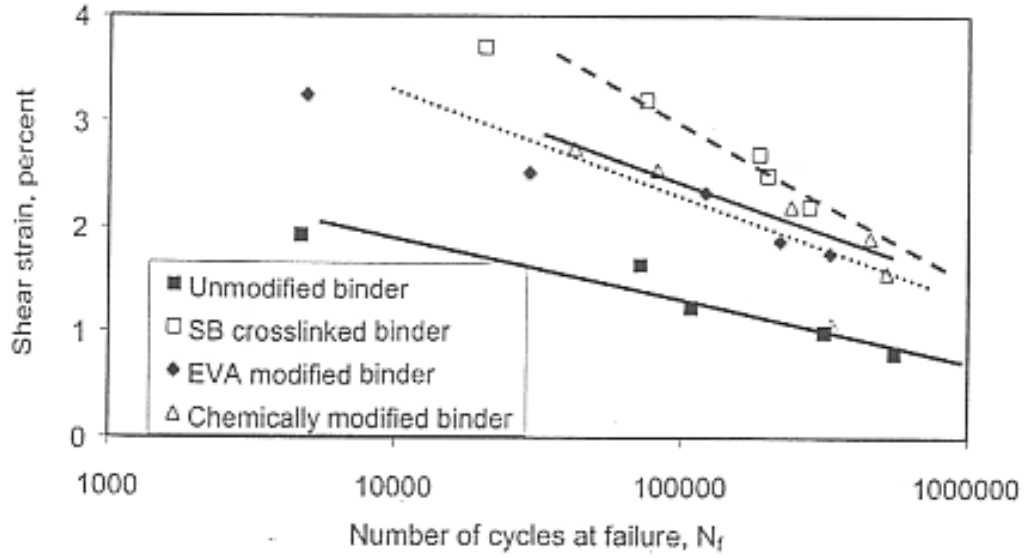

Figure 2.31: Fatigue lines for bituminous binders (Anderson et al., 2001)

Bahia et al. (2002) evaluated fatigue lives of bituminous binders by means of the phenomenological approach. They conducted time sweep tests on nine aged polymer modified bitumens under controlled strain mode of loading (3 percent strain) at 10 Hz at temperatures as close as possible to the mixture beam fatigue temperatures. The flexure beam fatigue tests were also performed on asphalt mixtures containing the same binder at 10 Hz under controlled strain mode of loading (400 microstrains). The fatigue lives of binders and mixtures were both determined by the number of cycles to 50 percent initial G* value. They found a high correlation for the fatigue relationship between the mixture performance and the binder fatigue life.

Soenen et al. (2004) also performed time sweeps on unmodified and modified bitumens at 25 Hz under controlled strain mode of loading and conducted two point bending fatigue tests on asphalt trapezoidal sample at 25 Hz. The binder and mixture fatigue tests were carried out at equi-stiffness conditions. The fatigue failure was determined as the 50 percent reduction of initial stiffness. The ε6 values (strain at which 1 million cycles causes a reduction in stiffness by 50 percent) of binder and mixture were compared. They found that a good agreement between binder and mixture fatigue for the unmodified bitumens. However, although there was an increase in fatigue life for

modified bitumens compared to plain bitumens in the binder fatigue testing, an increase in fatigue life for mixtures was not observed.

Dissipated Energy Method

Definitions of fatigue failure made on the basis of dissipated energy were considered since the criteria made based on phenomenological concept were arbitrary (for controlled strain mode of loading). Dissipated energy approach based on the viscoelastic theory has been used to analyse the fatigue behaviour of bituminous mixtures (Daniel et al., 2004; Fakhri and Shakel, 2003; Ghuzlan and Carpenter, 2000; Hopman et al., 1989; Pronk, 1997; Pronk and Hopman, 1990; Rowe, 1996; Rowe and Bouldin, 2000; Tayebali et al., 1992; Van Dijk, 1975; Van Dijk and Visser, 1977) as well as asphalt binders (Anderson et al., 2001; Bahia et al., 2002; Bonnetti et al., 2002; Martono and Bahia, 2003). The concept is that the amount of energy dissipated per loading cycle changes throughout a fatigue test. Figure 2.32 shows the difference in dissipation of energy between a linear elastic material and a viscoelastic material. With an elastic material, the energy stored in the system (when loaded) equals to the area under load-deflection curve, and during unloading, all the energy is recovered. A viscoelastic material, when unloaded, traces a different path to that when loaded. Therefore, the dissipated energy per cycle is equivalent to the area within the hysteresis loop as a bituminous material is sinusoidally loaded. If non-sinusoidal loading is applied, the area within the hysteresis loop can be calculated by means of numerical integration (Rowe, 1996).

When a bituminous material is subjected to sinusoidal loading, the dissipated energy (area within the hysteresis loop) per loading cycle can be given in terms of stress-strain behaviour:

$$W_i = \pi \sigma_i \varepsilon_i \sin \delta_i \tag{2.24}$$

where:

W_i = Dissipated energy at load cycle, i,

σ_t = Stress amplitude at load cycle, i,

ε_t = Strain amplitude at load cycle, i, and

δ_i = Phase angle between stress and strain wave signal at load cycle, i.

Hopman et al. (1989) proposed a ratio of energy dissipation and the further researchers (Anderson et al., 2001; Bahia et al., 2002) named it as dissipated energy ratio (DER), shown as follows:

$$DER = \frac{\sum_{i}^{n} W_i}{W_n} \tag{2.25}$$

where:

$\sum_{i}^{n} W_i$ = the total sum of dissipated energy up to cycle n, and

W_n =the dissipated energy at cycle n.

Anderson et al. (2001) proposed to use the DER to define fatigue failure. Figure 2.33 shows the typical plot of DER against number of cycles (for controlled strain mode of loading). A nonlinear transition is between two linear phases. They decided the failure as the point on the curve where the curve became nonlinear (point B) because using the intersections of two asymptotes as a fatigue criterion (point A) might overestimate the fatigue life of the material (Hopman et al., 1989). The transition between the two phases could be very wide.

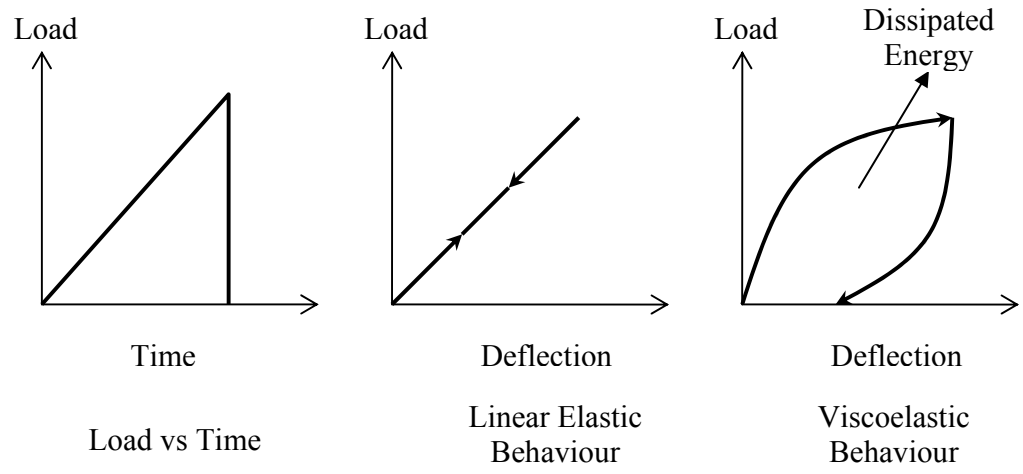

Figure 2.32: Dissipated energy for linear elastic and viscoelastic behaviour (after Rowe, 1996)

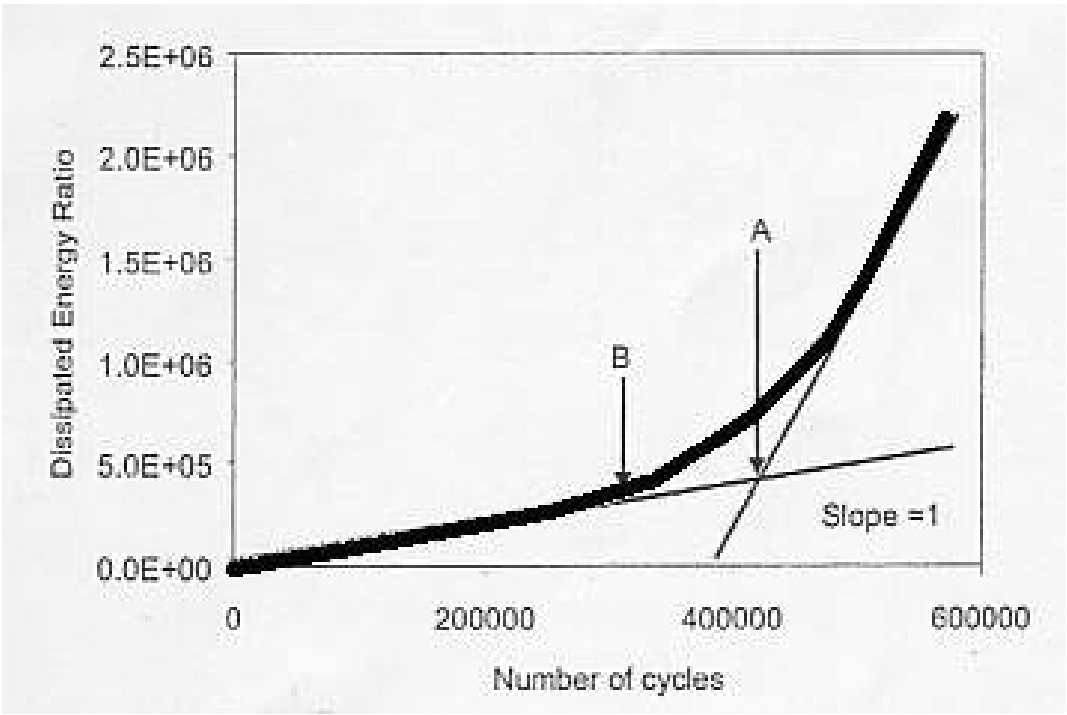

Figure 2.33: Typical plot of DER against number of cycles (after Anderson et al., 2001)

Bahia et al. (2002) also applied the DER concept to binder fatigue data. Figure 2.34 shows the plot of DER versus number of cycles for controlled strain and stress modes of loading. The intersection of the two asymptotes as a fatigue life criterion (N_p) was decided. They found the DER curves of the binder data were similar to the mixture data, indicating the main factor in the fatigue behaviour of mixtures could be well related to the fatigue damage in the binders. They also demonstrated the DER approach was selected because it was independent of the loading mode.

In addition, the number of load cycles to failure for the controlled stress testing can be easily determined from the peak of the energy ratio versus cycles. However, there is a difficulty of defining a sharp change in the controlled strain testing, and thus several parameters of failure definition were arbitrarily selected such as N_p (Bahia et al., 2002), N_1 (Hopman et al., 1989; Rowe, 1996) and N_{p20} (Bonnetti et al., 2002). N_p was defined as the number of cycles at which the intersection of two asymptotes. N_1 was determined as the number of cycles at where the curve becomes nonlinear. N_{p20} was defined as the number of cycles at which the dissipated energy ratio shows 20% deviation from the no-damage ratio.

Ghuzlan and Carpenter (2000) proposed a fatigue criterion based on dissipated energy for asphalt mixtures, named ratio of dissipated energy change (RDEC). The criterion was defined as the change in dissipated energy (ΔDE) between cycles a and a+1 divided by the total dissipated energy (DE) of load cycle a. The formula is shown as follows:

$$\frac{\Delta DE}{DE} = \frac{W_a - W_{a+1}}{W_a} \tag{2.26}$$

where:

W_a = the total dissipated energy at cycle a, and

W_{a+1} = the total dissipated energy at cycle a+1.

Ghuzlan and Carpenter (2000) found the damage accumulation ratio, ΔDE/DE, provided a consistent failure indicator for asphalt mixtures, which appeared to be independent of the mode of loading. However, Bahia et al. (2002) reported that for asphalt binders the RDEC was useful for the controlled stress testing because the failure point could be easily determined, while it was not for controlled strain testing due to the scattered results (see Figure 2.35).

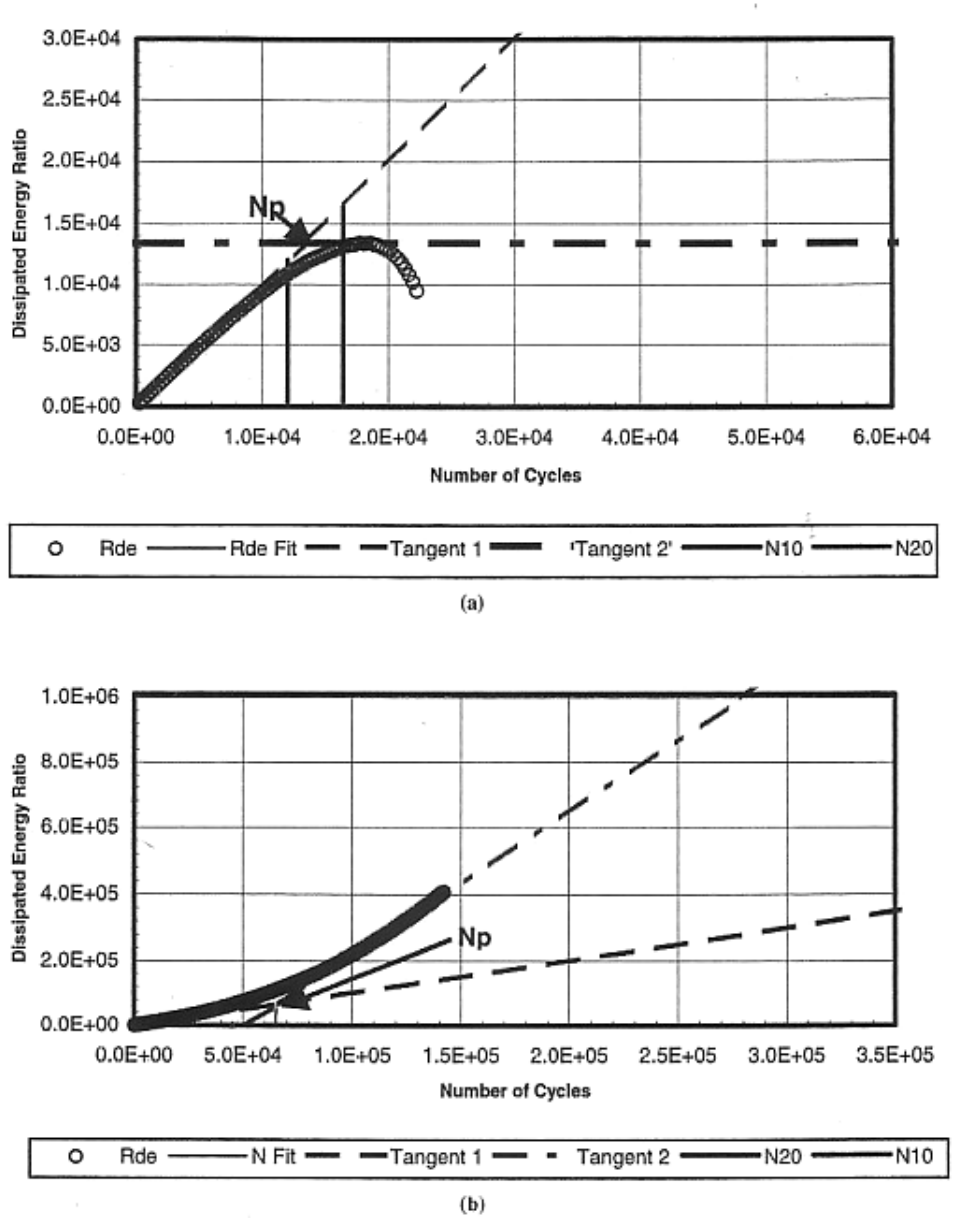

Figure 2.34: DER versus number of cycles : (a) stress controlled test; (b) strain controlled test (Bonnetti et al., 2002)

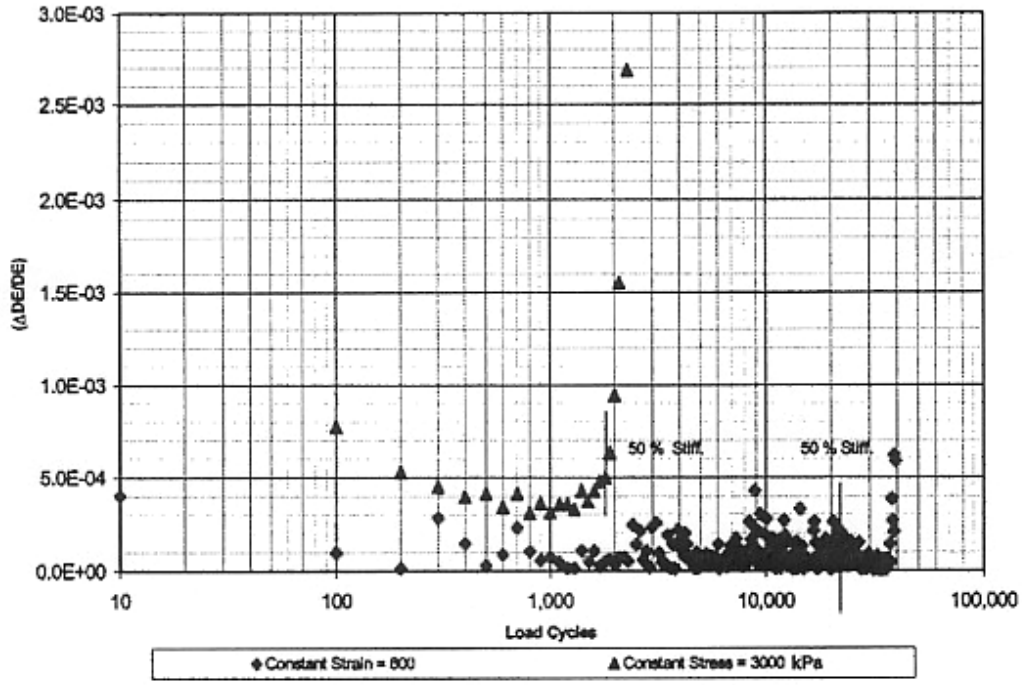

Figure 2.35: Determination of failure point using RDEC (Bahia et al., 2002)

2.6 Summary

The literature review presented in Chapter 2 has described the constitution and structure (colloidal system) of bitumens as well as the physical properties of mineral fillers. The effects of mineral filler properties such as particle size distribution, shape, Rigden voids, filler concentration and packing fraction on the physical and mechanical properties of bitumen-filler mastics and asphalt mixtures have also been reviewed in order to provide a background to understanding the role of mineral filler in mastics as well as mixtures in terms of the physical and chemical aspects. The mineral filler has been known to stiffen bitumen and significantly influence the mechanical properties of asphalt paving mixture as mineral filler particles are suspended in bitumen. However, as at high filler concentration or filler particles form a skeleton in bitumen, the rheological properties (viscosity and complex modulus) and mechanical properties (tensile strength) of bitumen-filler mastic are improved but the mechanical properties (tensile strength and

resilient modulus) of asphalt mixtures might be impaired due to the difficulties in asphalt mixing and compaction procedures.

This chapter also reviewed that the small strain shear oscillatory testing using a dynamic shear rheometer (DSR) provides a practical and relatively simple method to obtain a number of rheological parameters of bituminous binders within the linear region. The dynamic mechanical analysis (DMA) helps to understand the viscous and the elastic nature of binders over a wide range of temperatures and loading rates. In addition, the master curve also provides a form of presenting data, allowing the prediction of the complex modulus, phase angle, storage and loss stiffness modulus at any loading frequency or temperature and the comparison of dynamic data on an equal basis. However, practically, because bituminous binders exist as thin films in asphalt mixtures, they might perform in the non-linear region due to the considerable difference between modulus of aggregates and modulus of binders. The strain domains within binders are much higher than the bulk strain within asphalt mixtures (Bahia et al., 1999).

This chapter also presented the measurements of viscosity within linear range using different techniques. It is recognised that the binder contribution to rutting is a permanent deformation described by a viscosity. DSR creep testing using low stress levels provides a method of obtaining the steady state viscosity of binders. The only viscosity in the linear region has been selected to evaluate the permanent deformation resistance of asphalt mixtures. Measurement techniques performed on a DSR with the zero shear viscosity (ZSV) being determined directly from the plotted data or, particularly in the case of the oscillation test, extrapolated to zero frequency using an appropriate mathematical model have also been introduced in this chapter. However, again, the tests were performed using low stress and strain levels. The tests should be expanded to evaluate deformation properties of binders in non-linear viscoelastic response.

The concept of using damage characterisation by performing fatigue testing of bituminous binders has been considering as an alternative to predict the true fatigue behaviour of binders. Direct testing of bituminous binders in fatigue has been used to

generate load-associated fatigue characteristics for bituminous binders by means of time sweep tests using a DSR at various strain and stress levels in the linear and non-linear ranges. During the repeated shear loading fatigue testing, the dominance of the two failure mechanisms of true fatigue and edge fracture depending on the modulus of the binder should be considered. Two fatigue analyses of phenomenological approach and dissipated energy method for determination of failure point are also reviewed in this chapter.

In this investigation, a straight-run bitumen with three types (one active and two inert fillers) of mineral filler having different particle size distribution, specific gravity, specific surface area and Rigden voids will be tested using a DSR. Three filler concentration levels in bitumen-filler mastics are selected as filler particles are suspended in bitumen (low content) and filler particles form a skeleton in bitumen (high content). At low filler content, the bitumen/filler ratio in bitumen-filler mastic is the same as that in Dense Bitumen Macadam (DBM) mixture, while at high filler content the filler skeleton in bitumen-filler mastic might represent mineral aggregate skeleton in DBM.

Various techniques using a DSR will be conducted on bitumen-filler mastics in linear as well as non-linear range in order to understand the stiffness, permanent deformation property and fatigue characteristic of mastics. The mechanical properties of bitumen-filler mastics might reflect those of DBM mixtures.

The physical properties of bitumen and mineral fillers as well as small strain oscillatory tests will be described in Chapter 3. Creep tests and the extrapolation of ZSVs will be discussed in Chapter 4. Fatigue tests and analyses of bitumen-filler mastics will be also included in Chapter 5.

3

Small Strain Rheological Analysis

3.1 General

Empirical tests for bituminous binders have been used to represent the physical properties of binders and link these to the performance of asphalt mixtures. Penetration test (BS EN 1426, 2000) has been used to classify the grade of bitumen; the determination of softening point (BS EN 1427, 2000) for bitumen has been related to the permanent deformation of asphalt mixtures; and Fraass breaking point (BS EN 12593, 2000) for bitumen has been associated with the brittle fracture of asphalt pavements. However, these conventional specifications and tests only determine the binder's characteristics at particular temperature and loading rate conditions. Particularly, the use of specialist binders, such as polymer modified bitumens (PMBs) are not necessarily characterised by the traditional parameters from these empirical tests. Fundamental rheological testing using a dynamic shear rheometer (DSR) enables the complete rheological bitumen properties to be determined and related to pavement performance. Using the DSR, the viscoelastic properties of bituminous binders can be characterised over a wide range of temperature and loading time conditions.

Bituminous binder in an asphalt mixture occurs not as bitumen alone, but is mixed with mineral fillers forming the mastic. The physical properties and chemical constituents of mineral fillers significantly affect the rheological and mechanical properties of bitumen-filler mastic. The role of mineral fillers also has been known to considerably influence the mechanical properties of asphalt paving mixtures, as described in Chapter 2. In this study, a combination of one penetration grade bitumen, three filler types and three filler concentrations of 15%, 35% and 65% was selected to assess the filler effect on rheological properties of bitumen-filler mastics by performing dynamic shear oscillatory testing using small strains.

This chapter focuses on the strain and stress linear viscoelastic limits as well as filler stiffening effect on rheological characteristics of bitumen-filler mastics using a set of oscillatory testing with the Bohlin Gemini 200 Dynamic Shear Rheometer. Critical analysis of the rheological data indicates that the rheological character differs for pure bitumen (base bitumen) and various bitumen-filler mastics.

3.2 Materials

3.2.1 Bitumen

A conventional 50 penetration grade bitumen typically used for asphalt pavement construction in the United Kingdom was selected as the base bitumen to mix with mineral fillers in the test programme. This straight-run bitumen originated from a Venezuelan crude was supplied by Nynas Bitumen Limited. The specification parameters of penetration and softening point are presented in Table 3.1.

Table 3.1: Base bitumen properties

Bitumen type	Source	Specific gravity	Penetration (dmm)	Softening point (^{o}C)
50 penetration grade	Venezuelan	1.02	50	50.2

3.2.2 Mineral Filler

The mineral fillers in this study are defined as 90 percent of particles passing a 75 μm sieve. Three types of mineral fillers of limestone, cement and gritstone were selected for the investigation on the basis of their physical properties (particle size distribution, specific gravity, specific surface area and Rigden voids), chemical reaction with bitumen (inert and active) and potential for mastic stiffening. The description of the mineral fillers is briefly described as follows:

- Limestone is composed primarily of calcium carbonate ($CaCO_3$). Limestone filler is a typical material used in asphalt paving mixtures,

- Cement is made primarily from limestone, certain clay and gypsum in a high temperature process. Cement is a typical material used in building construction and is sometimes used in asphalt paving mixtures as filler. Cement can bind some materials together when combined with water, and
- Gritstone is a sedimentary rock composed of coarse sand grains with inclusions of small stones, containing quartz and/or feldspar. Gritstone filler is a natural material from crushed gritstone and is typically used in asphalt paving mixtures.

Table 3.2 lists the physical properties of specific gravity, specific surface and Rigden voids of mineral fillers. It is noted that the gritstone filler has the highest specific surface and Rigden void content compared to the limestone filler and cement filler. Craus et al. (1978) reported that variations in specific surface were mainly due to the variations in the geometric irregularity (shape and surface texture) of filler particles. Traxler et al. (1933) also proposed that the differences in void content of dry compacted filler might be attributed to differences in particle shape and texture. Therefore, the high specific surface and Rigden void content for the gritstone filler compared to limestone filler and cement filler should be caused by the increase in geometric irregularity (compared to smooth spheres) of filler particles.

Table 3.3 and Figure 3.1 show the gradation of each type of mineral filler which was measured by performing a laser diffraction technique. The limestone filler undoubtedly has the finest particles. The cement filler and gritstone filler have similar particle size distribution but the gritstone filler particles are slightly finer than cement filler particles below the particle size fraction of 10 μm. In terms of the physical properties of mineral fillers, limestone filler has the finest particles, gritstone filler has angular particles, and cement filler and gritstone have a similar size distribution but cement filler is rather coarser than gritstone filler.

Limestone filler (contains calcium carbonate) and gritstone filler (contains quartz and/or feldspar) are considered to be chemically stable materials, and bitumens are shown to have little chemical reaction with them (Anderson, 1987; Kavussi and Hicks, 1997;

Soenen and Teugels, 1999). They are embedded in bitumen and thus are considered as inert fillers. With regard to cement, it might have chemical reaction with bitumen. Little and Petersen (2005) reported carboxylic acids and 2-quinolone types which are present in bitumen react irreversibly with the carbon hydroxide ($Ca(OH)_2$). As water is present in the interface between bitumen and cement filler, carbon hydroxide is produced and thus cement filler might chemically react with bitumen. Therefore, cement filler will be considered to be an active filler.

Table 3.2: Physical properties of mineral fillers

Filler type	Source	Specific gravity[1]	Specific Surface[2] (m^2/g)	Rigden Voids[3] (%)
Limestone	Longcliffe	2.74	1.3	24.86
Cement	Ordinary	3.18	1.4	28.38
Gritstone	Bayston Hill	2.65	6.0	32.88

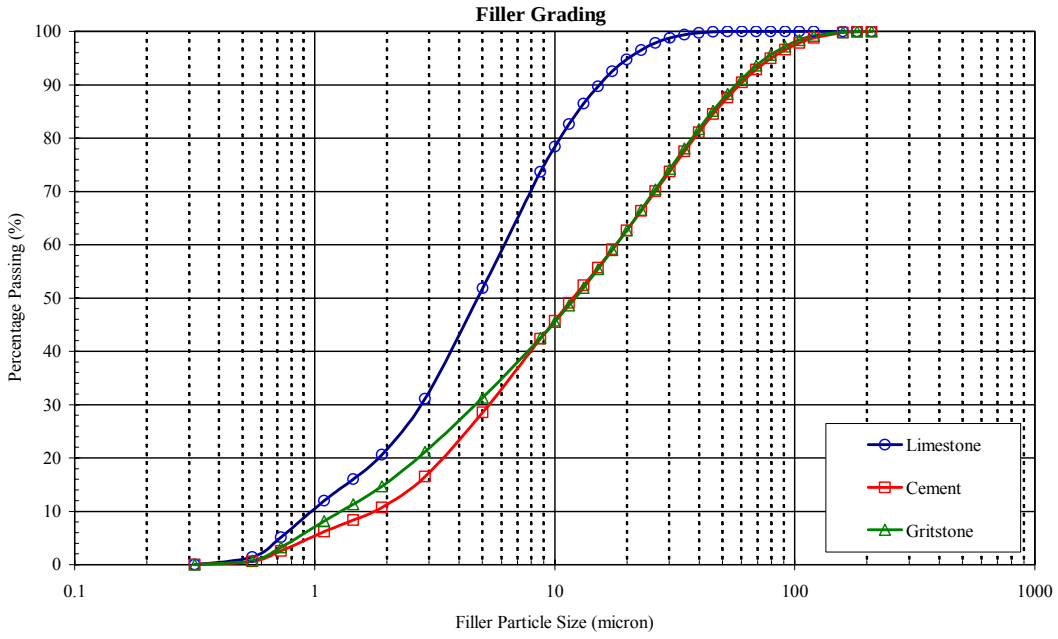

Figure 3.1: Particle size distributions for the mineral fillers by laser diffraction technique[4]

[1] Data were generated by Osman (2005) according to BS EN 1097-7: 1999
[2] Data were generated by BET nitrogen absorption technique according to BS 4359-1: 1996 at Ceram Research
[3] Data were generated using Rigden apparatus according to BS EN 1097-4: 1999
[4] Results of filler gradation were generated by Laser Diffraction technique at Minelco Specialities Limited

Table 3.3: Particle size distributions for the mineral fillers by laser diffraction technique[5]

Particle Size (micron)	Limestone Passing (%)	Cement Passing (%)	Gritstone Passing (%)
208.93	100	100	100
181.97	100	99.96	99.99
158.49	100	99.79	99.88
120.23	100	98.76	99.17
104.71	100	97.85	98.38
91.20	100	96.58	97.20
79.43	100	94.94	95.61
69.18	100	92.89	93.57
60.26	100	90.45	91.12
52.48	100	87.64	88.29
45.71	99.92	84.50	85.11
39.81	99.74	81.06	81.67
34.67	99.38	77.48	78.03
30.20	98.78	73.76	74.24
26.30	97.85	70.01	70.39
22.91	96.53	66.30	66.53
19.95	94.76	62.67	62.72
17.38	92.50	59.15	59.00
15.14	89.73	55.72	55.40
13.18	86.44	52.37	51.95
11.48	82.64	49.06	48.65
10.00	78.36	45.73	45.49
8.71	73.64	42.37	42.47
5.01	51.87	28.55	31.34
2.88	31.08	16.50	21.15
1.91	20.61	10.74	14.71
1.45	16.04	8.32	11.29
1.10	11.97	6.19	8.13
0.72	5.13	2.58	3.23
0.55	1.41	0.62	0.77
0.32	0.00	0.00	0.00
0.00	0.00	0.00	0.00

[5] Results of filler gradation were generated by laser diffraction technique at Minelco Specialities Limited

3.3 Bitumen-Filler Mastic System

The contribution of bituminous binders to asphalt mixtures is to fill the voids and lubricate between coarse aggregates. Bituminous binder within an asphalt mixture occurs not as bitumen alone, but is mixed with mineral fillers forming the mastic. It can be argued that rheological properties of bitumen-filler mastic rather than pure bitumen may be more appropriate in the search to establish correlations with mechanical properties of asphalt mixtures. If the physical contact between filler particles and other particles is absent, a suspension of filler in bitumen must be present. These suspended mineral particles should produce a measurable effect on the bitumen in an asphalt paving mixture (Tunnicliff, 1967). On the other hand, mineral filler is part of what is usually called aggregate. These fine particles might establish physical contact with other particles through the bitumen medium. The mechanical properties of asphalt mixtures might be reflected by those of bitumen-filler mastic as the filler skeleton is present in bitumen.

The purpose in this chapter is to investigate the rheological properties of bitumen-filler mastic as considering filler particles are suspended in bitumen as well as filler skeleton (physical contact) is present in bitumen. A total of seven bitumen-filler mastics were produced using a 50 penetration grade bitumen as the base bitumen, three filler types (limestone, cement and gritstone) and three filler concentrations of 15%, 35% and 65% by mass. The filler concentrations of 15% and 35% represent filler particles that are suspended in bitumen, while the filler concentration of 65% represents the filler skeleton that is present in bitumen. The filler concentration by mass is considered in order to easily compare with the filler proportion in asphalt mixture design. The filler proportion in asphalt mixture design is normally shown by mass content. The filler concentration by volume and effective volume will be also calculated by means of Rigden voids, specific gravity and mass of mineral filler.

The following sections look at the preparation of bitumen-filler mastic, combination of bitumen-filler mastic and filler effective volume in bitumen-filler system.

3.3.1 Bitumen-Filler Mastic Preparation

The bitumen-filler mastics were produced by adding the correct mass of filler to heated bitumen at a temperature of 160^{o}C while mixing the two components together with the Silverson L4RT high shear mixer (shown in Figure 3.2) until a homogeneous mastic was obtained. The mixing time was restricted to a maximum of 5 minutes. The mixing procedures are detailed as follows:

- Mineral filler was put into a 160^{o}C oven for 24 hours to ensure moisture-free particle surfaces.
- The 50 penetration grade bitumen stored in a 5 litre tin needed 5 hours to preheat in a 160^{o}C oven and to make bitumen liquid and ready to mix.
- The accurate quantity of the bitumen was poured into a 2.5 litre tin. The tin with the bitumen was left on a hot plate maintained at 160^{o}C.
- The bitumen was mechanically stirred for 30 seconds. The accurate mass of the mineral filler was added slowly while the mechanical stirring was continued for 4.5 minutes.
- The mastic was continuously stirred as it cooled to prevent settling and was then transferred to several vials to make samples for further testing.
- The mixing process was carefully followed so that the mineral filler was homogeneously dispersed in the bitumen.

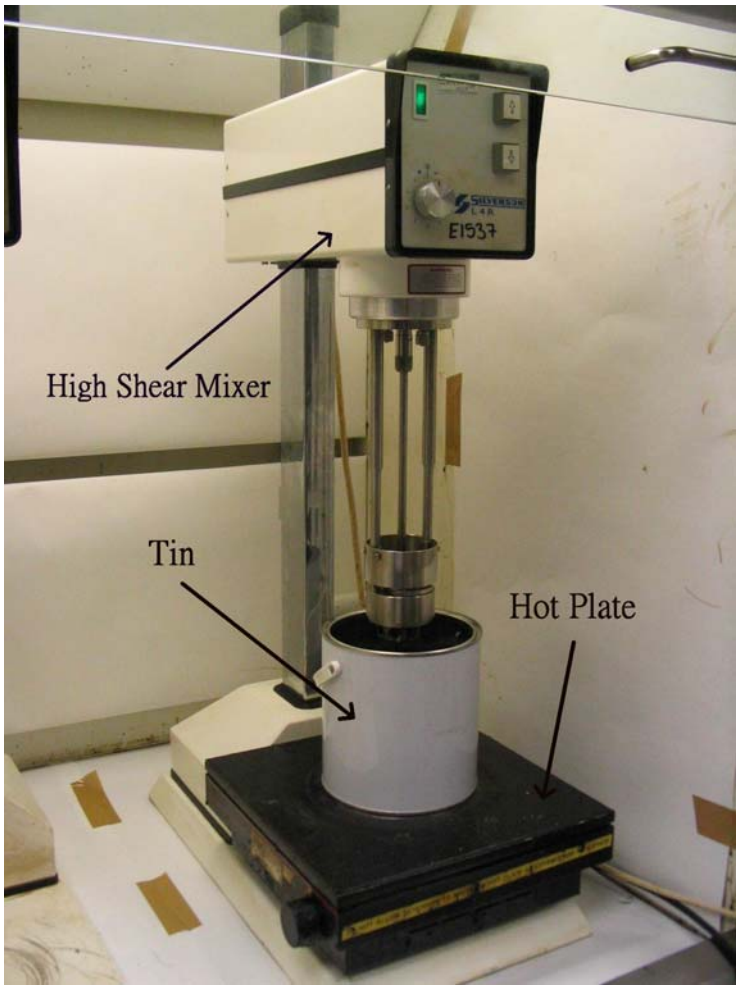

Figure 3.2: Bitumen-filler mastic blending facilities

3.3.2 Filler Concentration by Mass

A combination of one 50 penetration grade bitumen (base bitumen), three filler types and three filler concentrations of 15%, 35% and 65% by mass were included in the testing programme, as shown in Table 3.4. The filler concentration by mass is considered in order to easily compare with the filler proportion in asphalt mixture design because the filler proportion in asphalt mixture design is normally shown by mass content. The choices of using 15%, 35% and 65% to prepare the bitumen-filler mastics are based on the filler content for a DBM mixture. The selection of filler content will be discussed in the next section.

The determination of filler concentration in a bitumen-filler mastic is given by:

$$\text{Filler concentration by mass} = \frac{Mass_{filler}}{Mass_{filler} + Mass_{bitumen}} \quad (3.1)$$

The determination of ratio of filler to bitumen based on mass is given by:

$$\text{Ratio of filler to bitumen by mass} = \frac{Mass_{filler}}{Mass_{bitumen}} \quad (3.2)$$

Table 3.4: Matrix of bitumen-filler mastics

Materials / Filler Contents	Base Bitumen	Bitumen-Filler Mastics		
	50 Pen Bitumen	Limestone	Cement	Gritstone
0%	x			
15%		x		
35%		x	x	X
65%		x	x	X

The comparison of ratios of filler to bitumen (by mass) between the investigation and the Superpave requirement is shown in Table 3.5. The requirement within Superpave system for filler is a range of filler-to-bitumen ratios of between 0.6 and 1.2 based on mass. In this investigation, the filler-to-bitumen ratios of 0.18 and 0.54 can be considered as filler particles are suspended in bitumen, while the ratio of 1.86 can be considered as the physical contact between filler particles is present in bitumen. However, the use of limiting filler content based on mass may not be the best for investigating bitumen-filler system because it does not account the stiffening potential of a given filler to be evaluated. The physical properties such as particle size distribution, Rigden voids, particle shape and specific surface considerably influence the rheological properties of bitumen-filler mastics and the mechanical properties of asphalt mixtures. Filler volumetric concentration and packing effect within a bitumen-filler system should be considered.

Table 3.5: Ratio of filler to bitumen in bitumen-filler system

Selection of Filler Content in the Investigation		Filler Proportion in Superpave Mixture
Filler Content by Mass	Ratio of Filler to Bitumen	Ratio of Filler to Bitumen
15%	0.18 (15/65)	0.6
35%	0.54 (35/65)	to
65%	1.86 (65/35)	1.2

3.3.3 Filler Packing Fraction

Volumetric proportion of filler including Rigden voids is a main parameter to influence the rheological properties of bitumen-filler mastics, and thus filler packing fraction must be considered in the investigation. Tunnicliff (1967) stated that packing referred to the degree of dispersion of filler particles in bitumen-filler mastic. Packing and concentration were not the same because concentration was concerned only with the volume occupied by particles, whereas packing involved space between particles.

Lesueur and Little (1999) reported that filler maximum packing fraction would be lower than filler volume fraction measured on the dry filler (1-Rigden Voids). The effect is complicated by the presence of an adsorption layer around the filler particles, a certain extent of particle aggregation, or both. Any physicochemical interaction parameter between bitumen and filler should be considered. The same filler does not have the same maximum packing volume in different bitumens, which shows a different degree of dispersion of the filler in different bitumens or different interactions with different bitumens.

In this study, the determination of filler concentration by volume within a bitumen-filler mastic is given:

$$V_f = \frac{\frac{Mass_{filler}}{SG_{filler}}}{\frac{Mass_{filler}}{SG_{filler}} + \frac{Mass_{bitumen}}{SG_{bitumen}}} \tag{3.3}$$

where V_f is the filler concentration by volume.

The results of filler packing fraction for the bitumen-filler mastics were obtained in terms of the formulas in Heukelom's (1965) literature (has been reviewed in Section 2.2.5). Table 3.6 summarises the filler concentrations by volume and filler packing fractions.

At the same filler concentration by mass, the highest effective volume (solid phase) in a bitumen-filler mastic for the gritstone filler compared to the limestone and cement fillers is caused by the gritstone filler having angular particles, higher specific surface and higher Rigden voids. The lowest effective volume for the cement filler compared to the limestone and gritstone fillers might be because the cement filler has coarser particles and higher specific gravity. Because there is no water involved in the mixing process, the cement filler should have no/little effect on effective volume of bitumen-filler mastic. The cement filler is considered to be an inert filler and the particles are embedded in bitumen.

The choices of using 15, 35 and 65 mass percent to the prepare bitumen-filler mastics are based on the fact that the mineral fillers passing 75 μm sieve work out to about 35% to 60% by mass of the bitumen for a DBM mixture. As a 10 mm DBM mixture is produced by limestone aggregates (specific gravity = 2.7) mixed with an optimum bitumen (specific gravity = 1.02) content of 5.2%, the percentage of fillers by mass passing 75 μm sieve is between 3% and 8% of total mass of aggregates according to the specification of grading limits in British Standard. Table 3.7 shows the filler contents for the limestone bitumen-filler mastics in comparison with the filler (limestone) contents for a 10 mm DBM close graded wearing course (BS 4987-1: 1993).

Anderson (1987) suggested that the free bitumen content in the filler fraction should be maintained at 40% or less on the basis of the mechanical properties and the observed workability of asphalt mixtures in the laboratory. Chen and Peng (1998) indicated that the free bitumen volume should be larger than 30 percent. At a 30% ratio the mineral filler is floating in the bitumen and particle-particle contact between mineral filler no

longer exists. Soenen and Teugels (1999) claimed that above the filler content of 45% by volume the filler skeleton gradually started to influence the rheological behaviour as temperature increased. Although the literature revealed that the mineral filler particles might be considered to be suspended in the bitumen, Table 3.7 shows filler content by mass in mastic should not be greater than 60% in terms of the limit specification of aggregate gradation. The physical contact or filler skeleton should be present in bitumen and thus they influence the performance of asphalt mixture.

Table 3.6: Filler and bitumen contents in bitumen-filler system

Content / Filler	Filler Content by Mass	Filler Content by Volume (V_f)	Filler Content by Effective Volume (V_{fa}) (Solid Phase)	Free Bitumen Volume Content (Fluid Phase)
Limestone Filler	15 %	6.2 %	8.3%	91.7 %
	35 %	16.7 %	22.2%	77.8 %
	65 %	40.9 %	54.4%	45.6 %
Cement Filler	35 %	14.7 %	20.6%	79.4 %
	65 %	37.3 %	52.1%	47.9 %
Gritstone Filler	35 %	17.2 %	25.6%	74.4 %
	65 %	41.7 %	62.1%	37.9 %

Table 3.7: Comparison of limestone filler contents in bitumen-filler mastics and limestone filler contents in DBM mixture

Selection of Filler Content in the Investigation			10 mm DBM Mixture		
Filler Content by Mass of Mastic	Filler Content by Volume of Mastic	Filler Content by Effective Volume of Mastic	Filler Content by Mass of Aggregate	Filler Content by Mass of Mastic	Filler Content by Volume of Mastic
15%	6.2%	8.3%	3%	35.3%	17.1%
35%	16.7%	22.2%	5%	50.1%	27.5%
65%	40.9%	54.4%	8%	59.3%	35.5%

3.4 Testing Programme

The general principle of the dynamic oscillatory shear load test is to determine the dynamic rheological properties of bituminous binders in a wide range of angular frequencies and test temperatures by means of an oscillatory rheometer with a parallel plate test geometry. A hockey puck-shaped bituminous sample is squeezed between two concentric, circular, and parallel plates. The sample is subjected to either a sinusoidal torque or a sinusoidal angular displacement of constant angular frequency during the test. The introduction of DSR and dynamic mechanical analysis have been reviewed in Chapter 2. The following two sections look at the stress sweep and frequency sweep oscillatory DSR tests.

3.4.1 Stress Sweep Test

Using controlled stress mode, the range of the linear viscoelastic behaviour of the bitumen and bitumen-filler mastics was determined by performing a stress sweep. The test parameters were shown as follows:

- Test temperatures : 5, 30, 45 and 60^{o}C,
- Test frequencies : 1.6, 10 and 25 Hz,
- Mode of loading: stress controlled loading, and
- Test geometry and gap: 8-mm diameter thick shaft parallel plates with a 2-mm gap, 8-mm diameter standard parallel plates with a 2-mm gap and 25-mm diameter parallel plates with a 1-mm gap. Table 3.8 shows the use of test geometry for the bitumen and bitumen-filler mastics.

The bituminous specimen was tested by increasing the shear stress over a range of values. The stress linearity limits were determined as the point beyond which the measured shear complex modulus reduces to 95% of its zero stress value. The determination of linearity of bituminous binders has been reviewed in Chapter 2.

Table 3.8: The use of test geometry for bitumen and bitumen-filler mastics (stress sweeps)

Material	Geometry	5°C	30°C	45°C	60°C
50 Pen Bitumen	8-mm thick shaft PP	x			
	8-mm standard PP		x		
	25-mm standard PP			x	x
Bitumen-Filler Mastic	8-mm thick shaft PP	x			
	8-mm standard PP		x	x	
	25-mm standard PP				x

* PP is the acronym for parallel plate

3.4.2 Frequency Sweep Test

The data of rheological parameters were generated using a frequency sweep under small strain conditions to ensure response within linear viscoelastic range. The viscoelastic characteristics of the bitumen were interpreted in terms of various material functions such as complex modulus, phase angle, loss modulus, storage modulus and meaningful combinations of these functions. The frequency sweep testing was performed on the bitumen and bitumen-filler mastics under strain controlled loading conditions by applying a sinusoidal angular displacement of constant amplitude within the linear viscoelastic domain. Different diameter parallel plates for the small strain oscillatory testing were used, depending on the test temperatures as shown in Table 3.9. The test parameters are shown as follows:

- Test temperatures : 5°C to 85°C, and 5°C intervals,
- Test frequency : 0.1 to 20 Hz,
- Mode of loading: strain controlled loading (small strains), and
- Test geometry and gap: 8-mm thick shaft parallel plates with a 2-mm gap, 8-mm diameter standard parallel plates with a 2-mm gap and 25-mm diameter parallel plates with a 1-mm gap.

Table 3.9: The use of test geometry for bitumen and bitumen-filler mastics (frequency sweeps)

Material	Test Geometry	Temperature
Bitumen	8-mm thick shaft PP	5°C to 15°C
	8-mm standard PP	20°C to 40°C
	25-mm standard PP	45°C to 85°C
Bitumen-Filler Mastic	8-mm thick shaft PP	5°C to 15°C
	8-mm standard PP	20°C to 45°C
	25-mm standard PP	50°C to 85°C

3.5 Testing Equipment and Sample Preparation

3.5.1 Dynamic Shear Rheometer

Dynamic Shear Rheometers (DSRs) are used to measure the rheological characteristics of bituminous binders. The principles involving in dynamic shear rheometry testing and dynamic mechanical analysis have been reviewed in Chapter 2. In this investigation, a Bohlin Gemini 200 Dynamic Shear Rheometer having a torque range between 0.5 (μN·m) and 200 (mN·m) was used for measuring the rheological parameters of bitumen and bitumen-filler mastics. The DSR is a controlled stress and strain instrument, which either applies a stress to a specimen and thus measures a resultant displacement or applies a displacement to a specimen and thus measures a resultant stress. The principal component of this rheometer is schematically shown in Figure 3.3. A constant motor in the rheometer works by a drag cup system. An angular position sensor detects the movement of the measuring system attached to the shaft. The software converts the applied torque to a shear stress when displaying data, and the reading from the position sensor is converted to a shear strain.

Temperature Controlled System

A water bath temperature control system was used with the Bohlin Gemini 200 DSR. A bituminous sample was submerged in the circulating water bath during testing. It is a more accurate and reliable temperature control system for bituminous sample tested

between 0°C and 85°C compared to Peltier and ETM (extended temperature module) temperature controlled systems (Airey, 1997). The temperature controlled system is capable of maintaining a temperature to within 0.1°C.

Parallel Plates Geometry

Three types of test geometry used for the DSR testing include 25-mm standard diameter parallel plate geometry, 8-mm diameter standard parallel geometry and 8-mm diameter thick shaft parallel plate geometry. It is essential to select spindle geometry (upper plate) for DSR testing on bituminous binders due to the effect of spindle compliance on rheological measurements when testing stiff binders. Anderson et al. (1994) suggested that 25-mm standard parallel plates should be used as the complex modulus ranges from 10^3 to 10^5 Pa, and 8-mm standard parallel plates should be used as the complex modulus ranges from 10^5 to 10^7 Pa (above the complex modulus of 10^7 Pa, torsion bar test is suggested to be used). The 8-mm thick shaft spindle is suggested to be used as the complex modulus is above 10^6 Pa (Bohlin DSR Manual).

Figure 3.3: Bohlin Gemini 200 DSR

3.5.2 Sample Preparation

The sample preparation is essential because the sample geometry may cause inaccurate rheological measurements. Prior to mounting a bituminous sample between a parallel plate geometry, two plates should be sufficiently warm (approximately 45^{o}C) that a good adhesion between a sample and plates can be achieved. The procedure of bituminous sample preparation is listed as follows:

- The bituminous sample stored in a small vial needs 20 minutes to preheat in a 160^{o}C oven, and to make the sample liquid and ready to pour.
- Remove the bituminous sample from an oven and then stir it manually for 20 seconds to ensure the mineral filler were not settled.
- Pour directly the sufficient quantity of the bituminous sample onto the lower plate until it nearly covered the plate.
- Close the plates to the target gap plus 50 micron for the bulge.
- Trim the extra specimen by moving a heating trimming tool around the upper and lower plates.
- Adjust the gap to the desired testing gap after trimming.

The procedure causes a hockey puck-shaped specimen and a desired bulge at the periphery of specimen. It is noted that the periphery of a specimen retains a convex shape as the temperature is changed. The sample should not shrink to the point where the edge becomes concave (Petersen et al. 1994).

3.6 Test Results and Discussion

3.6.1 Linear Viscoelastic Limits

The linear viscoelastic (LVE) limits for the base bitumen (50 penetration grade bitumen) and bitumen-filler mastics at various test temperatures and frequencies were determined from a set of shear complex modulus (G*) versus strain, as well as stress, plots as the point at which G* reduces to 95% of initial value (zero strain or zero stress values) as shown in Figures 3.4 and 3.5.

Figures 3.6 and 3.7 show the LVE strain and stress limits as functions of complex modulus values. The SHRP LVE strain and stress criteria are also included to compare to the data of bitumen-filler mastics in this study. There is a general increase in the LVE strain limit with a reduction in complex modulus for the binders, while there is an increase in the LVE stress limit with an increase in complex modulus. The LVE strain and stress limits for the base bitumen and bitumen-filler mastics containing 15% and 35% filler concentrations are all very similar although the LVE limits for the pure bitumen is somewhat higher than those of the bitumen-filler mastics. However, a divergence in the linearity limit of the 65% bitumen-filler mastics appears that the LVE strain and stress limits are below the SHRP LVE criteria. It indicates that the 65% bitumen-filler mastics have relatively narrower linear ranges and therefore lower linearity limits compared to the base bitumen and bitumen-filler mastics containing low (15%) and intermediate (35%) filler contents.

In terms of the LVE limits of the bitumen and bitumen-filler mastics, the linearity results provide an evidence that at the low and intermediate filler concentrations the mineral filler particles are suspended in the bitumen, whereas at the high filler concentration the physical contact between particles or filler skeleton are present in the bitumen-filler system. Soenen and Teugels (1999) reported that as the filler concentration was above 45% by volume in a mastic, the filler skeleton gradually began to influence the rheological behaviour with increasing temperature. They claimed that it was difficult to find a linear viscoelastic region, and the modulus measurements became sensitive to small changes during mastic sample loading. The linear viscoelastic region was also shifted to very low strain levels. Figures 3.6 and 3.7 show an increase in data scatter for the 65% bitumen-filler mastics at the low modulus caused by the complex modulus measurements being sensitive to applied shear loading during testing. The results clearly reflect that the LVE limits for the bitumen-filler mastics are relatively lower compared to the base bitumen due to the stiffening effect on binders as well as the change in structure of bitumen-filler system (pure bitumen, filler suspension and filler skeleton).

Due to the considerably difference in modulus between bitumen and aggregate, it is known that the strain domains within binders are much higher than the bulk strain within

asphalt mixtures. Most of the bulk strain of an asphalt mixture should be concentrated in the binder domain. Airey and Rahimzadeh (2004) investigated the LVE strain limits of bitumen and asphalt mixtures using stress sweep tests at various temperature and frequency conditions. They performed stress sweeps using a DSR on a 50 penetration grade bitumen and also conducted dynamic uniaxial tension-compression testing using stress sweeps on a 10 mm DBM cylindrical specimen (82mm diametral by 220 mm long) incorporating the 50 penetration grade bitumen. They found that the LVE strain limits for the bitumen (10,000 micronstrain) are approximately 100 times greater than those for the asphalt mixture (100 microstrain). Figure 3.6 shows that at low stiffness modulus (high temperature/low frequency) the LVE strain limits for the bitumen are also approximately 100 times greater than those for the 65% bitumen-filler mastics, while at high stiffness (low temperature/high frequency) the LVE strain limits for the bitumen are approximately 10 times greater than those for the 65% bitumen-filler mastics. The only indication that at high temperature the behaviour of asphalt mixtures may be reflected by the behaviour of 65% bitumen-filler mastics can be seen by the difference in LVE strain limits between the bitumen and the bitumen-filler mastic having filler skeleton in bitumen.

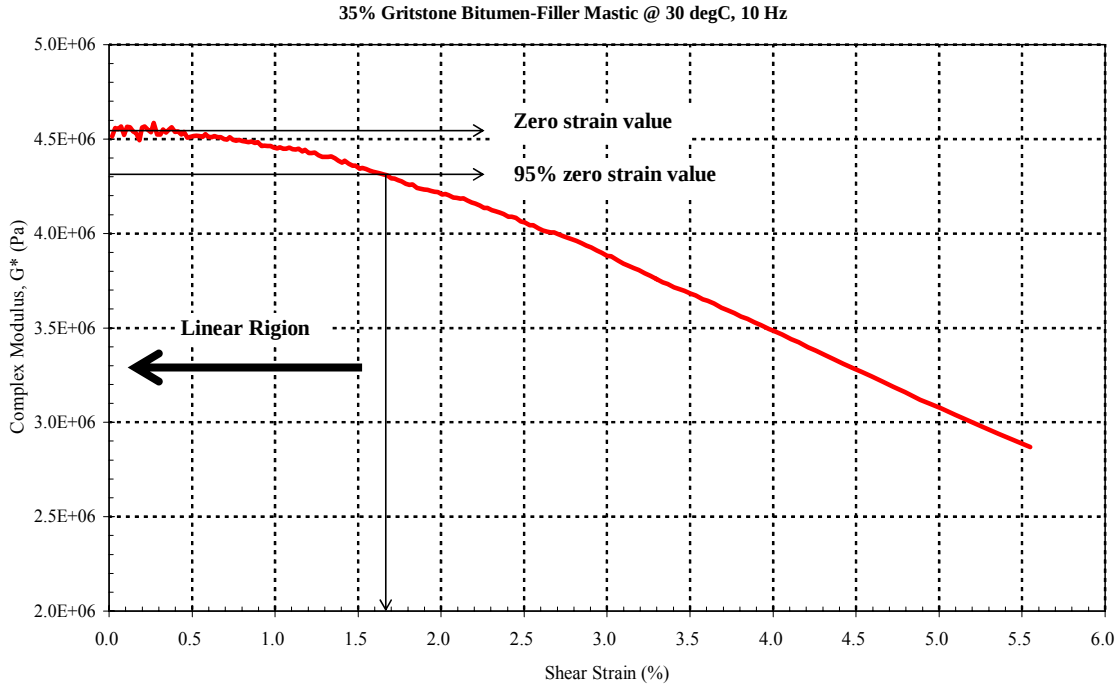

Figure 3.4: Strain sweep linearity limit for 35% gritstone bitumen-filler mastic

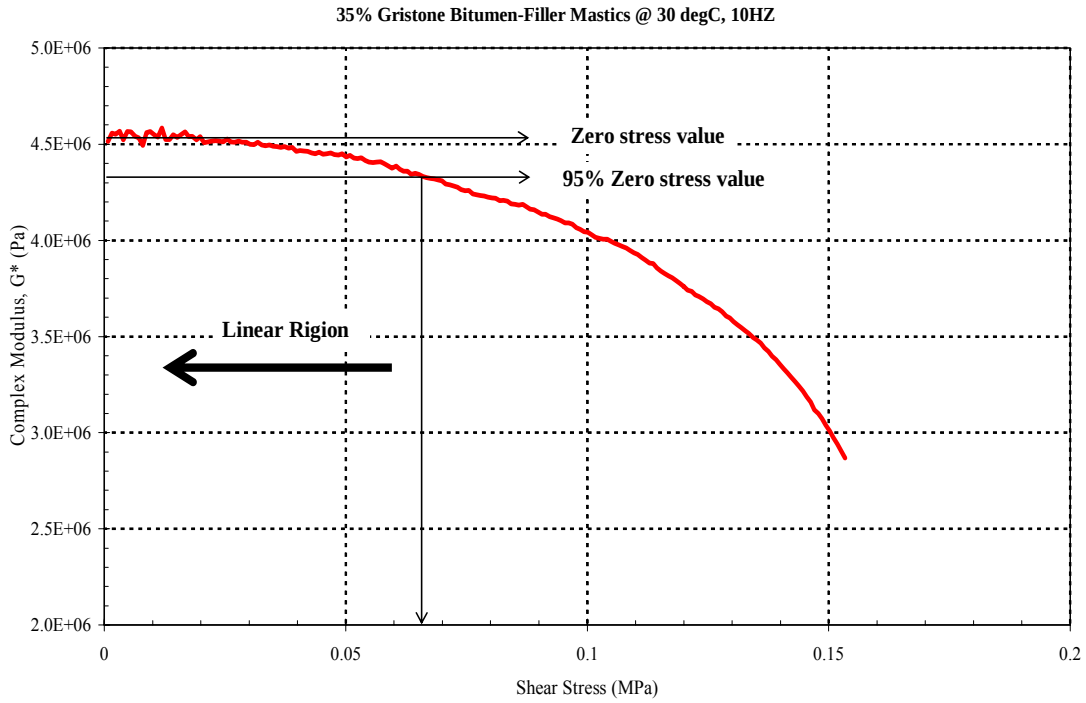

Figure 3.5: Stress sweep linearity limit for 35% gritstone bitumen-filler mastic

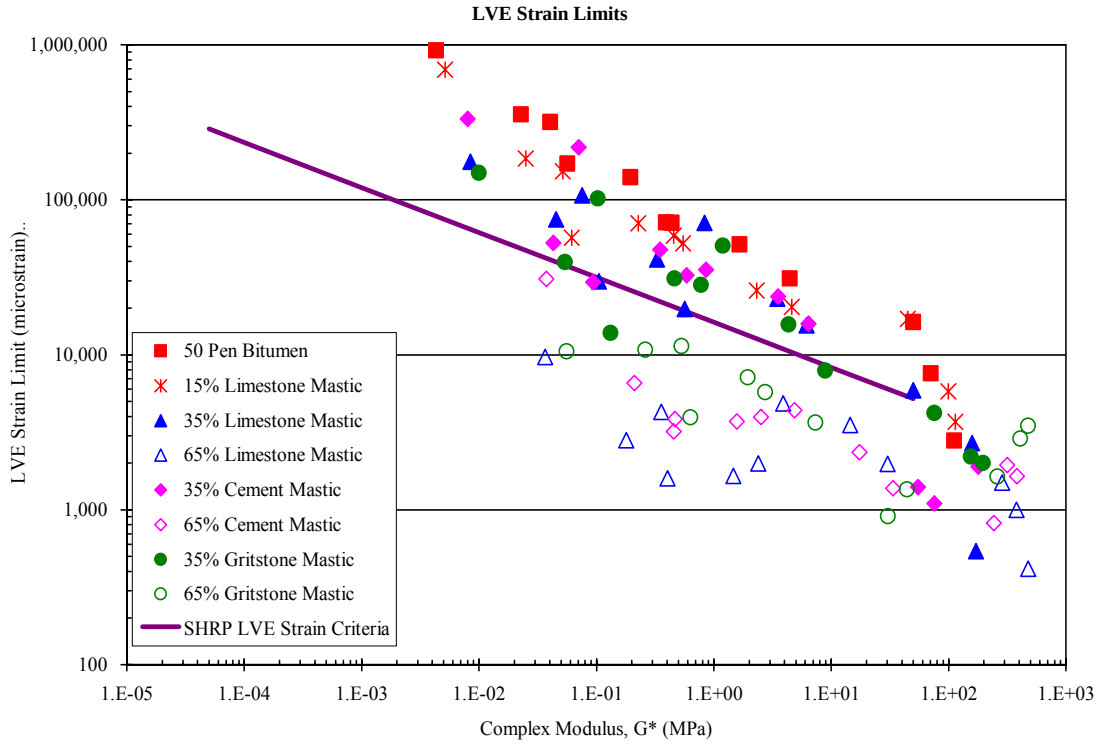

Figure 3.6: Strain LVE limits for bitumen and bitumen-filler mastics

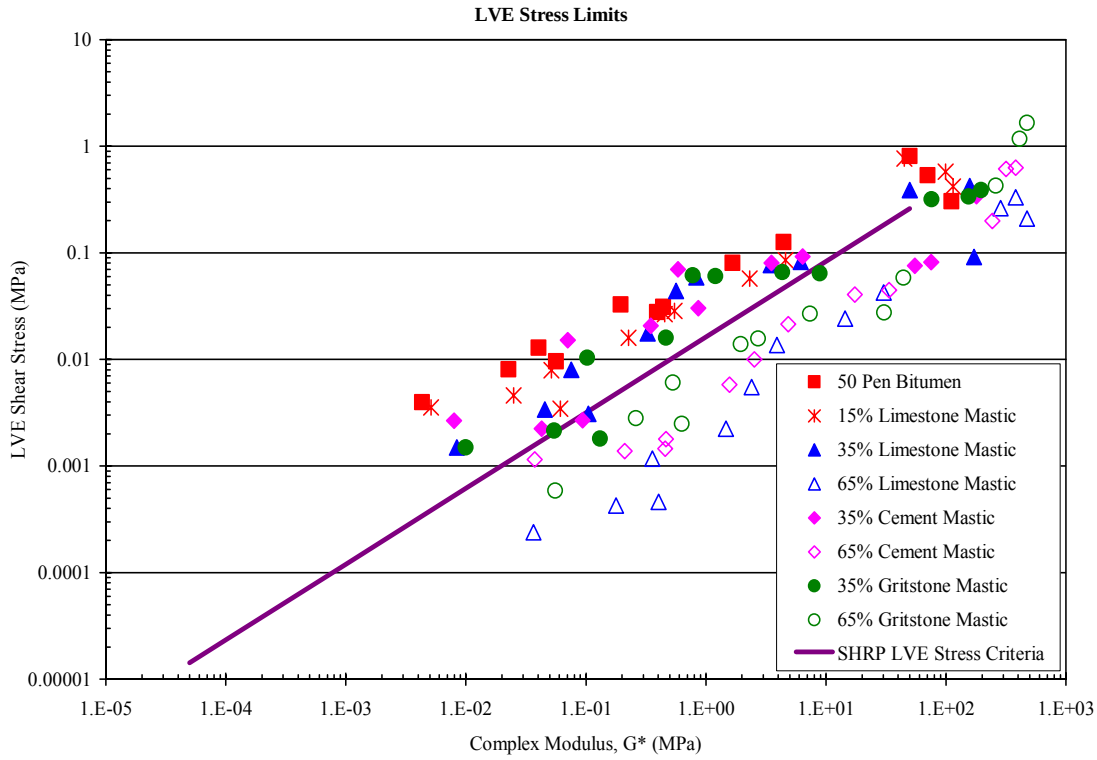

Figure 3.7: Stress LVE limits for bitumen and bitumen-filler mastics

3.6.2 Master Curves

The Bohlin Gemini 200 DSR was used to measure the dynamic shear modulus (G*) and phase angle (δ) of the bitumen and bitumen-filler mastics at temperature ranging from 5°C to 85°C. A frequency sweep covering the range of 0.1 Hz to 20 Hz was obtained at each test temperature. In order to facilitate the analysis of the rheological results, the dynamic shear data were combined into a single master curve using time-temperature superposition. The series of shift factors which are a function of temperature are the amounts of shift to form a single curve. One unit represents a shift of one logarithmic decade, positive/negative to the direction of high/low frequency. Thus, the master curve defines the time dependency of the stiffness and the shift factor defines the temperature dependency of the stiffness. In this investigation, the reference temperature was arbitrarily selected as 25°C. The details of the equipment, test procedure, dynamic mechanical analysis and construction of master curve have been reviewed in Chapter 2.

Complex Modulus Master Curve

Figures 3.8 through 3.10 show the complex modulus master curves for the base bitumen and bitumen-filler mastics. The addition of the filler has an effect on the overall complex modulus at all test temperatures due to the stiffening effect of mineral filler. There is a slight increase in complex modulus for the 15% and 35% bitumen-filler mastics compared to the base bitumen, while there is a significant increase in complex modulus for the 65% bitumen-filler mastics compared to the base bitumen. The indication that the considerably higher complex modulus for the 65% bitumen-filler mastic might be caused by the filler skeleton being present in the bitumen-filler system can be seen the difference in complex modulus curve between the 35% and 65% bitumen-filler mastics. Figure 3.9 shows that the effect of filler type is marginal on complex modulus for the 35% bitumen-filler mastics although the complex modulus for the 35% gritstone bitumen-filler mastic is somewhat higher than that for the limestone and cement bitumen-filler mastics. This is surely due to the fact that the 35% gritstone bitumen-filler mastic has the highest effective volume (25.6%), followed by the limestone (22.2%), then the cement (20.6%).

The master curves show an insignificant effect of filler type on complex modulus for the 65% bitumen-filler mastics at high frequency (low temperature) as shown in Figure 3.10. However, there is a considerable increase in complex modulus for the 65% gritstone bitumen-filler mastics at low frequency (high temperature) caused by the gritstone filler contributing the largest effective volume (62.1%) to the binder compared to the limestone (54.4%) and cement (52.1%) fillers.

Compared to the 35% bitumen-filler mastics, the addition of the filler in the 65% bitumen-filler mastic has slight effect on the elastic response (G') at all temperatures but increases the viscous component of the response (G") at high temperatures, as shown in Figure 3.11. It can be concluded that the filler particles become the predominant component in the 65% bitumen-filler system at high temperatures and low frequencies as seen by the deviation of the complex modulus master curve at low frequencies. Additionally, the master curves clearly show that the 65% bitumen-filler mastics have the lowest temperature susceptibility compared to the base bitumen and the bitumen-

filler mastics containing l5% and 35% filler concentrations. The difference between the complex modulus master curves for the mastics containing high filler content and those for the bitumen and the mastics containing low and intermediate filler contents is the loss of the viscous asymptote at low frequencies due to the elastic response afforded to the mastic by the filler skeleton.

Special attention should be paid that the effective volume for the cement bitumen-filler mastic is smaller than that for the limestone bitumen-filler mastic. However, the master curves clearly show the complex modulus values for the cement bitumen-filler mastics are higher than those for the limestone bitumen-filler mastic, particularly as the filler concentration is up to 65%. The cement bitumen-filler system is controlled not only by a mechanical filling effect of filler phase but also a physicochemical reinforcement. It is probably due to the fact that the cement bitumen-filler mastic specimen is submerged in the circulating water bath during testing, the cement filler provides a higher degree of reinforcement as combining with water.

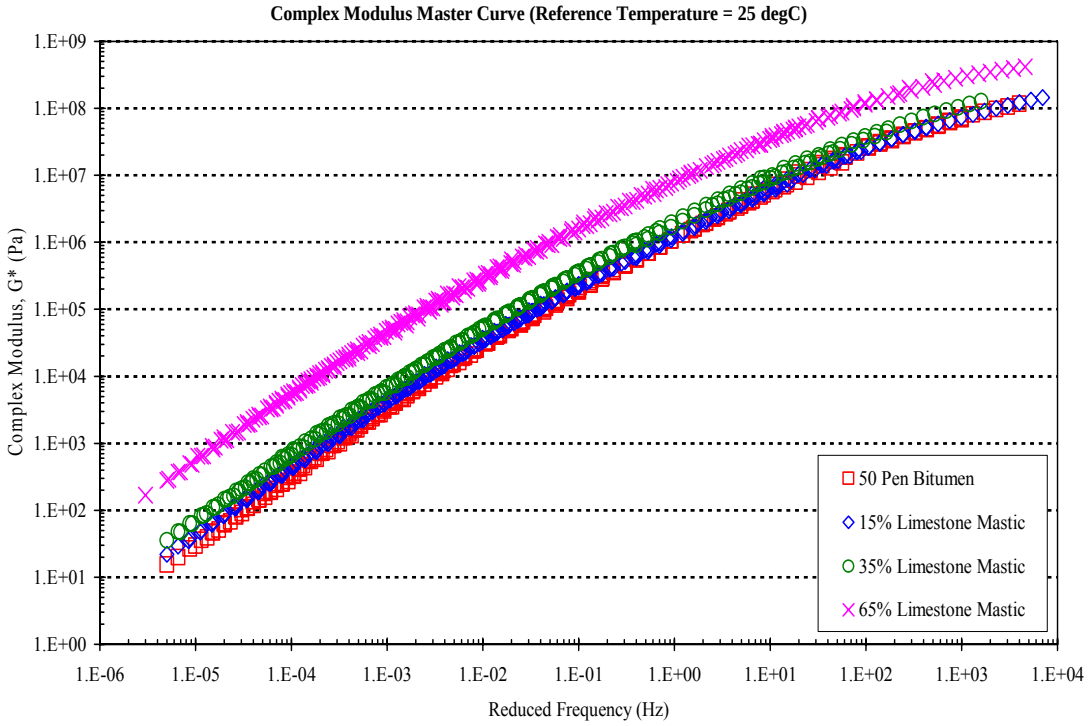

Figure 3.8: Complex modulus master curves for base bitumen and limestone bitumen-filler mastics

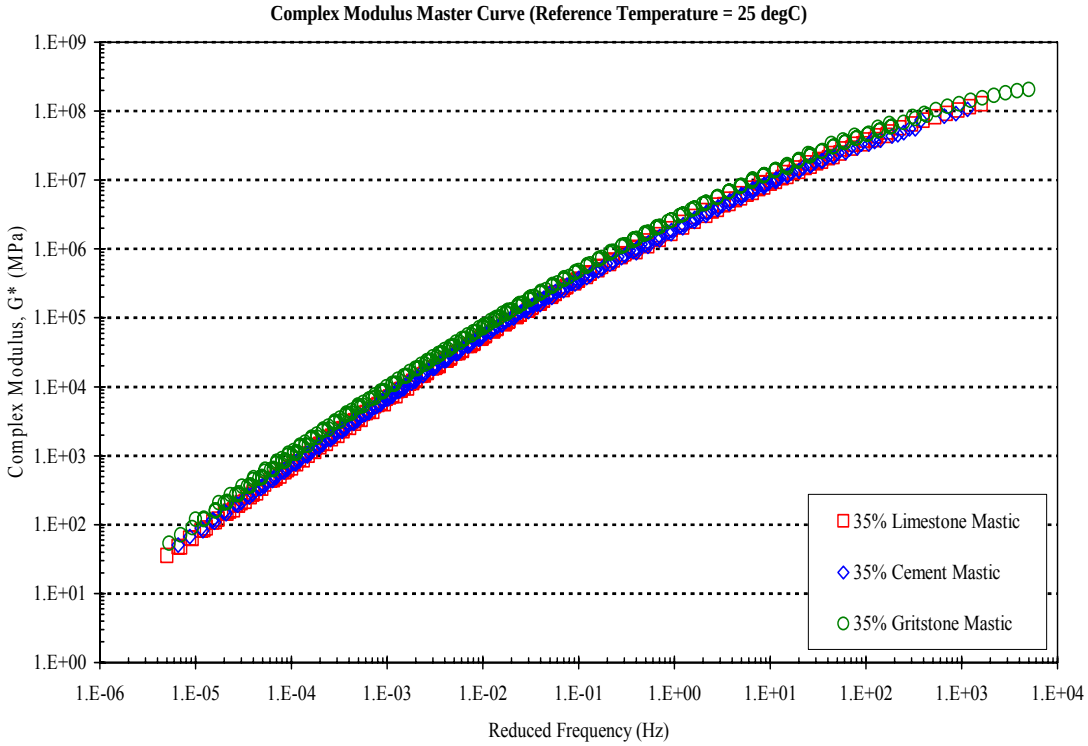

Figure 3.9: Complex modulus master curves for bitumen-filler mastics containing 35% filler content

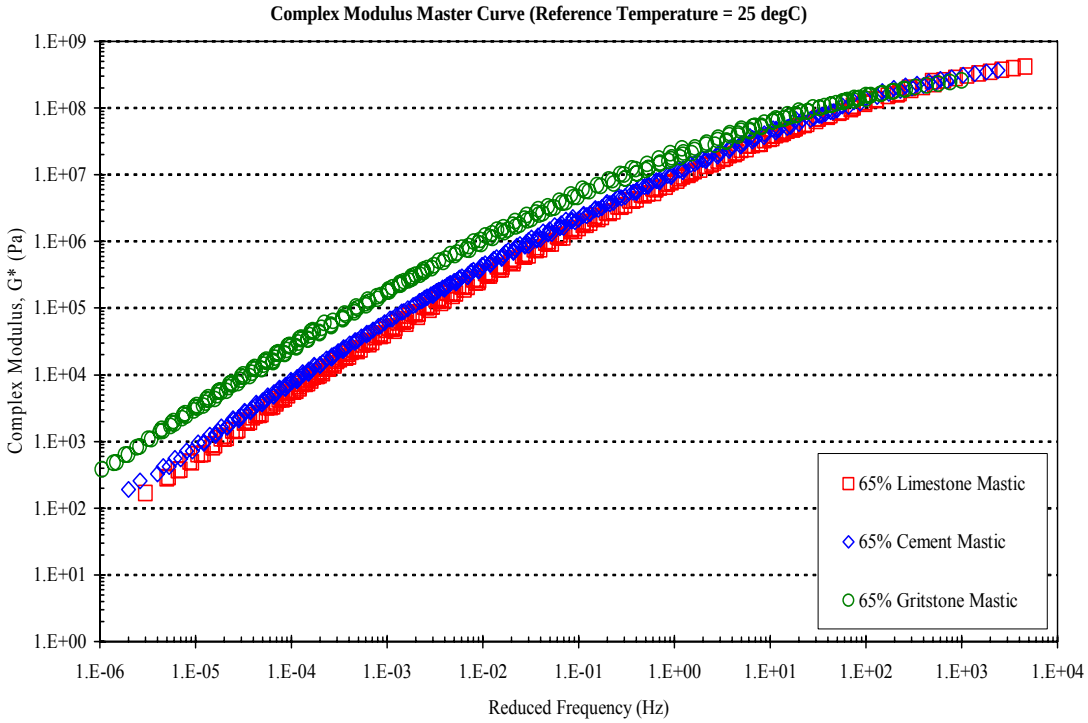

Figure 3.10: Complex modulus master curves for bitumen-filler mastics containing 65% filler content

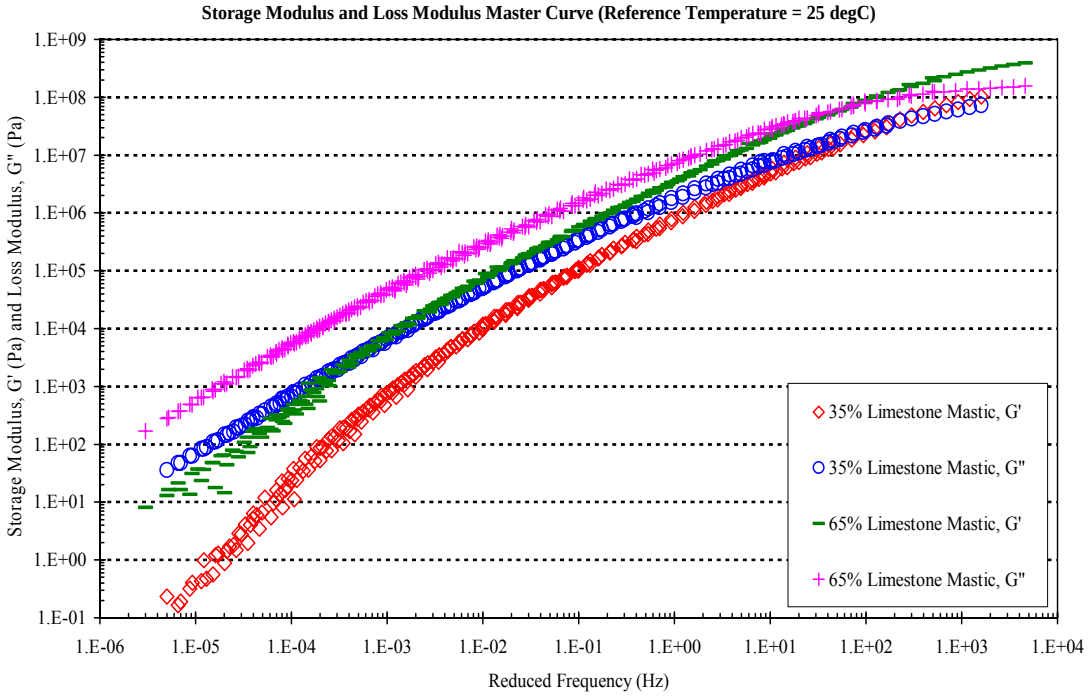

Figure 3.11: Storage modulus and loss modulus master curves for limestone bitumen-filler mastics containing 35% and 65% filler contents

Phase Angle Master Curve

Figures 3.12 through 3.14 show the phase angle master curves of the bitumen and bitumen-filler mastics. Figure 12 shows that the pure bitumen and the bitumen-filler mastics containing 15% and 35% filler concentrations tend towards the same phase angle versus frequency relationship at high frequencies. Figure 3.13 shows that the phase angle values for the 35% cement bitumen-filler mastic and the 35% gritstone bitumen-filler mastic somewhat tend to diverge at high frequencies compare to those for the 35% limestone bitumen-filler mastic due to the slight difference in effective volume of the mineral filler in the mastics. According to the literature by Kim and Little (2004), the phase angle of composite materials is theoretically equal to that of the matrix material when the matrix is incompressible and mixed with rigid particles. It can be inferred that material damping of composite is controlled by the damping ability of the matrix, as long as the second phase represents rigid particles without considerable interaction at interfaces between particles and surrounding matrix. Thus, it is not surprising that there is little difference in phase angle between pure bitumen and bitumen-filler mastic as the filler particles are suspended in the bitumen.

Figures 3.12 also shows the phase angle master curve for the 65% limestone bitumen-filler mastics significantly tend towards the lower phase angle values at high frequencies compared to the base bitumen and the bitumen-filler mastics containing 15% and 35% filler concentrations due to the higher elastic response of the bitumen-filler mastic containing high filler content. Over the central and low frequency regions, the phase angle master curves of the bitumen and bitumen-filler mastics differ slightly.

According to the literature by Airey and Rahimzadeh (2004), a smooth, continuous master curve relies on the bitumen exhibiting simple rheological behaviour and is generally found for unmodified bitumen. However, the simple rheological behaviour is not found for asphalt mixtures. An asphalt mixture shows a partial breakdown of smoothness of a master curve. Figure 3.14 shows that the phase angle master curve for the 65% gritstone bitumen-filler mastic also show a partial breakdown and discontinuity of smoothness of a master curve at high frequencies. The behaviour of bitumen-filler mastic containing high effective volume (62.1%) might mirror that of asphalt mixtures.

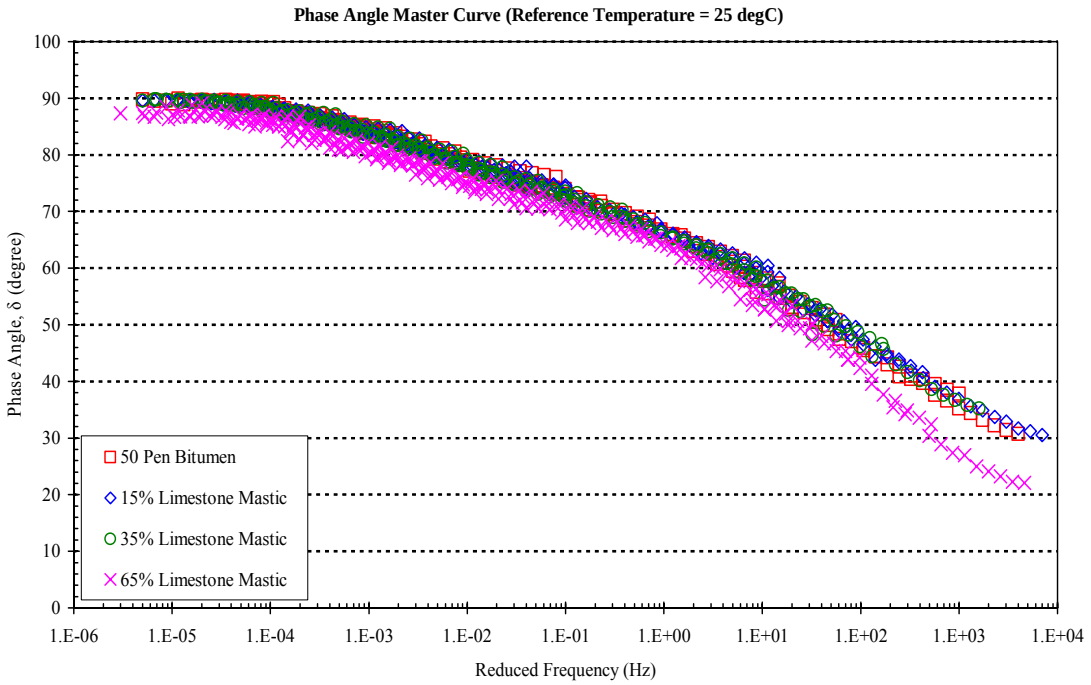

Figure 3.12: Phase angle master curves for base bitumen and bitumen-filler mastics

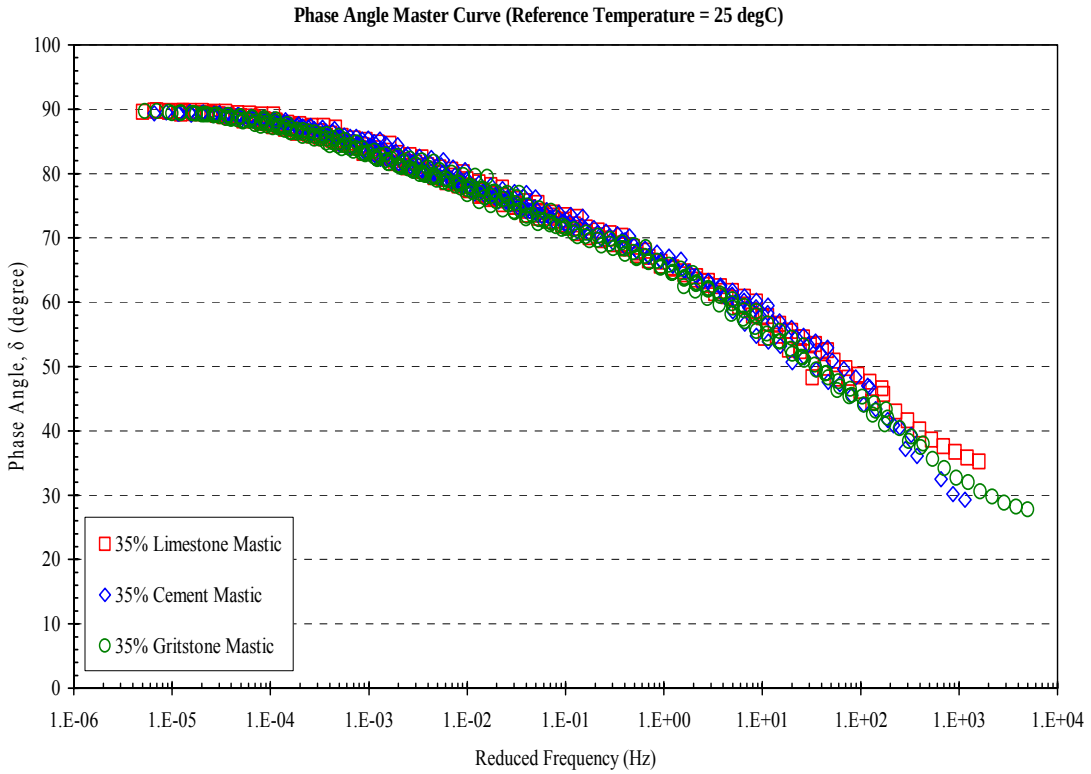

Figure 3.13: Phase angle master curves for bitumen-filler mastics containing 35% filler content

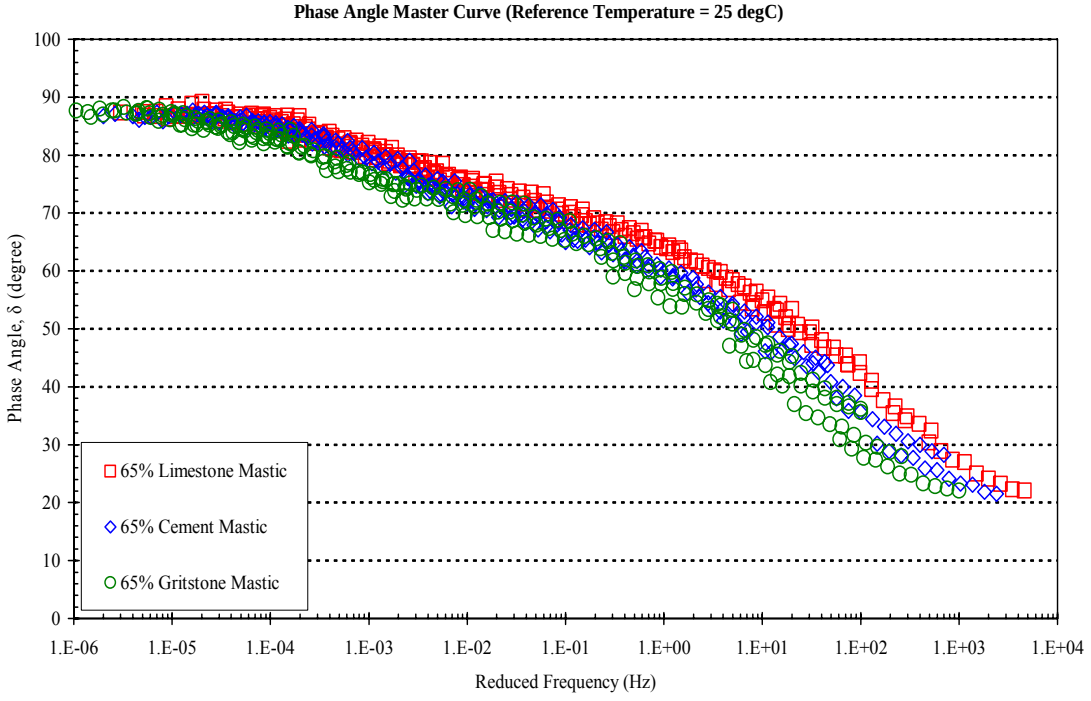

Figure 3.14: Phase angle master curves for bitumen-filler mastics containing 65% filler content

3.6.3 Black Diagram

Black diagram is also a common data presentation diagram for the understanding of the rheological characteristics of bituminous binders. The complex modulus and phase angle measurement obtained from a dynamic test are plotted in the graph of the Black diagram. The effects of temperature and loading time are eliminated from the plot, which allow the dynamic data to be presented in a plot without requiring the shifting of raw data. The Black diagrams for the 50 penetration grade bitumen as well as associated bitumen-filler mastics are presented in Figures 3.15 through 3.18. The smooth and continuous Black diagram curves for the base bitumen and bitumen-filler mastics containing 15% and 35% filler concentrations imply that simple rheological behaviour are found in the base bitumen and the mastic which filler particles are suspended in the pure bitumen. However, as with the phase angle master curve, the Black diagram curves for the 65% bitumen-filler mastics are distinctive. The disjointed and discontinuous Black diagram curves for the 65% bitumen-filler mastics indicate the complex rheological behaviour is found in the bitumen-filler mastics containing high filler content. The viscoelastic behaviour should be dominated by filler skeleton.

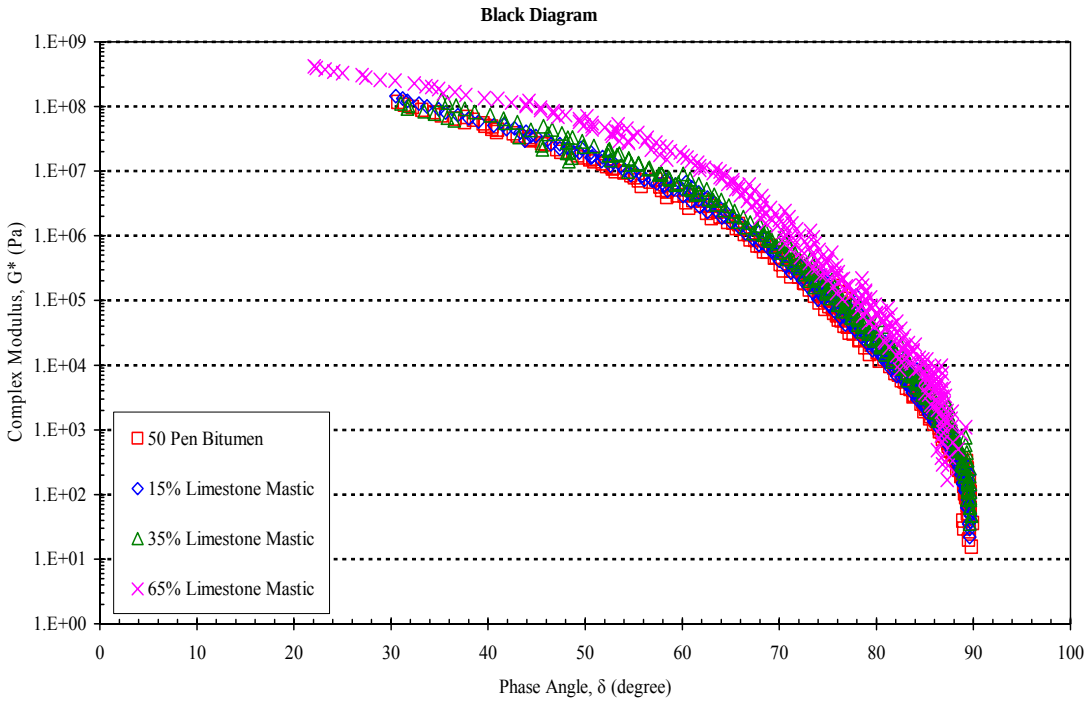

Figure 3.15: Black diagram for 50 penetration grade bitumen

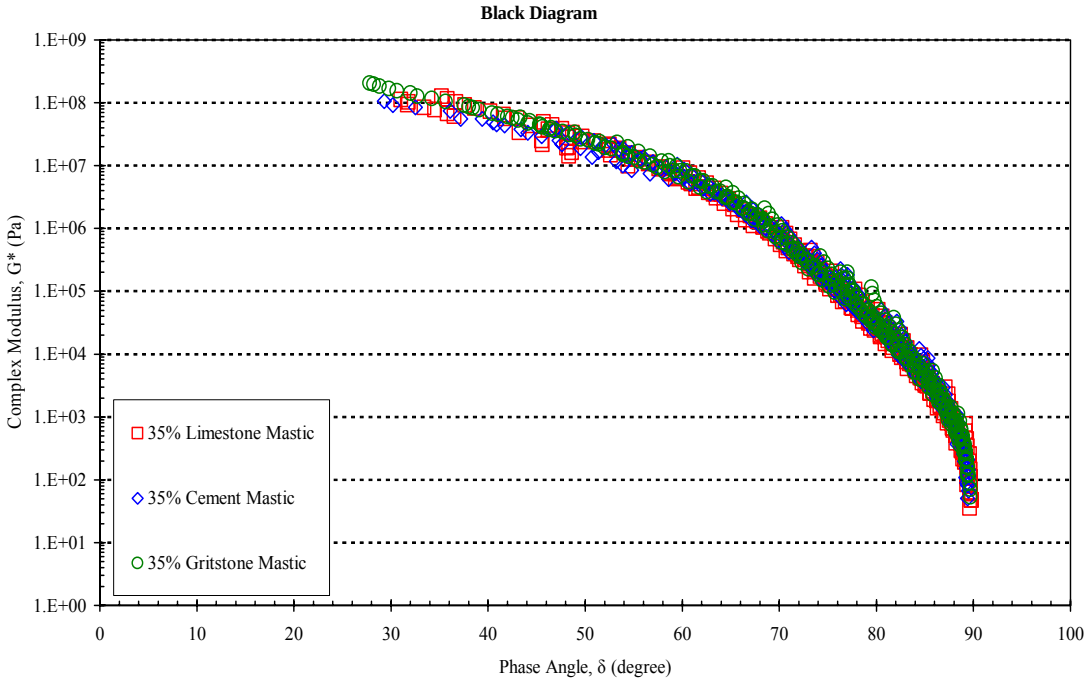

Figure 3.16: Black diagram for 35% bitumen-filler mastic

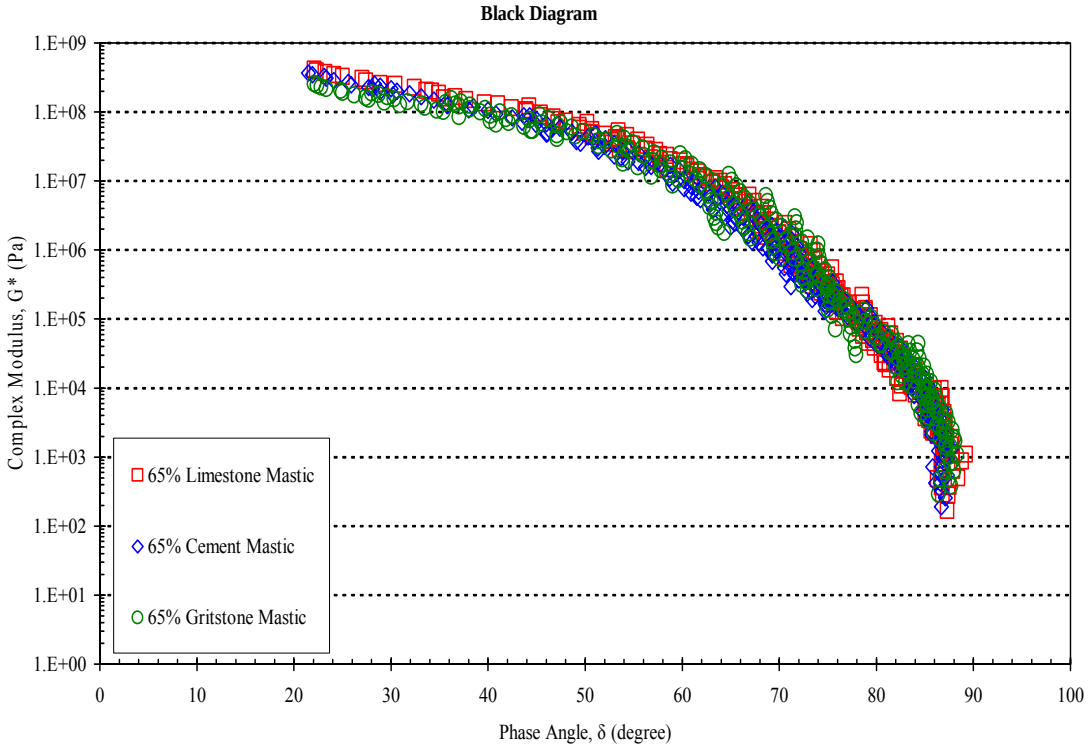

Figure 3.17: Black diagram for 65% bitumen-filler mastic

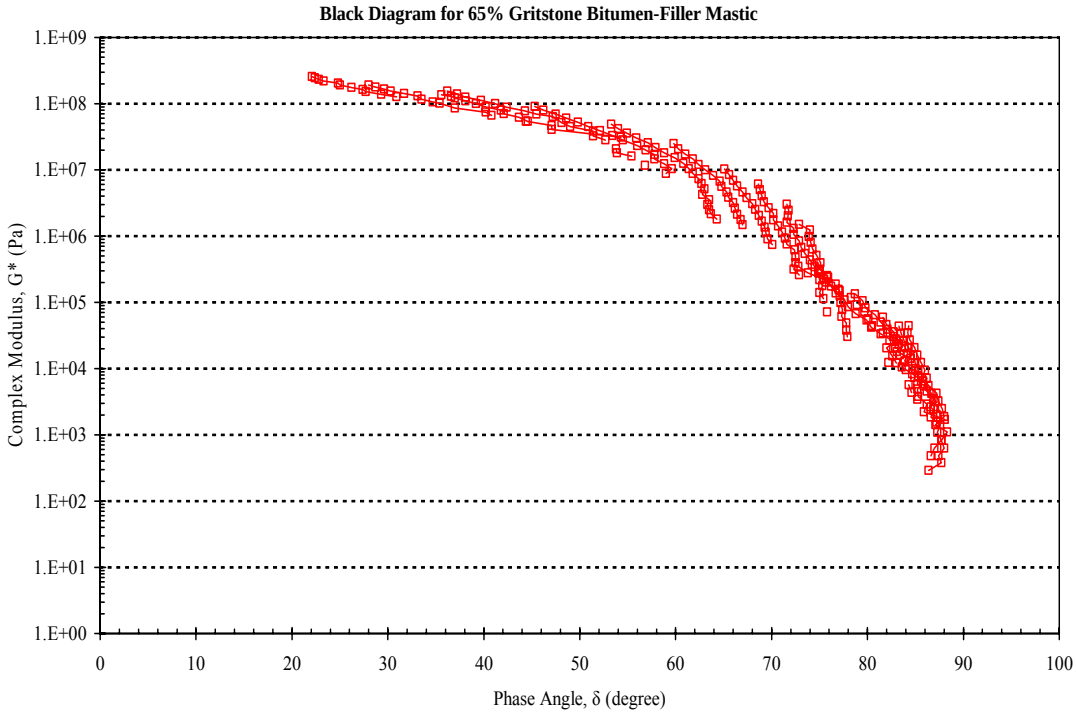

Figure 3.18: Black diagram for 65% gritstone bitumen-filler mastic

3.6.4 Stiffening Effect of Mineral Filler on Complex Shear Modulus

Table 3.10 compares the measurements of complex shear modulus (G*) obtained for the base bitumen and bitumen-filler mastics as measured using the small strain oscillation testing with frequency sweeps at 20°C, 40°C and 60°C and a loading frequency of 1.6 Hz. In addition to the values of complex shear modulus, the relative increase in complex modulus compared to the base bitumen is included as a ratio. The influence of filler type and concentration is also shown in Table 3.10, where the G* stiffening ratios for the base bitumen and bitumen-filler mastics are presented.

The results show that at 35% filler by mass the influence of filler type is marginal with all three mastics having a similar G* at 20°C, 40°C and 60°C although the G* for the 35% gritstone bitumen-filler mastic is somewhat higher. However, at 65% filler by mass the results show a significantly larger value of G* for the gritstone filler mastic compared to the limestone and cement fillers.

The results for the 50 penetration grade bitumen together with the bitumen-filler mastics show an increase in G* with increasing filler concentration. According to the G* stiffening ratios presented in Table 3.10, the results only show a slight increase in G* for the 15% and 35% bitumen-filler mastics but a considerable increase for the 65% filler content mastics. The sharp increase in G* is caused by the filler contributing such a large volume to the binder that it becomes the predominant component in the bitumen-filler mastic and therefore has a dramatic effect on complex modulus. Although the limestone and gritstone fillers (except cement filler) are inert additives added in the base bitumen, the stiffening ratios of G* of the bitumen-filler mastics are not directly proportional to filler content. It can be concluded that the rheological behaviour of the 15% and 35% bitumen-filler mastics is dominated by filler suspension system of mastic, while that of the 65% bitumen-filler mastics is dominated by mineral filler due to filler skeleton in the base bitumen.

It is noted that there is a significant stiffening effect of the filler skeleton of the 65% gritstone bitumen-filler mastic (filler effective volume content = 62.1%) compared to the base bitumen. The G* stiffening ratio for the 65% gritstone bitumen-filler mastic can go up to approximately 16 times.

Table 3.10: Stiffening Effect on Complex Modulus for bitumen and bitumen-filler mastics

Materials	G* @ 1.6 Hz (Pa)		
	20°C	40°C	60°C
50 Pen Bitumen	3,539,500	124,330	5,200
15% Limestone (by Mass) (8.3% by effective volume)	4,350,000 [1.23]	144,700 [1.16]	6,500 [1.25]
35% Limestone (by mass) (22.2% by effective volume)	6,585,400 [1.86]	225,000 [1.81]	8,777 [1.69]
65% Limestone (by mass) (54.4% by effective volume)	24,164,000 [6.83]	1,009,700 [8.12]	48,936 [9.41]
35% Cement (by mass) (20.6% by effective volume)	6,618,900 [1.87]	202,730 [1.63]	11,287 [2.17]
65% Cement (by mass) (52.1% by effective volume)	32,119,000 [9.07]	1,097,700 [8.83]	53,659 [10.32]
35% Gritstone (by mass) 25.6% by effective volume)	9,846,800 [2.78]	231,270 [1.86]	12,795 [2.46]
65% Gritstone (by mass) (62.1% by effective volume)	51,795,000 [14.63]	2,059,800 [16.57]	85,739 [16.49]

3.7 Summary

The aim of the research in this chapter is to ascertain the effects of filler content and filler type on the LVE linearity limits and rheological characteristics (using small strains) of bitumen-filler mastics by means of dynamic shear rheometry. The mineral filler concentrations in the bitumen-filler mastics have been selected as the filler particles are suspended in bitumens (15% and 35% by mass) and the filler skeleton is present in bitumens (65% by mass). The following detailed conclusions can be drawn from this chapter:

- Based on the physical properties including voids of dry compacted fillers (Rigden Voids) and specific surface area for the three types of mineral fillers, the gritstone filler contributes the largest effective volume, V_{fa}, to the base bitumen compared to the cement and limestone fillers as the same filler mass contents (35% and 65%) are added in the base bitumen. It is essential to consider the volumetric content of

filler within the bitumen-filler mastic rather than mass content due to the rheological characteristics of the bitumen-filler mastic are considerably affected by percentage of filler content by volume. In addition, the chemical reaction between the cement filler and the base bitumen should be considered as the complex modulus for the cement bitumen-filler mastic is higher than the limestone bitumen-filler mastic although the volumetric content for the cement filler is lower than that for the limestone filler.

- The linearity limits results show that the LVE strain and stress limits for the base bitumen and the bitumen-filler mastics having filler particle suspension in bitumen (15% and 35% by mass) are similar although those for the base bitumen are somewhat higher. A divergence in the linearity limit of the 65% bitumen-filler mastics shows that the LVE strain and stress limits are below the SHRP LVE criteria, implying the filler skeleton considerably influences the linearity limits of mastics. At low stiffness modulus (high temperature/low frequency), the LVE strain limits for the bitumen are approximately 100 times greater than those for the 65% bitumen-filler mastics. The indication that at high temperature the behaviour of asphalt mixtures may be reflected by the behaviour of 65% bitumen-filler mastics can be seen by the difference in LVE strain limits between the bitumen and the bitumen-filler mastic having filler skeleton in bitumen.
- The complex modulus master curves show that the addition of the filler has an effect on the overall complex modulus at all test temperatures due to the stiffening effect of mineral filler. The effect of filler type is marginal on complex modulus for the 35% bitumen-filler mastics although the complex modulus for the 35% gritstone bitumen-filler mastic is somewhat higher than that for the limestone and cement bitumen-filler mastics. This is surely due to the fact that the 35% gritstone bitumen-filler mastic has the highest effective volume (25.6%), followed by the limestone (22.2%), then the cement (20.6%). It also can be concluded that the filler particles become the predominant component in the 65% bitumen-filler system at high temperatures and low frequencies as seen by the deviation of the complex modulus master curve at low frequencies.
- The phase angle master curves show that the pure bitumen and the bitumen-filler mastics containing 15% and 35% filler concentrations tend towards the same phase

angle versus frequency relationship at high frequencies, while those for the 65% bitumen-filler mastics significantly tend towards the lower phase angle values at high frequencies due to the higher elastic response of the bitumen-filler mastic containing high filler content. The simple rheological behaviour can be found for the 15% and 35% bitumen-filler mastics because they show smooth and continuous master curves. However, the phase angle master curve for the 65% gritstone bitumen-filler mastic shows a partial breakdown and discontinuity of smoothness of a master curve at high frequencies. The complex rheological behaviour of bitumen-filler mastic containing high effective volume (62.1%) might mirror that of asphalt mixtures.

- The smooth and continuous Black diagram curves for the base bitumen and bitumen-filler mastics containing 15% and 35% filler concentrations imply simple rheological behaviour can be found in the base bitumen and the mastic where filler particles are suspended in the pure bitumen. However, the disjointed and discontinuous Black diagram curves for the 65% bitumen-filler mastics indicate the complex rheological behaviour is found in the bitumen-filler mastics containing high filler content. The viscoelastic behaviour of the 65% bitumen-filler mastics is dominated by filler skeleton.

Steady State Rheological Analysis

4.1 General

The rheological properties of a bitumen have a direct influence on the permanent deformation performance of asphalt mixtures. When asphalt mixtures are subjected to deformation upon application of a stress, the aggregates act as load-bearing entities while the binders deform in response to the applied stress. However, a good relationship between the rheological properties of binders and the permanent deformation of mixtures does not exist in some cases (Shenoy et al., 2003). There could be the possible interactions between aggregate and bitumen, which does not get reflected in the rheological properties of plain bitumen. Bitumen-filler mastics might provide a better correlation because they take account of physicochemical aspects of the interaction between bitumen and mineral filler. The rheological properties and permanent deformation performance of mastics rather than those of bitumen may be more appropriate in terms of establishing a correlation with asphalt mixture rutting performance.

Rheological parameters such as the Superpave bitumen rutting parameter, $G^*/\sin\delta$, have been used as a performance indicator for rutting (Anderson et al., 1994). For conventional, penetration grade bitumens this parameter may provide a good indication and correlation with the rutting behaviour of asphalt mixtures. However, this correlation is not particular good for specialist binders such as polymer modified bitumens (PMBs) (Phillips and Robertus, 1996) due to the inability of the Superpave parameter to account for the effect of delayed elasticity. The use of the concept of zero shear viscosity (ZSV) has therefore been suggested as more appropriate rutting parameter (Phillips and Robertus, 1996; Sybilsky, 1996a). The ZSV of a binder is an intrinsic property that has been shown to correlate with the rutting performance of an asphalt mixture.

Bitumen viscosity, as a rational, physical material property, has commonly been accepted as an indicator of asphalt mixture permanent deformation resistance (Sybilski, 1996b). However, as bitumen and bitumen-filler mastics tend to show non-Newtonian behaviour at 40^{o}C and 60^{o}C, the viscosity needs to be determined in the form of ZSV, which is independent of shear rate and testing condition. Within this linear regime, the ZSV reflects dissipated motions in a negligibly perturbed, equilibrium "no-flow" structure (Phillips and Robertus, 1995).

This chapter looks at the permanent deformation behaviour and ZSVs of bitumen-filler mastics. Different filler concentration levels of mastics including pure bitumen (0% filler), filler suspension in bitumen (15% and 35% filler concentration by mass) and filler skeleton in bitumen (65% filler concentration by mass) were tested using a DSR. Three techniques were used to measure low shear and steady state viscosity, including small amplitude, low frequency oscillations, low strain rate viscometry measurements and low stress creep tests. Two mathematical models were used to extrapolate measurements of complex viscosity to zero frequency and apparent viscosity to zero shear rate as measurements are practically not taken down to zero shear conditions. Additionally, measurements of viscosity at steady state were obtained by performing creep and pulse creep testing. The comparison of ZSV of bitumen-filler mastics using different measurement techniques was also presented in this chapter.

4.2 Materials and Equipments

4.2.1 Materials

A combination of one penetration grade bitumen, three filler types and three filler concentrations by mass were included in the testing programme. The matrix of materials that were tested is listed in Table 4.1. The base bitumen consisted of a 50 penetration grade bitumen with the filler being limestone, cement and gritstone. The details of physical properties of the bitumen, physical properties of the mineral fillers and filler concentrations in bitumen-filler system have been described in Chapter 3.

Table 4.1: Matrix of bitumen-filler mastics

Materials / Filler Contents	Base Bitumen	Bitumen-Filler Mastics		
	50 Pen Bitumen	Limestone	Cement	Gritstone
0%	x			
15%		x		
35%		x	x	X
65%		x	x	X

4.2.2 Dynamic Shear Rheometer

The Bohlin Gemini 200 Dynamic Shear Rheometer having a torque range between 0.5 (μN·m) and 200 (mN·m) was used for measuring the rheological characteristics of bitumen and bitumen-filler mastics. The details of the principal components of the DSR, temperature controlled system and sample preparation have been described in Chapter 3.

4.3 Testing Programme

4.3.1 Oscillation Testing

The principle of the dynamic oscillatory shear testing has been described in Chapter 3. The measurements of dynamic complex viscosity of the bitumen and bitumen-filler mastics were obtained by performing frequency sweep testing over a range of test frequencies between 0.1 and 20 Hz at 40^{o}C and 60^{o}C. The oscillation testing was performed on the bitumen and bitumen-filler mastics under strain controlled loading conditions by applying a sinusoidal angular displacement of constant amplitude within the linear viscoelastic region. Different diameter parallel plates for the small strain oscillation testing were used, depending on the test temperatures of 40^{o}C and 60^{o}C. The test parameters are shown as follows:

- Test temperatures : 40^{o}C and 60^{o}C,
- Test frequency : 0.1 to 20 Hz,
- Mode of loading: strain controlled loading,

- Test geometry and gap: 8-mm diameter standard parallel plates with a 2-mm gap (40^{o}C) and 25-mm diameter parallel plates with a 1-mm gap (60^{o}C), and
- Load mode: sinusoidal wave shown in Figure 4.1.

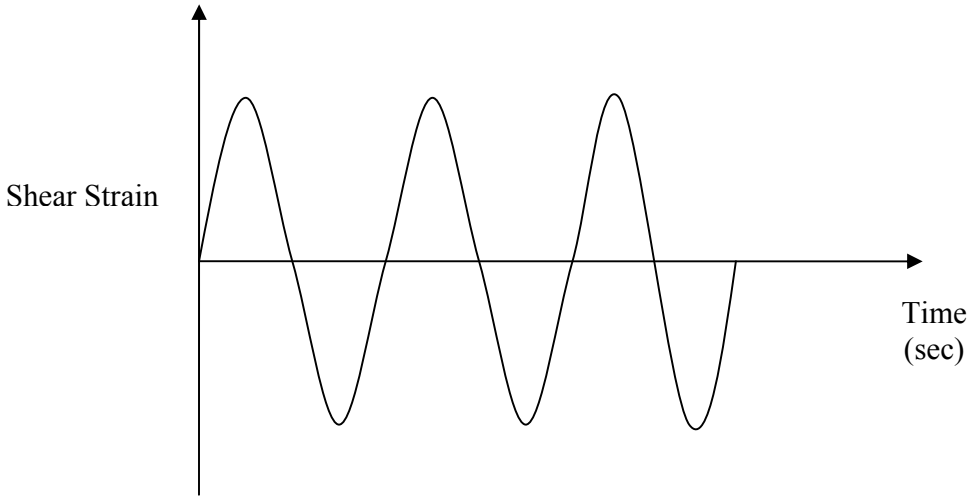

Figure 4.1: Sinusoidal wave

The ZSV of the bitumen and bitumen-filler mastics can be determined by means of dynamic oscillatory testing using the DSR. Using this testing technique, measurements of complex viscosity approach a value equal to ZSV, as loading frequency tends to zero or at least at very low oscillation frequencies. The ZSV extrapolated from dynamic oscillation measurements has been presented in Section 2.4.4.

4.3.2 Viscometry Testing

Viscometry testing using the DSR can be undertaken to determine the measurements of viscosity of a bitumen over a range of shear rate (rate of change of shear strain). A shear stress is applied to the bituminous sample by rotation. The shear stress and shear rate are varied continuously from one value to another. The viscosity is the measure of the resistance to flow of a bituminous binder, and is the ratio of the shear stress to the shear rate. The viscometry testing was carried out on the bitumen and the bitumen-filler mastics within a range of shear rates between 0.01 and 10 (1/sec) at the test temperatures of 40^{o}C and 60^{o}C. The test parameters are given as follows:

- Test temperatures : 40 and 60^{o}C,
- Test shear rate : 0.01 to 10 (1/s),
- Test geometry and gap : 8-mm diameter standard parallel plates with-2 mm gap (40^{o}C) and 25-mm diameter parallel plates with 1-mm gap (60^{o}C), and
- Load mode: stepped shear rate shown in Figure 4.2.

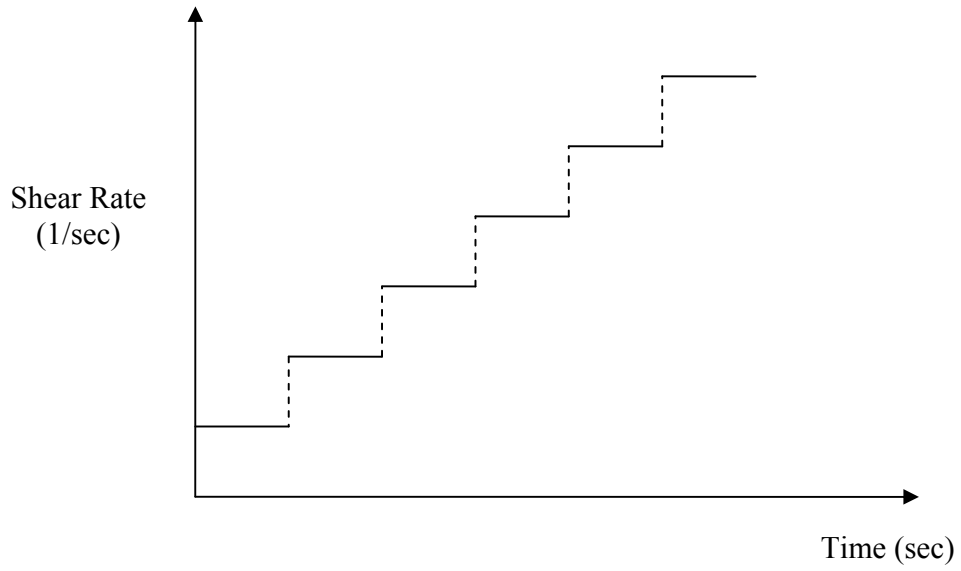

Figure 4.2: Stepped shear rate mode

Using this testing technique the ZSV can be determined as strain rate tends to zero and the viscosity becomes Newtonian in nature. Figure 4.3 shows that a Newtonian behaviour followed by a shear-thinning behaviour (non-Newtonian behaviour) for a bitumen in the relation between shear stress and shear rate. The power law relationship between shear stress and shear strain rate can be shown as follows:

$$\tau = \eta \dot{\gamma}^{n} \tag{4.1}$$

where τ is the shear stress (Pa), η is the viscosity (Pa.s), $\dot{\gamma}$ is the shear rate (1/s) and n is the power exponent.

Figure 4.4 shows a tendency to approach an upper limiting viscosity at very low shear rate and the measurements of apparent viscosity are independent of loading time (shear rate). Using this testing technique, the viscosity approaches a value equal to ZSV as shear rate tends to zero.

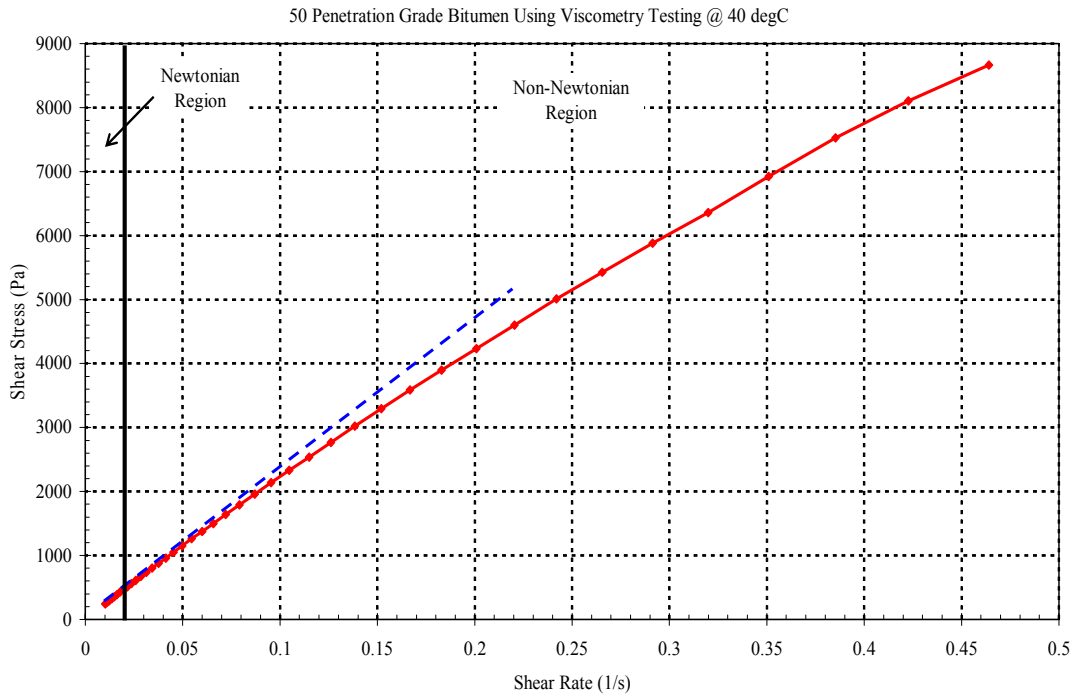

Figure 4.3: Shear stress versus shear rate

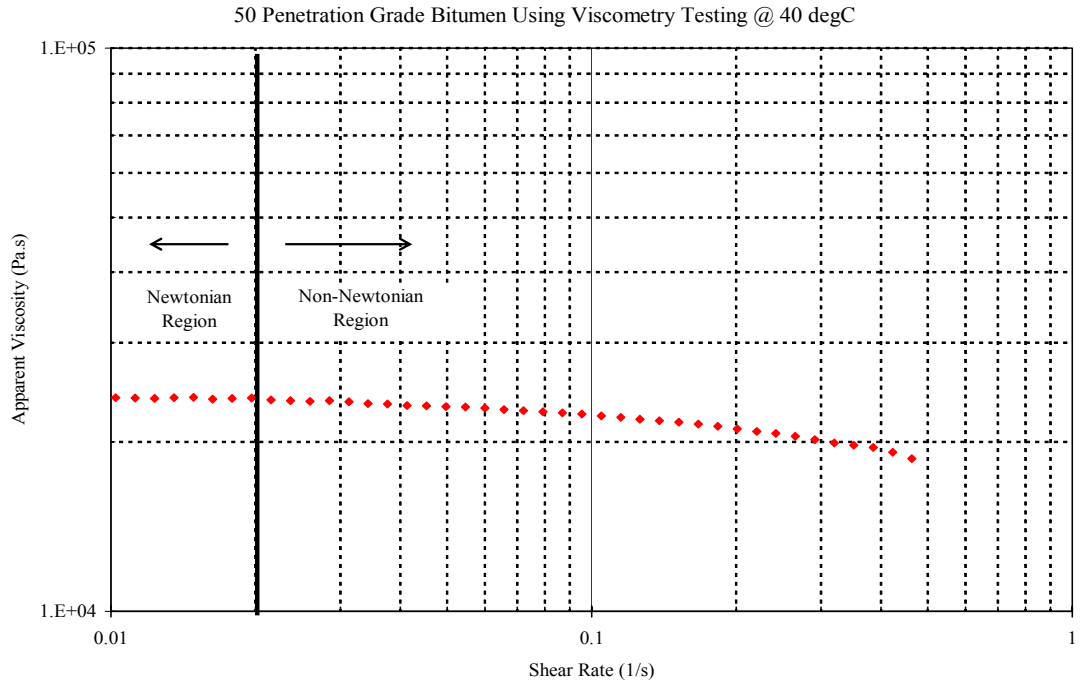

Figure 4.4: Apparent viscosity versus shear rate

4.3.3 Creep Testing

Creep testing using the DSR can be carried out to determine the shear deformation behaviour with increasing time of loading. At low stress levels and with increasing time of loading, ZSV can be measured in a creep test as a limiting value (steady state viscosity). The calculation of ZSV has been reviewed in Section 2.4.2. A constant shear stress is applied to a bituminous sample for a long time period followed by a rest period. In a long creep test, the effect of delayed elasticity decreases with time. The rheological behaviour of the bituminous binder is dominated by viscous flow after a sufficient long time. Under low stress creep, structures within the bitumen or bitumen-filler mastic deform so slowly that they can continuously adapt thereby maintaining a situation close to equilibrium without building up any significant structural change in the material.

In this study, a creep followed by rest period test was undertaken using a DSR on the base bitumen and bitumen-filler mastics at test temperatures of 40^{o}C and 60^{o}C at low stress levels. Two creep modes of single creep-recovery test and pulse creep (100 cycles of 1 second loading time and 9 seconds unloading time) test were performed for

sufficiently long time to achieve steady state. The 8-mm diameter standard parallel plate with-2 mm gap was used to test bitumen and mastic samples at 40°C, whereas the 25-mm diameter parallel plates with 1-mm gap was used to test bitumen and mastic samples at 60°C. The creep test conditions are detailed in Table 4.2.

Table 4.2: Creep testing programme of bitumen-filler mastics

	Temperature (°C)	Shear Stress (Pa)	Creep Time (sec)	Rest Time (sec)
Single Creep and Recovery	40	300 to 1000	5000 to 30000	5000 to 30000
	60	300 to 1000	5000	5000
Pulse Creep (100 Cycles)	40	300 to 1000	1	9
	60	300 to 1000	1	9

Single Creep-Recovery Testing

Figure 4.5 shows that a typical creep curve (without rest) for the 50 penetration grade bitumen is divided into three regions. In the primary creep region, the shear strain rate decreases with time and the bitumen behaviour is dominated by elastic and delay elastic effects. In the steady state creep region, the shear strain rate remains approximately constant with time and the bitumen behaviour is dominated by viscous effect. In the tertiary creep region, the shear strain rate increases with time, and the bitumen is progressively damaged.

In the steady state creep region, the shear strain is proportional to the loading time. The bitumen viscosity is independent of shear rate and test conditions. The viscosity can be calculated as a limiting viscosity value called SSV (steady state viscosity) or ZSV in steady state creep region. The equation is shown as follows:

$$\eta_0 = \left(\frac{dJ_c(t_c)}{dt_c} \right)^{-1} = \left(\frac{d\left(\gamma(t_c) / \tau \right)}{dt_c} \right)^{-1} \tag{4.2}$$

where η_0 is the ZSV (Pa.s), J_c is the creep compliance (1/Pa), γ is the shear strain, τ is the shear stress (Pa) and t_c is the creep loading time (sec).

Figure 4.6 shows a cycle of creep-recovery curve for the 50 penetration grade bitumen with sufficient loading time and recovery time to achieve steady state. The ZSV was determined from either creep part (loading period) at steady state stage (see Figure 4.5) or recovery part (unloading period) (see Figure 4.6). The ZSV obtained from loading period can be calculated based on Equation 4.2, while the ZSV determined from unloading period can be calculated from irrecoverable strain using Equation 4.3.

$$\eta_0 = \frac{t_c}{J_r} = \frac{t_c}{\left(\gamma_{ir} \diagup \tau\right)} \tag{4.3}$$

where η_0 is the ZSV (Pa.s), J_r is the recoverable compliance (1/Pa), γ_{ir} is the irrecoverable shear strain, τ is the shear stress (Pa) and t_c is the creep loading time (sec).

Pulse Creep Testing

Some researchers have reported that ZSV calculated from pulse creep testing is related to permanent deformation of asphalt pavements (Bahia et al., 2002; Carswell and Moglia, 2003; Visscher et al., 2004; Vlachovicova et al., 2005). The pulse creep testing performed on bituminous binders can eliminate the effect of delayed elastic response if it is performed with a sufficient magnitude of shear stress together with loading time. In this study, a set of 100 cycles of pulse creep experiment was performed on the bitumen and the bitumen-filler mastics with a loading time of 1 second followed by an unloading time of 9 seconds. The repeated shear loads caused an irrecoverable strain of a bituminous binder to achieve steady state. Figure 4.7 shows the last 5 cycles of pulse creep curve. The ZSVs were determined at the last cycle (100^{th} cycle) using Equations 4.2 and 4.3.

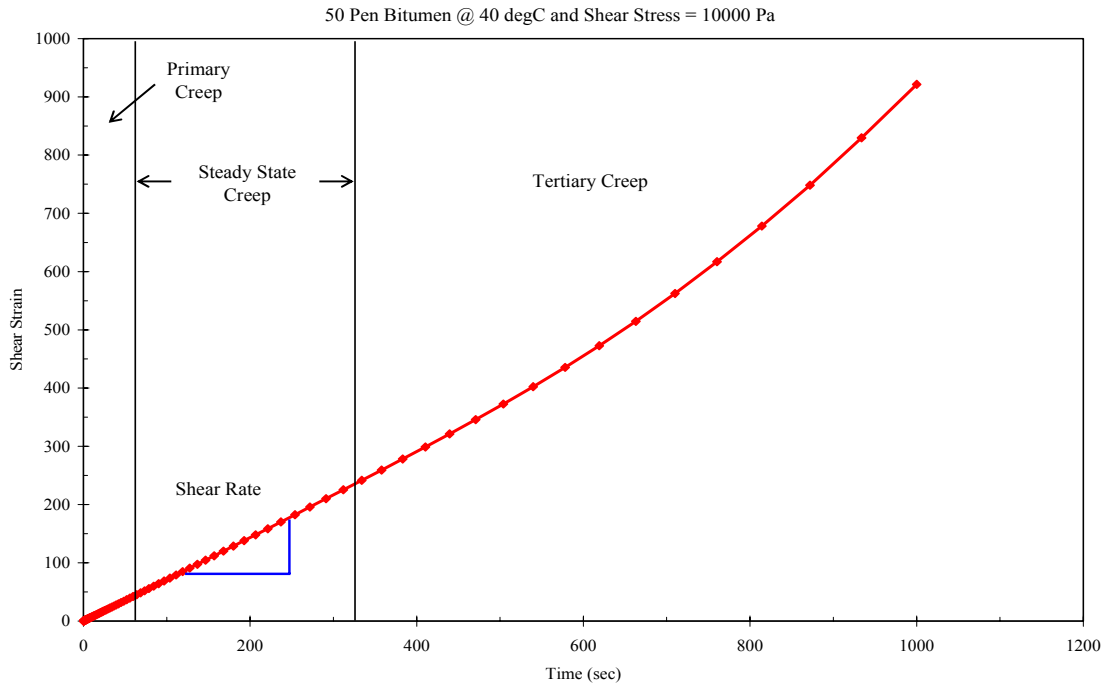

Figure 4.5: Creep curve of bitumen

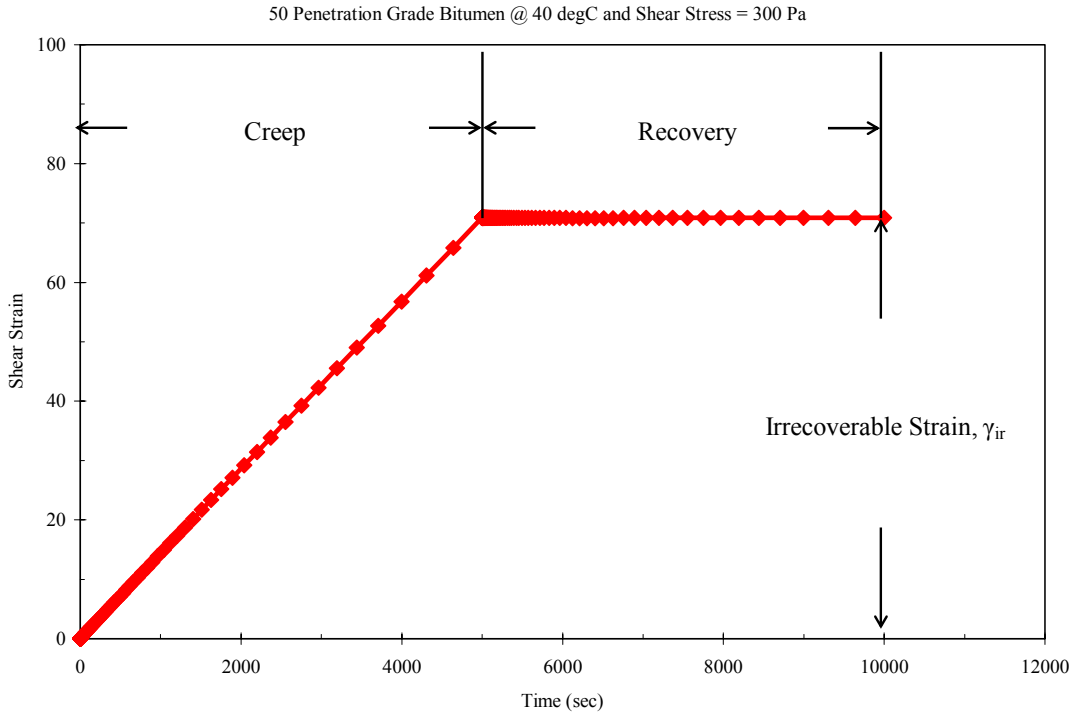

Figure 4.6: Creep followed by rest period

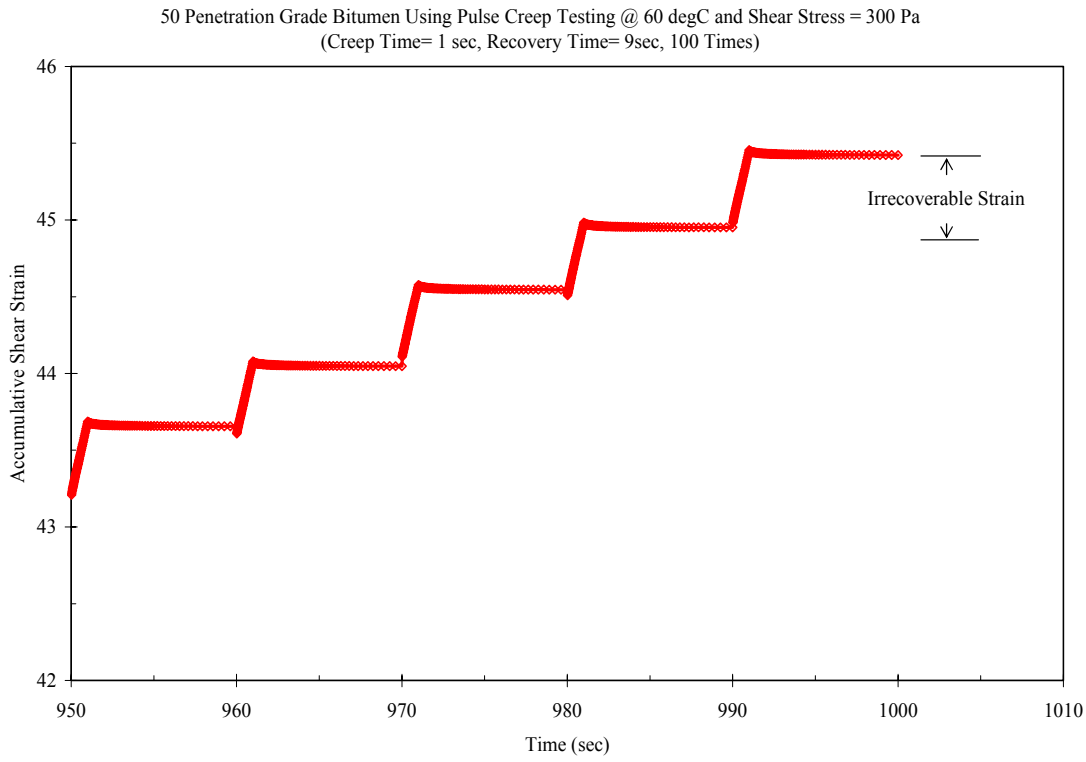

Figure 4.7: Pulse creep testing

4.4 Extrapolation of Zero Shear Viscosity

As the viscosity measurements are not possibly taken down to the "zero" frequency or "zero" shear rate, the limiting viscosity at very low shear rate or frequency can be extrapolated using a flow equation relating viscosity to shear rate or frequency. In this section, two appropriate mathematical models, the four-parameter Cross model (Cross, 1965) and Carreau model (Carreau et al., 1968), are selected to extrapolate the measurements of viscosity to zero frequency or shear rate.

4.4.1 ZSV Extrapolated Using the Cross Model

The four-parameter Cross model was derived by Cross (1965) based on the assumption that psuedoplastic flow (a decrease in viscosity with increasing rate of shear) is associated with the formation and rupture of structural linkages. The equation fits to the experimental results which are presented on a wide range of pseudoplastic systems, ranging from suspensions (aqueous media) to optically solutions (nonaqueous media).

Chapter 2 has reviewed that the Cross model was selected by some researchers for ZSV extrapolation of bitumens and fitting to measurements of bitumen complex viscosity/apparent viscosity over a wide range of frequencies/shear rates.

In this section, the Cross model has been selected for the bitumen and bitumen-filler mastics to extrapolate sinusoidal oscillation measurements of complex viscosity (η^*) to zero frequency as well as viscometry measurements of apparent viscosity (η) to zero shear strain rate. The Cross model describes a flow curve of pseudoplastic liquids which show a decrease in viscosity with increasing rate of shear in the form of a four parameter equation:

For oscillation measurements:

$$\eta^* = \eta_\infty + \frac{\eta_0 - \eta_\infty}{\left(1 + k_1 \omega^{n_1}\right)} \tag{4.4}$$

where η^* is the complex viscosity (Pa.s), η_0 is the zero shear viscosity (Pa.s), η_∞ is the infinite viscosity (Pa.s), ω is the frequency (rad/s), and k_1 and n_1 are material constants.

For viscometry measurements:

$$\eta = \eta_\infty + \frac{\eta_0 - \eta_\infty}{\left(1 + k_2 \dot{\gamma}^{n_2}\right)} \tag{4.5}$$

where η is the apparent viscosity (Pa.s), η_0 is the zero shear viscosity (Pa.s), η_∞ is the infinite viscosity (Pa.s), $\dot{\gamma}$ is the shear strain rate (1/s), and k_2 and n_2 are material constants.

4.4.2 ZSV Extrapolated Using the Carreau Model

In order to calculate ZSV, the Carreau model (Carreau et al., 1968) used in this investigation is fitted to the viscosity curves allowing extrapolating of the viscosity at a zero frequency and zero shear rate, with a non-linear regression. The Carreau model applied to viscosity measurements of bituminous binders has been reviewed in Chapter 2, and it has a similar profile as the Cross Model:

For oscillation measurements:

$$\eta^* = \eta_\infty + \frac{\eta_0 - \eta_\infty}{\left[1 + (k_3 \omega)^2\right]^{n_3}} \tag{4.6}$$

where η^* is the complex viscosity (Pa.s), η_0 is the zero shear viscosity (Pa.s), η_∞ is the infinite viscosity (Pa.s), ω is the frequency (rad/s), and k_3 and n_3 are material constants.

For viscometry measurements:

$$\eta = \eta_\infty + \frac{\eta_0 - \eta_\infty}{\left[1 + \left(k_4 \dot{\gamma}\right)^2\right]^{n_4}} \tag{4.7}$$

where η is the apparent viscosity (Pa.s), η_0 is the zero shear viscosity (Pa.s), η_∞ is the infinite viscosity (Pa.s), $\dot{\gamma}$ is the shear rate (1/s), and k_4 and n_4 are material constants.

4.4.3 Cox-Merz Rule

Theoretically there is no reason for correspondence to exist between complex viscosity (frequency dependence) and apparent viscosity (shear rate dependence) measurements because the dynamic oscillation test and the rotational viscometry test are quite independent. An empirical correlation, called the Cox-Merz rule, between dynamic and

steady flow viscosity measurements was proposed by Cox and Merz (1958). The correlation is given by:

$$\eta^*(\omega) = \eta\left(\dot{\gamma}\right)_{\dot{\gamma}=\omega} \tag{4.8}$$

where η^* is the complex viscosity (Pa.s), ω is the angular frequency (rad/s) in the dynamic oscillation testing, η is the apparent viscosity (Pa.s), and $\dot{\gamma}$ is the shear rate (1/s) in the rotational viscometry testing.

Cox and Merz (1958) demonstrated that for a non-Newtonian character of the flow of polystyrene the apparent viscosity in steady flow should be analogous to the absolute magnitude of the complex viscosity. The Cox-Merz rule has also been used by researchers (Partal et al., 1999; Perez-Lepe et al., 2003; Stastna et al., 2003) for relating linear viscoelastic functions as a function of frequency to the viscometry functions as a function of shear rate for unmodified bitumens and PMBs. In this investigation, the Cox-Merz rule is selected to compare measurements of complex viscosity (η^*) with those of apparent viscosity (η) for the bitumen and bitumen-filler mastics.

4.5 Test Results and Discussion

4.5.1 ZSV Extrapolated from Oscillatory Measurements

The complex viscosities for the base bitumen and bitumen-filler mastics are plotted versus the corresponding frequencies on a log-log plot. Figures 4.8 through 4.13 show that the Cross and Carreau models are fitted to the oscillatory measurements of the complex viscosity allowing extrapolating of the viscosity at a zero frequency. The Cross and Carreau models applied to the data points obtained from the frequency sweep test are adapted to the base bitumen and bitumen-filler mastics. However, at lower frequencies the complex viscosity curves obtained from the Carreau model are lower than those obtained from the Cross model. Binard et al. (2003) reported that the curve

fitting parameters from the Carreau model forced the formation of a plateau at low frequencies, artificially bending the curves, leading to a more pronounced curvature than with the Cross model, resulting in smaller ZSVs. It is not surprising that at low frequencies the predicted values obtained from the Carreau model are lower than those obtained from the Cross model if the measurements of complex viscosity do not reach steady state or the bitumen and mastics are not an aqueous system.

The two mathematical models can be used to check if the bitumen and the bitumen-filler mastics behave in the linear viscoelastic domain. Observing a plateau at low frequencies indicates that the complex viscosity is independent of frequency. At 60^{o}C the viscosities of the base bitumen and bitumen-filler mastics containing 15% and 35% filler contents at low frequencies reach constant values using the two models, but those of the 65% bitumen-filler mastics do not reach constant values using the Cross model. It is not surprising that the viscosity values of the 65% bitumen-filler mastics reach constant values using the Carreau model because the curve fitting parameters from the Carreau model can bend the curve at low frequencies. However, as seen from the upturn of predicted curve using the Cross model for the 65% bitumen-filler mastics, the particle-particle interaction of fillers must be considered.

Stastna et al. (2003) reported that particle-particle interaction in PMBs was believed to be responsible for the upturn of the viscosity curve (at low shear rate) in filled polymers. Thus, for the 65% bitumen-filler mastics having filler skeleton structure in the system, the mineral filler could be responsible for the rheological behaviour at low frequencies. This mechanism can have a role in forming the viscosity curves of the bitumen-filler mastics at low frequencies. Another explanation is that the steady state of the 65% bitumen-filler mastics may be not attained at 60^{o}C.

At 40^{o}C the significant difference in fitting curves at low frequencies for the bitumen and bitumen-filler mastics is shown using the Cross and Carreau models. The plateau at low frequency is observed for the predicted curves using the Carreau model because the curve fitting parameters always force the formation of a plateau. Additionally, the indication that the measurements of complex viscosity do not reach steady state at 40^{o}C

can be seen from the upturn of the predicted curve at low frequency using the Cross model.

In addition, the Cross model is only fitted to the experimental results which are associated with a pseudoplastic system, ranging from suspensions (aqueous media) to optically solutions (nonaqueous media). The steady state of the filler skeleton of the 65% bitumen-filler mastics could not be attained at the test temperatures of 40°C and 60°C, and the viscosity values may therefore not be reliable at low frequencies. In order to overcome the problem of reaching the steady state, the solution would be to run the frequency sweep test at higher temperatures than 60°C or lower frequencies than 0.001 rad/s. However, the accuracy of viscosity measurements should be considered due to the settling of filler particles and rheometer sensibility while testing at high temperature and long loading time conditions. Another solution is to test the stiff mastics using rotational viscometry test or creep test.

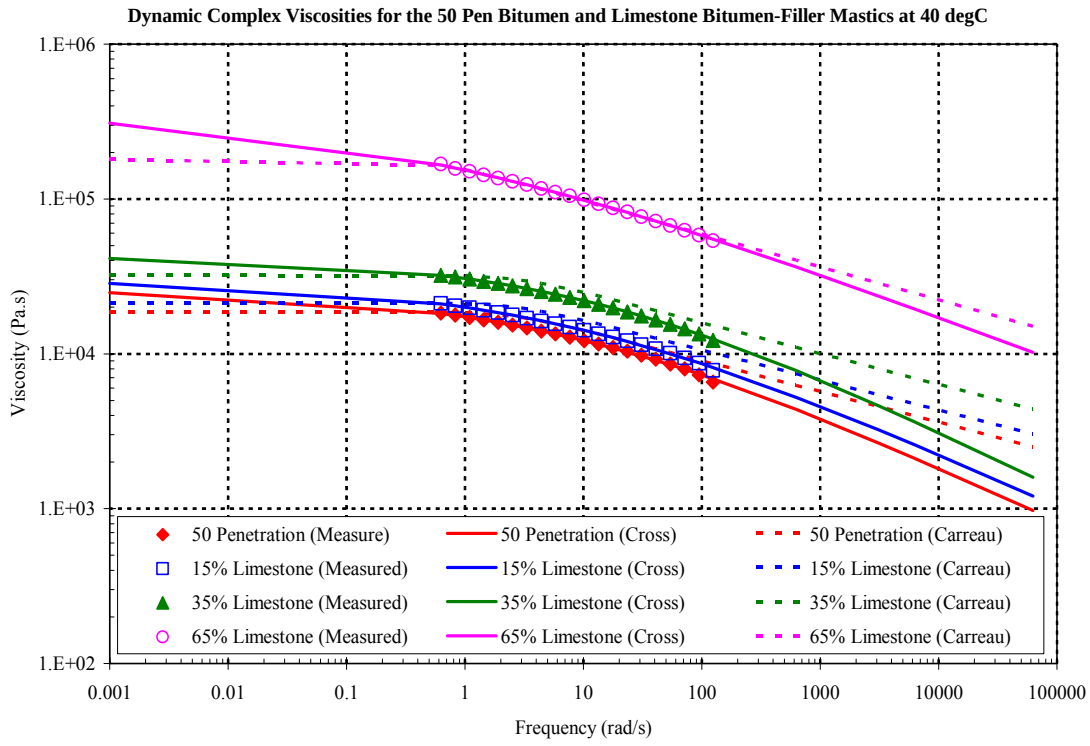

Figure 4.8: Effect of filler content on complex viscosity at 40°C for base bitumen and limestone bitumen-filler mastics

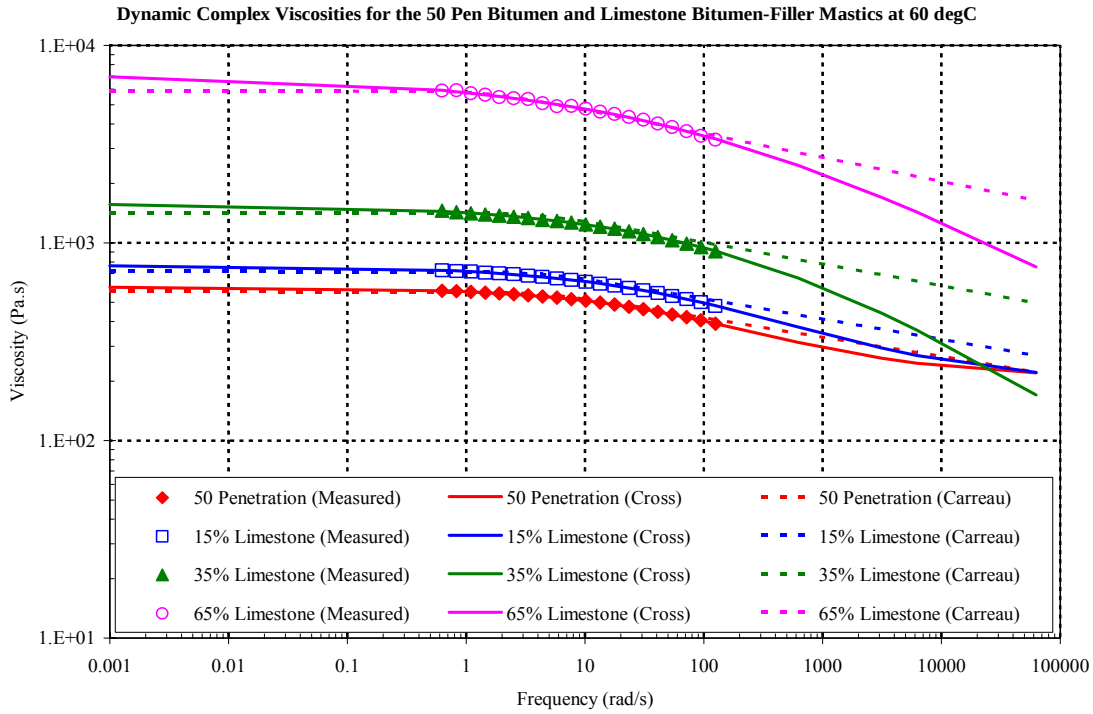

Figure 4.9: Effect of filler content on complex viscosity at 60°C for base bitumen and limestone bitumen-filler mastics

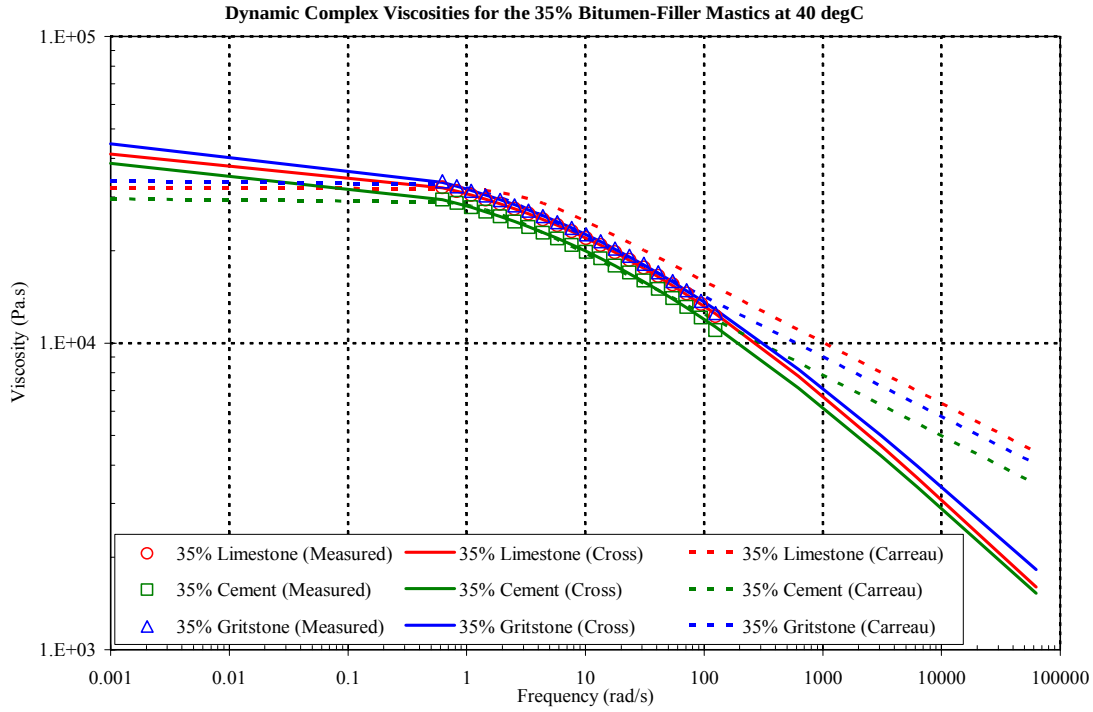

Figure 4.10: Effect of filler type on complex viscosity at 40°C for 35% bitumen-filler mastics

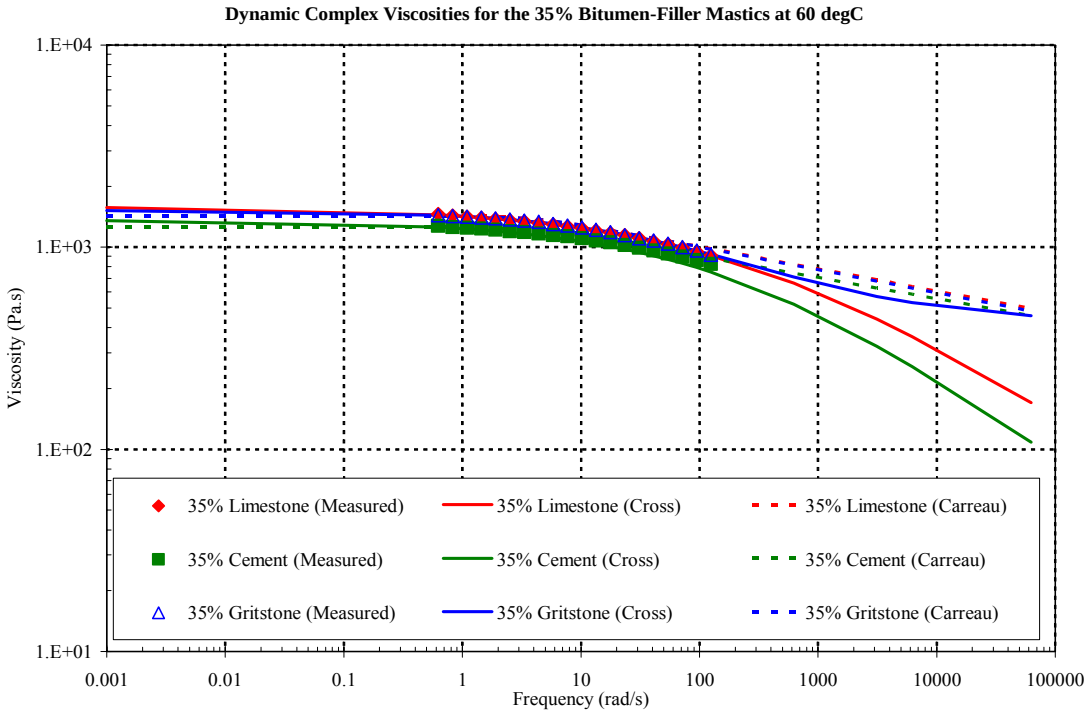

Figure 4.11: Effect of filler type on complex viscosity at 60°C for 35% bitumen-filler mastics

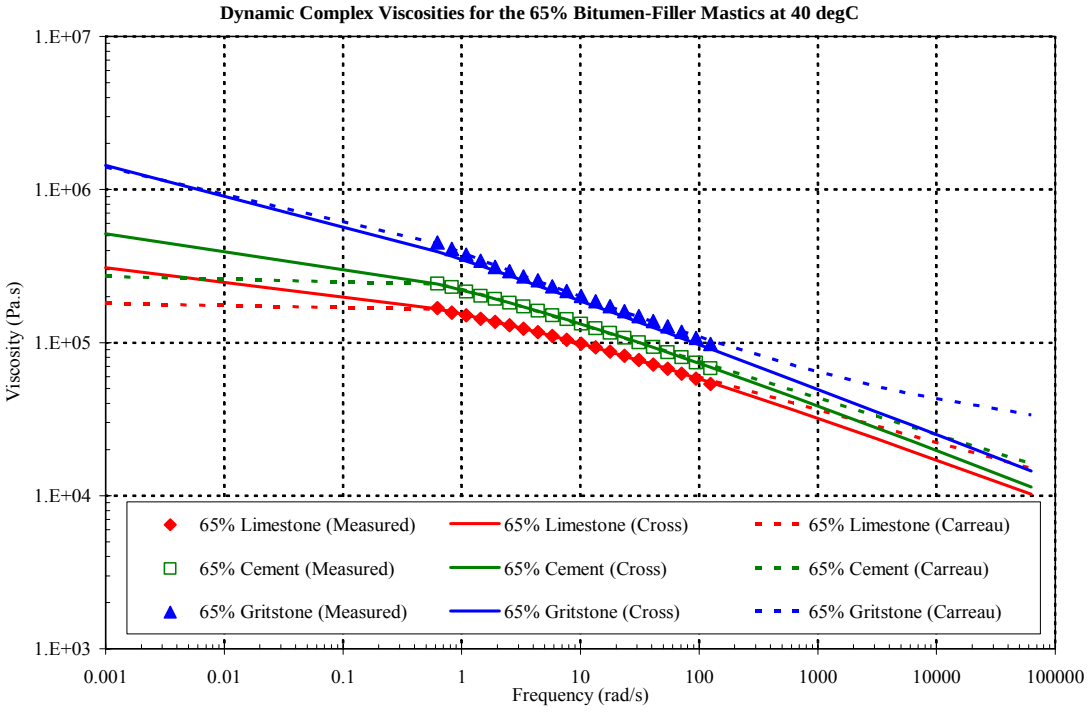

Figure 4.12: Effect of filler type on complex viscosity at 40°C for 65% bitumen-filler mastic

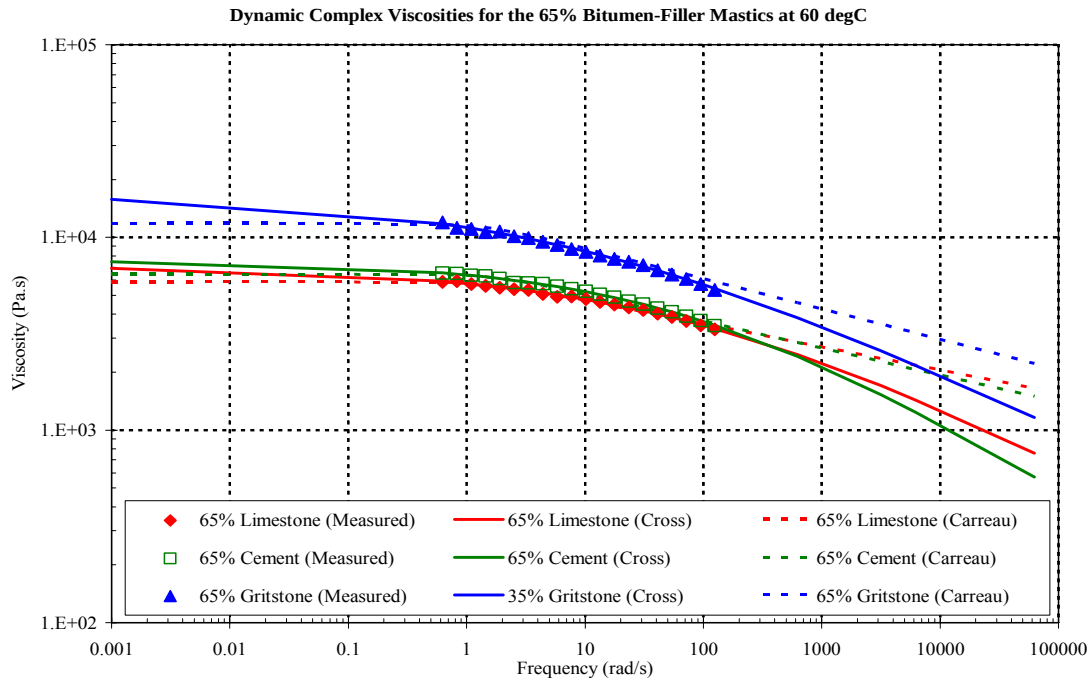

Figure 4.13: Effect of filler type on complex viscosity at 60°C for 65% bitumen-filler mastics

Influence of Filler Concentration and Type

Table 4.3 compares the ZSV results obtained for the base bitumen and bitumen-filler mastics as measured using low frequency oscillatory testing at both 40°C and 60°C. In addition to the values of ZSV, the relative increase in viscosity compared to the base bitumen is included as a ratio. Figures 4.14 to 4.17 show the 95% confidence for the ZSV values. The influence of filler type and concentration is also shown in Figures 4.18 and 4.19, where the ZSV stiffening ratios for the base bitumen and bitumen-filler mastics are presented.

The results show that at 35% filler by mass, the influence of filler type is marginal with all three mastics having a similar ZSV at both 40°C and 60°C. However, at 65% filler by mass the results show a significantly larger value of ZSV for the gritstone filler mastic compared to the limestone and cement fillers. It is noted that at 35% filler by mass, the ZSVs for the cement bitumen-filler mastics are slightly lower than those for the limestone bitumen-filler mastics because the cement bitumen-filler mastics have the

lower filler volume contents. However, at 65% filler by mass, the ZSVs for the cement bitumen-filler mastics are higher than those for the limestone bitumen-filler mastic. It can be speculated that some of the cement filler particles at the edge of DSR specimen may chemically react with bitumen as combining with water during testing. For the 35% cement bitumen-filler mastic, because the cement filler particles are suspended in the base bitumen, less chemical reaction occurred between the cement filler and the base bitumen, and therefore less stiffening effect is present in mastic.

The results for the 50 penetration grade bitumen together with the bitumen-filler mastics show an increase in ZSV with increasing filler concentration. According to the ZSV stiffening ratios presented in Table 4.3, the results only show a slight increase in ZSV for the 15% and 35% bitumen-filler mastics but a considerable increase for the 65% filler content mastics. The sharp increase in ZSV is caused by the filler contributing such a large volume to the binder that it becomes the predominant component in the bitumen-filler mastic and therefore has a dramatic effect on viscosity. Although the limestone and gritstone fillers (except cement filler) are inert additives added in the base bitumen, the stiffening ratios of ZSV of the bitumen-filler mastics are not directly proportional to filler content. It can be concluded that the rheological behaviour of the 15% and 35% bitumen-filler mastics is dominated by filler suspension system of mastic, while that of the 65% bitumen-filler mastics is dominated by mineral filler due to filler skeleton in the base bitumen.

It is noted that there is a significant stiffening effect of the filler skeleton of the 65% gritstone bitumen-filler mastic (filler effective volume content = 62.1%) compared to the base bitumen. At 40^{o}C, the ZSV stiffening ratio for the 65% gritstone bitumen-filler mastic can go up to approximately 100 times. The stiffening effect of 100 times corresponds with the 100 times factor between mastic linearity and bitumen linearity as described previously in Chapter 3. The ZSVs for the bitumen-filler mastic having filler skeleton structure might reflect the permanent deformation behaviour of asphalt mixtures.

Table 4.3: ZSVs extrapolated from oscillatory measurements using the two mathematical models

Materials	ZSV @ 40°C (Pa.s)		ZSV @ 60°C (Pa.s)	
	Cross	Carreau	Cross	Carreau
50 Pen Bitumen	25,800	18,600	597	567
15% Limestone (by mass)	29,700	21,400	768	718
(8.3% by effective volume)	[1.15]	[1.15]	[1.29]	[1.27]
35% Limestone (by mass)	42,500	32,100	1,581	1,427
(22.2% by effective volume)	[1.65]	[1.73]	[2.65]	[2.52]
65% Limestone (by mass)	364,000	180,000	7,093	5,907
(54.4% by effective volume)	[14.11]	[9.68]	[11.88]	[10.42]
35% Cement (by mass)	39,900	29,500	1,363	1,253
(20.6% by effective volume)	[1.55]	[1.59]	[2.28]	[2.21]
65% Cement (by mass)	629,000	271,000	7,572	6,484
(52.1% by effective volume)	[24.38]	[14.57]	[12.68]	[11.44]
35% Gritstone (by mass)	46,300	33,800	1,518	1,423
(25.6% by effective volume)	[1.79]	[1.82]	[2.54]	[2.51]
65% Gritstone (by mass)	2,590,000	1,410,000	16,740	11,860
(62.1% by effective volume)	[100.39]	[75.81]	[28.04]	[20.98]

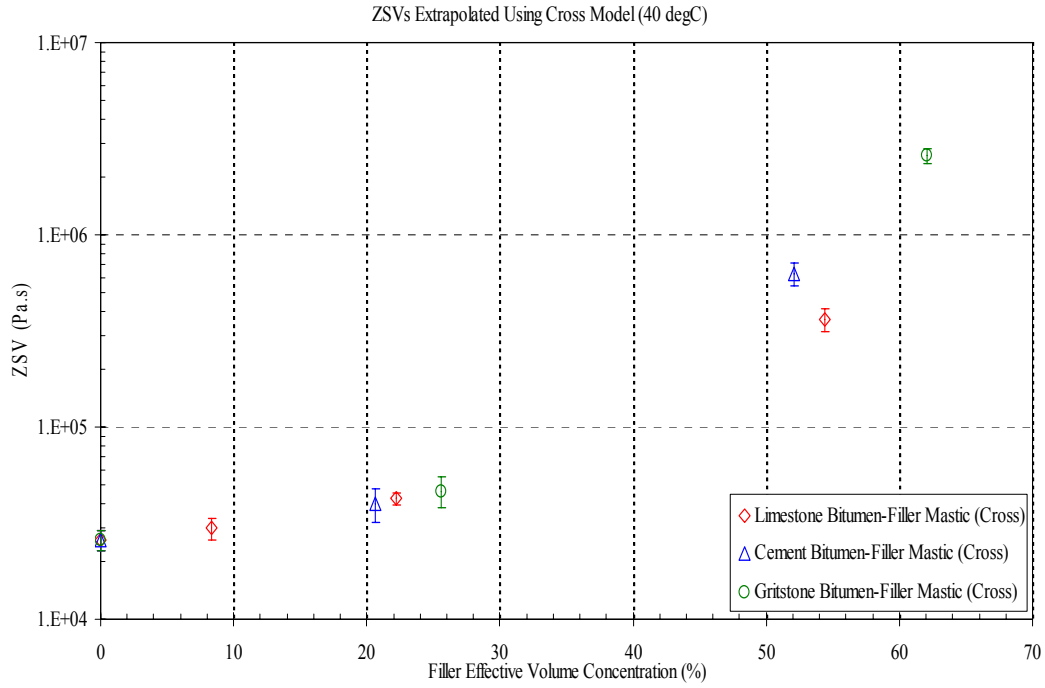

Figure 4.14: Variability of ZSVs for bitumen-filler mastics at 40°C (oscillation testing, Cross model)

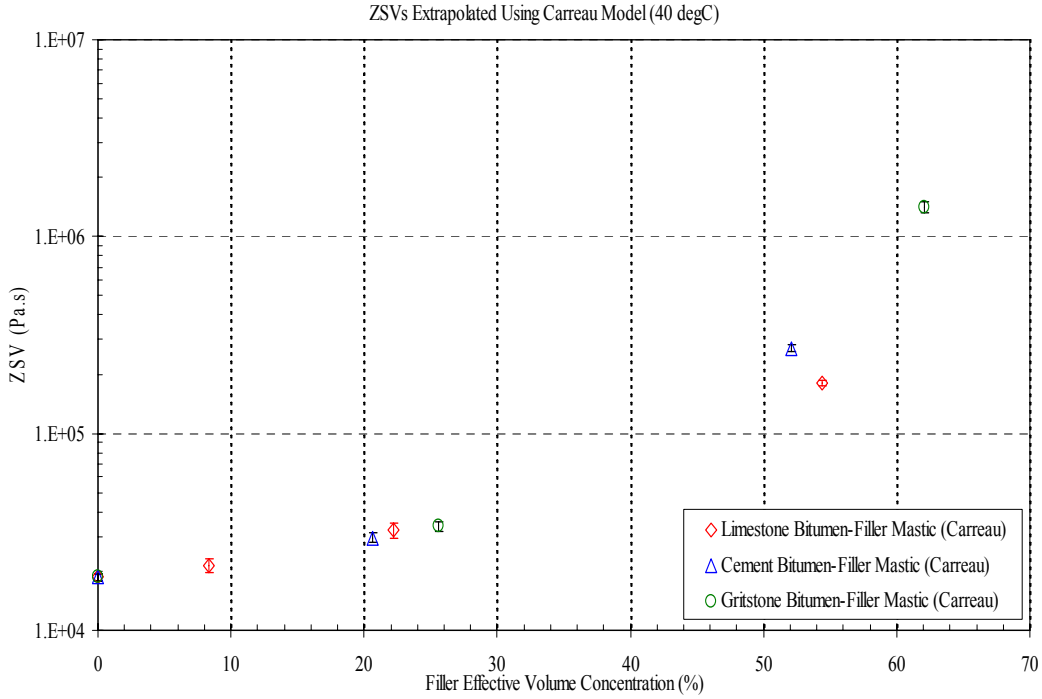

Figure 4.15: Variability of ZSVs for bitumen-filler mastics at 40°C (oscillation testing, Carreau Model)

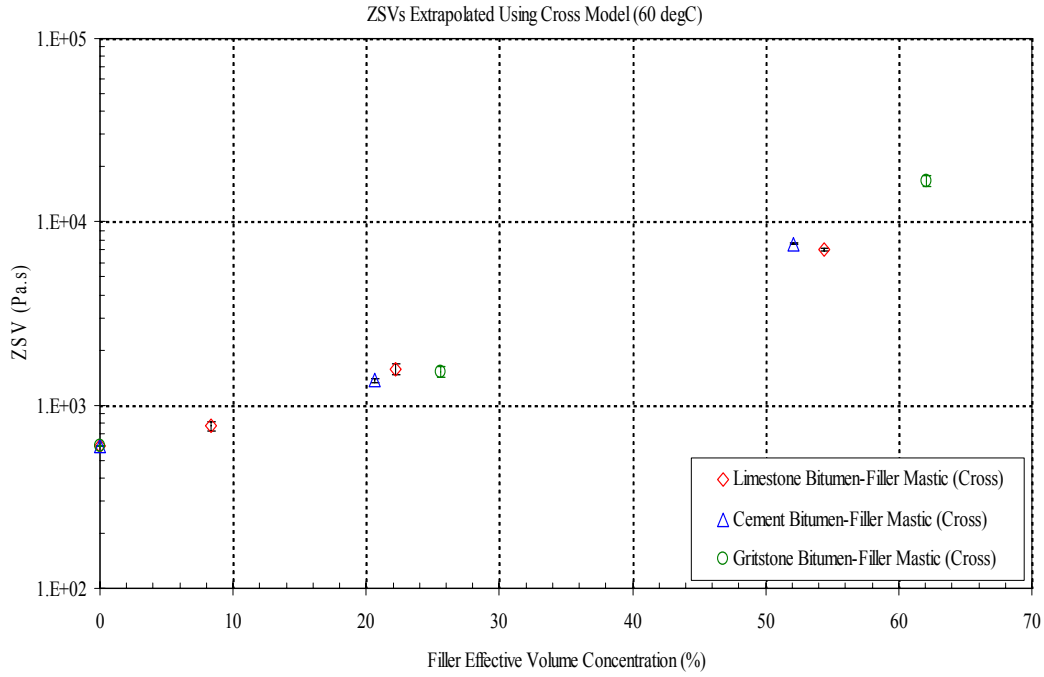

Figure 4.16: Variability of ZSVs for bitumen-filler mastics at 60°C (oscillation testing, Cross model)

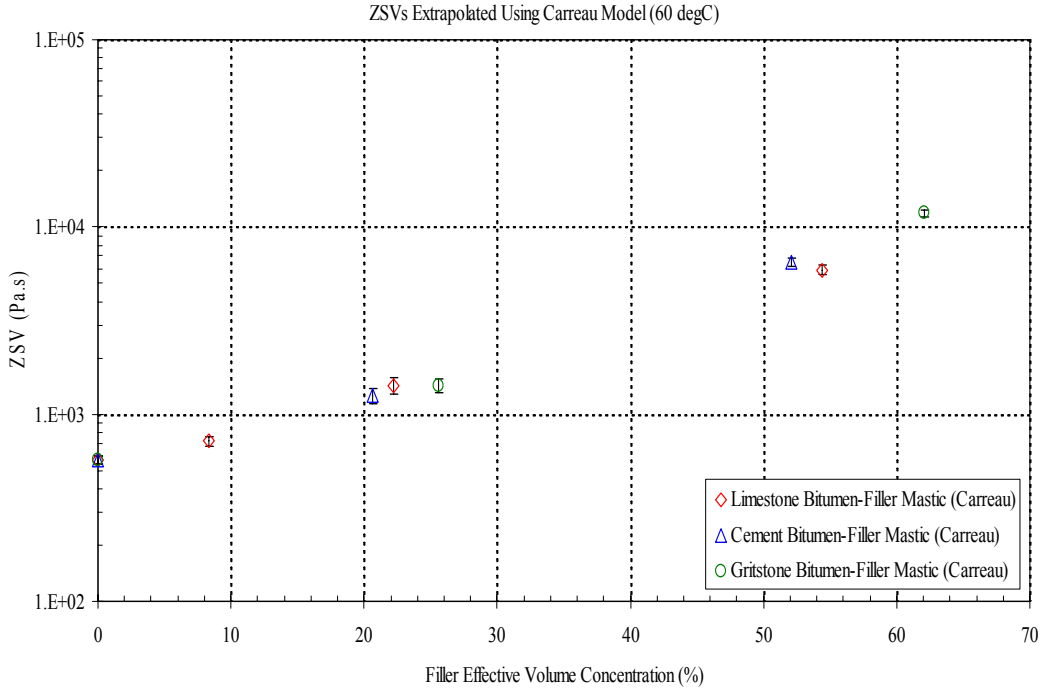

Figure 4.17: ZSV stiffening ratio for bitumen-filler mastics at 60°C (oscillation testing, Carreau model)

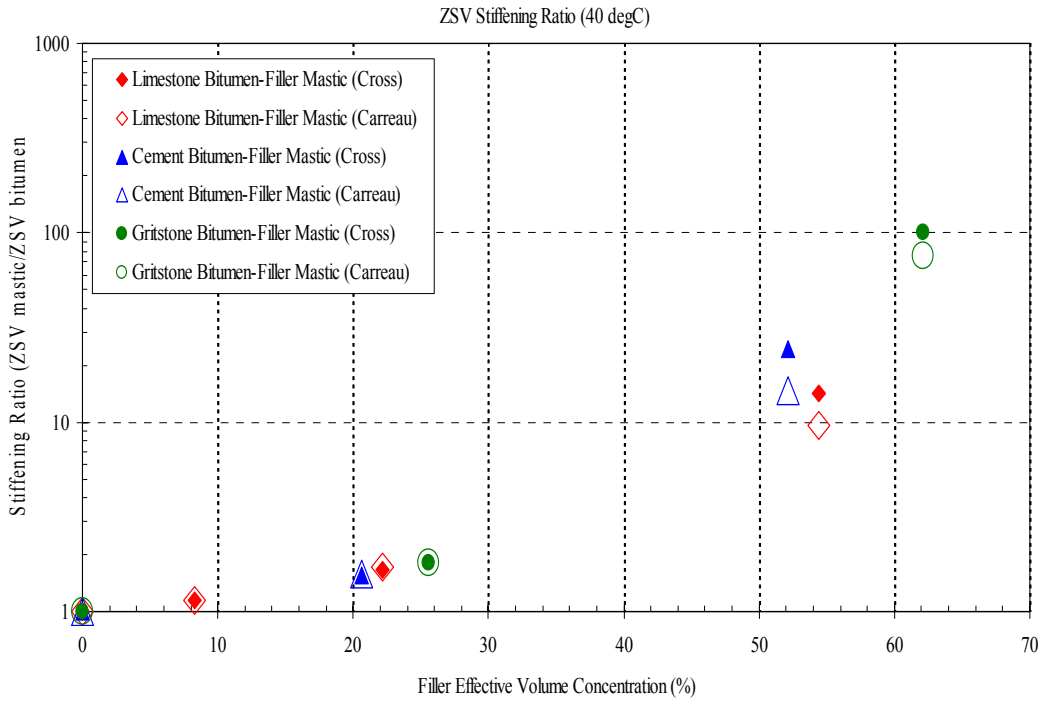

Figure 4.18: ZSV stiffening ratio for bitumen-filler mastics at 40°C (oscillation testing)

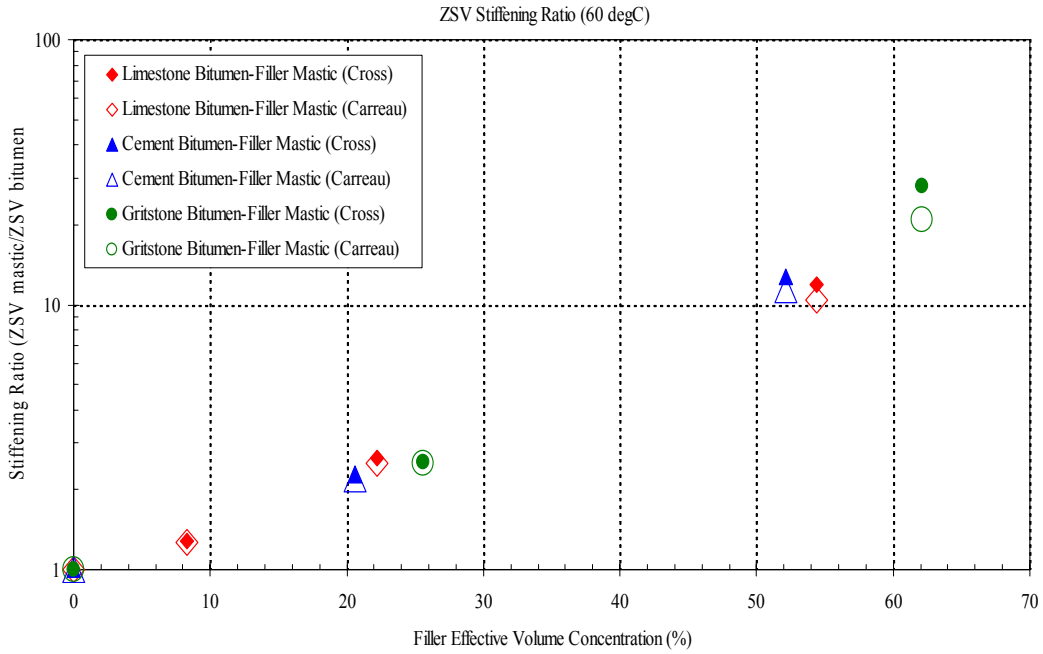

Figure 4.19: ZSV stiffening ratio for bitumen-filler mastics at 60°C (oscillation testing)

Material Constants from Oscillatory Measurements

Tables 4.4 and 4.5 compare the material constants for the base bitumen and bitumen-filler mastics at both 40°C and 60°C as calculated using a nonlinear regression analysis. The material constants, k_1 (Cross model) and k_3 (Carreau model), are related to viscosity and associated with rupture of material structural linkage (Cross, 1965). The higher values of k_1 and k_3 imply relatively large shear dependent contribution to structural damage (Cross, 1965). A significant increase in k_1 and k_3 with increasing ZSV at 40°C and 60°C is shown in Figure 4.20 also implies an increase in k_1 and k_3 with increasing filler concentration. The outliers of k_1 (65% gritstone bitumen-filler mastic at 40°C) and k_3 (65% gritstone bitumen-filler mastic at 40°C) on Figure 4.16 represents a highly modified system (filler skeleton) under shear conditions which may exhibit more rapid increases of rupture of structural linkage.

The material constants, n_1 (Cross model) and n_3 (Carreau model), are not related to ZSV but regarded as a measure of shear compliance of the bitumen and mastics. Sybilsky (1996a) reported that shear compliance was related to penetration index (PI) or shear susceptibility although the PI was calculated from measurements at 15°C and 25°C. The constants can be regarded as the slopes of the linear relationship between logarithmic complex dynamic viscosity and logarithmic frequency. The higher the n_1 and n_3 values, the higher is the shear susceptibility. Figure 4.20 shows that a decrease in the constant n_1 with increasing ZSV (or increasing filler concentration) implies that the shear susceptibility for the bitumen-filler mastic is not significant compared to that for the base bitumen using the Cross model. However, a slight increase in constant n_3 with increasing ZSV (or increasing filler concentration) indicates that there is a slightly higher shear susceptibility for the bitumen-filler mastics using the Carreau model. There is a good agreement that highly modified systems (65% bitumen-filler mastic) under shear conditions may exhibit a more rapid decrease of viscosity.

Table 4.4: Material constants from oscillatory measurements at 40°C

Materials	Cross Model		Carreau Model	
	k_1	n_1	k_3	n_3
50 Pen	0.941	0.358	5.632	0.099
15% limestone	0.923	0.352	5.575	0.097
35% limestone	0.775	0.380	4.483	0.100
65% limestone	2.343	0.293	11.220	0.107
35% cement	0.839	0.369	4.865	0.099
65% cement	3.239	0.306	12.840	0.120
35% gritstone	0.885	0.360	5.293	0.098
65% gritstone	11.140	0.301	460.800	0.156

Table 4.5: Material constants from oscillatory measurements at 60°C

Materials	Cross Model		Carreau Model	
	k_1	n_1	k_3	n_3
50 Pen	0.225	0.540	1.762	0.049
15% limestone	0.235	0.483	1.982	0.051
35% limestone	0.229	0.390	2.305	0.055
65% limestone	0.419	0.325	16.650	0.060
35% cement	0.224	0.428	2.096	0.053
65% cement	0.373	0.379	13.086	0.070
35% gritstone	0.252	0.523	1.902	0.057
65% gritstone	0.847	0.300	17.744	0.079

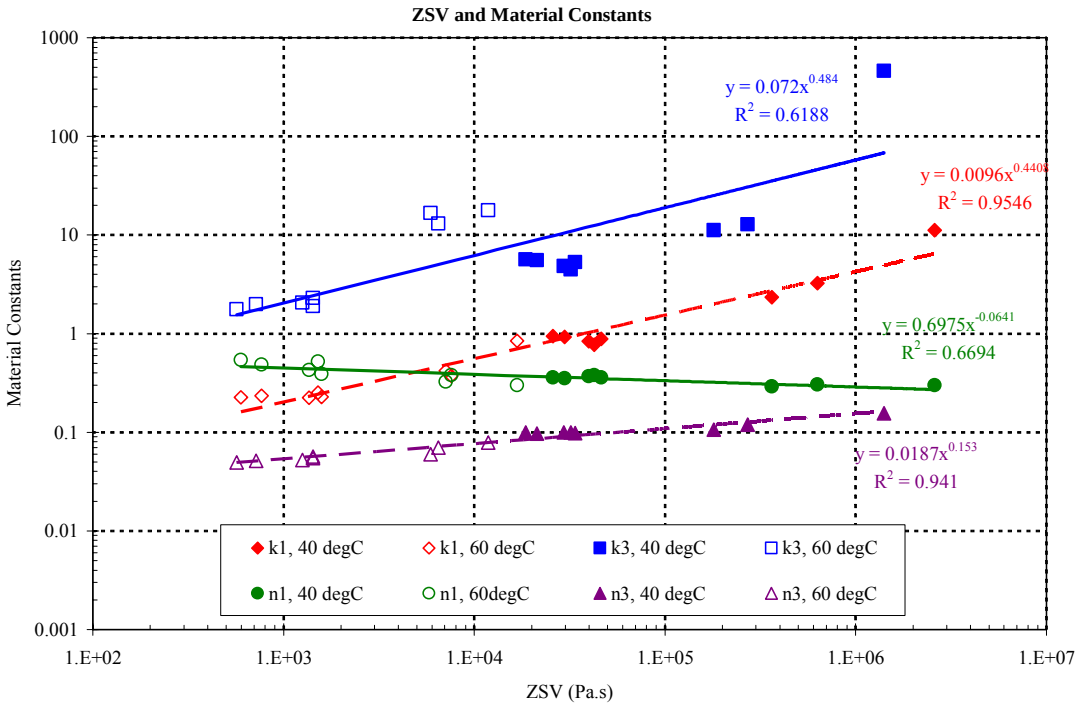

Figure 4.20: Material constant calculated from oscillation measurements

4.5.2 ZSV extrapolated from Viscometry Measurements

Due to the fact that the settling of filler particles in bitumens occurs while running oscillation testing at higher temperature and lower frequency conditions in order to reach steady state, the use of rotational viscometry testing using a DSR is an alternative for determining ZSV values of the bitumen and mastics at low shear rates. The apparent viscosities for the base bitumen and bitumen-filler mastics are plotted versus the corresponding shear rate on a log-log plot. Figures 4.21 through 4.26 show that the Cross and Carreau models are fitted to the viscometry measurements of the apparent viscosity allowing extrapolation of the viscosity at a zero shear rate. The Cross and Carreau models applied to the data points obtained from the rotational viscometry testing are adapted to the base bitumen and bitumen-filler mastics. At low shear rates the apparent viscosity curves obtained from the Carreau model are approximately equal to those obtained from the Cross model. It is because the apparent viscosity measurements of the bitumen-filler mastics reach steady state because the rotational viscometry testing is performed down to lower shear rate (0.01 1/s) without a very long test duration.

The two mathematical models can be used to check if the bitumen and bitumen-filler mastics behave in the linear viscoelastic range. Observing a plateau at low shear rate indicates that the apparent viscosity is independent of shear rate. The indication that at 40°C and 60°C the viscosities of the base bitumen and bitumen-filler mastics at low shear rate are independent of shear rate using the Cross and Carreau models reflects the viscosity measurements of the bitumen and mastics reach steady state.

It is a reasonable fact that there is little difference in low shear rate viscosity using the two mathematical models. The lowest test shear rate of the rotational viscometry testing is carried out down to 0.01 1/s compared to the lowest test frequency of the dynamic oscillation testing is 0.625 rad/s (0.1 Hz).

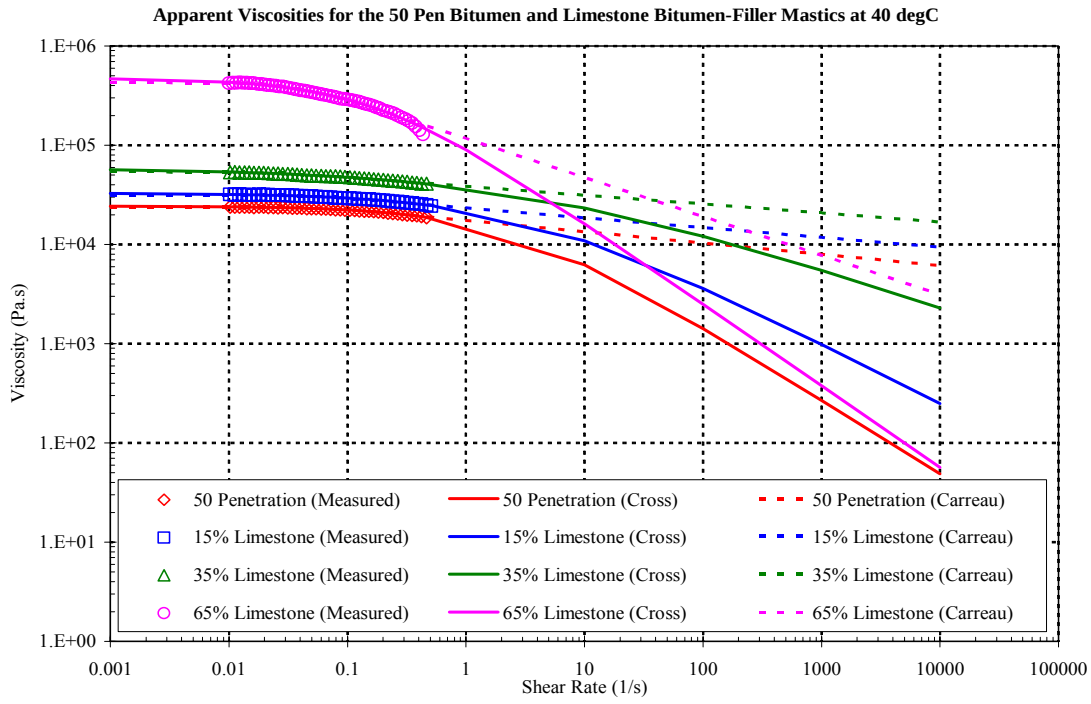

Figure 4.21: Effect of filler content on apparent viscosity at 40°C for limestone bitumen-filler mastics

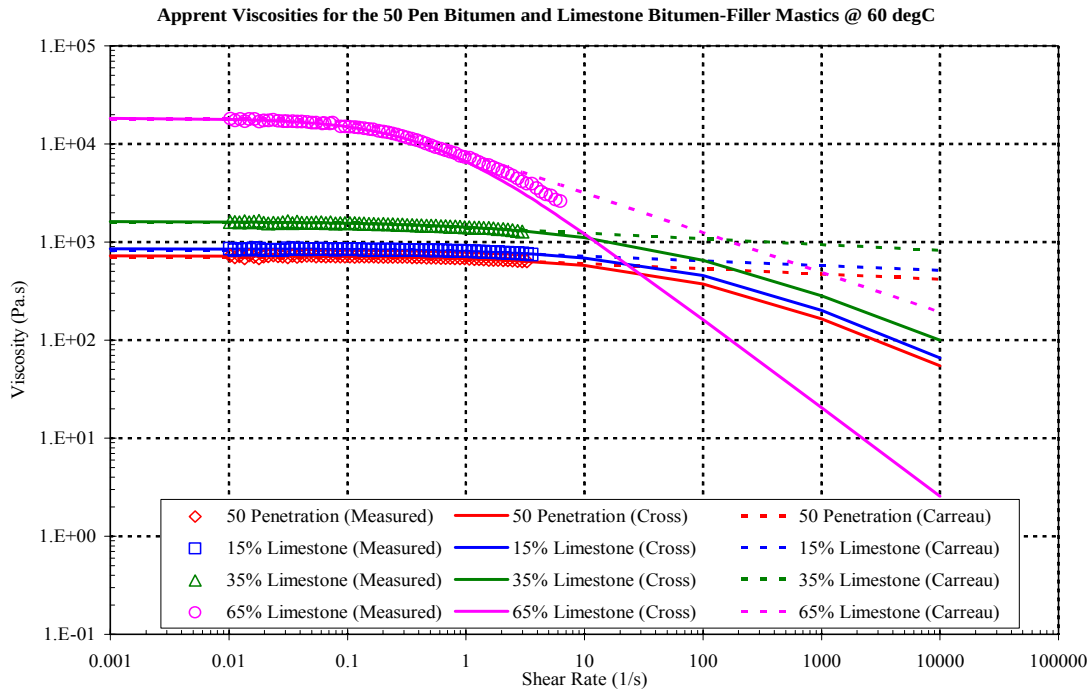

Figure 4.22: Effect of filler content on apparent viscosity at 60°C for limestone bitumen-filler mastics

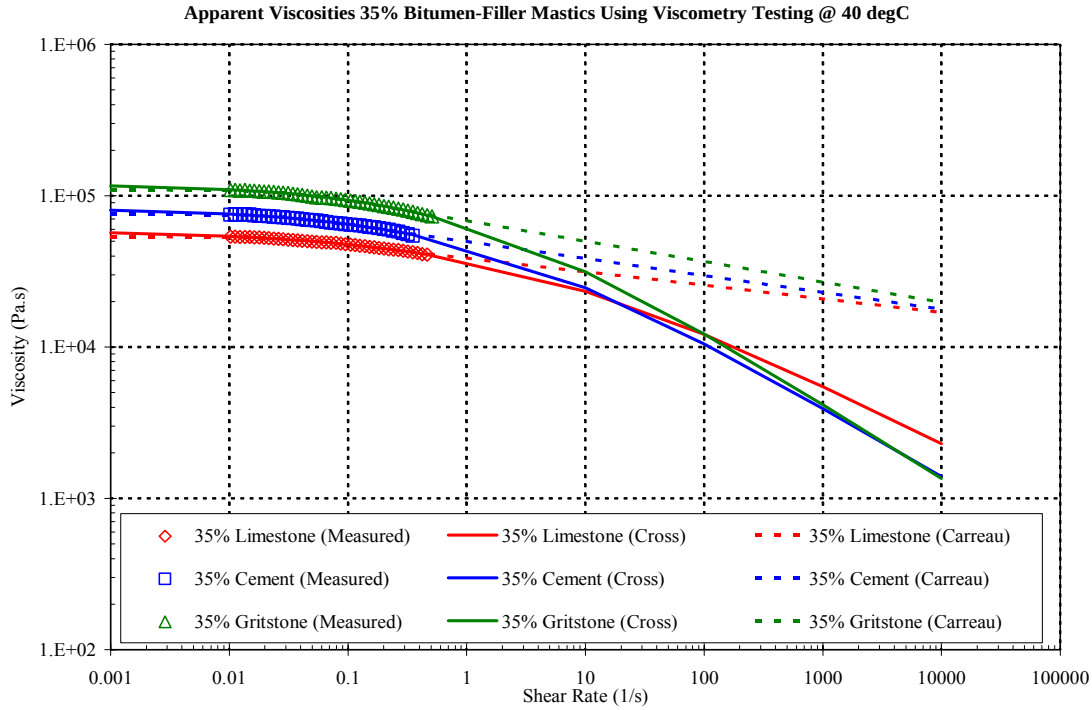

Figure 4.23: Effect of filler type on apparent viscosity at 40°C for 35% bitumen-filler mastics

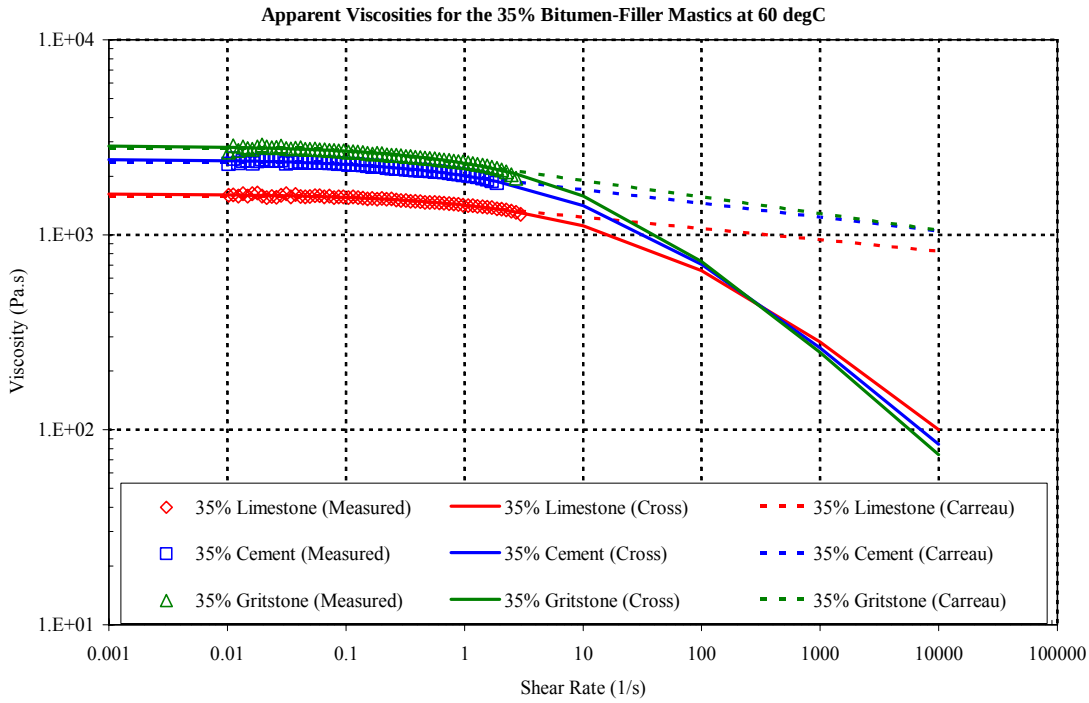

Figure 4.24: Effect of filler type on apparent viscosity at 60°C for 35% bitumen-filler mastics

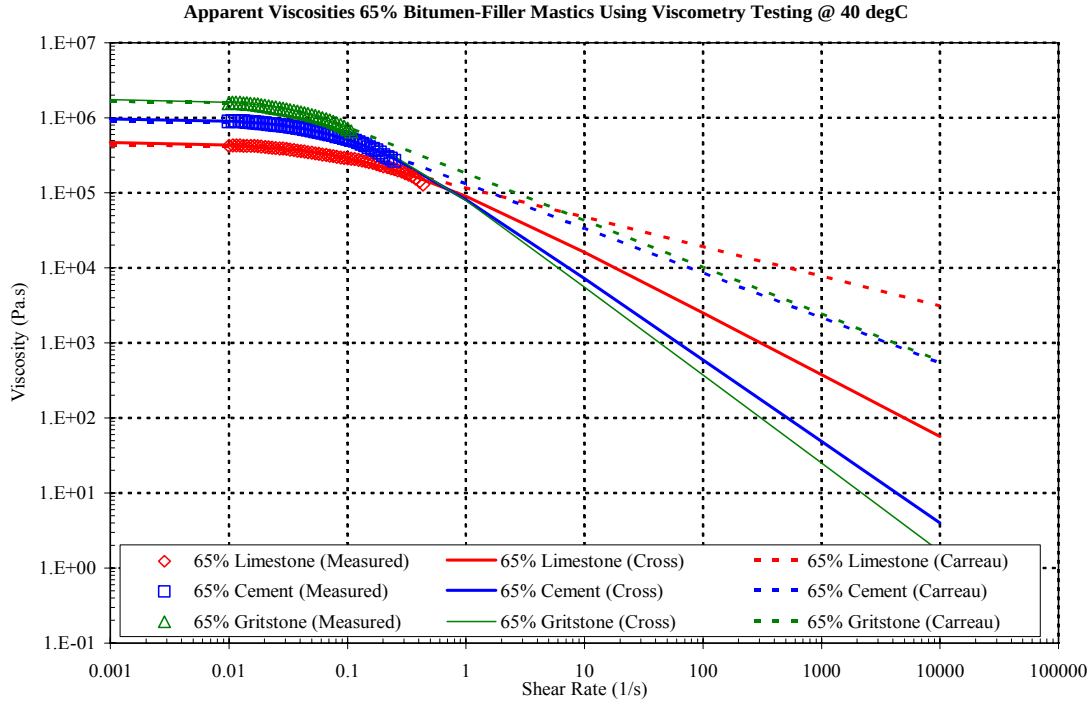

Figure 4.25: Effect of filler type on apparent viscosity at 40°C for 65% bitumen-filler mastics

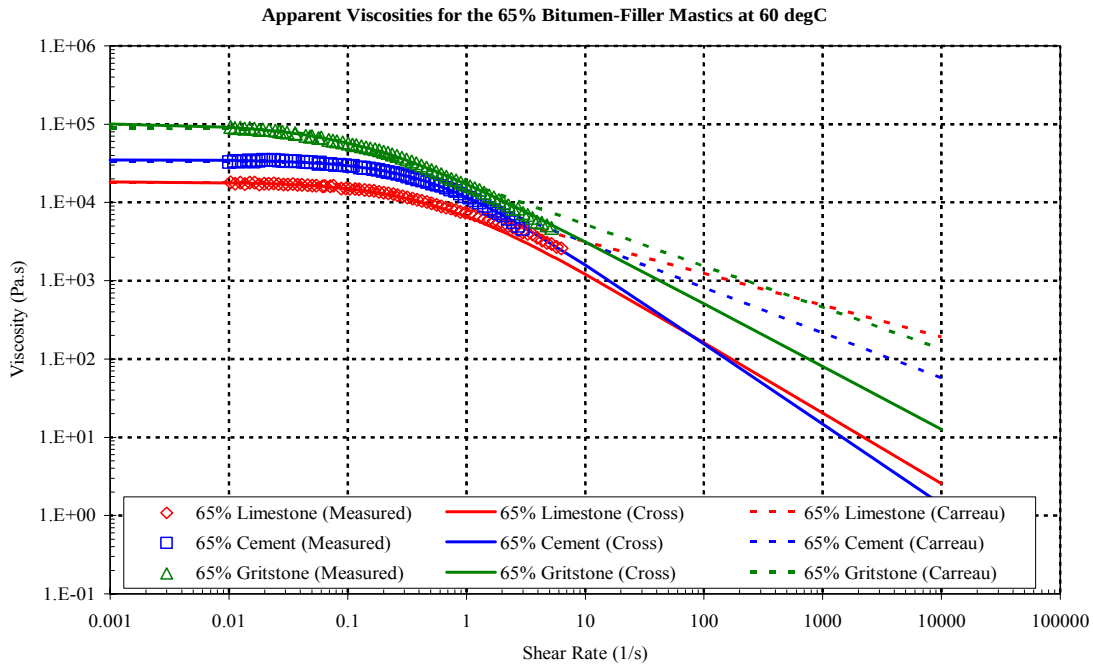

Figure 4.26: Effect of filler type on apparent viscosity at 60°C for 65% bitumen-filler mastics

Influence of Filler Concentration and Type

Table 4.6 compares the ZSV results obtained for the base bitumen and bitumen-filler mastics as measured using the technique of low shear rate viscometry testing at both 40°C and 60°C. In addition to the values of ZSV, the relative increase in viscosity compared to the base bitumen is included as a ratio. Figures 27 through 30 show 95% confidence for the ZSV values. The influence of filler type and concentration is also shown in Figures 4.31 and 4.32, where the ZSV stiffening ratios for the base bitumen and bitumen-filler mastics are presented.

The results show that at 35% filler by mass, the influence of filler type is slightly different among the three types of mastics at both 40°C and 60°C. The grtistone bitumen-filler mastic has the highest stiffening effect, followed by the cement bitumen-filler mastic, then the limestone bitumen-filler mastic. At 65% filler by mass the results show a significantly larger value of ZSV for the gritstone filler mastic compared to the limestone and cement fillers. It is noted that at 35% filler by mass, the ZSVs for the cement bitumen-filler mastics are slightly higher than those for the limestone bitumen-

filler mastics. It is believed that the cement fillers chemically react with the bitumen as combining water while testing. The ZSV results of the 35% cement bitumen-filler mastic obtained from the viscometry testing is opposite to those from the oscillation testing. It can be speculated that the rotational testing may cause much more chemical reaction between the cement filler particles and the bitumen compared to dynamic oscillation testing.

The results for the 50 penetration grade bitumen together with the bitumen-filler mastics show an increase in ZSV with increasing filler concentration. According to the ZSV stiffening ratios presented in Table 4.6, the results only show a slight increase in ZSV for the 15% and 35% bitumen-filler mastics but a considerable increase for the 65% filler content mastics. The sharp increase in ZSV is caused by the filler contributing such a large volume to the binder that it becomes the predominant component in the bitumen-filler mastic and therefore has a dramatic effect on viscosity. Although the limestone and gritstone fillers (except cement filler) are inert additives added in the base bitumen, the stiffening ratios of ZSV of the bitumen-filler mastics are not directly proportional to filler content. It can be concluded that the rheological behaviour of the 15% and 35% bitumen-filler mastics is dominated by filler suspension system of mastic, while that of the 65% bitumen-filler mastics is dominated by mineral filler due to the filler skeleton in the base bitumen.

It is noted that there is a significant stiffening effect of the filler skeleton of the 65% gritstone bitumen-filler mastic (filler effective volume content = 62.1%) compared to the base bitumen. At 60^{o}C, the ZSV stiffening ratio for the 65% gritstone bitumen-filler mastic can be over 100 times. The stiffening effect of 100 times corresponds with the 100 times factor between mastic linearity and bitumen linearity as described previously in Chapter 3. The ZSVs for the bitumen-filler mastic having filler skeleton structure might potentially reflect the permanent deformation behaviour of asphalt mixtures.

Table 4.6: ZSVs extrapolated from viscometry measurements using the two mathematical models

Materials	ZSV @ 40 degC (Pa.s)		ZSV @ 60 degC (Pa.s)	
	Cross	Carreau	Cross	Carreau
50 Pen Bitumen	24,400	23,900	725	713
15% Limestone by mass (8.3% by effective volume)	33,000 [1.35]	31,700 [1.33]	854 [1.18]	841 [1.18]
35% Limestone (by mass) (22.2% by effective volume)	59000 [2.42]	53,800 [2.25]	1,626 [2.24]	1589 [2.23]
65% Limestone (by mass) (54.4% by effective volume)	474,000 [19.43]	430,000 [17.99]	18,320 [25.27]	18,130 [25.43]
35% Cement (by mass) (20.6% by effective volume)	82,900 [3.40]	75,700 [3.17]	2,444 [3.37]	2,379 [3.34]
65% Cement (by mass) (52.1% by effective volume)	968,000 [39.67]	901,000 [37.70]	35,050 [48.34]	33,510 [47.00]
35% Gritstone (by mass) 25.6% by effective volume)	120,000 [4.92]	109,000 [4.56]	2,858 [3.94]	2,783 [3.90]
65% Gritstone (by mass) (62.1% by effective volume)	1,760,000 [72.13]	1,650,000 [69.04]	102,500 [141.38]	88,310 [123.86]

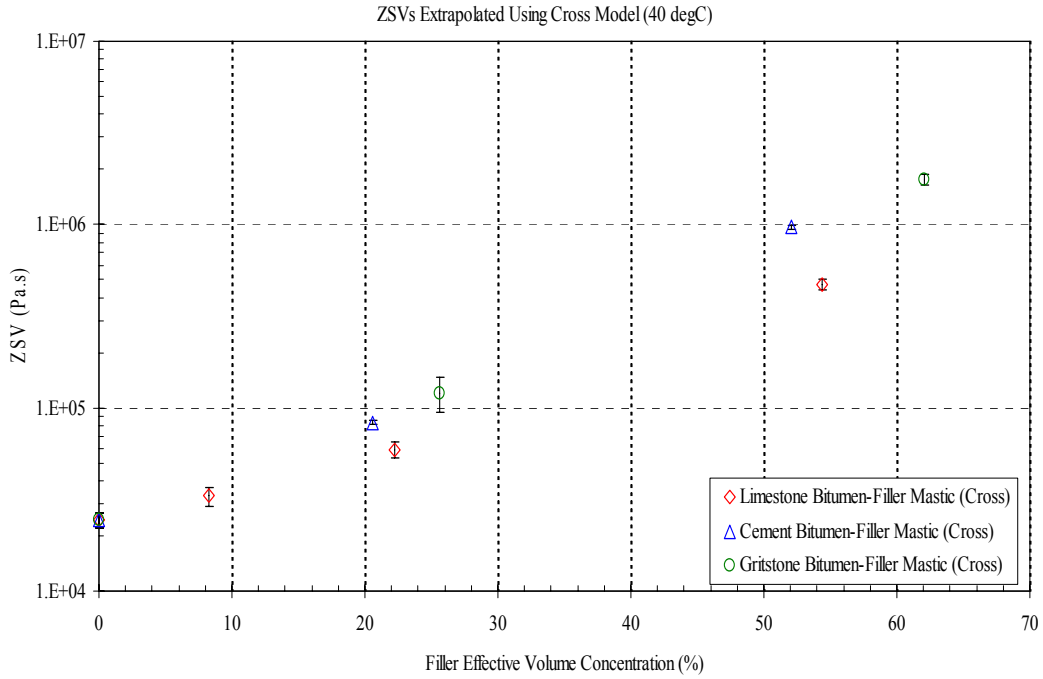

Figure 4.27: Variability of ZSVs for btumen-filler mastics at 40°C (viscometry testing, Cross model)

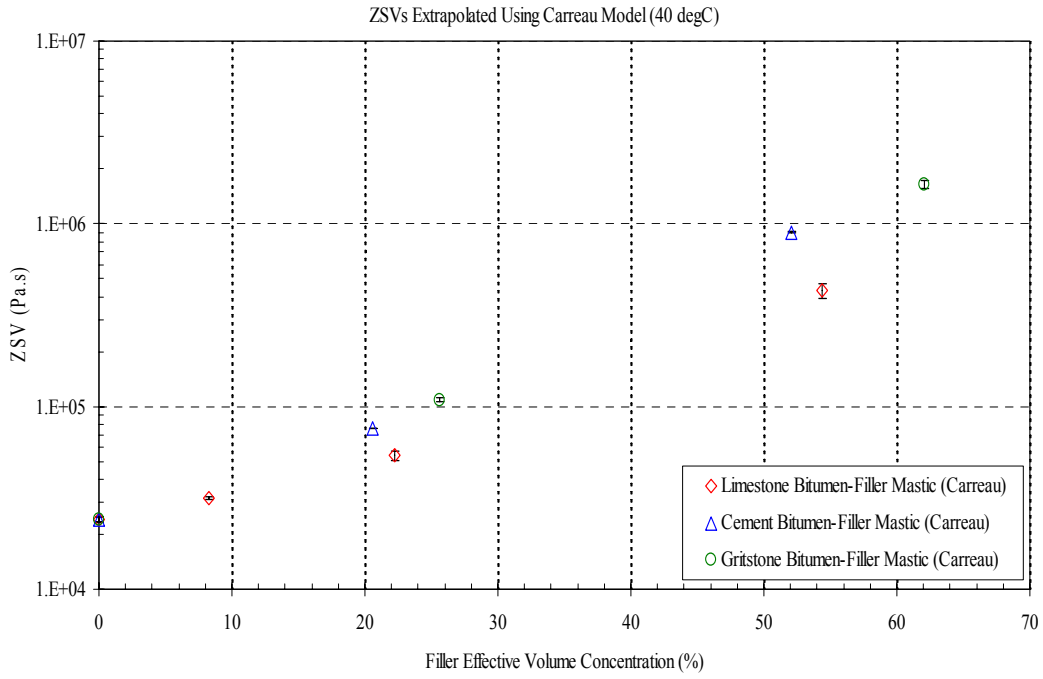

Figure 4.28: Variability of ZSVs for btumen-filler mastics at 40°C (viscometry testing, Carreau model)

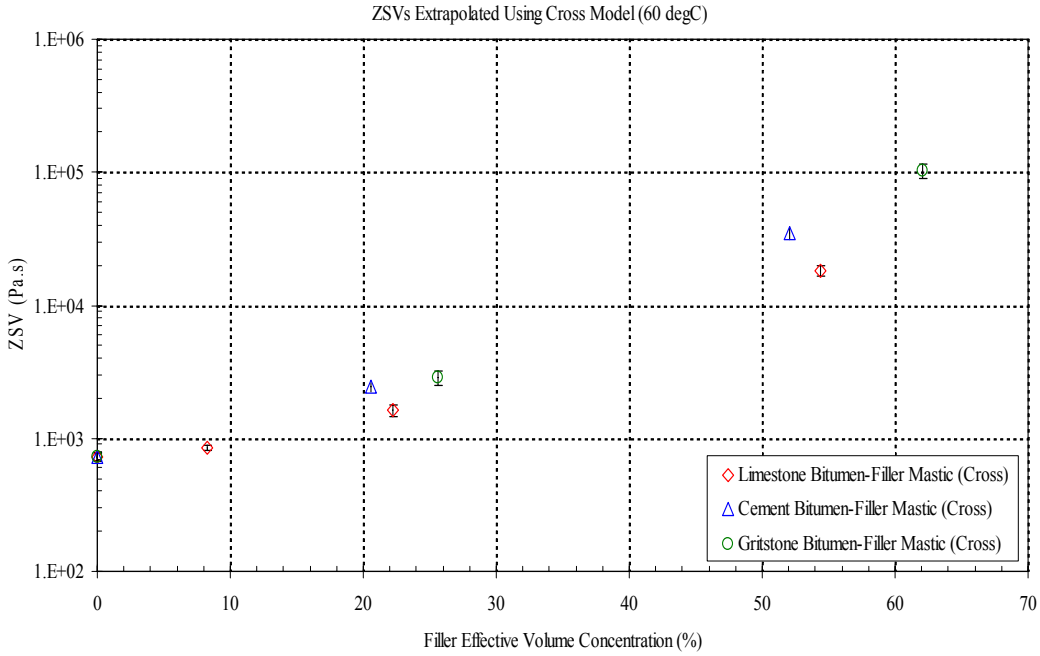

Figure 4.29: Variability of ZSVs for bitumen-filler mastics at 60°C (viscometry testing, Cross model)

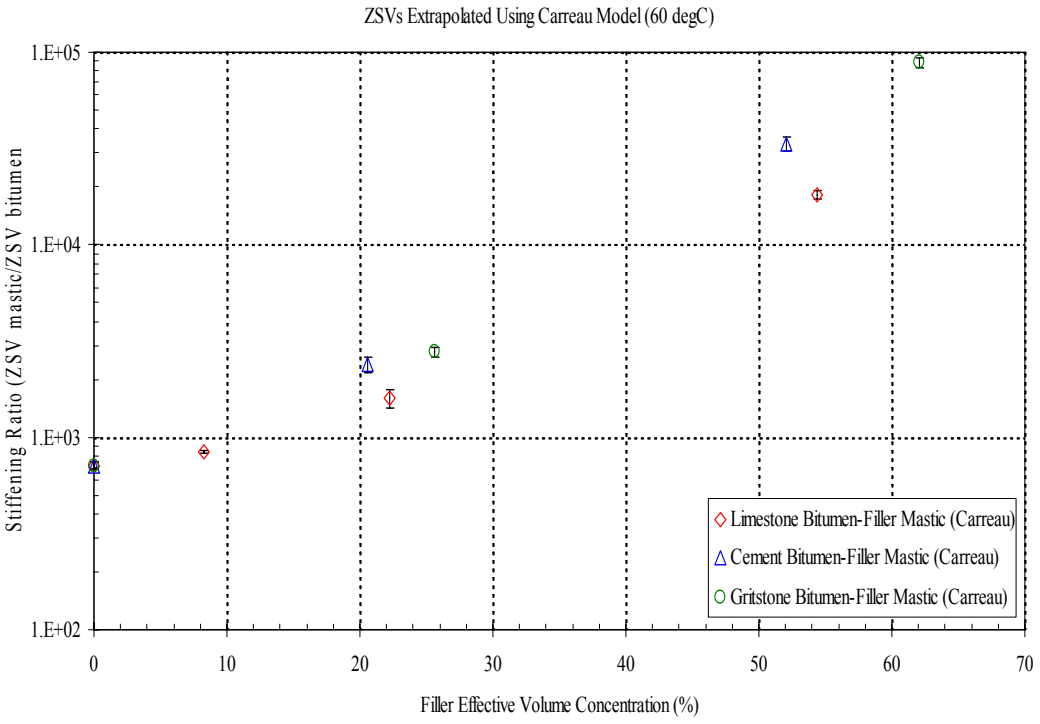

Figure 4.30: ZSV stiffening ratio for bitumen-filler mastics at 60°C (viscometry testing, Carreau model)

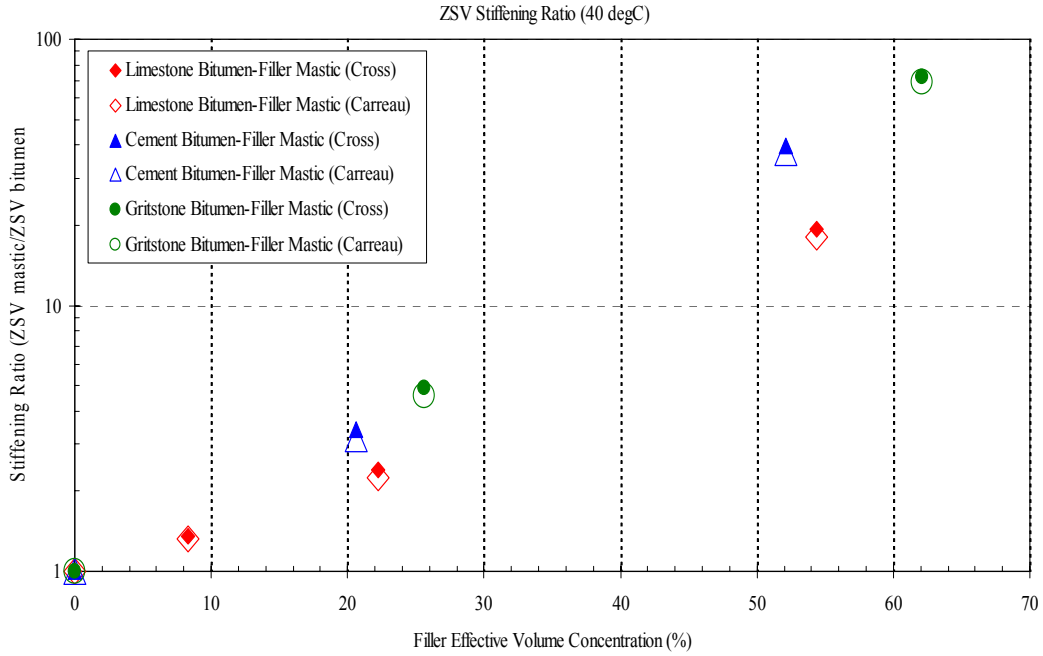

Figure 4.31: ZSV stiffening ratio for bitumen-filler mastics at 40°C (viscometry testing)

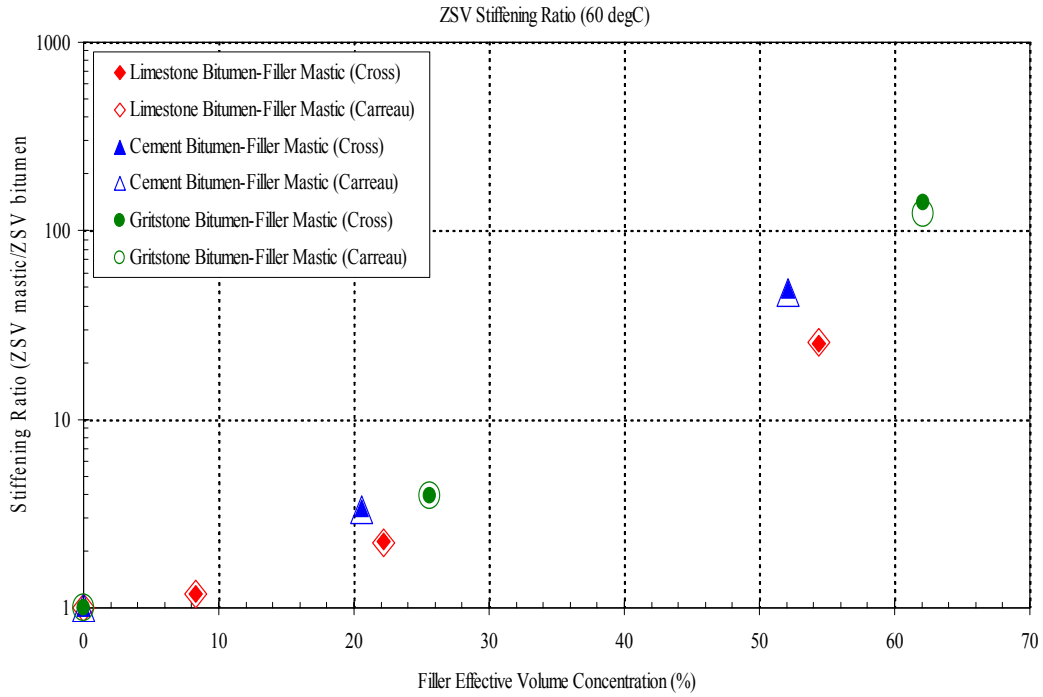

Figure 4.32: ZSV stiffening ratio for bitumen-filler mastics at 60°C (viscometry testing)

Material Constants from Viscometry Measurements

Tables 4.7 and 4.8 compare the material constants for the base bitumen and bitumen-filler mastics at both 40°C and 60°C as calculated using the nonlinear regression analysis. Figure 4.33 shows a significant increase in k_2 (Cross model) and k_4 (Carreau model) with increasing ZSV at 40°C and 60°C. It also indicates that an increase in k_2 and k_4 with increasing filler concentration. The fact shows a more rapid increase of rupture of structural linkage for the 65% bitumen-filler mastics compared to the base bitumen and the bitumen-filler mastic containing 15% and 35% filler contents.

The material constants, n_2 (Cross model) and n_4 (Carreau model), are not related to ZSV but regarded as a measure of shear susceptibility of the bitumen and mastics. The two constants can be regarded as the slopes of the linear relationship between logarithmic apparent viscosity and logarithmic shear rate. The higher the n_2 and n_4 values, the higher is the shear susceptibility. Figure 4.33 shows that an increase in the constant n_2 with increasing ZSV (and increasing filler concentration) implies that the shear susceptibility for the bitumen-filler mastic is not significant compared to the base bitumen using the Cross model. However, a considerable increase in constant n_4 with increasing ZSV (and increasing filler concentration) indicates that the higher shear susceptibility for the bitumen-filler mastics is shown using the Carreau model. There is a good agreement that highly modified systems under shear conditions may exhibit a more rapid decrease of viscosity.

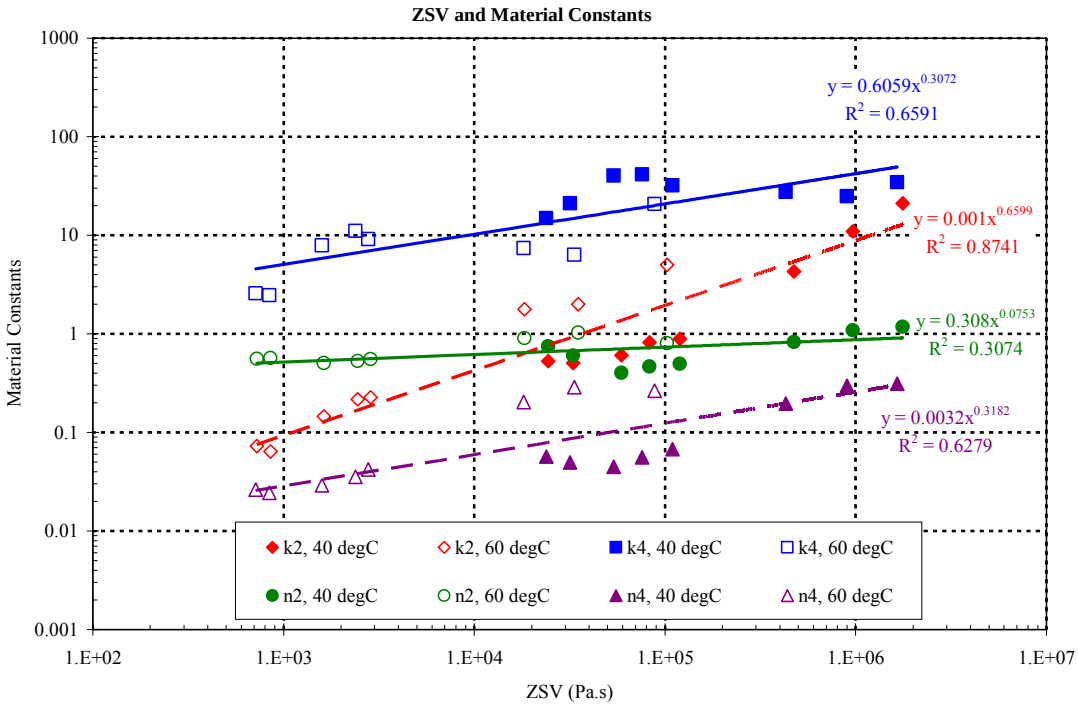

Figure 4.33: Material constants from viscometry measurements

Table 4.7: Material constants from viscometry measurements at 40°C

Materials	Cross Model		Carreau Model	
	k_2	n_2	k_4	n_4
50 Pen	0.527	0.744	14.870	0.057
15% limestone	0.507	0.603	21.100	0.050
35% limestone	0.605	0.403	40.090	0.045
65% limestone	4.274	0.823	27.390	0.197
35% cement	0.815	0.464	41.220	0.056
65% cement	10.930	1.087	24.850	0.298
35% gritstone	0.890	0.498	32.190	0.068
65% gritstone	21.180	1.174	34.550	0.312

Table 4.8: Material constants from viscometry measurements at 60°C

Materials	Cross Model		Carreau Model	
	k_2	n_2	k_4	n_4
50 Pen	0.072	0.557	2.586	0.026
15% limestone	0.064	0.568	2.459	0.024
35% limestone	0.146	0.505	7.863	0.029
65% limestone	1.773	0.901	7.410	0.203
35% cement	0.216	0.528	11.090	0.035
65% cement	1.999	1.025	6.336	0.288
35% gritstone	0.227	0.554	9.161	0.042
65% gritstone	5.001	0.802	20.700	0.265

4.5.3 ZSV Calculated from Creep Measurements

Chapter 2 has reviewed that ZSV can be estimated from the steady state part of the creep phase (retardation phase), and is also derived from the residual compliance in the recovery phase (relaxation phase). Table 4.9 compares the ZSV results for the bitumen and bitumen-filler mastics as measured using the two creep techniques of single creep-recovery and pulse creep testing at 40°C and 60°C. In addition to the values of ZSV, the relative increase in viscosity compared to the base bitumen is included as a ratio. In order to obtain the accurate ZSVs, steady state must be attained during testing time. Additionally, the ZSV value is independent of the shear stress as the applied shear stress is sufficient low. The measurement is then performed in the linear viscoelastic domain.

Effect of Filler Concentration and Type on ZSV

In terms of the limestone bitumen-filler mastics, the results for the 50 penetration grade bitumen together with the three limestone bitumen-filler mastics are presented in Figures 4.34 and 4.35. The results show a marginal increase in ZSV for the 15% and 35% filler mastics but a considerable increase for the 65% filler concentration mastic. The dramatic increase in ZSV is caused by the filler contributing such a large volume to the binder that it becomes the predominant component in the bitumen-filler system and therefore has a dramatic effect on viscosity.

The influence of filler type is also shown in Figures 4.36 and 4.37, where the ZSVs for the 35% and 65% bitumen-filler mastics as determined using the two techniques of single creep-recovery creep and pulse creep testing are presented. The results show that at 35% filler by mass, the influence of filler type is marginal with all three mastics having a similar ZSV at 60^{o}C but the gritstone bitumen-filler mastic has the higher ZSV, followed by the cement bitumen-filler mastic, then the limestone bitumen-filler mastic at 40^{o}C. In addition, at 65% filler by mass the results show a significant larger value of ZSV for the gritstone bitumen-filler mastic compared to the limestone and cement bitumen-filler mastics. In addition the stiffening effect is greater for the cement mastic compared to the limestone due to the fact that the cement filler particles chemically react with the base bitumen as combining with water while testing.

It is noted that the ZSV derived from the steady state in the creep phase is the same as that derived from residual compliance in the recovery phase. For the comparison of test techniques, there is no difference in ZSV for the base bitumen and bitumen-filler mastics using the single creep-recovery testing and the pulse creep testing. The similar values in ZSV for the base bitumen and mastics implies that the viscosity estimated from creep testing approaches the value of ZSV as long as the steady state is attained during testing.

Additionally, there is a significant stiffening effect of the filler skeleton of the 65% gritstone bitumen-filler mastic (filler effective volume content = 62.1%) compared to the other bitumen-filler mastics. At 40^{o}C and 60^{o}C, the ZSV stiffening ratio for the 65% gritstone bitumen-filler mastic can be approximately 200 times. The ZSV stiffening effect may correspond with the 100 times factor between mastic linearity and bitumen linearity as described previously in Chapter 3. Delgadillo et al (2004 and 2006) claimed that repeated creep loading (pulse creep) represented better the actual loading on the pavement than fully reserved load from dynamic oscillation testing because the load that causes rutting in the real pavement is not fully reserved. Thus, the ZSVs obtained from creep testing for the bitumen-filler mastic having filler skeleton structure might better reflect the permanent deformation behaviour of asphalt mixtures compared to dynamic oscillation and rotational viscometry testing.

Table 4.9: ZSVs extrapolated from single creep and pulse creep measurements

Materials	ZSV @ 40°C (Pa.s)		ZSV @ 60°C (Pa.s)		ZSV @ 60°C (Pa.s)	
	Single Creep-Recovery		Single Creep-Recovery		Pulse Creep	
	Creep	Recovery	Creep	Recovery	Creep	Recovery
50 Pen Bitumen	21,300	21,200	723	742	628	667
15%Limestone	26,600 [1.25]	26,900 [1.27]	839 [1.16]	836 [1.15]	752 [1.20]	806 [1.21]
35%Limestone	49,100 [2.31]	49,000 [2.31]	1,267 [1.75]	1,267 [1.71]	1,290 [2.05]	1,344 [2.01]
65%Limestone	627,000 [29.44]	627,000 [28.58]	15,700 [21.72]	15,723 [21.19]	13,100 [20.86]	12,903 [19.34]
35%Cement	64,300 [3.02]	63,900 [3.01]	1,280 [1.77]	1,276 [1.72]	1,230 [1.96]	1,328 [1.99]
65%Cement	1,190,000 [55.87]	1,110,000 [52.36]	35,700 [49.38]	35,211 [47.45]	-- [--]	-- [--]
35%Gritstone	77,500 [3.64]	76,300 [3.60]	1,380 [1.91]	1,374 [1.85]	1,380 [2.20]	1,443 [2.16]
65%Gritstone	4,860,000 [228.17]	4,270,000 [201.42]	147,000 [203.32]	142,248 [191.71]	-- [--]	-- [--]

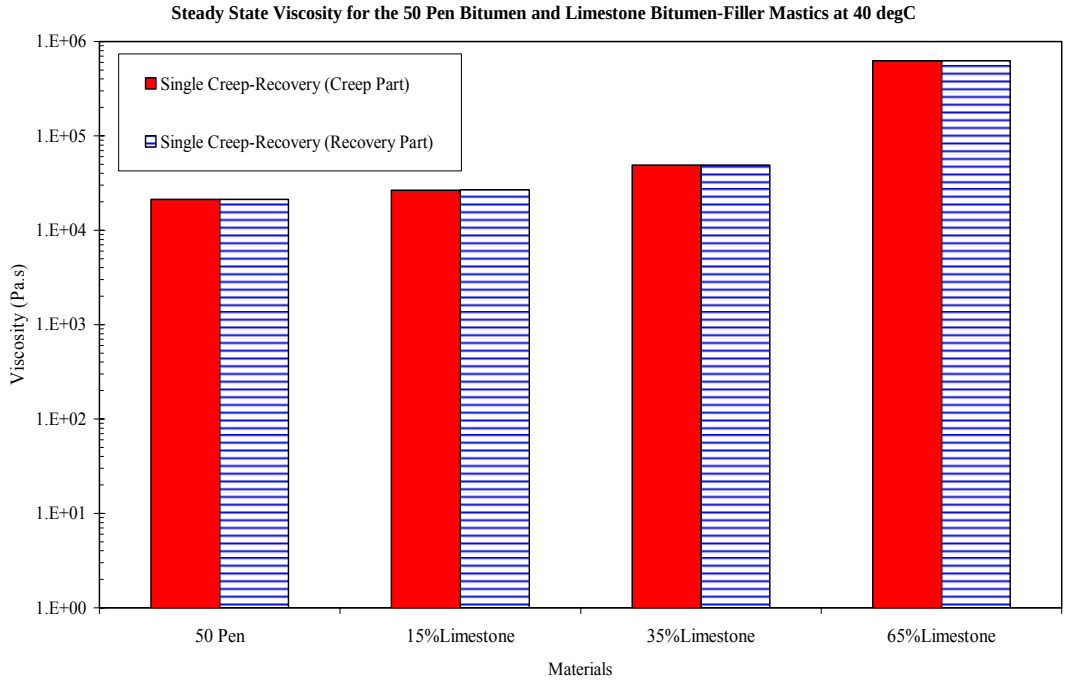

Figure 4.34: Effect of filler content on ZSV for 50 pen bitumen and limestone bitumen-filler mastics at 40°C

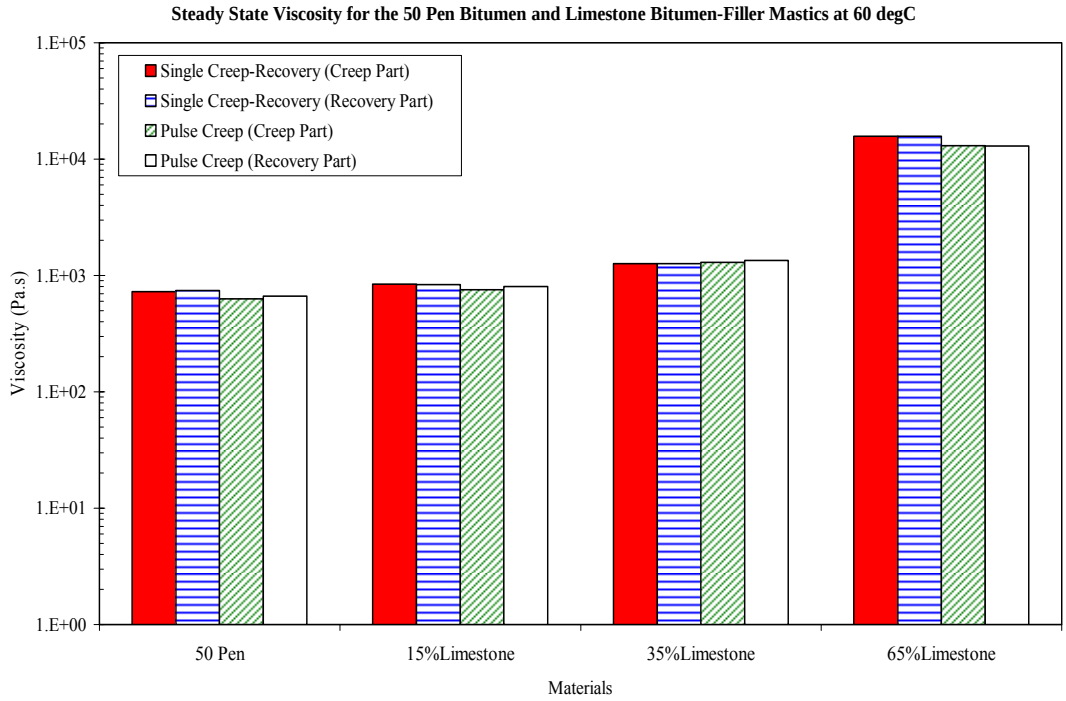

Figure 4.35: Effect of filler content on ZSV for 50 pen bitumen and limestone bitumen-filler mastics at 60°C

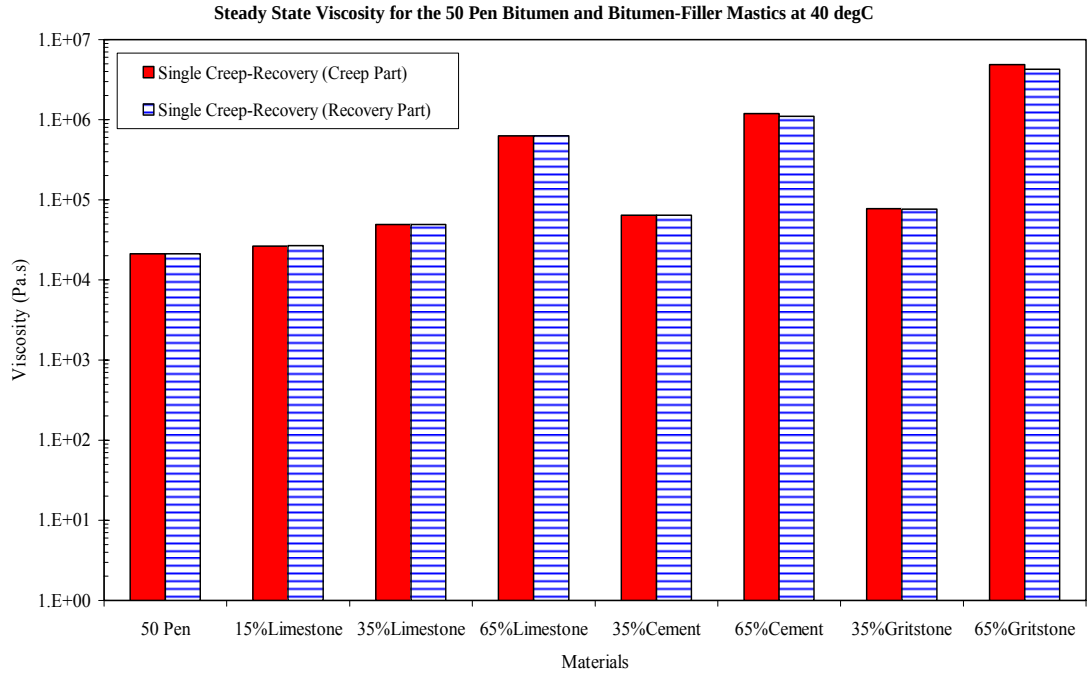

Figure 4.36: Effect of filler type on ZSV for 50 pen bitumen and bitumen-filler mastics at 40°C

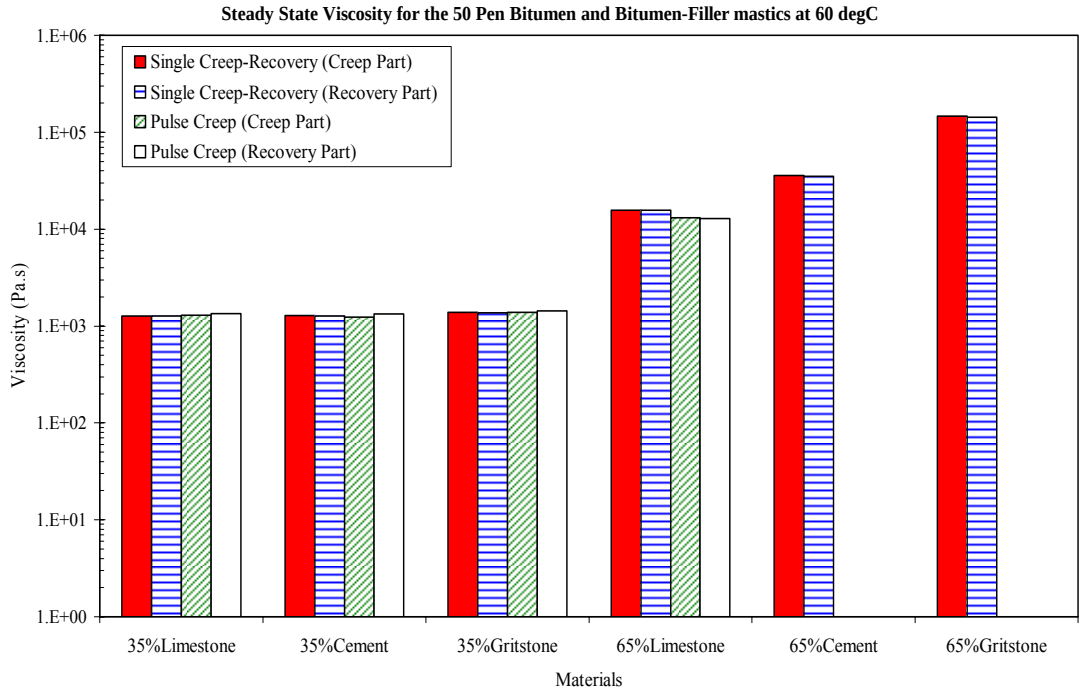

Figure 4.37: Effect of filler type on ZSV for 50 pen bitumen and bitumen-filler mastics at 60°C

4.6 Comparisons of ZSVs Using Different Measurement Techniques

4.6.1 Cox-Merz Rule for the Complex Dynamic Viscosity and Apparent Viscosity

Bituminous binders may exhibit a similarity between viscometry functions as a function of shear rate (rotational viscometry testing) and linear viscoelastic functions as a function of frequency (dynamic oscillation testing). The most successful of those relations is the Cox-Merz rule, which relates the viscosity, η, at a shear rate to the complex dynamic viscosity, η^*, at a frequency. The apparent viscosity and complex dynamic viscosity are plotted in Figures 4.38 through 4.43, which shows that the Cross model and the Carreau model are fitted to the measurements of apparent viscosity and complex dynamic viscosity for the base bitumen and limestone bitumen-filler mastics at 40^oC and 60^oC. On these plots the validity of the Cox-Merz rule at domains can be checked, where the apparent viscosity and the complex dynamic viscosity are overlapping.

It can be observed that the base bitumen and the 35% limestone bitumen-filler mastics show a shear-thinning behaviour (viscosity decrease with increasing shear rate or frequency) and an upper limiting viscosity (ZSV) is displayed. The base bitumen and the mastics having a filler suspension structure reasonably follow the Cox-Merz Rule. Consequently, the simple rheological behaviour is apparent for the bitumen and 35% bitumen-filler mastics in steady state. It can be seen that the apparent viscosity and the complex dynamic viscosity overlap over the interval of the shear rate and frequency. The Cross model and the Carreau model show that the measurements of apparent viscosity and complex dynamic viscosity approach approximately the same upper limiting viscosity value although there is a considerable difference in predicted viscosity at high shear rate.

The 65% limestone bitumen-filler mastics are also shear thinning in the whole range of shear rate/frequency, but a significant deviation from the Cox-Merz rule is observed. The simple rheological behaviour of the highly structured mastic is not found. The comparison of the apparent viscosity and complex dynamic viscosity for the highly modified mastics points to a significant change in the rheological behaviour of the

mastic. The fact is related to its more complicated structure (filler skeleton) in the bitumen. Here a relatively large difference between the upper limiting viscosity estimated from the dynamic and apparent viscosity is seen. The particle-particle interaction is believed to change the viscosity curves of the 65% bitumen-filler mastic.

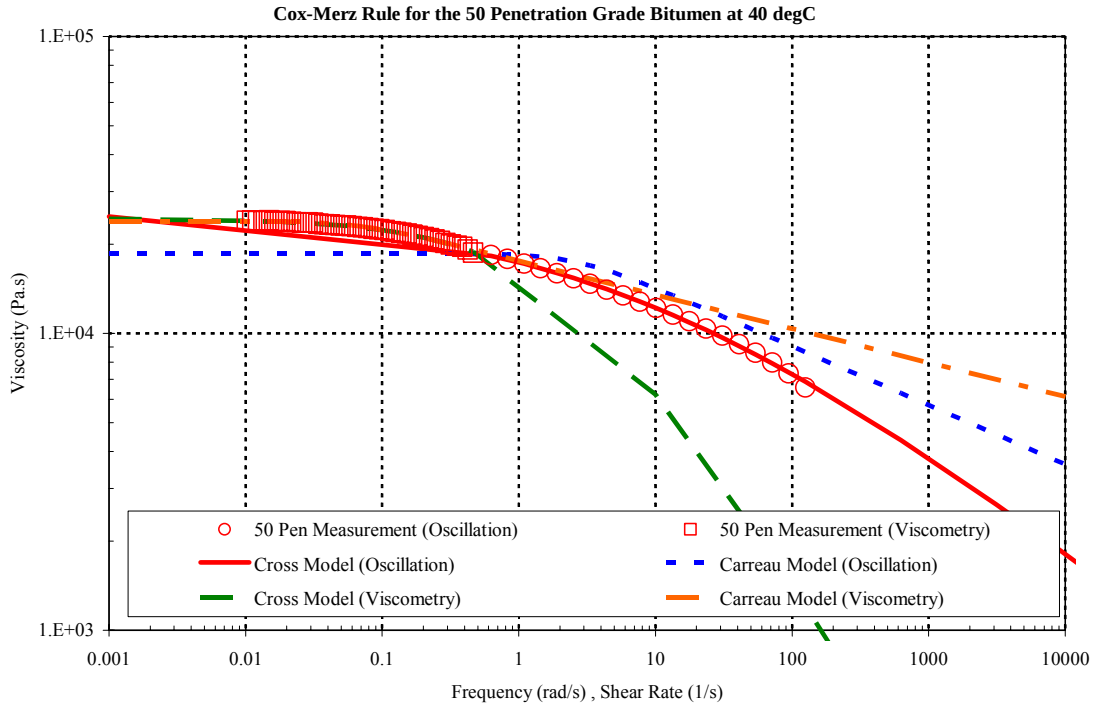

Figure 4.38: Cox-Merz rule for 50 penetration grade bitumen at 40°C

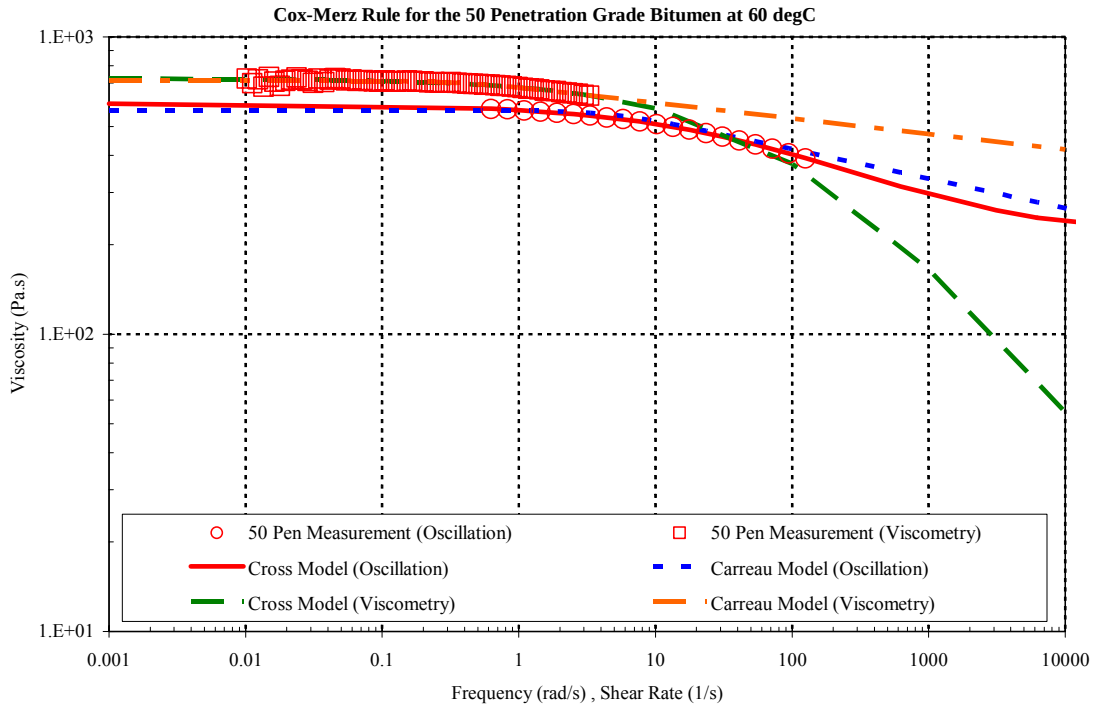

Figure 4.39: Cox-Merz rule for 50 penetration grade bitumen at 60 °C

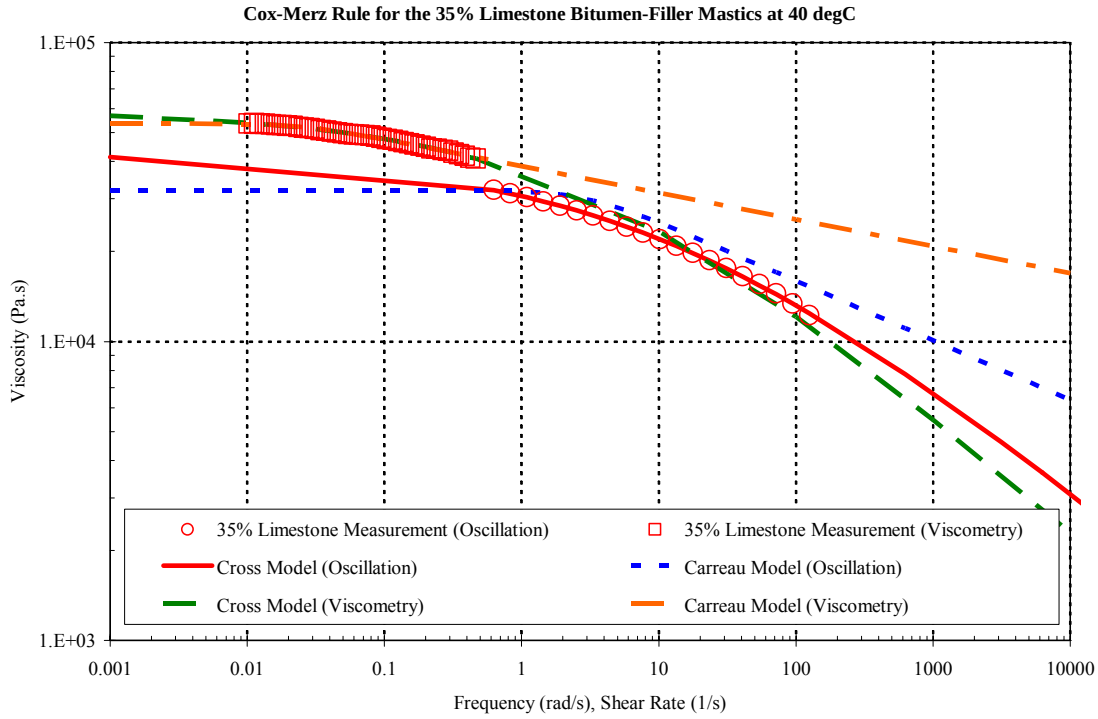

Figure 4.40: Cox-Merz rule for 35% limestone bitumen-filler mastic at 40 °C

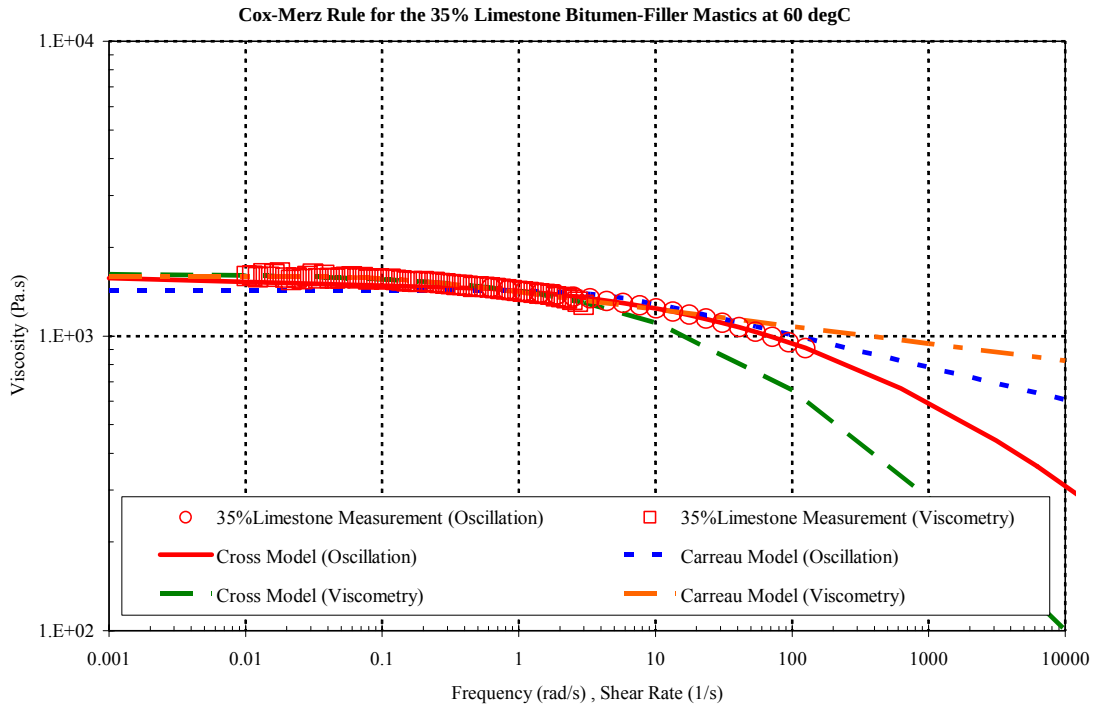

Figure 4.41: Cox-Merz rule for 35% limestone bitumen-filler mastics at 60 °C

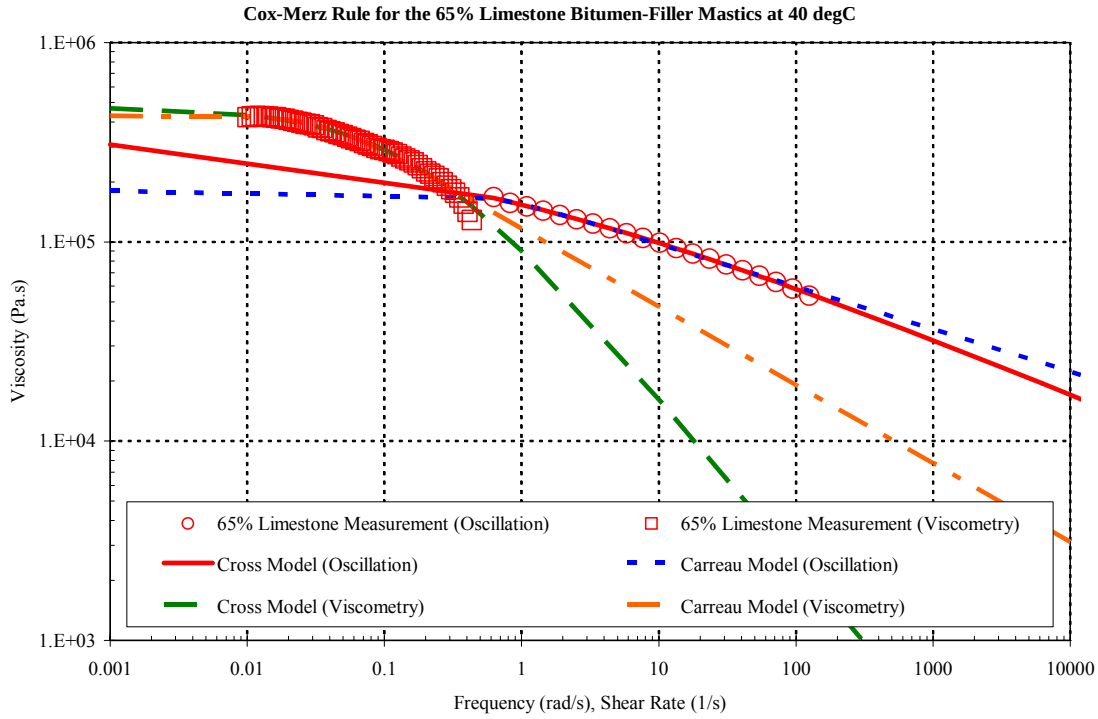

Figure 4.42: Cox-Merz rule for 65% limestone bitumen-filler mastics at 40 °C

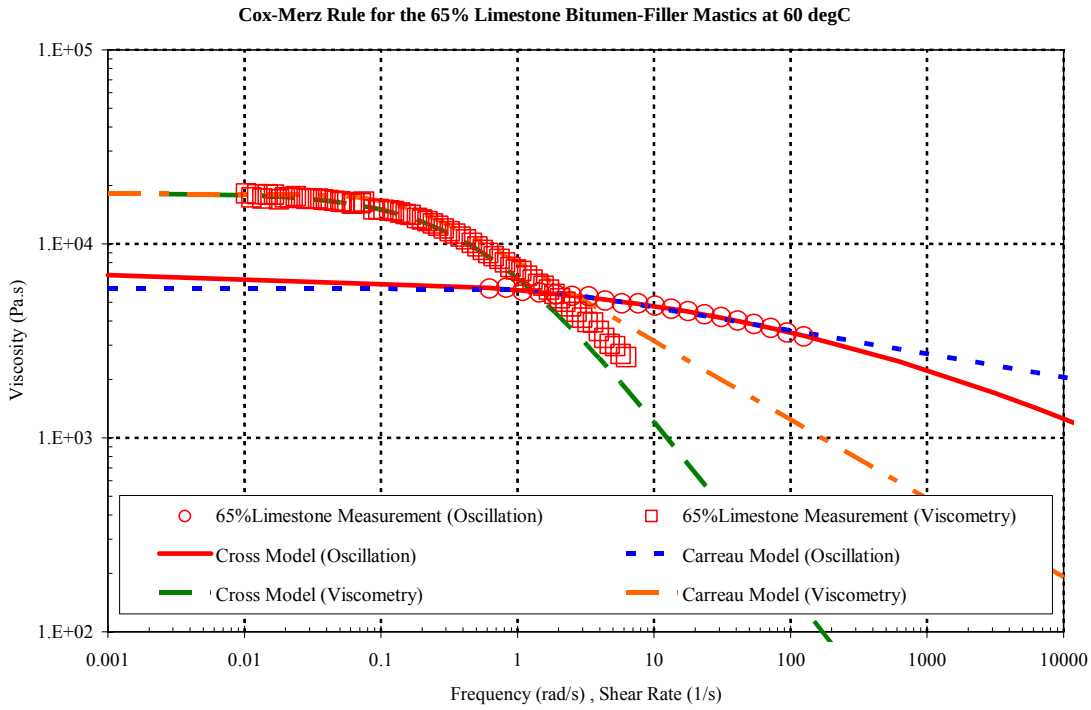

Figure 4.43: Cox-Merz rule for 65% limestone bitumen-filler mastic at 60 ^{o}C

4.6.2 Comparisons of ZSVs

The influence of test method on the ZSVs determined for the 50 penetration grade bitumen and various bitumen-filler mastics is shown in Figures 4.44 through 4.46. In general the two techniques, viscometry and creep tests produce basically the same results for the bitumen and bitumen-filler mastics. The comparison of ZSV values obtained from the two methods show a good correlation. The outliers at the higher range of the ZSV values come primarily from the 65% gritstone bitumen-filler mastic (see Figure 4.44). Excellent agreement is shown between the ZSVs obtained from the viscometry measurements and ZSVs obtained from the creep measurements, which can be concluded that the values of apparent viscosity and creep viscosity can approach similar ZSV as long as the steady state is attained during testing.

However, the ZSV results obtained from the oscillation testing are lower compared to those obtained from the viscometry and creep testing. That is because the oscillation testing is only performed at the range of frequency between 0.1 Hz (0.625 rad/s) and 20 Hz (125 rad/s). Visscher et al. (2004) suggested that the complex viscosity at 0.001 Hz

(0.00625 rad/s) was used as an approximation of ZSV. The fact that the measurements of complex dynamic viscosity of some mastics might not reach steady state can be observed in Section 4.6.1. The ZSV values obtained from oscillation measurements are therefore underestimated compared to those obtained from viscometry and creep measurements.

The advantages and disadvantages of using the three measurement techniques can be discussed for ease of comparing the different methods and included here. It is noted that only the simple rheological behaviour of bitumens are considered here.

For oscillation testing, the measurements of complex dynamic viscosity can be obtained by performing regular small-strain rheological oscillation testing. There is no need to create an extra test for determining ZSV. However, since it is not possible to measure down to zero frequency, extrapolation to zero frequency using mathematical models with nonlinear regression analysis produces ZSV values. The selection of different parameters of mathematical models may result in different ZSV values.

For viscometry testing, the measurements of apparent viscosity can be obtained by performing shear strain rate sweeps without long test duration. However, the viscosity measurements could be unreliable at very low shear rates because the viscosity values are sensitive to shear rate in the low shear range. The viscosity measurements could not be accurate at high shear rate because the specimen may be damaged during testing. Checking the plot of shear stress versus shear rate is necessary. In addition, the extrapolation to zero shear rate using mathematical models is required for ZSV calculation. Again, the selection of different parameters may result in different ZSV values.

For single creep-recovery and pulse creep testing, the ZSV value can be directly calculated from either the creep curve at steady state in retardation phase or recovery compliance in relaxation phase, without any extrapolation to zero shear rate using mathematical models. However, the selection of shear stress levels influences the change in ZSV value. Although Binard et al. (2004) recommended running the test in the linear

domain where viscosity at steady state is independent of stress level, it may be very time consuming to reach steady state using a lower shear stress level. Additionally, lowering the shear stresses reduces the measured torque to a very low level that may not be appropriate to rheometer sensibility. It is also noted that in order to attain steady state for the bitumen-filler mastics, the solution is to run the test at higher temperature, but the settling of filler particles in the mastic while testing should be considered.

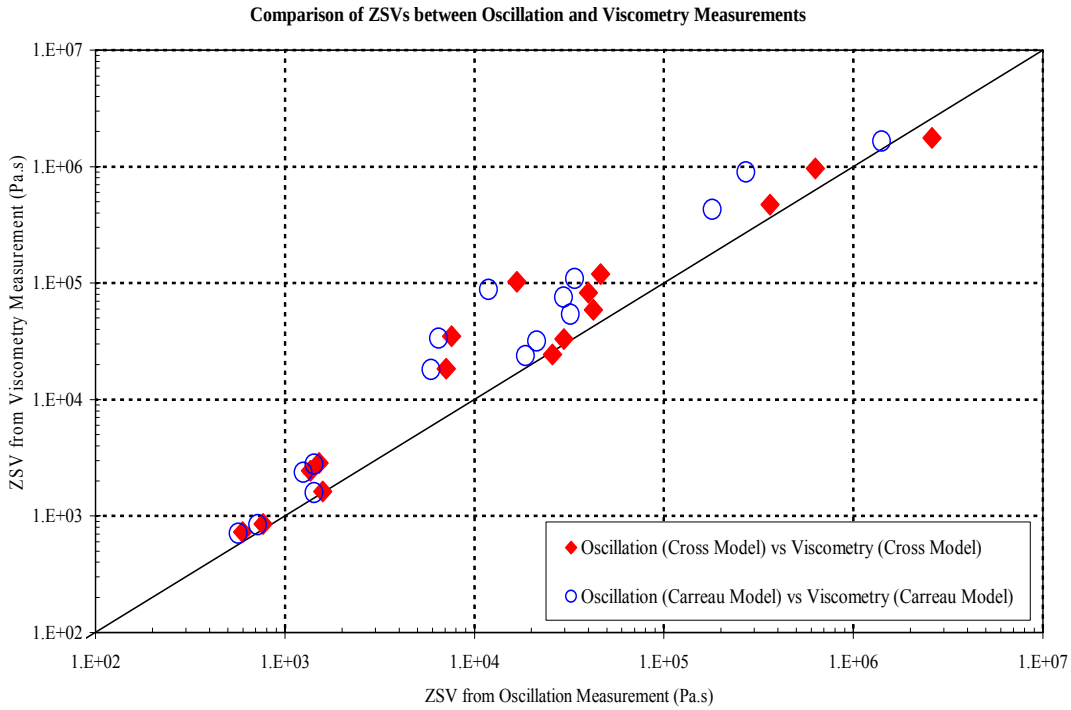

Figure 4.44: Comparison of ZSV between oscillation and viscometry measurements

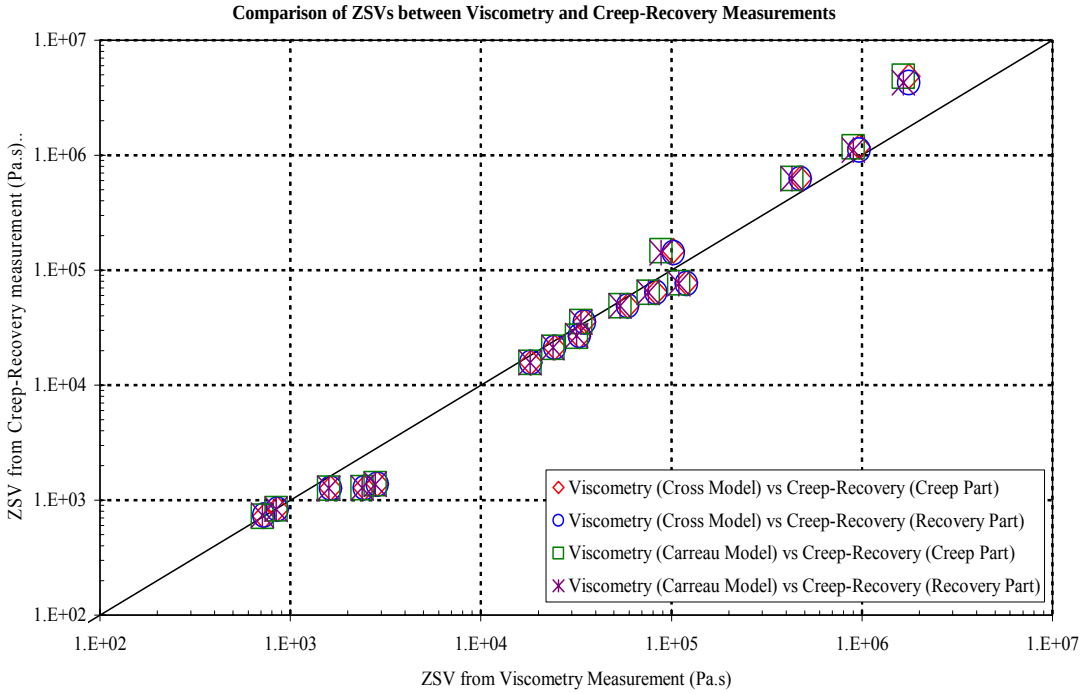

Figure 4.45: Comparison of ZSV between viscometry and creep-recovery measurements

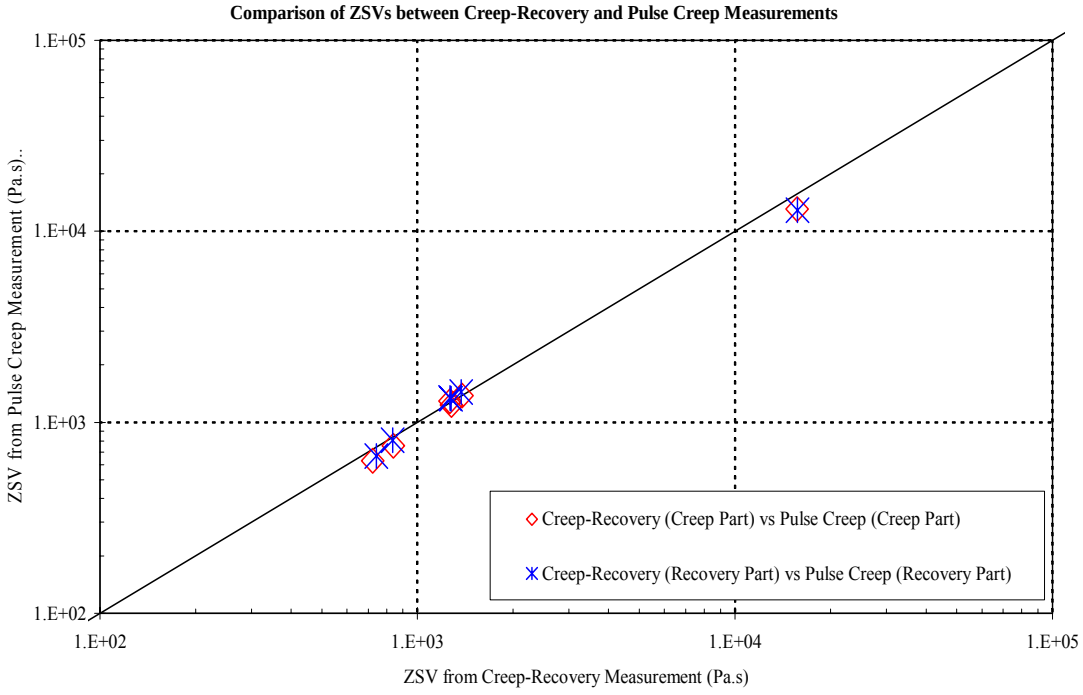

Figure 4.46: Comparison of ZSV between creep-recovery and pulse creep measurements

4.7 Summary

Chapter 4 showed the feasibility to obtain ZSV values using three techniques of oscillation, viscometry and creep methods for the 50 penetration grade bitumen and bitumen-filler mastics by means of dynamic shear rheometry. Based on the test procedures used and the materials tested, a number of findings and conclusions are drawn as follows:

- According to the ZSV stiffening ratios presented in this investigation using the three techniques, the results only show a slight increase in ZSV for the 15% and 35% bitumen-filler mastics but a considerable increase for the 65% filler content mastics. The sharp increase in ZSV is caused by the filler contributing such a large volume to the binder that it becomes the predominant component in the bitumen-filler mastic and therefore has a dramatic effect on viscosity. The ZSV stiffening ratios for the 65% gritstone bitumen-filler mastic (effective filler volume = 62.1%) obtained from the single creep-recovery and pulse creep tests can be up to 200 times. The viscosity at steady state of the highly modified system, such as bitumen-filler mastics with high filler concentrations, may potentially mirror the permanent deformation behaviour of asphalt mixtures.
- The base bitumen and the mastics having a filler suspension structure reasonably follow the Cox-Merz Rule. The simple rheological behaviour is apparent for the bitumen and 35% bitumen-filler mastics in steady state. However, the simple rheological behaviour of the 65% limestone bitumen-filler mastic is not found, with a significant deviation from the Cox-Merz rule being observed. The comparison of the apparent viscosity and complex dynamic viscosity for the highly modified mastics points to a significant change in the rheological behaviour of the mastic. The fact is related to its filler skeleton structure in the bitumen. Here a relatively large difference between the upper limiting viscosity estimated from the dynamic and apparent viscosity is seen. The particle-particle interaction is believed to change the viscosity curves of the 65% bitumen-filler mastic.
- Excellent agreement is shown between the ZSVs obtained from the viscometry measurements and ZSVs obtained from the creep measurements, which can be

concluded that the values of apparent viscosity and creep viscosity can approach similar ZSV as long as the steady state is attained during testing.

- The Cross model and Carreau model with nonlinear regression analysis can fit well to the measurements of the complex dynamic viscosity and apparent viscosity in the range of the test frequencies and shear rates. The extrapolation of ZSV value can be similar if the viscosity measurements reach steady state. However, a considerable difference in viscosity value is presented in the predicted viscosity curves at higher frequencies and shear rates.

Fatigue Characterisation

5.1 General

Fatigue cracking is one of the primary distresses of a flexible pavement caused by repeated traffic loading, temperature variations and construction practices generating tensile stresses and strains in the asphalt layers. Although it is recognised that fatigue damage is mainly caused by cracking or damage within the bituminous binder and/or bitumen-filler mastic, fatigue testing has generally been limited to the asphalt mixture. However, since the introduction of the dynamic shear rheometer (DSR), direct testing of bituminous binders in fatigue has become relatively common with a number of research groups having successfully generated fatigue characteristics for both pure and modified bitumens by means of time sweep tests using the DSR. However, it can be argued that fatigue of bitumen-filler mastics rather than pure bitumen may be more appropriate in the search to establish fatigue correlations with asphalt mixtures due to the fact that the bituminous binder occurs not as bitumen alone but is mixed with mineral filler forming the mastic.

Attempts have been made to include a binder parameter in asphalt mixture fatigue prediction with the Superpave fatigue criterion, $G^*\sin\delta$, being the most recent. However, these parameters determined in the linear viscoelastic region at low strain levels have generally failed to establish a comprehensive correlation with asphalt mixture fatigue performance (Bahia et al., 2002). Bahia et al. (1999) claimed that strains within binder films could be as high as 10 to 100 times the bulk strains of asphalt mixture. Because binders exist as thin films, they can be performing in the non-linear region due to the considerable difference between modulus of mineral aggregates and modulus of binders.

This chapter looks at the fatigue characteristics of pure bitumen and bitumen-filler mastics containing three types of mineral fillers by means of dynamic shear rheometry.

Fatigue tests have been carried out on a wide range of bitumen-filler mastic (35% and 65% filler mass with limestone, cement and gritstone filler) to investigate the effect of filler content as well as mineral type on mastic fatigue. The fatigue tests were performed using oscillatory shear loading in the DSR at 10^{o}C and 20^{o}C and a loading frequency of 10Hz. These binder fatigue studies have been undertaken under both controlled stress and strain conditions, both in the linear and non-linear response of the materials.

5.2 Materials and Equipments

5.2.1 Materials

A total of six bitumen-filler mastics were produced using a 50 penetration grade bitumen as the base bitumen, three filler types (limestone, cement and gritstone) and two filler concentrations of 35% and 65% by mass. The limestone and gritstone fillers can be considered as inert fillers, while the cement filler can be considered to be an active filler. The matrix of materials that were tested is listed in Table 5.1. The details of physical properties of the bitumen, physical properties of the mineral fillers and filler concentrations in bitumen-filler system have been described in Chapter 3.

Table 5.1: Matrix of bitumen-filler mastics

Materials / Filler Contents	Base Bitumen	Bitumen-Filler Mastics		
	50 Pen Bitumen	Limestone	Cement	Gritstone
0%	x			
35%		x	x	x
65%		x	x	x

5.2.2 Dynamic Shear Rheometer

The Bohlin Gemini 200 Dynamic Shear Rheometer having a torque range between 0.5 (μN·m) and 200 (mN·m) was used for measuring the fatigue characteristics of bitumen and bitumen-filler mastics. The details of the principal components of the DSR, temperature controlled system and sample preparation have been described in Chapter 3.

5.3 Testing Programme

The principle of the dynamic oscillatory shear testing using the DSR has been described in Chapter 3. The measurements of rheological parameters of the bitumen and bitumen-filler mastics were obtained by performing a time sweep testing at different strain and stress levels within the linear and non-linear viscoelasic domains at 10^{o}C and 20^{o}C with a loading frequency of 10 Hz. The 8-mm diameter parallel plates was used. The testing parameters are shown as follows:

- Testing temperatures : 10^{o}C and 20^{o}C,
- Testing frequency : 10 Hz,
- Mode of loading : strain and stress controlled loading (large strains and stresses),
- Testing geometry and gap: 8-mm diameter thick shaft parallel plates with a 2-mm gap (10^{o}C and 20^{o}C).

The 8-mm thick shaft parallel plates was used in the DSR fatigue testing due to the fact that the machine compliance at high stiffness value is a concern. As can be seen from the complex modulus master curves in Chapter 3, the measurements of complex modulus at 10^{o}C and 20^{o}C and a loading frequency of 10 Hz for the bitumen and mastics can be above 10 MPa. In addition, it is noted that there must be a good adhesion of bituminous specimen to the parallel plates during the testing.

5.4 Definition of Fatigue Failure Point

The phenomenological approach was used for fatigue failure definition of the bitumen and bitumen-filler mastics in this investigation. The definition of fatigue failure can be considered in terms of strain and stress controlled oscillatory testing with time sweeps. The two fatigue failure definitions are presented in the following two sections.

5.4.1 Time Sweeps under Controlled Strain Loading Mode

Figure 5.1 illustrates a typical change in complex modulus during the course of a strain controlled fatigue test for the DSR oscillatory shear configuration. The characteristic of the fatigue curve has an initial drop in complex modulus within a small number of load

cycles, then a slight decrease in stiffness at a constant reducing rate followed by a dramatic reduction in complex modulus. The failure criterion is defined as an arbitrary 50% reduction in initial complex modulus for the controlled strain tests.

In the first stage, a decrease in complex modulus within a small number of load cycles may be due to a thermal effect (self-heating) of bituminous specimen on stiffness reduction (Bodin et al. 2004; Planche et al. 2003). However, Bodin et al. (2004) reported that the thermal effects in the shear binder fatigue tests presented were minor, and had only a marginal interaction with the fatigue criterion, based on a 50% reduction in stiffness. Shenoy (2002) claimed that an initial drop in stiffness was due to yield behaviour.

In the second stage, microcracks initiate and damage accumulates inside the binders, producing a slight decrease in stiffness at a constant reducing rate. Due to the non-uniform shear strain and stress on the plane of the specimen, the cracks propagate from edge towards centre of specimen. In this stage, the stabilised material starts responding to the experimental conditions before it begins to show a sharp reduction in complex modulus.

With increasing load cycles, the propagation of macrocracks can be recognised by a dramatic drop in stiffness in the third stage. The stage should be characterised by a stiffness approaching zero but never reaching zero. In practice, real failure of the bitumen does not occur. A decelerating stiffness reducing rate in the end of strain controlled testing is because of decreasing stress amplitude in order to achieve the same applied strain amplitude. Due to the difficulties associated with the determination of fatigue failure, the failure criterion used in this study is based on the 50% reduction of initial complex modulus.

5.4.2 Time Sweeps under Controlled Stress Loading Mode

Figure 5.2 shows a typical change in complex modulus during the course of a stress controlled fatigue test for the DSR oscillatory shear configuration. The characteristic of

the fatigue curve has an initial drop in complex modulus within a small number of load cycles, then a slight decrease in stiffness at a constant reducing rate followed by an abrupt drop in complex modulus. The failure criterion is defined as complete fracture of the specimen for the controlled stress tests.

There are also three stages presented on the fatigue curve for the stress controlled testing. An initial decrease in complex modulus is due to yield behaviour in the first stage. The microcracks initiate with increasing number of load cycles and cause a reduction in stiffness at a constant reducing rate in the second stage. In the third zone, a sharp reduction in complex modulus is due to the propagation of macrocracks. In practice, the stiffness reaches zero and real failure of the bitumen can be observed. The fatigue failure point is clearly determined as the number of load cycles that correspond to the specimen being completely fractured.

An accelerating stiffness reducing rate in the end of stress controlled testing is because of increasing strain amplitude in order to achieve the same applied stress amplitude. Generally, binders tested under controlled strain tests tend to have longer fatigue lives than those tested under controlled stress conditions.

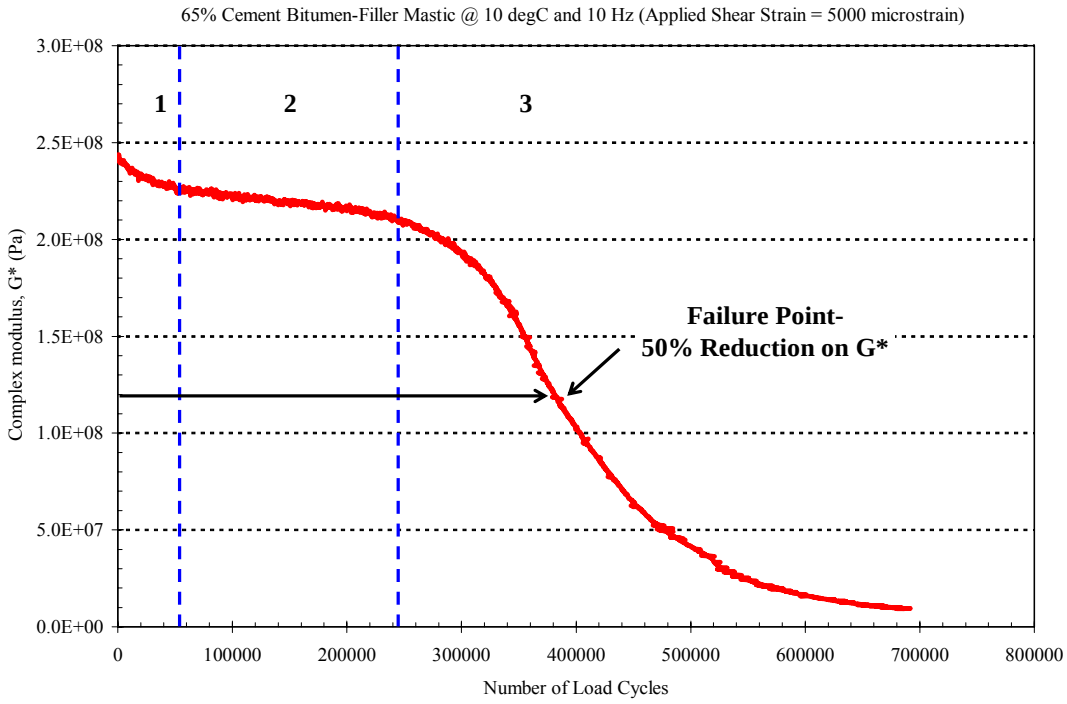

Figure 5.1: Fatigue curve and failure point under strain controlled loading mode

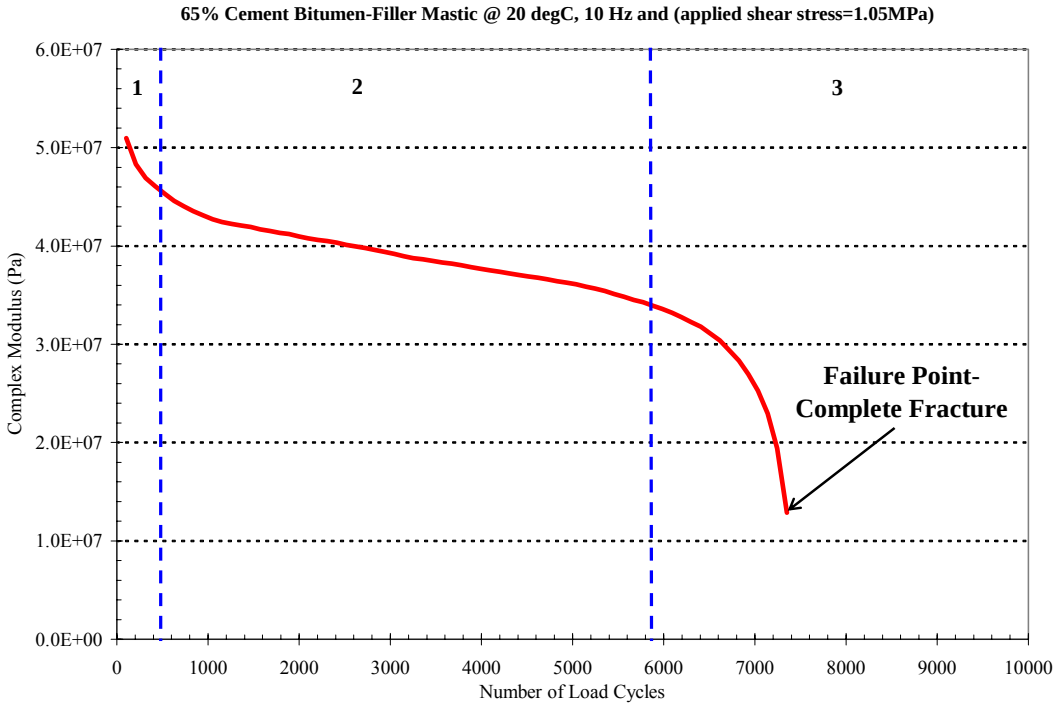

Figure 5.2: Fatigue curve and failure point under stress controlled loading mode

5.5 Test Results and Discussion

In terms of fatigue, two considerations need to be addressed. Firstly, the type of loading mode (controlled stress or strain) that is used to determine the fatigue properties of the material needs to be selected and, secondly, the manner in which the fatigue life is presented (versus stress or strain) needs to be chosen. Pell (1972) suggests that controlled strain tests are applicable for thin asphalt layers (<50 mm), while controlled stress tests should be used for thicker, stiffer layers (>150 mm). Materials tested under controlled strain conditions tend to have longer fatigue lives than those tested under controlled stress conditions. In this study both conditions are used. In terms of fatigue presentation, traditionally for asphalt mixtures the "strain criterion" has been used (Pell, 1962; Pell, 1967), while recent research on bitumen fatigue suggests that fatigue data for binders should probably be plotted against stress (Airey et al., 2004).

5.5.1 Influence of Filler Concentration

Table 5.2 compares the average complex modulus values of the base bitumen and bitumen-filler mastics used in the DSR fatigue tests. Fatigue results for stress controlled tests on the pure 50 pen bitumen as well as the 35% and 65% limestone filler mastics are presented in Figure 5.3 with the data plotted against stress level. Standard power law type fatigue lines (straight lines in logarithmic space) have been fitted to the data with reasonable high levels of fit (R^2 values included in figure). The data is presented to compare the fatigue performance of the pure bitumen and bitumen-filler mastics at a test temperature of 20°C and a loading frequency of 10 Hz. Additional 50 pen bitumen fatigue data is provided at the lower test temperature of 10°C.

The fatigue results in Figure 5.3 show that there is a considerable difference between the results for pure bitumen and those for the bitumen/filler mastics, although the slopes of the three fatigue lines at 20°C are very similar (see Figure 5.3 and Table 5.3). The effect of increasing filler content results in an increase in fatigue life, as a function of stress level, for the mastics relative to the pure bitumen, or stated differently, increases the applied stress level for a constant fatigue life. The increase in stress with increasing filler content is synonymies with the increase in tensile strength (stress) found for the same mastics but subjected to fracture testing rather than fatigue (Thom et al. 2005). It is also

interesting to note that the effect of reducing the test temperature to 10°C for the 50 pen bitumen has a similar effect to that of the mastics with a considerable increase in fatigue life compared to the binder fatigue results at 20°C. The fatigue relationships for the 65% limestone mastic at 20°C and 50 pen bitumen at 10°C are similar, with the pure bitumen having a slightly better fatigue performance but greater slope. In addition, as shown by the average stiffness values in Table 5.2, the stiffening effect of either reducing the test temperature for the 50 pen bitumen or adding 65% by mass of filler are almost identical.

In an attempt to provide more clarity on the effect of filler content on fatigue performance, the results in Figure 5.3 were repeated for the pure bitumen and mastics but under controlled strain conditions (fatigue equations in Table 5.4) and with fatigue data generated for the 35 and 65% limestone mastics at 10°C as well as 20°C. The fatigue results are shown in Figure 5.4 plotted against initial stress level (stress decreasing throughout controlled strain test).

The fatigue results show the same pattern as seen for the controlled stress tests in Figure 5.3. For both the 10°C and 20°C tests, there is an increase in fatigue life for the 35% and 65% mastics compared to the pure bitumen. The magnitude of this increase is also similar at both 10°C and 20°C, with the increase in fatigue being considerably larger between 35% and 65% than between the pure bitumen and 35% limestone mastic. However, unlike the stress controlled tests, the slopes for the fatigue lines at 20°C in Figure 5.4 differ for each material, although the slopes are very consistent for the tests at 10°C. The order of the six fatigue lines is also identical to the order of the average stiffness values for the material/temperature combinations under controlled strain conditions (see Table 5.2).

The fatigue results have also been plotted against strain, used for asphalt mixture fatigue analysis due to the strain dependency of mixture fatigue, in Figures 5.5 and 5.6 for the controlled strain and controlled stress tests respectively. The individual fatigue results and the fitted power law fatigue lines show that there is no strain dependent criterion, with results undertaken on the same material but at different temperatures lying on

separate fatigue lines. In terms of strain, the fatigue order for the three materials, at both 10°C and 20°C, in terms of increasing fatigue life is 65% mastic followed by 35% mastic with the pure bitumen having the highest fatigue performance. However, this order is not simply the reverse of the fatigue relationships versus stress seen in Figures 5.3 and 5.4, or even increasing fatigue with decreasing stiffness, as the pure bitumen fatigue results at 10°C show a better fatigue performance than what would be expected based on the overall trend of decreasing fatigue with increasing stiffness in Figures 5.5 and 5.6. In terms of the effect of testing mode, the results in Figure 5.5 (controlled strain) and Figure 5.6 (controlled stress) confirm the accepted understanding that controlled strain testing conditions produce longer fatigue lives than the more severe controlled stress conditions.

Table 5.2: Average complex modulus values of bitumen and bitumen-filler mastics used in the fatigue tests

Bitumen / Mastic Material	Initial Stiffness (G*) MPa			
	Controlled Strain Loading Mode		Controlled Stress Loading Mode	
	10°C	20°C	10°C	20°C
50 Pen Grade Bitumen	44	12	44	12
35% Limestone Mastic	76	18	-	16
35% Cement Mastic	79	18	-	20
35% Gritstone Mastic	75	20	-	21
65% Limestone Mastic	221	39	-	43
65% Cement Mastic	245	41	-	47
65% Gritstone Mastic	-	55	-	58

Table 5.3: Fatigue equations versus stress and strain for stress controlled testing

Fatigue Tests @ 10°C (Fatigue versus Stress Relationship)		
Materials	Fatigue Equation	Stress Equation
50 Pen Bitumen	$N_f = 1.89*10^4 \tau^{-2.113}$	$\tau = 96.97\ N_f^{-0.465}$
Fatigue Tests @ 10°C (Fatigue versus Strain Relationship)		
Materials	Fatigue Equation	Strain Equation
50 Pen Bitumen	$N_f = 3.85*10^{16} \gamma^{-2.136}$	$\gamma = 2.14*10^6\ N_f^{-0.461}$
Fatigue Tests @ 20°C (Fatigue versus Stress Relationship)		
Materials	Fatigue Equation	Stress Equation
50 Pen Bitumen	$N_f = 2.73*10^2\ \tau^{-3.534}$	$\tau = 3.30\ N_f^{-0.244}$
35% Limestone Mastic	$N_f = 6.00*10^2 \tau^{-4.001}$	$\tau = 4.88\ N_f^{-0.248}$
35% Cement Mastic	$N_f = 1.15*10^3 \tau^{-3.708}$	$\tau = 6.46\ N_f^{-0.266}$
35% Gritstone Mastic	$N_f = 7.78*10^2 \tau^{-4.304}$	$\tau = 4.62\ N_f^{-0.230}$
65% Limestone Mastic	$N_f = 5.41*10^3 \tau^{-4.323}$	$\tau = 6.59\ N_f^{-0.219}$
65% Cement Mastic	$N_f = 9.66*10^3 \tau^{-5.267}$	$\tau = 5.71\ N_f^{-0.190}$
65% Gritstone Mastic	$N_f = 9.11*10^3 \tau^{-5.551}$	$\tau = 5.05\ N_f^{-0.177}$
Fatigue Tests @ 20°C (Fatigue versus Strain Relationship)		
Materials	Fatigue Equation	Strain Equation
50 Pen Bitumen	$N_f = 6.92*10^{17} \gamma^{-3.081}$	$\gamma = 4.51*10^5\ N_f^{-0.294}$
35% Limestone Mastic	$N_f = 1.82*10^{18} \gamma^{-3.217}$	$\gamma = 4.73*10^5\ N_f^{-0.311}$
35% Cement Mastic	$N_f = 5.21*10^{16} \gamma^{-2.863}$	$\gamma = 6.65*10^5\ N_f^{-0.345}$
35% Gritstone Mastic	$N_f = 2.40*10^{18} \gamma^{-3.249}$	$\gamma = 4.49*10^5\ N_f^{-0.307}$
65% Limestone Mastic	$N_f = 2.30*10^{14} \gamma^{-2.452}$	$\gamma = 6.79*10^5\ N_f^{-0.401}$
65% Cement Mastic	$N_f = 3.01*10^{17} \gamma^{-3.137}$	$\gamma = 3.67*10^5\ N_f^{-0.317}$
65% Gritstone Mastic	$N_f = 8.88*10^{17} \gamma^{-3.349}$	$\gamma = 2.29*10^5\ N_f^{-0.298}$

Table 5.4: Fatigue equations versus stress and strain for strain controlled testing

Fatigue Tests @ 10°C (Fatigue versus Strain Relationship)		
Materials	Fatigue Equation	Strain Equation
50 Pen Bitumen	$N_f = 1.93*10^{16} \gamma^{-2.704}$	$\gamma = 1.02*10^{6} N_f^{-0.367}$
35% Limestone Mastic	$N_f = 9.98*10^{15} \gamma^{-2.750}$	$\gamma = 6.51*10^{5} N_f^{-0.363}$
35% Cement Mastic	$N_f = 2.76*10^{14} \gamma^{-2.378}$	$\gamma = 1.02*10^{6} N_f^{-0.406}$
35% Gritstone Mastic	$N_f = 2.47*10^{15} \gamma^{-2.608}$	$\gamma = 7.05*10^{5} N_f^{-0.371}$
65% Limestone Mastic	$N_f = 1.64*10^{20} \gamma^{-3.974}$	$\gamma = 1.22*10^{5} N_f^{-0.252}$
65% Cement Mastic	$N_f = 1.01*10^{24} \gamma^{-4.983}$	$\gamma = 6.55*10^{4} N_f^{-0.201}$
Fatigue Tests @ 10°C (Fatigue versus Stress Relationship)		
Materials	Fatigue Equation	Stress Equation
50 Pen Bitumen	$N_f = 3.45*10^{4} \tau^{-3.818}$	$\tau = 14.07 N_f^{-0.253}$
35% Limestone Mastic	$N_f = 6.26*10^{4} \tau^{-3.994}$	$\tau = 15.87 N_f^{-0.250}$
35% Cement Mastic	$N_f = 7.49*10^{4} \tau^{-3.851}$	$\tau = 18.11 N_f^{-0.258}$
35% Gritstone Mastic	$N_f = 6.20*10^{4} \tau^{-3.4.01}$	$\tau = 14.84 N_f^{-0.244}$
65% Limestone Mastic	$N_f = 4.38*10^{5} \tau^{-4.128}$	$\tau = 17.29 N_f^{-0.217}$
65% Cement Mastic	$N_f = 8.99*10^{5} \tau^{-5.001}$	$\tau = 11.95 N_f^{-0.178}$
Fatigue Tests @ 20°C (Fatigue versus Strain Relationship)		
Materials	Fatigue Equation	Strain Equation
50 Pen Bitumen	$N_f = 8.19*10^{15} \gamma^{-2.559}$	$\varepsilon = 1.60*10^{6} N_f^{-0.387}$
35% Limestone Mastic	$N_f = 1.67*10^{16} \gamma^{-2.696}$	$\varepsilon = 9.85*10^{5} N_f^{-0.365}$
35% Cement Mastic	$N_f = 2.34*10^{13} \gamma^{-2.074}$	$\varepsilon = 2.29*10^{6} N_f^{-0.459}$
35% Gritstone Mastic	$N_f = 1.20*10^{16} \gamma^{-2.642}$	$\varepsilon = 1.21*10^{6} N_f^{-0.378}$
65% Limestone Mastic	$N_f = 3.75*10^{17} \gamma^{-3.056}$	$\varepsilon = 5.43*10^{5} N_f^{-0.323}$
65% Cement Mastic	$N_f = 2.73*10^{17} \gamma^{-3.035}$	$\varepsilon = 5.55*10^{5} N_f^{-0.329}$
65% Gritstone Mastic	$N_f = 6.20*10^{19} \gamma^{-3.630}$	$\varepsilon = 2.83*10^{5} N_f^{-0.275}$
Fatigue Tests @ 20°C (Fatigue versus Stress Relationship)		
Materials	Fatigue Equation	Stress Equation
50 Pen Bitumen	$N_f = 1.72*10^{3} \tau^{-2.872}$	$\tau = 11.50 N_f^{-0.334}$
35% Limestone Mastic	$N_f = 1.49*10^{3} \tau^{-3.410}$	$\tau = 8.15 N_f^{-0.289}$
35% Cement Mastic	$N_f = 2.23*10^{3} \tau^{-3.091}$	$\tau = 10.40 N_f^{-0.306}$
35% Gritstone Mastic	$N_f = 3.74*10^{3} \tau^{-3.818}$	$\tau = 8.21 N_f^{-0.256}$
65% Limestone Mastic	$N_f = 1.41*10^{4} \tau^{-5.322}$	$\tau = 5.90 N_f^{-0.186}$
65% Cement Mastic	$N_f = 2.26*10^{4} \tau^{-4.915}$	$\tau = 7.59 N_f^{-0.202}$
65% Gritstone Mastic	$N_f = 2.94*10^{4} \tau^{-5.087}$	$\tau = 7.45 N_f^{-0.195}$

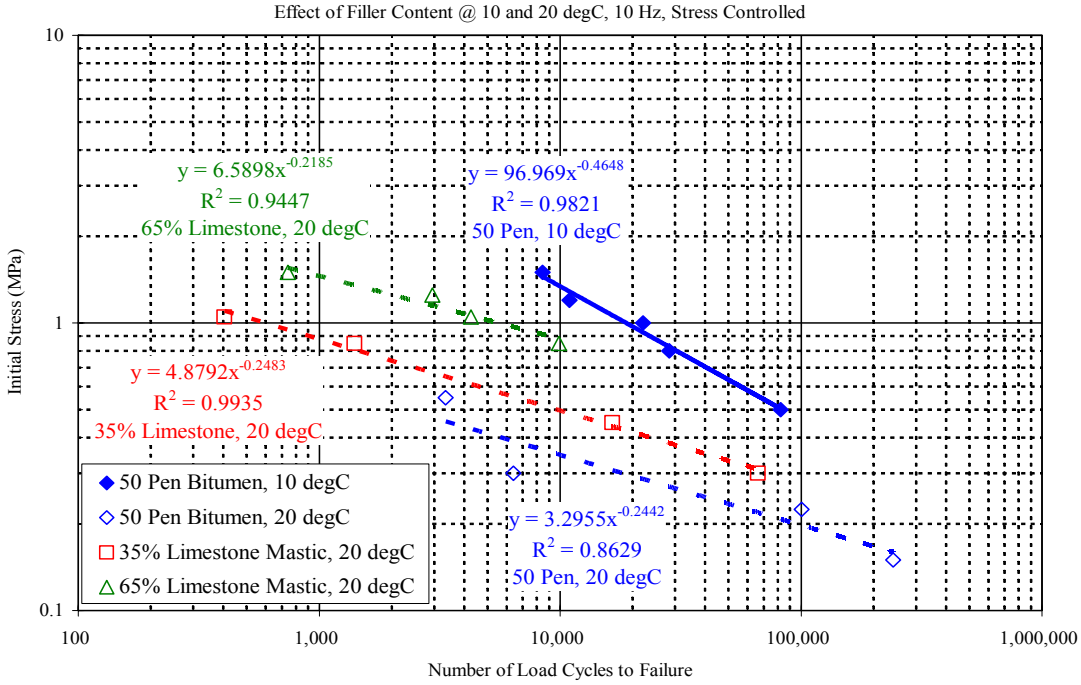

Figure 5.3: Effect of filler concentration on fatigue – controlled stress, 10°C and 20°C, 10 Hz versus initial stress

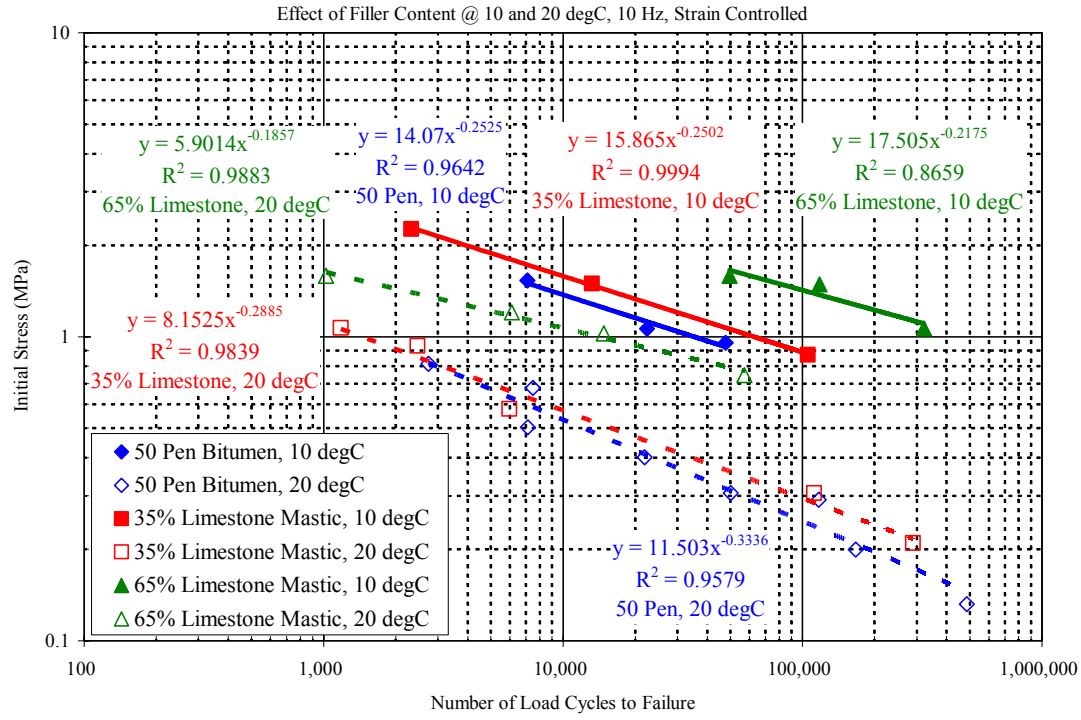

Figure 5.4: Effect of filler concentration on fatigue – controlled strain, 10°C and 20°C, 10 Hz versus initial stress

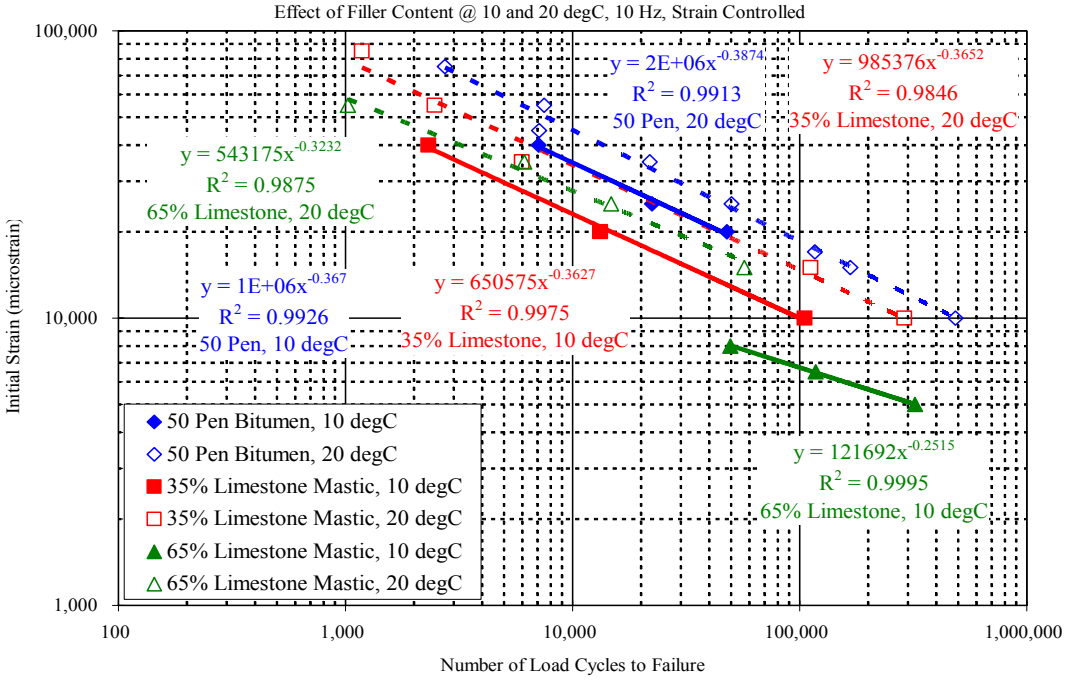

Figure 5.5: Effect of filler concentration on fatigue – controlled strain, 10°C and 20°C, 10 Hz versus initial strain

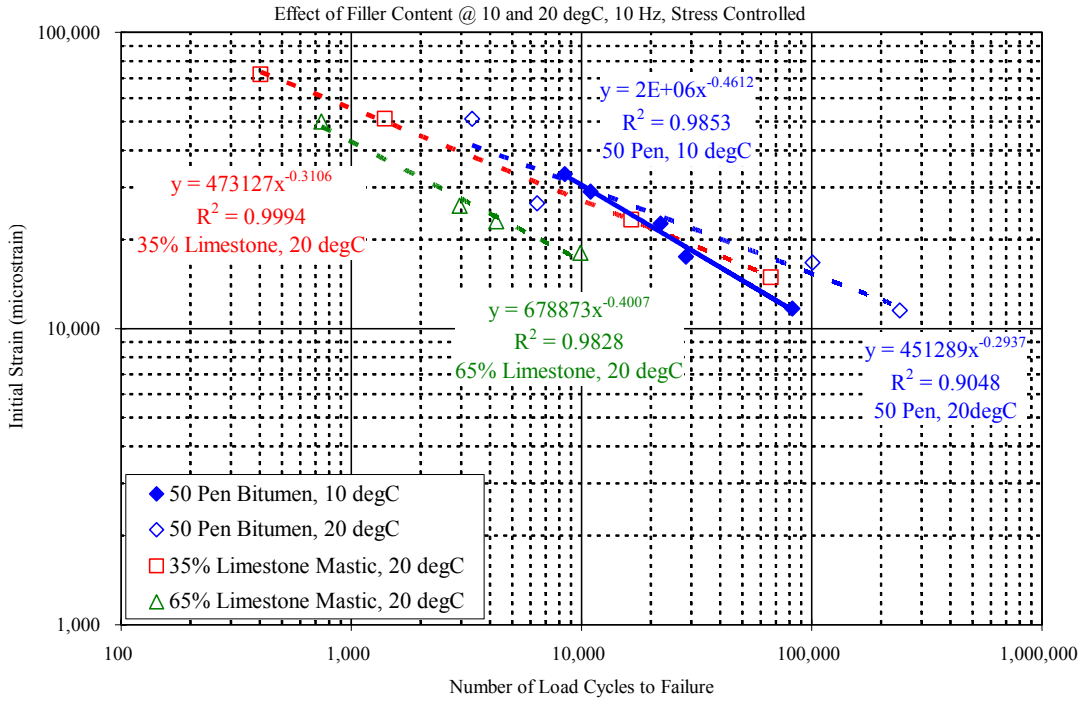

Figure 5.6: Effect of filler concentration on fatigue – controlled stress, 10°C and 20°C, 10 Hz versus initial strain

5.5.2 Influence of Filler Type

The fatigue results for the 35 and 65% mastics at 10°C are shown in Figures 5.7 (plotted against stress) and Figure 5.8 (against strain). Only the controlled strain tests have been presented although similar observations were made based on the controlled stress tests.

The results in Figure 5.7 show that the three 35% mastics (limestone, cement and gritstone) and the two 65% mastics (limestone and cement) can be separated into two groups. The 65% gritstone mastic was not tested at 10°C, due to difficulties involved in testing a mastic that showed a significantly higher stiffness compared to the other two 65% mastics. The results indicate that the effect of filler type can be considered to be negligible compared to the effect of filler content. The results in both Figures 5.7 and 5.8 show that a single fatigue relationship could be produced for the three 35% mastics and, secondly, for the two 65% mastics. As would be expected, the stiffer 65% mastics demonstrated better fatigue performance versus stress (Figure 5.7) while the opposite was true (better fatigue performance for the 35% mastics) versus strain in Figure 5.8. Based on these findings, it appears that it is the stiffening effect (probably simply related to bulk properties) of the fillers that is important rather than the actual type of filler.

In general, the fatigue results at 20°C in Figures 5.9 and 5.10 support the conclusion that the stiffness of the mastic is more influential on the fatigue performance than the type of filler. The results of the six mastics can be grouped into two groups based on filler concentration, although there is slightly more separation of fatigue lines within these two broad groups. This can be explained once the average stiffness values of the mastics at 20°C are taken into account. Whereas the stiffness values for the 35% mastics at 10°C are very similar (see Table 5.2), the values at 20°C differ slightly more. The same can be seen for the 65% mastics with the stiffness of the 65% gritstone mastic being over 40% higher than that of the 65% limestone mastic. These larger relative differences in stiffness at 20°C do result in different fatigue lines, as clearly seen for the 65% limestone and gritstone mastics in Figure 5.10.

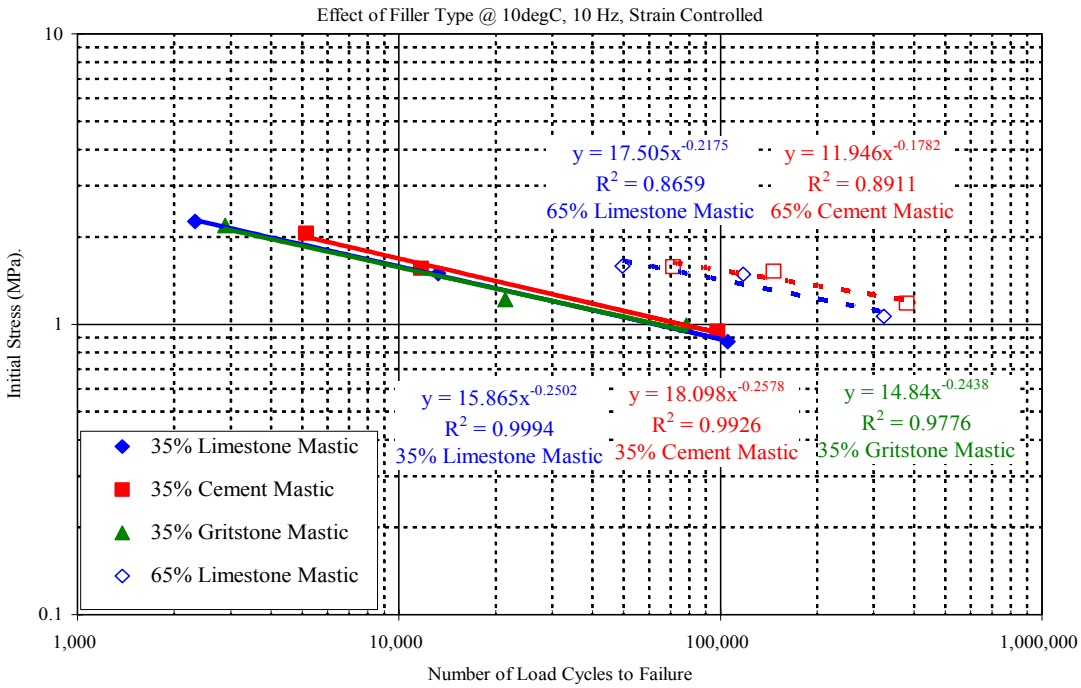

Figure 5.7: Effect of filler type on fatigue – controlled strain, 10°C, 10 Hz versus initial stress

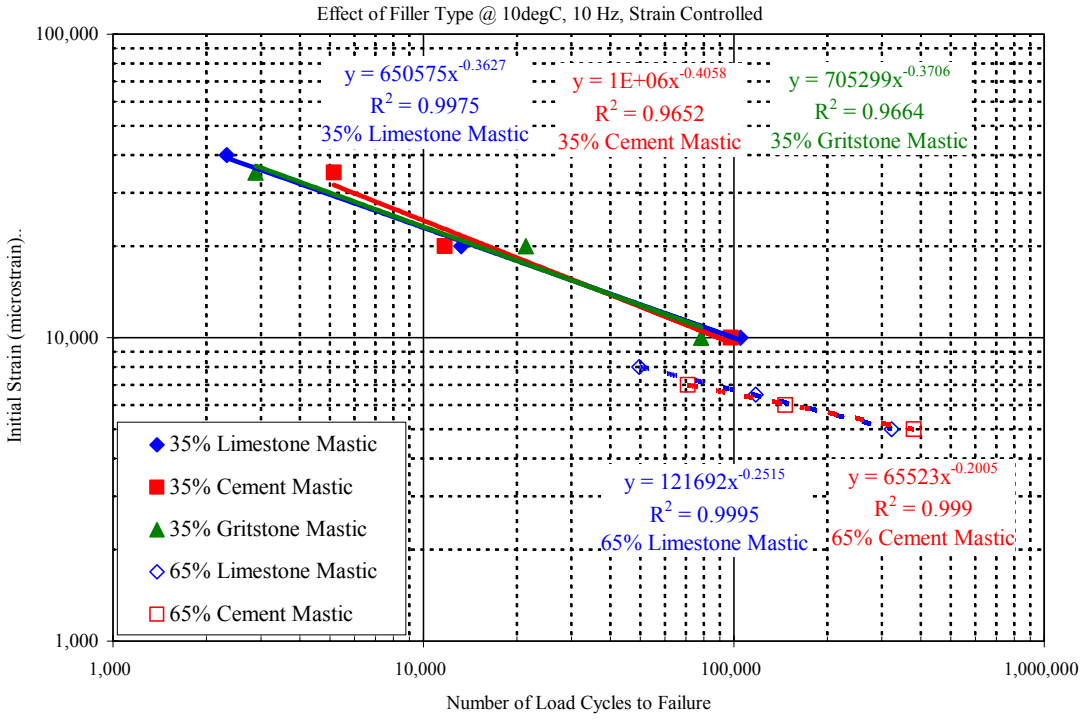

Figure 5.8: Effect of filler type on fatigue – controlled strain, 10°C, 10 Hz versus initial strain

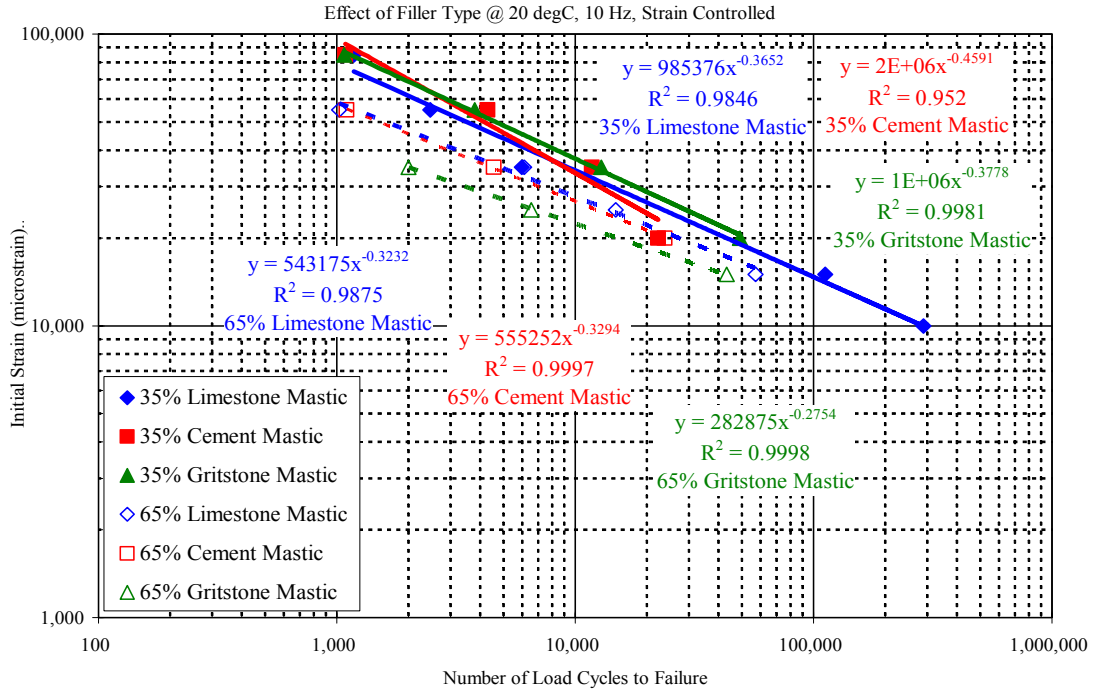

Figure 5.9: Effect of filler type on fatigue – controlled strain, 20°C, 10 Hz versus initial strain

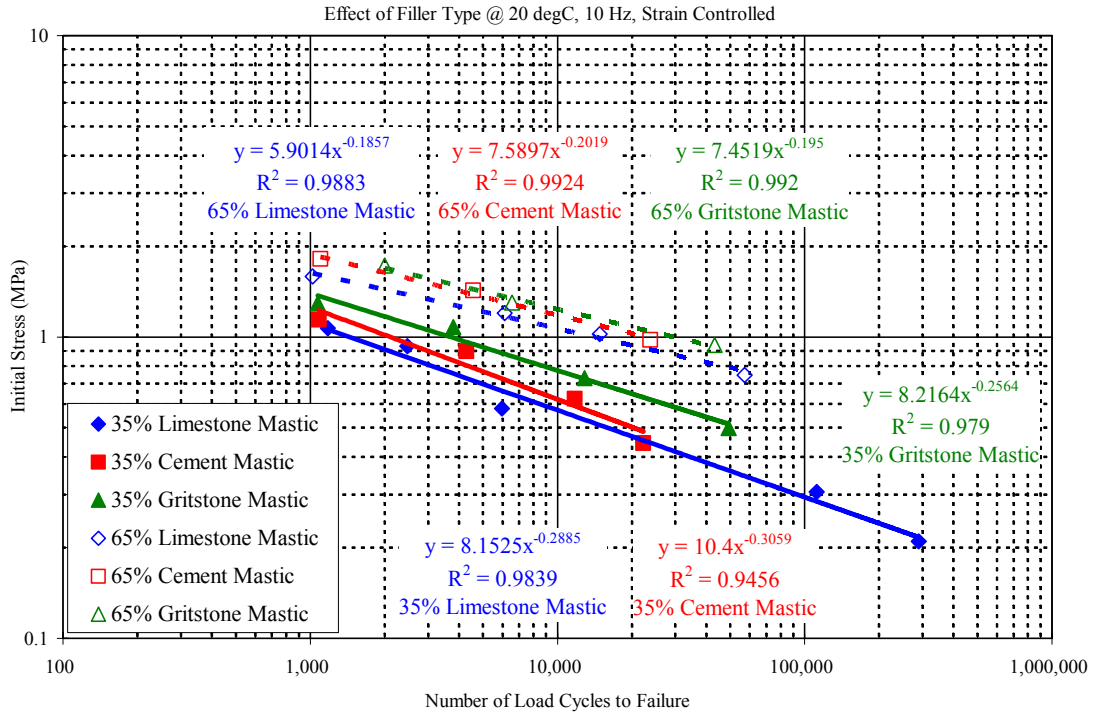

Figure 5.10: Effect of filler type on fatigue – controlled strain, 20°C, 10 Hz versus initial stress

5.6 Comparisons of Fatigue Characteristics of Bitumen, Mastics and Mixtures

The purpose in this section is to compare the fatigue characterisation of the pure bitumen, bitumen-filler mastic and asphalt mixture. It can be considered that fatigue properties of bitumen-filler mastic rather than pure bitumen may be more appropriate in the search to establish correlations with fatigue properties of asphalt mixtures. Additionally, if the physical contact between filler particles and other particles is absent, a suspension of filler in bitumen is present. The bitumen-filler mastic (35% filler concentration by mass) could be considered as an enhanced binder. On the other hand, if mineral filler particles establish physical contact with other particles through the bitumen medium, the fatigue properties of asphalt mixtures might be reflected by those of bitumen-filler mastic (65% filler concentration by mass) as the filler skeleton is formed in bitumen. In this section, the fatigue results obtained from a four point bending test for asphalt mixtures are used to compare with those obtained from the DSR fatigue tests for the bitumen and mastics. The fatigue data of asphalt mixtures were generated by Dr. Osman at the University of Nottingham (Osman, 2004).

5.6.1 Four-Point Bending Test

The four point bending test is one of the flexural tests developed to study the fatigue characteristics of asphalt mixtures. During such a loading method a state of predominantly uniaxial tensile bending is created within an asphalt mixture specimen, which is an appropriated approach for simulating fatigue damage that occurs at the bottom of an asphalt layer. In this test, the dimensions of an asphalt beam are 305 mm long with a cross section measuring 50 mm by 50 mm, which allows it to be cut from a roller compacted slab of material. The tests were carried out in displacement control and each test was continued until the load had dropped to 50% of its initial value. The definition of fatigue life is the number of load cycles until the 50% reduction in the initial stiffness.

Figure 5.11 shows the schematic diagram of the four point bending test apparatus. During the test, a displacement was applied to the specimen through a servo hydraulic

actuator. A linear variable differential transformer (LVDT) connected to the actuator piston monitored the crosshead stroke and provided a feedback signal for the control system. The actuator piston was connected to a load cell to record the applied load. The test schematic diagram of loading, deformation and specimen geometry are shown in Figure 5.12. The test fixture incorporated a clamping mechanism and used a displacement mode of control. To measure the vertical deformation of the asphalt beam on the neutral axis, one LVDT was used and positioned at the centre of the neutral axis of the beam. The tensile strain generated at the bottom of the asphalt beam can be determined by measuring the vertical deformation on the specimen using the LVDT. All specimens were tested at different tensile strain levels up to 700 microstrain at 10^{o}C with a loading frequency of 10 Hz.

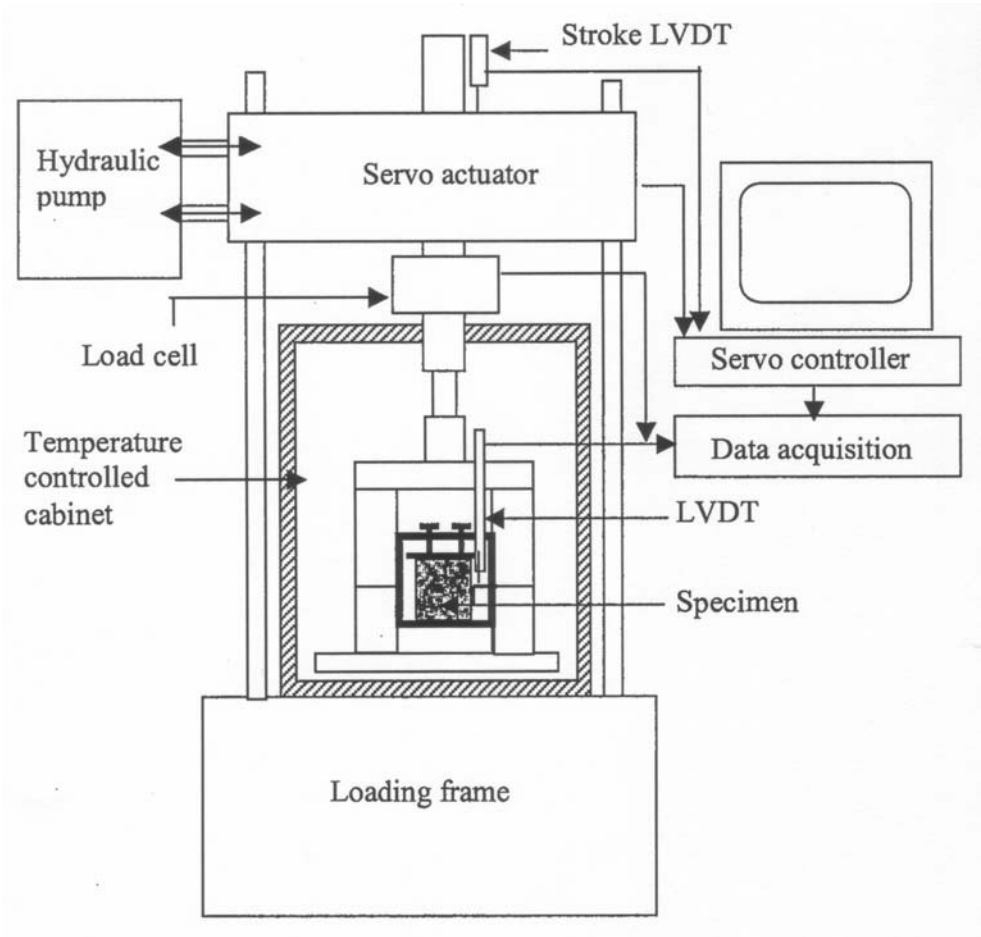

Figure 5.11: Schematic diagram of four point bending test apparatus (Osman, 2004)

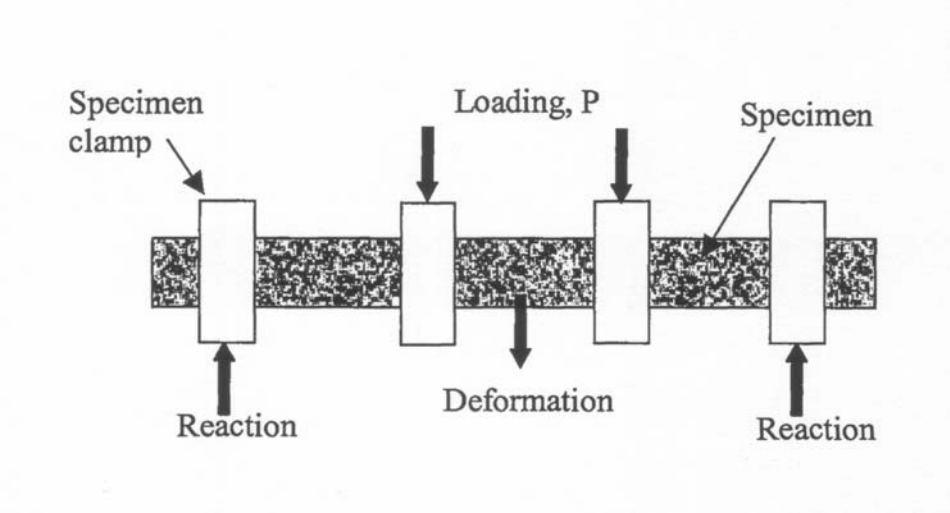

Figure 5.12: Schematic diagram of four point bending fatigue test (Osman, 2004)

5.6.2 Asphalt Mixtures

The four point bending testing was carried out on a 10 mm nominal size Dense Bitumen Macadam (DBM) which was designed according to the specification limits of 10 mm size closed graded wearing course BS 4987-1 (1993). A straight-run 50 penetration grade bitumen used as the binder in the four point bending test for mixtures was the same as that used in the mastics DSR fatigue tests. The bitumen content was maintained at 5.2% by mass for all mixtures while the filler type was varied. Crushed limestone aggregates and three filler types of limestone, cement and gritstone fillers were included in the testing programme. The target air voids content was set at 4%. Table 5.5 shows the aggregate gradation and mixture design for the 10 mm DBM.

Table 5.5: Mixture design for 10 mm DBM

Constituent	Percentage by Mass (%)
10 mm Aggregate	37
6 mm Aggregate	26
Dust	34
Filler	3
Ratio of Filler to Bitumen	0.54 (35/65)
Bitumen Content	5.2%
Target Air Voids	4%

5.6.3 Comparisons of Fatigue Characteristics

The fatigue results at 10^{o}C and 10 Hz from the DSR fatigue tests and four point bending tests are plotted in Figures 5.13 and 5.14, against strain and stress. A single fatigue characteristic has been drawn for the asphalt mixtures since there is no clear pattern differentiating the different filler types (Osman, 2004). For the bitumen and mastics DSR tests, only the controlled strain tests have been presented. A single fatigue line has also been produced for the 35% and 65% bitumen-filler mastics due to the fact that the effect of filler type can be considered to be negligible. It is noted that the fatigue values plotted for the asphalt mixtures are tensile components whereas those plotted for the bitumen and mastics are shear components. It is clear that the fatigue results for the pure bitumen and 35% bitumen-filler mastic are compatible. The slopes of the fatigue characteristic for the pure bitumen are about 0.37 (against strain) and 0.25 (against stress) compared to about 0.38 (against strain) and 0.25 (against stress) for the 35% bitumen-filler mastic. It implies that the fatigue behaviour for the 35% bitumen-filler mastic is similar to that for the pure bitumen. The 35% bitumen-filler mastic is an enhanced binder and its fatigue behaviour is dominated by the base bitumen.

It is also clear that the fatigue results for the asphalt mixture and 65% bitumen-filler mastic are compatible. The gradients of the characteristic lines for the asphalt mixture are about 0.26 (against strain) and 0.18 (against stress) compared to about 0.23 (against strain) and 0.19 (against stress) for the 65% bitumen-filler mastic. Although a significantly large difference in strain level (about 40 times) between the 65% bitumen-filler mastic and the asphalt mixture, the strain dependency of the highly modified mastic is similar to that of the 10 mm DBM. The similar slope for the high filler content mastic and asphalt mixture implies that the fatigue characteristics of mixtures could be reflected by those of mastics having a filler skeleton structure. When fatigue data plotted against stress, the fatigue lines for the 65% bitumen-filler mastic and DBM are almost at the same stress levels. It appears that the shear stress levels for the highly modified mastic are only up to 1.6 MPa due to difficulties involved in testing such a stiff mastic that shows a poor adhesion between the DSR parallel plates and the mastic. Additionally, the applied shear strain levels for the 65% bitumen-filler mastic only can be performed at shear strain levels up to 0.8% (8000 microstrain).

The failure plane generated in the four point bending test is caused by tension whereas there is no tension in the DSR on the failure plane on which the specimen is forced to fail by shear. However, the fatigue characteristics for the asphalt mixtures with respect to strain and stress have apparently similar slopes to those for the highly modified mastics. It also can be speculated that the stiffnesses of the asphalt mixtures are therefore about 40 times those of the 65% bitumen-filler mastics. Table 5.6 shows the stiffness modulus values of the 10 mm DBM generated from four point bending test are approximately 40 times those of the highly modified mastic generated from DSR test.

Table 5.6: Stiffness modulus values for 65% bitumen-filler mastics and 10 mm DBM at 10^{o}C and 10 Hz

Filler used in Mastic or DBM	65% Bitumen-Filler Mastic Complex Modulus (MPa)	10 mm DBM Tensile Stiffness Modulus (MPa)
Limestone	221	7620
Cement	245	7889
Gritstone	-	7882

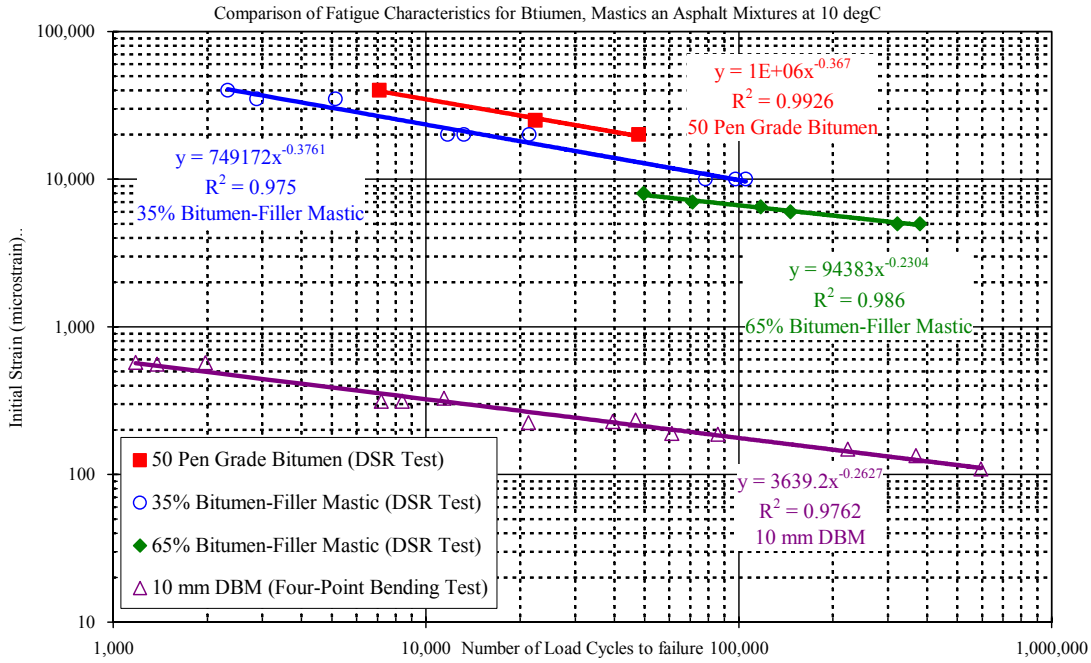

Figure 5.13: Fatigue data plotted against strain for bitumen, mastics and mixture at 10°C and 10 Hz

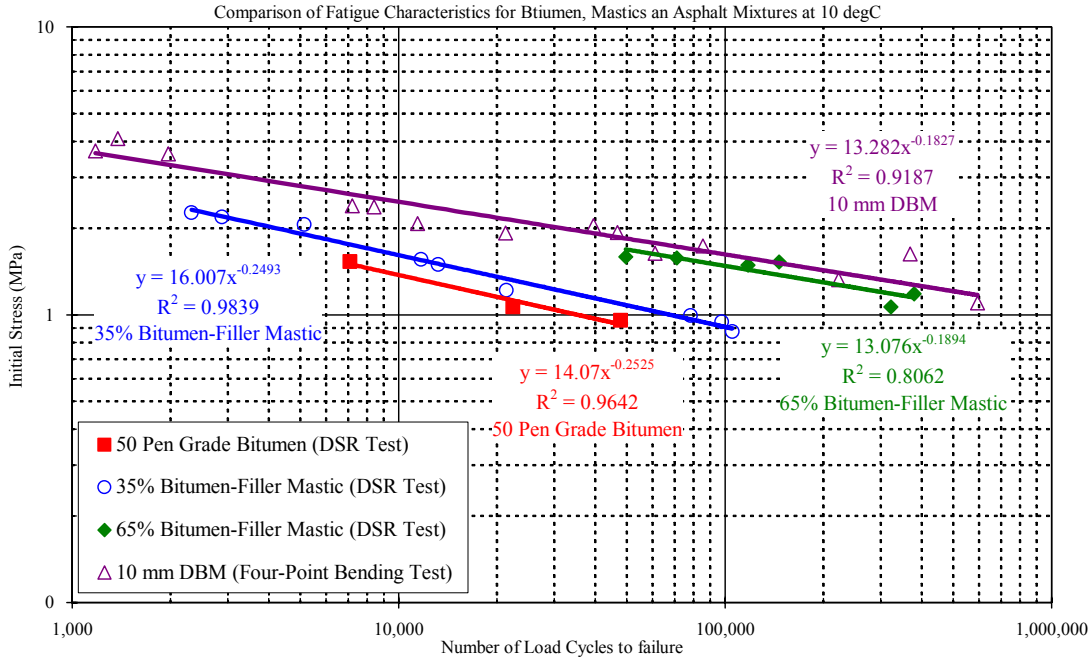

Figure 5.14: Fatigue data plotted against stress for bitumen, mastics and mixture at 10°C and 10 Hz

5.7 Summary

In this chapter, oscillation testing using time sweeps has been used to determine the fatigue properties of a range of bitumen-filler mastics and a control bitumen (50 penetration grade bitumen) at two temperatures of 10^{o}C and 20^{o}C and a loading frequency of 10 Hz. The comparison of bitumen, mastic and mixture has also been presented by plotting fatigue results against strain as well as stress. The following conclusions can be drawn from the fatigue data presented in this chapter:

- Both controlled stress and controlled strain fatigue tests are possible on bitumen-filler mastics using the DSR.
- For the large range of stiffness values found for the different filler content mastics and pure bitumens at different testing temperatures, there does not appear to be a definite stress or strain dependency criterion.
- Filler content has a significant influence on the fatigue life of bitumen-filler mastics with the higher contents (65%) showing an increase in fatigue life versus stress similar to the increase in fracture strength seen for the mastics.
- However, filler type does not appear to influence fatigue performance of bitumen-filler mastics, other than in terms of the stiffening effect of the individual filler type and its concentration in the mastic.
- The 35% bitumen-filler mastics show similar patterns of fatigue behaviour to the pure bitumen. It is therefore proposed that the mastics having filler suspension should be considered as enhanced binders.
- The fatigue characteristics for the 10 mm DBM with respect to strain and stress show similar slopes to those for the highly modified mastics (65% bitumen-filler mastic). The fatigue behaviour of highly modified mastic using the DSR time sweep testing can reflect that of the asphalt mixtures using four point bend testing.

Summary, Conclusions and Recommendations for Future Work

6.1 Summary

A total of seven bitumen-filler mastics produced using the 50 penetration grade bitumen as the base bitumen, three filler types (limestone, cement and gritstone) and three filler concentrations of 15%, 35% and 65% by mass has been tested using the Bohlin Gemini 200 Dynamic Shear Rheometer (DSR). The selection of filler concentrations in the bitumen-filler mastics was considered as (1) filler particles are suspended in the bitumen (15% and 35% by mass) and (2) filler particles form a skeleton in the bitumen (65% by mass). Taking into consideration the problem statements mentioned in Chapter 1, the research objectives in this thesis are concerned with three areas:

1. Small Strain Rheological Analysis

Using the DSR, the linear viscoelastic properties of the mastics can be characterised over a wide range of temperature and loading time conditions. Oscillation testing using stress sweeps and frequency sweeps was performed on the base bitumen and bitumen-filler mastics.

2. Steady State Rheological Analysis

This research objective looks at the suitability of different laboratory testing techniques at measuring zero shear viscosity (ZSV) of bitumen-filler mastics and the relative effect of filler type and concentration on the measured ZSV. Various techniques were used to measure ZSV, including small amplitude, low frequency oscillations, low stress creep tests and low shear strain rate viscometry measurements.

3. Fatigue Characterisation (large strain)

Oscillation testing using time sweeps was performed using large strains and stresses to investigate fatigue characteristics of the bitumen and bitumen-filler mastics. To establish a picture of the factors affecting pavement fatigue at every stage from bitumen to mixture, comparisons of fatigue characteristics of bitumen, mastics and mixtures were discussed.

This research investigates the small and large strain rheological and fatigue characterisation of bitumen-filler mastics. This chapter summarises the conclusions from this thesis and provides recommendations for future work in this field.

6.2 Conclusions

The main conclusions that can be drawn from the bitumen-filler mastic investigation undertaken in this thesis are:

- In this research, the gritstone filler contributes a larger volume to the binder compared to the limestone and cement fillers and therefore it has a dramatic effect on rheological and mechanical behaviour of mastic.
- The 15% and 35% bitumen-filler mastics can be considered as an enhanced binder since they show similar patterns of rheological and mechanical behaviour to the pure bitumen. The considerable stiffening effect for the 65% bitumen-filler mastics on complex modulus, ZSV and fatigue characteristics indicates that filler skeleton structures are present in the highly modified mastics. The mechanical properties of asphalt mixtures can be mirrored by those of the bitumen-filler mastics at high filler concentrations.

In addition to these main conclusions, the following conclusions have been drawn from the work done in various chapters of the thesis.

Literature Review (Chapter 2)

- The effects of mineral filler properties such as particle size distribution, shape, Rigden voids, specific surface, filler concentration, packing fraction and filler chemical compositions significantly influence the physical and mechanical properties of bitumen-filler mastics as well as asphalt mixtures in terms of the physical and chemical aspects.
- The mineral filler has been known to stiffen bitumen and considerably influence the mechanical properties of asphalt paving mixture as mineral filler particles are suspended in bitumen.
- Small strain shear oscillatory testing using a dynamic shear rheometer (DSR) provides a practical and relatively simple method to obtain a number of rheological parameters of bituminous binders within the linear viscoelastic range.
- The dynamic mechanical analysis (DMA) helps to understand the viscous and the elastic nature of binders over a wide range of temperatures and loading rates.
- Various measurement techniques (oscillation test and creep test) performed on a DSR with the ZSV being determining directly from the plotted data or, particularly in the case of the oscillation test, extrapolated to zero frequency using an appropriate mathematical model have also been introduced in this chapter.
- Direct testing of bituminous binders in fatigue has been used to generate load-associated fatigue characteristics for bituminous binders by means of time sweep tests using a DSR at various strain and stress levels in the linear and non-linear ranges.

Small Strain Rheological Analysis (Chapter 3)

- It is essential to consider the volumetric content of filler within the bitumen-filler mastic rather than mass content as the rheological characteristics of the bitumen-filler mastic are considerably affected by percentage of filler content by effective volume.
- At high temperature the behaviour of asphalt mixtures may be reflected by the rheological behaviour of the 65% bitumen-filler mastics can be seen from the difference in LVE strain limits between the bitumen and the bitumen-filler mastic having filler skeleton in bitumen (65% filler content by mass).

- The mineral filler particles become the predominant component in the 65% bitumen-filler system at high temperatures and low frequencies as seen by the deviation of the complex modulus master curve.
- Simple rheological behaviour can be found for the 15% and 35% bitumen-filler mastics, while the complex rheological behaviour of bitumen-filler mastic containing high effective volume (62.1%) mirrors that of asphalt mixtures.

Steady State Rheological Analysis (Chapter 4)

- The viscosity under steady state conditions for the highly modified system (65% bitumen-filler mastic) potentially mirrors the permanent deformation behaviour of asphalt mixtures.
- The simple rheological behaviour of the 65% limestone bitumen-filler mastic is not found, but a significant deviation from the Cox-Merz rule is observed. The fact is related to its filler skeleton structure in the bitumen. The particle-particle interaction is believed to change the viscosity curves of the 65% bitumen-filler mastic.
- Excellent agreement is shown between the ZSVs obtained from the viscometry measurements and ZSVs obtained from the creep measurements. It can be concluded that the values of apparent viscosity and creep viscosity can approach similar ZSV as long as the steady state is attained during testing.
- The Cross model and Carreau model with a nonlinear regression analysis can fit well to the measurements of the complex dynamic viscosity and apparent viscosity in the range of the test frequencies and shear rates. The extrapolation of ZSV value can be similar if the viscosity measurements reach steady state.

Fatigue Characterisation (Chapter 5)

- For the large range of stiffness values found for the different filler content mastics and pure bitumens at different testing temperatures, there does not appear to be a definite stress or strain dependency criterion.

- Filler content has a significant influence on the fatigue life of bitumen-filler mastics with the higher contents (65%) showing an increase in fatigue life versus stress similar to the increase in fracture strength seen for the mastics.
- However, filler type does not appear to influence fatigue performance of bitumen-filler mastics, other than in terms of the stiffening effect of the individual filler type and its concentration in the mastic.
- The 35% bitumen-filler mastics show similar patterns of fatigue behaviour to the pure bitumen. It is therefore proposed that the mastics having filler suspension should be considered as enhanced binders.
- The fatigue characteristics for the 10 mm DBM with respect to strain and stress show similar slopes to those for the highly modified mastics (65% bitumen-filler mastic). The fatigue behaviour of highly modified mastic using the DSR time sweep testing can reflect that of the asphalt mixtures using four point bend testing.

6.3 Recommendations for Future Work

A fundamental rheological study, with regard to the small and large strain rheological and fatigue characterisation of bitumen-filler mastics, has been undertaken and presented in this thesis. The rheological measurements have shown the complex rheological behaviour and dramatic stiffening effect on viscosity at steady state for the highly modified mastics. It can be speculated that the filler skeleton exhibiting in the mastics is similar to the aggregate skeleton occurring in asphalt mixtures. However, further research is needed to investigate whether the values of complex modulus and ZSV are evident to the permanent deformation of asphalt mixtures. It is, therefore, recommended that creep testing, dynamic oscillatory type testing and wheel track testing of DBM, incorporating the 50 pen bitumen and mineral aggregates (limestone or gritstone), should be undertaken. Although the 65% bitumen-filler mastics show similar patterns of fatigue behaviour to the 10 mm DBM, the fatigue characterisation also needs to be identified and quantified for the DBM by means of dynamic fatigue testing such as direct uniaxial tension-compression tests, diametral tests and various flexure tests.

Although the filler concentrations of 15%, 35% and 65% by mass were tested in this study, further rheological and fatigue testing on bitumen-filler mastic at different filler content levels are recommended. Additionally, the filler grading such as continuous graded and gap graded mastics, may considerably affect the rheological behaviour of bitumen-filler mastics. Similar filler grading for mastics and aggregate grading for asphalt mixtures could show very similar rheological and mechanical properties between the mastics and mixtures. In addition, although the limestone filler, cement filler, gritstone filler and 50 penetration grade bitumen were used in this mastic investigation, the study should be extended to include various penetration grade bitumens and polymer modified bitumens (PMBs) to study filler stiffening effects on rheological properties and fatigue characterisation.

The fundamental rheological tests were carried out in the dynamic shear rheometer (DSR) because of the convenience and availability of the equipment. The DSR is a standard piece of binder test equipment and it delivers repeated torsional load to a hockey puck-shaped disc of bitumen or mastic. The advantages of the DSR are the accurate temperature control and load (or displacement) control. The disadvantages are that the non-uniform shear strains and shear stresses are generated in the specimen. The values of shear strain and shear stress are dependent on the radius of the parallel plates and vary in magnitude from the centre to the extremities of disks. The shear stress, shear strain and shear complex modulus, which is a function of the radius to fourth power, are calculated at the outside (maximum value) of the disk. Therefore, uniaxial tension-compression fatigue tests (Osman, 2004) are recommended to be performed on the highly modified mastics since relatively uniform tensile stress conditions can be generated.

The debonding between the stainless steel parallel plates and mastics is a main problem of the DSR equipment, particularly during the fatigue testing at low temperatures (below 10^{o}C). The modifications made to a base plate and spindle to allow for an aggregate-type interface with the mastic could be a solution.

The research in this thesis has focused on moderate to high temperature testing of bitumen and bitumen-filler mastics. In order to create a better understanding of the rheological and mechanical properties of mastics, future work can be carried out using the Bending Beam Rheometer (BBR) and the Direct Tension Testing (DDT). In addition to the various fundamental rhological testing, the recent development of X-ray tomography may allow scanning of the filler skeleton of dry compacted filler (related to Rigden voids) and internal structure of bitumen-filler mastic to help obtain a better understanding of packing effect of filler on mastic rheological and mechanical behaviour. The fundamental rheological and mechanical properties of mastics can be compared and validated with those of asphalt mixtures.

References

Airey, G.D. (1997). "Rheological Characteristics of Polymer Modified and Aged Bitumens", Ph.D. Thesis, Department of Civil Engineering, University of Nottingham, United Kingdom.

Airey, G.D. and Rahimzadeh, B. (2004). "Combined Bituminous Binder and Mixture Linear Rheological Properties", *Construction and Building Materials*, Issue 18, pp.535-548, 2004.

Airey, G.D. and Rahimzadeh, B. and Collop, A.C. (2002). "Linear and Nonlinear Rheological Properties of Asphalt Mixtures", *Journal of the Association of Asphalt Paving Technologists*, Vol. 71, pp. 160-196.

Airey, G.D., Thom, N.H., Osman, S., Huang, H. and Collop, A.C. (2004). "A Comparison of Fatigue Test Data from Different Test Methods", 5th International RILEM Conference, Limoges, France.

Anderson, D.A. (1987). "Guidelines for Use of Dust in Hot-Mix Asphalt Concrete Mixtures" *Journal of the Association of Asphalt Paving Technologists*, Vol. 56, pp. 492-516.

Anderson, D.A., Christensen, D.W. and Bahia, H. (1991). "Physical Properties of Asphalt Cement and the Development of Performance-Related Specifications", *Journal of the Association of Asphalt Paving Technologists*, Vol. 60, pp. 437-532.

Anderson, D.A., Christensen, D.W., Bahia, H. U., Dongre, R., Sharma, M. G., Antle, C. E. and Button, J. (1994). "Binder Characterization and Evaluation, Volume 3: Physical Characterization", SHRP-A-369, Strategic Highway Research Program, National Research Council, Washington, DC, United State.

Anderson, D.A., Le Hir, Y.M., Marasteanu, M.O., Planche, J.-P., Martin, D. and Gauthier, G. (2001). "Evaluation of Fatigue Criteria for Asphalt Binders", *Transportation Research Record*, No. 1766, pp. 48-56.

Anderson, D.A., Le Hir, Y.M., Planche, J. and Martin, D. (2002). "Zero Shear Viscosity of Asphalt Binders", *Transportation Research Record*, No. 1810, pp. 54-62.

Bahia, H.U., Zhai, H., Bonnetti, K. and Kose, S. (1999). "Non-Linear Viscoelastic and Fatigue Propertise of Asphalt binders", *Journal of the Association of Asphalt Paving Technologies*, Vol.68, pp. 1-34.

Bahia, H.U., Zhai, H., Zeng, M., Hu, Y. and Turner, P. (2002). "Development of Binder Specification Parameters Based on Characterization of Damage Behavior", *Journal of the Association of Asphalt Paving Technologies*, Vol. 70, pp. 442-470.

Binard, C., Anderson, D., Lapalu, L. and Planche, J.P. (2004). "Zero Shear Viscosity of Modified and Unmodified Binders", 3rd Euroasphalt & Eurobitume Congress, Book II, Paper 236, pp. 1721-1733, Vienna.

Bodin, D., Soenen, H. and Roche, C. (2004). "Temperature Effects in Binder Fatigue and Healing Tests", 3rd Euroasphalt & Eurobitume Congress, Book II, Paper 136, pp. 1996-2004, Vienna.

Bonnetti, K.S., Nam, K. and Bahia, H. (2002). "Measuring and Defining Fatigue Behavior of Asphalt Binders", *Transportation Research Record*, No. 1810, pp. 33-43.

Bohlin Instruments Ltd.(2004). "User Manual for Bohlin Rheometers".

British Standards Institution, BS 812: Part 2: 1995 "Testing Aggregates, Part2. Methods of Determination of Density".

British Standards Institution, BS 4359-1: 1996 "Determination of the Specific Surface area of Powders, Part 1: BET Method of Gas Adsorption for Solids (including Porous Materials)".

British Standards Institution, BS 4987-3: 1993 "Coated Macadam for Roads and Other Paved Area- Part 1: Specification for Constituent Materials and for Mixtures".

British Standards Institution, BS EN 1097-4: 1999 "Tests for Mechanical and Physical properties of Aggregates- Part 4: Determination of Voids of Dry Compacted Filler".

British Standards Institution, BS EN 1097-7: 1999 "Tests for Mechanical and Physical properties of Aggregates- Part 7: Determination of the Particle Density of Filler-Pyknometer Method".

British Standards Institution, BS EN 12593: 2000 "Methods of Test for Petroleum and Its Products—BS 2000-80: Bitumen and Bituminous Binders—Determination of the Fraass Breaking Point".

British Standards Institution, BS EN 1426: 2000 "Methods of Test for Petroleum and Its Products—BS 2000-49: Bitumen and Bituminous Binders—Determination of

Needle Penetration (Identical with IP 49-2000)".

British Standards Institution, BS EN 1427: 2000 "Methods of Test for Petroleum and Its Products—BS 2000-58: Bitumen and Bituminous Binders—Determination of Softening Point—Ring and Ball Method (Identical with IP 58-2000)".

British Standards Institution, BS EN 12593: 2000 "Methods of Test for Petroleum and Its Products—BS 2000-80: Bitumen and Bituminous Binders—Determination of the Fraass Breaking Point".

Carreau, P.J., Macdonald, I.F. and Bird, R.B. (1968). "A Nonlinear Viscoelastic Model for Polymer Solutions and Melts-II", Chemical Engineering Science, Vol. 23, pp. 901-911.

Carswell, J. and Green P.J. (2000). "Prediction of Rutting Resistance in Hot Rolled Asphalt Using Rheological Parameters" *The Asphalt Year Book* (Institute of Asphalt Technology).

Carswell, J. and Moglia, O. (2003). "Assessment of the Pulsed Creep Test to Predict the Rutting Performance of Asphalt Mixtures", *Europeanroads Review*, Special Issue, RGRA 1, pp. 64-68.

Chen, J.S. and Peng, C.H. (1998). "Analyses of Tensile Failure Properties of Asphalt-Mineral Filler Mastics", *Journal of Materials in Civil Engineering*, Vol. 10, No. 4, pp.256-262.

Christensen, D.W. and Anderson, D.A. (1992). "Interpretation of Dynamic Mechanical Test Data for Paving Grade Asphalt Cements", *Journal of the Association of Asphalt Paving Technologies*, Vol.61, pp. 67-116.

Collop, A.C., Airey, G.D. and Khanzada, S. (2002). "Creep Testing of Bitumens Using the Dynamic Shear Rheometer", *the International Journal of Pavement Engineering*, Vol.3 (2), pp. 107-116.

Cox, W.P. and Merz, E.H. (1958). "Correlation of Dynamic and Steady Flow Viscosities", *Journal of Polymer Science*, Vol.28 (118), pp. 619-622.

Craus, J., Ishai, I. and Sides, A. (1978). "Some Physico-Chemical Aspects of The Effect and The Role of The Filler in Bituminous Paving Mixtures" *Journal of the Association of Asphalt Paving Technologists*, Vol. 46, pp. 558-588.

Cross, M.M. (1965). "Rheology of Non-Newtonian Fluids: A New Flow Equation for

Pseudoplastic Systems", *Journal of Colloid Science*, Vol. 20, pp. 417-437.

Daniel, J.S., Bisirri, W. and Kim, Y.R. (2004). "Fatigue Evaluation of Asphalt Mixtures Using Dissipated Energy and Viscoelastic Continuum Damage Approaches", *Journal of the Association of Asphalt Paving Technologies*, Vol. 73, pp. 557-583.

Delgadillo, R., Cho, D.W. and Bahia, H. (2006). "Non Linearity of Repeated Creep and Recovery Binder Test and the Relationship with Mixture permanent Deformation" Transportation Research Board, 85ft Annual Meeting, Paper No. 06-3016.

Desmazes, C., Lecomte, M., Lesueur, D. and Philips, M. (2000) "A Protocol for Reliable Measurement of Zero-Shear-Viscosity in Order to Evaluate the Anti-Rutting Performance of Binders", 2nd Eurasphalt & Eurobitume Congress, Proc.0073, Book I, pp. 203-211, Barcelona.

De Visscher, Soenen, H. Vanelstraete, A. and Redelius, P. (2004). "A Comparison of the Zero Shear Viscosity from Oscillation Tests and the Repeated Creep Test", 3rd Eurasphalt & Eurobitume Congress, Book II, Paper 153, pp. 1501-1513, Vienna.

Dongre, R. and D'Angelo, J. (2003). "Refinement of Superpave High-Temperature Binder Specification Based on Pavement Performance in the Accelerated Loading Facility", *Transportation Research Record*, No.1829, pp. 39-46.

Fakhri, M. and Shackel, B. (2003). "Fatigue Characterisation of Asphaltic Concrete Using Dissipated Energy Approach", *Proceedings - Conference of the Australian Road Research Board*, Vol. 21, pp. 231-242.

Ferry, J.D. (1980). "Viscoelastic Properties of Polymers", 3rd Ed., Wiley, New York.

Ghuzlan, K.A. and Carpenter, S.H. (2000) "Energy-Derived, Damage-Based Failure Criterion for Fatigue Testing", *Transportation Research Record*, No.1723, pp. 141-149.

Girdler, R.B. (1965). "Constitution of Asphaltenes and Related Studies", *Journal of the Association of Asphalt Paving Technologists*, Vol. 34, pp. 45-79.

Goodrich, J.L. (1991). "Asphaltic Binder Rheology, Asphalt Concrete Rheology and Asphalt Concrete Mix Properties", *Journal of the Association of Asphalt Paving Technologists*, Vol. 60, pp. 80-120.

Goodrich, J.L. (1988). "Asphalt and Polymer Modified Asphalt Properties Related to the

Performance of Asphalt Concrete Mixes", *Journal of the Association of Asphalt Paving Technologists*, Vol. 57, pp. 116-175.

Hammoum, F. De La Roche, Piau, T.-M., and Stefani, C. (2002). "Experimental Investigation of Fracture and Healing of Bitumen of Pseudo-contact of Two Aggregate", Proceedings of the 9th International Conference on Asphalt Pavement, Copenhagen.

Harris, B. M. and Stuart, K. D. (1995). "Analysis of Mineral Fillers and Mastics Used in Stone Matrix Asphalt", *Journal of the Association of Asphalt Paving Technologists*, Vol. 64, pp. 54-95.

Hatman, A.M. and Gilchrist, M.D. (2004). "Evaluation Four-Point Bend Fatigue of Asphalt Mix Using Image Analysis", *Journal of Materials in Civil Engineering*, pp. 60-68.

Heukelom, W. (1965). "The Role of Filler in Bitumen Mixes" *Journal of the Association of Asphalt Paving Technologists*, Vol. 34, pp. 396-429.

Hopman, P.C, Kunst, P.A.J.C. and Pronk, A.C. (1989). "A renewed Interpretation Method for Fatigue Measurement, Verification of Miner's Rule, ", 4th Eurobitume Symposium, Vol. 1, pp. 557-561.

Huschek, S. and Angst, CH. (1980). "Mechanical Properties of Filler-Bitumen Mixes at High and Low Service Temperatures" *Journal of the Association of Asphalt Paving Technologists*, Vol. 49, pp. 440-475.

Ishai, I. and Craus, J. (1977). "Effect of the Filler on Aggregate-Bitumen Adhesion Properties in Bituminous Mixtures" *Journal of the Association of Asphalt Paving Technologists*, Vol. 46, pp. 228-258.

Kavussi, A. and Hicks, R.G. (1997). "Properties of Bituminous Mixtures Containing different Fillers" *Journal of the Association of Asphalt Paving Technologists*, Vol. 66, pp. 153-186.

Kim, Y.-R. and Little, D.N. (2004). "Linear Viscoelastic Analysis of Asphalt Mastics", *Journal of Materials in Civil Engineering*, Vol. 16, No. 2, pp. 122-132.

Lesueur, D. and Little, D. N., "Effect of Hydrated Lime on Rheology, Fracture and Ageing of Bitumen", *Transportation Research Record*, No. 1661, pp. 93-105, 2003.

Little, D.N. and Petersen, J.C. (2005). “Unique Effects of Hydrated Lime Filler on the Performance-Related Properties of Asphalt Cements : Physical and Chemical Interactions Revisited”, *Journal of Materials in Civil Engineering*, Vol. 17, No. 2, pp. 207-218.

Lu, X., Soenen, H. and Redelius, P. (2003). “Fatigue and Healing Characteristics of Bitumens Studied Using Dynamic Shear Rheometer”, 6th RILEM Symposium PTEBM’03, pp. 408-415, Zurich.

Mack, C. (1932). “Colloid Chemistry of Asphalts”, *Journal of Physical Chemistry*, Vol. 36, Issue 12, pp. 2901-2914.

Martono, W. and Bahia, H.U. (2003). “Defining Asphalt Binder Fatigue as a Function of Pavement Temperature and Pavement Structure”, *Transportation Research Board*, Paper No. 03-4162.

Osman, S.A. (2004). “The Role of Bitumen and Bitumen/Filler Mortar in Bituminous Mixture Fatigue”, Ph.D. Thesis, Department of Civil Engineering, University of Nottingham, United Kingdom.

Partal, P., Martinez-Boza, F., Conde, B. and Gallegos, C. (1999). “Rheological Characterisation of Synthetic Binders and Unmodified Bitumens”, *Fuel*, 78, pp. 1-10.

Pell, P.S. (1962). “Fatigue Characteristics of Bitumen and Bituminous Mixes”, Proceedings of the International Conference on the Structural Design of Asphalt Pavements, Ann Arbor, pp. 310-323.

Pell, P.S. (1967). “Fatigue of Asphalt Pavement Mixes”, Proceedings of the Second International Conference on the Structural Design of Asphalt Pavements, pp. 577-593.

Pell, P.S. (1973). “Characterization of Fatigue Behaviour” Structural Design of Asphalt Concrete Pavements to Prevent Fatigue Cracking, Special Report 140, Highway Research Board, Washington, D.C., pp. 49-64.

Perez-Lepe, A., Martinez-Boza, F.J., Gallegos, C., Gonzalez, O., Munoz, M.E. and Santamaria, A. (2003). “Influence of the Processing Conditions on the Rheological Behaviour of Polymer-Modified Bitumen”, *Fuel*, 82, pp. 1339-1348.

Petersen, J.C. (1984). “Chemical Composition of Asphalt as Related to Asphalt

Durability: State of the Art", *Transportation Research Record*, No. 999, pp. 13-30.

Petersen, J.C., Robertson, R.E., Branthaver, J.F., Harnsberger, P.M., Duvall, J.J., Kim, S.S., Anderson, D.A., Christiansen, D.W., Bahia, H.U., Dongre, R., Antle, C.E. Sharma, M.G., Button, J.W. and Glover, C.J. (1994). "Binder Characterization and Evaluation, Volume 4:Test Method", SHRP-A-370 Report, Strategic Highway Research Program, National Research Council, Washington D.C.

Petersen, J.C., Plancher, H. and Harnsberger, P.M. (1987). "Lime Treatment of Asphalts to Reduce Age Hardening and Improve Flow Properties", *Journal of the Association of Asphalt Paving Technologists*, Vol. 56, pp. 632-653.

Philips, M.C. and Robertus, C. (1995). "Rheological Characterisation of Bitumen Binders in Connection with Permanent Deformation in Asphaltic Pavement; the Zero-Shear Viscosity Concept", No.50, The Rheology of Bituminous Binders Eurobitume Workshop, Brussels.

Philips, M.C. and Robertus, C. (1996). "Binder Rheology and Asphaltic Pavement Permanent Deformation; the Zero-Shear-Viscosity", No.5134, Euroasphalt & Eurobitume Congress.

Pfeiffer, J.PH. and Saal, R.N.J. (1940). "Asphaltic Bitumen as Colloid System", *Journal of Physical Chemistry*, Vol. 44, Issue 2, pp. 139-149.

Planche, J.-P., Anderson, D.A., Gauthier, G., Le Hir, Y.M. and Martin, D. (2003). "Fatigue and Healing Characteristics of Bitumens Studied Using Dynamic Shear Rheometer", *6th RILEM Symposium PTEMB'03*, pp. 408-415, Zurich.

Pronk, A.C. (1997). "Evaluation of the Dissipated Energy Concept for the Interpretation of Fatigue Measurements in the Crack Initiation Phase. Report No. W-DWW-97-056. *Minister van Verkeer en Waterstaat*.

Pronk, A.C. and Hopman, P.C. (1990). "Energy Dissipation : the Leading Factor of Fatigue", the United States Strategic Highway Research Program, London, pp. 225-237.

Read, J.M. (1996). "Fatigue Cracking of Bituminous Paving Mixtures", Ph.D. Thesis, Department of Civil Engineering, University of Nottingham, United Kingdom.

Read, J. and Whiteoak, D., "The Shell Bitumen Hand Book", Fifth Edition, Thomas

Telford Publishing, London, United Kingdom, 2003.

Rowe, G.M. (1996). “Application of the Dissipated Energy Concept to Fatigue Cracking in Asphalt Pavements”, Ph.D. Thesis, Department of Civil Engineering, University of Nottingham, United Kingdom.

Rigden, P.J. (1947). “The Use of Fillers in Bituminous Road Surfacings. A Study of Filler-Binder Systems in Relation to Filler Characteristics”, *Journal Society of Chemical Industry*, Vol. 66, pp. 299-309.

Romberg, J.W. Nesmith, S.D. and Traxler, R.N. (1959). “Some Chemical Aspects of the Components of Asphalt”, *Journal of Chemical and Engineering Data*, Vol. 4, pp. 159-161.

Rowe, G.F. and Bouldin, M.G. (2000) “Improved Techniques to Evaluate the Fatigue Resistance of Asphaltic Mixtures”, 2nd Eurasphalt & Eurobitume Congress, Proc. 0081, Book I, pp. 754-763, Barcelona.

Saal, R.N.J. and Labout, J.W.A. (1940). “Rheological Properties of Asphaltic Bitumens”, *Journal of Physical Chemistry*, Vol. 44, Issue 2, pp. 149-165.

Shashidhar, N., Needham, S.P., Chollar, B.H. and Romeo, P. (1999). “Prediction of the Performance of Mineral Fillers in Stone Matrix Asphalt”, *Journal of the Association of Asphalt Paving Technologists*, Vol. 68, pp. 222-251.

Shenoy, A. (2002). “Fatigue Testing and Evaluation of Asphalt Binders Using the Dynamic Shear Rheometer”, *Journal of Testing and Evaluation*, JTEVA, Vol. 30, No.4, pp. 303-312.

Shenoy, A., Stuart, K. and Mogawer, W. (2003). “Do Asphalt Mixtures Correlate Better with Mastics or Binders in Evaluating Permanent Deformation”, *Transportation Research Record*, No. 1829, pp. 16-25.

Soenen, H., De La Roche, C. and Redelius, P. (2004). “Predict Mix Fatigue Tests from Binder Fatigue Properties, Measured with a DSR”, 3rd Eurasphalt & Eurobitume Congress, Paper 134, Vienna.

Soenen, H. and Eckmann, B. (2000). “Fatigue Testing of Bituminous Binders with a Dynamic Shear Rheometer”, 2nd Eurasphalt & Eurobitume Congress, Proc. 0209, Book I, pp. 827-834, Barcelona.

Soenen, H. and Teugels, W. (1999). “Rheological Investigation on Binder-Filler

Interactions", Eurobitume Workshop 99 – Performance Related Properties for Bituminous Binders, Paper No. 102.

Stastna, J., Zanzotto, L. and Vacin, O.J. (2003). "Viscosity Function in Polymer-Modified Asphalts", *Journal of Colloid and Interface Science*, Vol. 259, pp. 200-207.

Sybilski, D. (1996a). "Zero-Shear Viscosity of Bituminous Binder and Its Relation to Bituminous Mixture's Rutting Resistance", *Transportation Research Record*, No. 1535, pp. 15-21.

Sybilski, D. (1996b). "Zero-Shear Viscosity: Phenomenon at Measurement, Interpretation and Relation to Permanent Deformation", Euroasphalt & Eurobitume Congress, No. 5142, Strasbourg.

Tayebali, A.A., Rowe, G.M. and Sousa, J.B. (1992). "Fatigue Response of Asphalt-Aggregate Mixtures", *Journal of the Association of Asphalt Paving Technologies*, Vol. 61, pp. 333-360.

Thom, N.H., Airey, G.D., Osman, S. and Collop, A.C. (2006). "Fracture and Fatigue of Binder and Binder/Filler Mastic", 10th international Conference on Asphalt Pavements, Quebec City.

Traxler, R.N. (1936a). "Bituminous Plastics", *Industrial and Engineering Chemistry*, Vol. 8, No.3, pp. 185-188

Traxler, R.N. (1936b). "The Physical Chemistry of Asphaltic Bitumen", *Chemical Review*, Vol. 19, No.2, pp. 119-143.

Traxler, R.N. (1938). "Flow Properties of Asphalts", *Industrial and Engineering Chemistry*, Vol. 30, No.3, pp. 322-324..

Traxler, R.N., Baum, L.A.H, and Pittman, C.U. (1933). "Experimental Determination of Void Content of Close-Packed Mineral Powders", *Industrial and Engineering Chemistry*, Vol. 5, No.3, pp. 155-168.

Traxler, R.N. and Coombs, C.E. (1936). "The Colloidal Nature of Asphalt as Shown by Its Flow Properties", *Journal of Physical Chemistry*, Vol. 40, No.9, pp. 1133-1147.

Traxler, R.N. and Coombs, C.E. (1938). "Structure in Asphalts", *Industrial and Engineering Chemistry*, Vol. 30, No.4, pp. 440-443.

Traxler, R.N. and Miller, J.S. (1936). “Mineral Powders, Their Physical Properties and Stabilizing Effects”, *Proceedings of the Association of Asphalt Paving Technologies*, Vol. 7.

Traxler, R.N. and Romberg, J.W. (1952). “Asphalt, a Colloid Material”, Industrial *and Engineering Chemistry*, Vol. 44, No.1, pp. 155-158.

Tunnicliff, D.G. (1962). “A Review of Mineral Filler”, *Journal of the Association of Asphalt Paving Technologies*, Vol. 31, pp. 119-147.

Tunnicliff, D.G. (1967). “Binding Effects of Mineral Filler”, *Journal of the Association of Asphalt Paving Technologies*, Vol. 36, pp. 114-156.

Vlachovicova, Z., Zanzotto, L. and Stastna, J. (2005). “Creep and Recovery in Asphalt Modified by Radial SBS”, Transportation Research Board Annual Meeting.

Van Dijk, W. (1975). “Practical Fatigue Characterization of Bituminous Mixes”, *Journal of the Association of Asphalt Paving Technologies*, Vol. 44, pp. 38-74.

Van Dijk, W. and Visser, W. (1977). “The Energy Approach to Fatigue for Pavement Design”, *Journal of the Association of Asphalt Paving Technologies*, Vol. 46, pp. 1-40.

Warden, W.B., Hudson, S.B. and Howell, H.C. (1959). “Evaluation of Mineral Fillers in Terms of Practical Pavement Performance”, *Journal of the Association of Asphalt Paving Technologies*, Vol. 28, pp. 316-342.

Appendix A

Determination of Filler Content by Mass, Volume and Effective Volume

With reference to 35% limestone bitumen-filler mastic, the determination of filler content by mass, volume and effective volume is shown as follows:

1. Determination of filler content by mass within a bitumen-filler mastic:

Filler content by mass = $\dfrac{Mass_{filler}}{Mass_{filler} + Mass_{bitumen}} = \dfrac{35}{35+65} = 35\%$

Ratio of filler to bitumen = $\dfrac{Mass_{filler}}{Mass_{bitumen}} = \dfrac{35}{65} = 0.54$

2. Determination of filler content by volume within a bitumen-filler mastic, V_f :

Filler content by volume, $V_f = \dfrac{\dfrac{Mass_{filler}}{SG_{filler}}}{\dfrac{Mass_{filler}}{SG_{filler}} + \dfrac{Mass_{bitumen}}{SG_{bitumen}}} = \dfrac{\dfrac{35}{2.74}}{\dfrac{35}{2.74} + \dfrac{65}{1.02}} = 16.7\%$

Where $SG_{filler} = 2.74$ and $SG_{bitumen} = 1.02$, as shown in Tables 3.1 and 3.2.

3. Determination of filler content by effective volume within a bitumen-filler mastic, V_{fa} :

The voids of compacted filler measured from Rigden test for the 35% limestone bitumen-filler mastic is 24.86%, as shown in Table 3.2.

Volume percentage of filler granules, $V_{fR} = (100\% - 24.86\%) = 77.14\%$

Volume percentage of filler within mastic, $V_f = 16.7\%$

Effective volume percentage of filler, $V_{fa} = \dfrac{100}{V_{fR}} V_f = \dfrac{100}{(100 - 24.86)} \times (16.7) = 22.2\%$

Appendix B

Determination of Steady State from Creep Measurements Using the Bohlin Software

During the creep test, the instantaneous viscosity is calculated from a moving window of the data in Bohlin software. The steady state viscosity is calculated from these data. The steady state value is the rate of change of creep compliance J_c with creep time t_c. The sample is in steady viscous flow when this value of rate (slope) becomes constant $(d \log J_c / d \log t_c \sim 1.0)$, as shown in Figure A.1. The window shows the creep parameters of viscosity value, shear rate, steady state and creep compliance, and recovery parameters of recovery compliance. In addition, the boxes can be selected the start and end indices to calculated the viscosity value between any two data, and select individual run (loading cycle) in pulse creep test, as shown in Figures A.1 and A.2 (User Manual for Bohlin Rheometers).

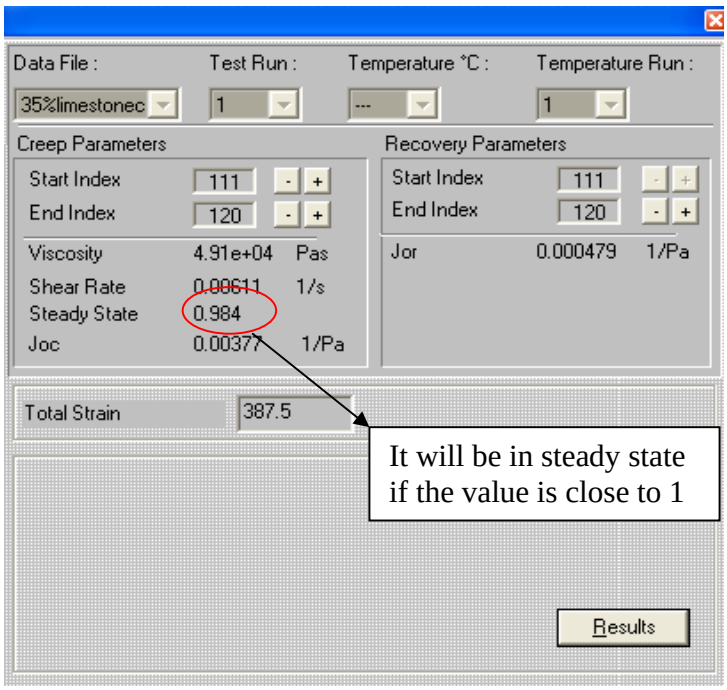

Figure A.1: Determination of steady state from creep measurements using the Bohlin software

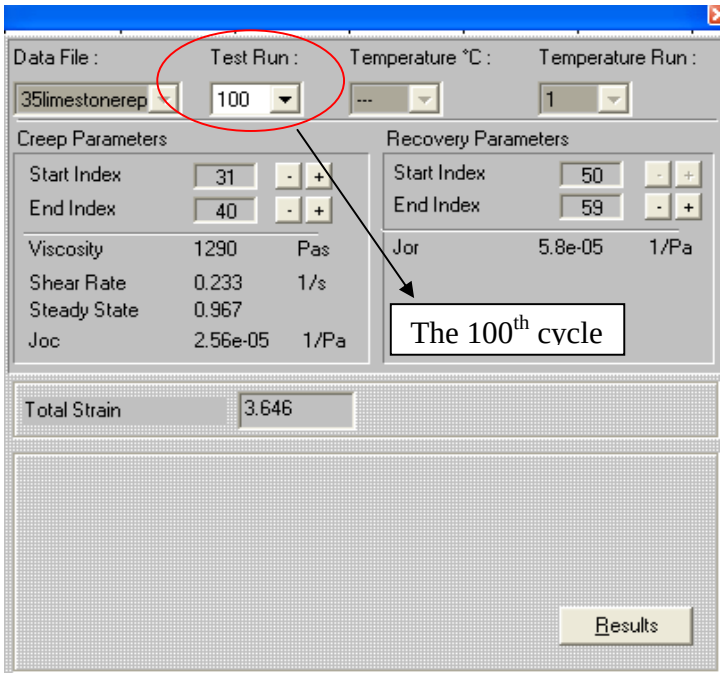

Figure A.2: Determination of creep parameters from pulse creep measurements using the Bohlin software

Appendix C

DSR Data of Strain and Stress LVE Limits

50 Penetration Grade Bitumen				
Temperature	Frequency	Complex Modulus	Shear Strain	Shear Stress
^{o}C	(Hz)	(MPa)	(microstrain)	(MPa)
5	1.6	49.99	16,200	0.810
5	10	70.61	7,600	0.533
5	25	111.48	2,800	0.304
30	1.6	0.44	70,900	0.031
30	10	1.66	51,400	0.081
30	25	4.43	31,100	0.126
45	1.6	0.04	317,500	0.013
45	10	0.20	139,400	0.033
45	25	0.39	71,500	0.028
60	1.6	0.004	922,800	0.004
60	10	0.02	355,800	0.008
60	25	0.06	170,600	0.010

15% Limestone Bitumen-Filler Mastic				
Temperature ^{o}C	Frequency (Hz)	Complex Modulus (MPa)	Shear Strain (microstrain)	Shear Stress (MPa)
5	1.6	45.02	17,000	0.767
5	10	99.66	5,800	0.576
5	25	114.44	3,700	0.418
30	1.6	0.55	52,400	0.028
30	10	2.32	25,900	0.057
30	25	4.60	20,300	0.085
45	1.6	0.05	152,700	0.008
45	10	0.23	70,500	0.016
45	25	0.46	58,700	0.027
60	1.6	0.01	693,400	0.004
60	10	0.03	185,300	0.005
60	25	0.06	56,800	0.003

35% Limestone Bitumen-Filler Mastic				
Temperature ^{o}C	Frequency (Hz)	Complex Modulus (MPa)	Shear Strain (microstrain)	Shear Stress (MPa)
5	1.6	50.08	5,900	0.387
5	10	158.02	2,700	0.423
5	25	171.20	540	0.092
30	1.6	0.83	71,100	0.059
30	10	3.47	23,100	0.077
30	25	6.18	15,500	0.083
45	1.6	0.08	107,200	0.008
45	10	0.33	41,200	0.018
45	25	0.56	19,800	0.044
60	1.6	0.01	176,580	0.001
60	10	0.05	75,000	0.003
60	25	0.11	29,700	0.003

65% Limestone Bitumen-Filler Mastic				
Temperature ^{o}C	Frequency (Hz)	Complex Modulus (MPa)	Shear Strain (microstrain)	Shear Stress (MPa)
5	1.6	285.00	1,500	0.262
5	10	380.00	1,000	0.332
5	25	475.00	417	0.209
30	1.6	3.901	4,866	0.014
30	10	14.48	3,521	0.024
30	25	30.23	1,982	0.042
45	1.6	0.36	4,276	0.001
45	10	1.47	1,652	0.002
45	25	2.40	1,995	0.006
60	1.6	0.04	9,704	0.0002
60	10	0.18	2,810	0.0004
60	25	0.40	1,601	0.0005

35% Cement Bitumen-Filler Mastic				
Temperature ^{o}C	Frequency (Hz)	Complex Modulus (MPa)	Shear Strain (microstrain)	Shear Stress (MPa)
5	1.6	55.04	1,400	0.076
5	10	75.56	1,100	0.082
5	25	179.90	1,900	0.341
30	1.6	0.86	35,300	0.030
30	10	3.52	23,700	0.080
30	25	6.39	15,900	0.092
45	1.6	0.07	217,800	0.015
45	10	0.35	47,700	0.021
45	25	0.59	32,500	0.070
60	1.6	0.01	333,600	0.003
60	10	0.04	52,700	0.002
60	25	0.09	29,500	0.003

65% Cement Bitumen-Filler Mastic				
Temperature ^{o}C	Frequency (Hz)	Complex Modulus (MPa)	Shear Strain (microstrain)	Shear Stress (MPa)
5	1.6	243.25	820	0.199
5	10	315.26	1,940	0.611
5	25	382.38	1,650	0.628
30	1.6	4.86	4,400	0.021
30	10	17.43	2,350	0.041
30	25	33.50	1,380	0.045
45	1.6	0.47	3,850	0.002
45	10	1.57	3,710	0.006
45	25	2.53	3,970	0.010
60	1.6	0.04	30,800	0.001
60	10	0.21	6,580	0.001
60	25	0.46	3,210	0.001

35% Gritstone Bitumen-Filler Mastic				
Temperature ^{o}C	Frequency (Hz)	Complex Modulus (MPa)	Shear Strain (microstrain)	Shear Stress (MPa)
5	1.6	75.78	4,200	0.317
5	10	154.64	2,200	0.339
5	25	196.52	2,000	0.387
30	1.6	1.20	50,600	0.060
30	10	4.33	15,700	0.066
30	25	8.92	7,900	0.064
45	1.6	0.10	102,100	0.010
45	10	0.46	31,100	0.016
45	25	0.78	28,200	0.061
60	1.6	0.01	149,200	0.001
60	10	0.05	39,700	0.002
60	25	0.13	13,800	0.002

65% Gritstone Bitumen-Filler Mastic				
Temperature ^{o}C	Frequency (Hz)	Complex Modulus G*(MPa)	Shear Strain (microstrain)	Shear Stress (MPa)
5	1.6	261.16	1,640	0.427
5	10	409.50	2,870	1.176
5	25	475.21	3,490	1.656
30	1.6	7.36	3,640	0.027
30	10	30.47	910	0.028
30	25	44.23	1,350	0.058
45	1.6	0.53	11,350	0.006
45	10	1.95	7,140	0.014
45	25	2.74	5,740	0.016
60	1.6	0.06	10,500	0.001
60	10	0.26	10,760	0.003
60	25	0.63	3,950	0.002

Appendix D

DSR Shear Complex Viscosity Data

Complex Viscosity

	50 Pen Bitumen		15% Limestone		35% Limestone		65% Limestone	
Frequency (Hz)	40°C (Pa.s)	60°C (Pa.s)	40°C (Pa.s)	60°C (Pa.s)	40°C (Pa.s)	60°C (Pa.s)	40°C (Pa.s)	60°C (Pa.s)
0.10	18,352	573	21,160	725	32,200	978	167,880	5,889
0.13	17,812	570	20,463	721	31,300	970	156,780	5,936
0.17	17,166	565	19,791	715	30,400	966	150,630	5,721
0.23	16,557	561	19,097	708	29,400	959	142,870	5,614
0.31	15,948	556	18,401	702	28,500	953	136,420	5,481
0.40	15,320	551	17,739	694	27,400	940	129,690	5,394
0.53	14,690	544	17,009	683	26,400	930	123,430	5,346
0.70	14,047	535	16,295	673	25,300	917	116,930	5,084
0.93	13,412	529	15,569	660	24,200	896	110,350	4,923
1.23	12,792	519	14,867	649	23,100	879	104,620	4,931
1.63	12,171	509	14,165	636	22,000	859	98,842	4,791
2.15	11,572	498	13,465	622	20,900	839	92,966	4,620
2.84	10,975	487	12,776	606	19,800	818	87,360	4,486
3.75	10,384	474	12,130	591	18,700	795	82,262	4,337
4.96	9,808	462	11,432	574	17,600	774	77,014	4,195
6.56	9,198	448	10,760	557	16,500	753	72,012	4,025
8.66	8,600	435	10,063	539	15,500	730	67,432	3,857
11.45	7,978	421	9,416	520	14,500	704	62,807	3,679
15.13	7,321	406	8,673	501	13,400	673	58,246	3,491
20.00	6,561	390	7,817	480	12,200	649	53,683	3,329

Complex Viscosity

	35% Cement		65% Cement		35% Gritstone		65% Gritstone	
Frequency (Hz)	40°C (Pa.s)	60°C (Pa.s)	40°C (Pa.s)	60°C (Pa.s)	40°C (Pa.s)	60°C (Pa.s)	40°C (Pa.s)	60°C (Pa.s)
0.10	29,446	1,272	243,150	6,541	33,739	1,439	450,990	11,956
0.13	28,618	1,258	230,890	6,495	32,494	1,427	408,280	11,222
0.17	27,741	1,246	215,440	6,372	31,375	1,417	375,930	11,052
0.23	26,766	1,235	202,400	6,306	30,300	1,403	343,170	10,669
0.31	25,862	1,220	192,780	6,111	29,300	1,391	312,220	10,719
0.40	24,924	1,200	182,120	5,823	28,163	1,374	293,880	10,144
0.53	23,887	1,188	171,860	5,795	27,053	1,351	270,140	9,929
0.70	22,852	1,168	161,200	5,758	25,929	1,334	255,950	9,500
0.93	21,862	1,149	151,140	5,583	24,830	1,304	232,910	9,155
1.23	20,876	1,131	142,020	5,409	23,725	1,281	217,270	8,709
1.63	19,846	1,105	132,610	5,253	22,640	1,253	201,640	8,393
2.15	18,860	1,080	124,070	5,061	21,493	1,222	186,890	8,068
2.84	17,925	1,054	115,530	4,893	20,365	1,185	173,160	7,748
3.75	16,964	1,024	107,620	4,666	19,244	1,146	161,000	7,467
4.96	15,970	992	100,320	4,508	18,154	1,109	148,800	7,183
6.56	15,022	963	93,408	4,297	17,036	1,080	138,480	6,774
8.66	14,045	930	86,603	4,102	15,936	1,042	127,740	6,414
11.45	13,068	898	80,077	3,901	14,890	1,004	117,660	6,086
15.13	12,097	863	74,079	3,709	13,744	962	107,630	5,724
20.00	11,034	825	68,069	3,484	12,523	918	98,202	5,329

Appendix E

DSR Fatigue Data

50 Penetration Grade Bitumen					
Load Mode	Temperature (^{o}C)	Initail Strain (microstrain)	Initial Stress (MPa)	Initial Stiffness (MPa)	No of Cycles to Failure (Cycles)
Strain	10	10,000	0.452	47.50	96,498
Strain	10	25,000	1.063	43.90	22,379
Strain	10	40,000	1.531	39.30	7,100
Stress	10	11,700	0.500	43.00	82,376
Stress	10	17,500	0.800	45.90	28,381
Stress	10	22,600	1.000	44.50	22,083
Stress	10	29,000	1.200	41.50	10,929
Stress	10	33,200	1.500	45.50	8,454
Strain	20	10,000	0.132	13.50	484,689
Strain	20	15,000	0.200	13.50	166,868
Strain	20	17,000	0.291	13.50	116,798
Strain	20	25,000	0.306	12.40	50,066
Strain	20	35,000	0.401	11.70	21,889
Strain	20	45,000	0.503	10.90	7,117
Strain	20	55,000	0.679	12.50	7,484
Strain	20	75,000	0.814	11.00	2,741
Stress	20	11,500	0.150	13.20	241,293
Stress	20	16,700	0.225	13.70	100,605
Stress	20	26,500	0.300	11.50	6,404
Stress	20	51,000	0.550	10.97	3,344

35% Limestone Bitumen-Filler Mastic					
Load Mode	Temperature (^{o}C)	Initail Strain (microstrain)	Initial Stress (MPa)	Initial Stiffness (MPa)	No of Cycles to Failure (Cycles)
Strain	10	10,000	0.873	91.20	105,177
Strain	10	20,000	1.496	77.40	13,231
Strain	10	40,000	2.264	58.50	2,323
Strain	20	10,000	0.210	21.40	289,263
Strain	20	15,000	0.306	20.80	111,858
Strain	20	35,000	0.579	16.70	5,973
Strain	20	55,000	0.932	17.00	2,467
Strain	20	85,000	1.070	12.60	1,179
Stress	20	14,900	0.300	20.70	66,331
Stress	20	23,300	0.450	19.00	16,470
Stress	20	51,000	0.850	14.60	1,399
Stress	20	72,000	1.050	10.20	404

65% Limestone Bitumen-Filler Mastic					
Load Mode	Temperature (^{o}C)	Initail Strain (microstrain)	Initial Stress (MPa)	Initial Stiffness (MPa)	No of Cycles to Failure (Cycles)
Strain	10	5,000	1.064	219.00	321,817
Strain	10	6,500	1.488	240.00	117,614
Strain	10	8,000	1.587	203.00	49,555
Strain	20	15,000	0.747	50.70	57,133
Strain	20	25,000	1.024	41.30	14,804
Strain	20	35,000	1.201	34.30	6,119
Strain	20	55,000	1.588	28.50	1,024
Stress	20	18,000	0.850	47.80	9,899
Stress	20	23,000	1.050	45.80	4,257
Stress	20	26,000	1.250	48.30	2,949
Stress	20	50,000	1.500	30.20	742

35% Cement Bitumen-Filler Mastic					
Load Mode	Temperature (^oC)	Initail Strain (microstrain)	Initial Stress (MPa)	Initial Stiffness (MPa)	No of Cycles to Failure (Cycles)
Strain	10	10,000	0.946	98.50	97,785
Strain	10	20,000	1.557	79.80	11,721
Strain	10	35,000	2.055	57.60	5,145
Strain	20	20,000	0.444	22.60	22,260
Strain	20	35,000	0.623	18.10	11,760
Strain	20	55,000	0.898	16.50	4,289
Strain	20	85,000	1.142	13.50	1,085
Stress	20	12,600	0.300	24.00	79,113
Stress	20	20,000	0.450	22.40	32,405
Stress	20	52,000	0.850	16.50	1,924
Stress	20	59,000	1.050	18.10	922

65% Cement Bitumen-Filler Mastic					
Load Mode	Temperature (^oC)	Initail Strain (microstrain)	Initial Stress (MPa)	Initial Stiffness (MPa)	No of Cycles to Failure (Cycles)
Strain	10	5,000	1.180	244.00	379,448
Strain	10	6,000	1.524	261.00	146,414
Strain	10	7,000	1.577	231.00	71,134
Strain	20	20000	0.978	49.50	23,765
Strain	20	35,000	1.429	41.00	4,560
Strain	20	55,000	1.815	32.80	1,099
Stress	20	15,600	0.850	54.60	23,025
Stress	20	21,000	1.050	50.95	7,349
Stress	20	29,000	1.250	43.20	2,956
Stress	20	40,000	1.500	37.50	1,155

35% Gritstone Bitumen-Filler Mastic					
Load Mode	Temperature (^oC)	Initail Strain (microstrain)	Initial Stress (MPa)	Initial Stiffness (MPa)	No of Cycles to Failure (Cycles)
Strain	10	10,000	0.993	99.00	78,351
Strain	10	20,000	1.217	61.00	21,381
Strain	10	35,000	2.189	64.00	2,877
Strain	20	20,000	0.499	25.50	49,177
Strain	20	35,000	0.730	21.10	12,850
Strain	20	55,000	1.080	19.80	3,787
Strain	20	85,000	1.295	15.20	1,074
Stress	20	12,000	0.300	24.90	119,809
Stress	20	20,000	0.450	23.10	28,407
Stress	20	46,000	0.850	18.80	1,945
Stress	20	64,000	1.050	16.60	500

65% Gritstone Bitumen-Filler Mastic					
Load Mode	Temperature (^oC)	Initail Strain (microstrain)	Initial Stress (MPa)	Initial Stiffness (MPa)	No of Cycles to Failure (Cycles)
Strain	20	15,000	0.941	63.60	43,166
Strain	20	25,000	1.302	52.30	6,547
Strain	20	35,000	1.725	49.30	2,001
Stress	20	16,600	1.050	63.50	6,445
Stress	20	21,000	1.250	59.90	3,058
Stress	20	30,000	1.500	50.70	893